SPECTRUM FATIGUE LIFETIME AND RESIDUAL STRENGTH FOR FIBERGLASS LAMINATES

Neil K. Wahl
Montana Tech of The University of Montana

and

John F. Mandell
Daniel D. Samborsky
Montana State University

Sandia National Laboratories

SPECTRUM FATIGUE LIFETIME AND RESIDUAL STRENGTH FOR FIBERGLASS LAMINATES

Neil K. Wahl
Montana Tech of The University of Montana
Butte, Montana 59701

John F. Mandell
Daniel D. Samborsky
Department of Chemical Engineering
Montana State University
Bozeman, Montana 59717

ABSTRACT

This report addresses the effects of spectrum loading on lifetime and residual strength of a typical fiberglass laminate configuration used in wind turbine blade construction. Over 1100 tests have been run on laboratory specimens under a variety of load sequences. Repeated block loading at two or more load levels, either tensile-tensile, compressive-compressive, or reversing, as well as more random standard spectra have been studied. Data have been obtained for residual strength at various stages of the lifetime. Several lifetime prediction theories have been applied to the results.

The repeated block loading data show lifetimes that are usually shorter than predicted by the most widely used linear damage accumulation theory, Miner's sum. Actual lifetimes are in the range of 10 to 20 percent of predicted lifetime in many cases. Linear and nonlinear residual strength models tend to fit the data better than Miner's sum, with the nonlinear providing a better fit of the two. Direct tests of residual strength at various fractions of the lifetime are consistent with the residual strength models. Load sequencing effects are found to be insignificant. The more a spectrum deviates from constant amplitude, the more sensitive predictions are to the damage law used. The nonlinear model provided improved correlation with test data for a modified standard wind turbine spectrum. When a single, relatively high load cycle was removed, all models provided similar, though somewhat non-conservative correlation with the experimental results. Predictions for the full spectrum, including tensile and compressive loads were slightly non-conservative relative to the experimental data, and accurately captured the trend with varying maximum load. The nonlinear residual strength based prediction with a power law S-N curve extrapolation provided the best fit to

the data in most cases. The selection of the constant amplitude fatigue regression model becomes important at the lower stress, higher cycle loading cases.

The residual strength models may provide a more accurate estimate of blade lifetime than Miner's rule for some loads spectra. They have the added advantage of providing an estimate of current blade strength throughout the service life.

TABLE OF CONTENTS

INTRODUCTION

The development of predictive design tools for the lifetime of fiberglass laminates has lagged that of metals [2-4] for a number of reasons, one of which is the anisotropic nature of the laminates. While metals have the single damage metric or parameter of crack size, composites have many more complicated failure modes. Failure of composites may include matrix cracking, delamination, fiber debonding, fiber pullout, fiber buckling, ply delamination, ply failure, and fiber fracture; a typical failure may involve a complex contribution of some or all these possible mechanisms. Although lifetime rules based upon nearly every laminate property have been proposed, many seem to have limited validity, with theoretical and actual lifetimes sometimes decades apart [5]. The more complicated models do not seem to yield better results than the linear damage accumulation law first proposed by M. A. Miner in the 1940's [4, 6, 7]. Despite this law's shortcomings, it is used throughout the wind industry, for estimating laminate wind turbine blade lifetimes, e.g., Sandia National Laboratories' computer code LIFE2 [8-10], as well as by many researchers in laminate fatigue [11-13].

Fatigue testing of fiberglass laminates typically involves the constant amplitude sinusoidal loading of a specimen until failure. Illustrated in Figure 1 is data, captured by use of a digital storage oscilloscope. The data is typical of load cycles used in constant amplitude fatigue testing. In the test; the cycle rate was 10 Hz, with maximum and minimum loads of 6.4 and 0.64 kN, respectively. Shown on the oscilloscope screen capture are both the demand and feedback signals from the test machine controller. The demand signal slightly leads the feedback signal. There is a slight amplitude deviation between the demand and feedback of approximately 1 percent in this example. The variation is a function of the laminate, test frequency, load levels and controller tuning.

Data such as found in References 13 and 14, which consist of the results of constant amplitude testing, are readily available. Unfortunately, constant amplitude testing and the Miner's rule ignore any possibility of load interaction and load sequence effects, which may be particularly important for load spectra that are random in nature. Shown in Figures 2 and 3 are variable amplitude spectrum loading histories for wind turbine blades. Figure 2 is a portion of a European standard loading spectrum [15, 16]; note the single, relatively large cycle of higher stress that must be considered in any fatigue model. This European spectrum is a distillation of flap load data collected from near the root of the blades of nine wind turbines in Europe. A portion of the edge bending moment loading of a blade of a Micon 65/13 wind turbine in California is shown in Figure 3 [17]. This loading is typical of a variable amplitude loading spectrum that may be encountered in industry. An arbitrary time scale is shown, as the frequency can be set by the operator when applying these load histories in a laboratory testing program.

Researchers and wind energy industry authorities have spelled out a need for improved life estimating rules and for the study of variable amplitude or spectrum loading [5, 9, 19]. The goal of

the research presented by this dissertation was to investigate improvements to lifetime
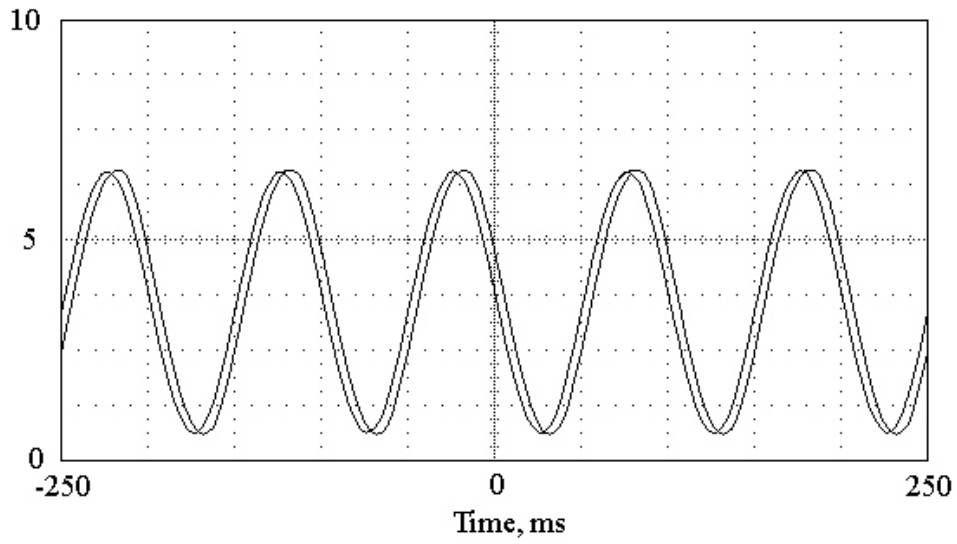
Figure 1.Constant Amplitude Load History.
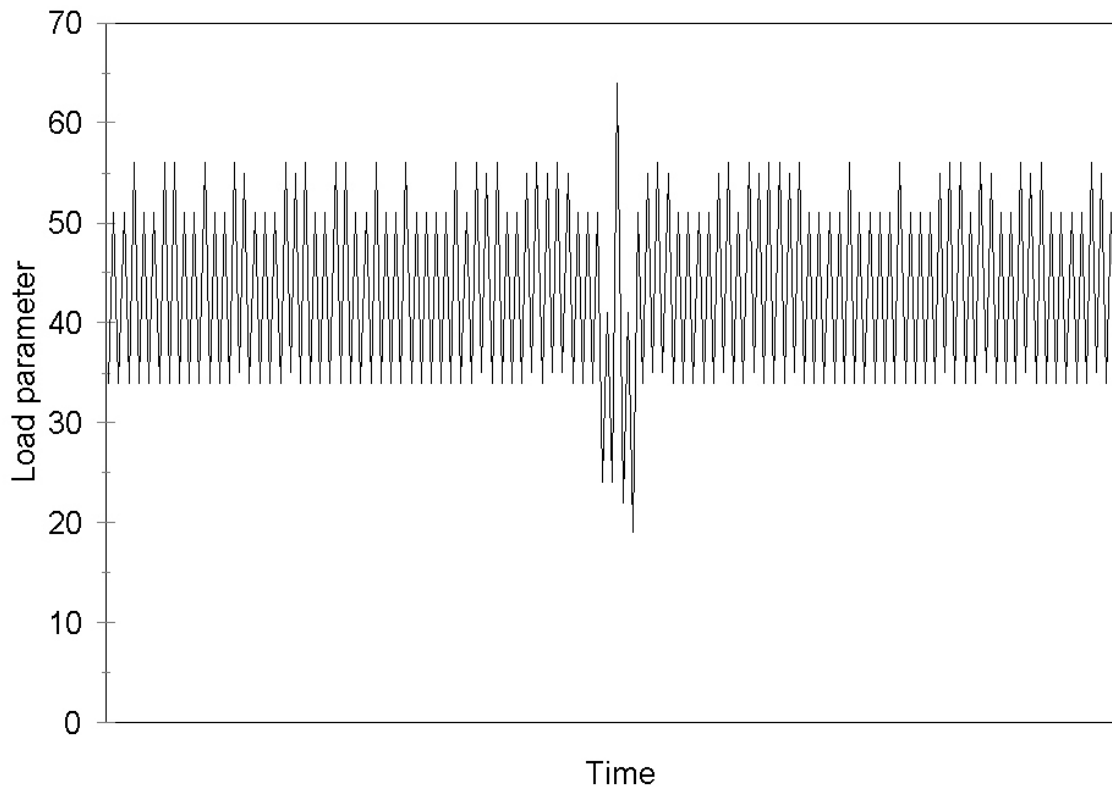
Figure 2. Portion of European Standard Variable Amplitude Fatigue Load History.
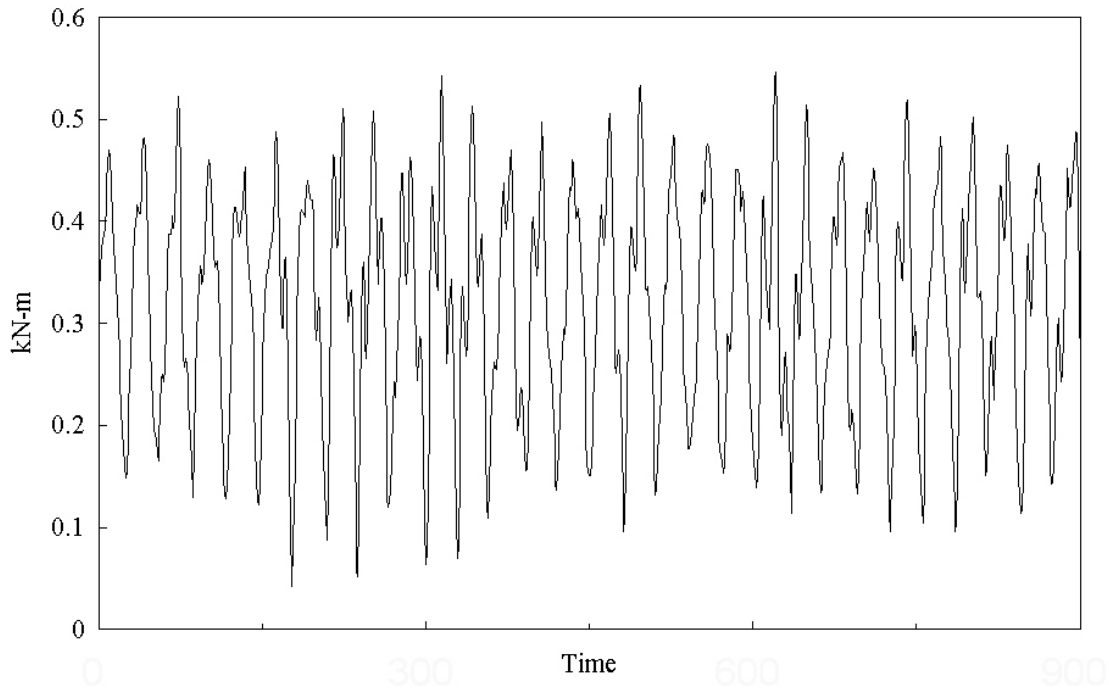
Figure 3. Portion of European Standard Variable Amplitude Fatigue Load History.

prediction rules for fiberglass laminates used in the construction of wind turbine blades. Any model that would be readily accepted must be easy to use, contain a minimum of parameters, and be accurate [20].

Very few researchers have undertaken an investigation of lifetime prediction models that started at the simplest of fatigue cases and logically progressed through an ever increasing complexity. Most research efforts can be characterized as a study of constant amplitude fatigue followed by the development of a lifetime prediction model, and, finally, an attempt to verify the model by analyzing the fatigue of specimens subjected to a two-block spectrum, with the second block run to failure. Sendeckyj [20] and Bond [21] itemized a research program that would lead to the development of a rational life prediction model. The work, herein summarized, attempts to follow those guidelines [20]; namely,

1. establish an experimental program to investigate the damage process of the laminate
2. determine a valid damage measurement method (metric)
3. develop a life prediction rule based upon the established metric
4. experimentally validate the life prediction rule.

The experimental program should begin with constant amplitude fatigue testing and progress to block spectra fatigue testing [21].

9

FATIGUE OF MATERIALS

Fatigue is typically defined as the failure of a material due to repeated loading at levels below the ultimate strength. The general nature of fatigue for the two common materials, metals and fiberglass laminates, will be reviewed in this chapter along with some fundamentals of fatigue testing.

Background

Fatigue of materials subjected to cyclic loading (Figures 1, 2 and 3) is dependent upon not only the maximum stress level encountered, but also the range of the stresses applied. Generally, the greater the maximum stress, and the greater the range, greater damage is encountered. Although there are a variety of methods for describing each cycle of loading of a specimen, the method normally accepted for laminates is the maximum stress and R-value.

$$R - value = R = \frac{\sigma_{min}}{\sigma_{max}} \tag{1}$$

where σ_{min} is the minimum stress level
σ_{max} is the maximum stress level

Summarized in Figure 4 are the basic descriptions of the various cycle stress parameters.
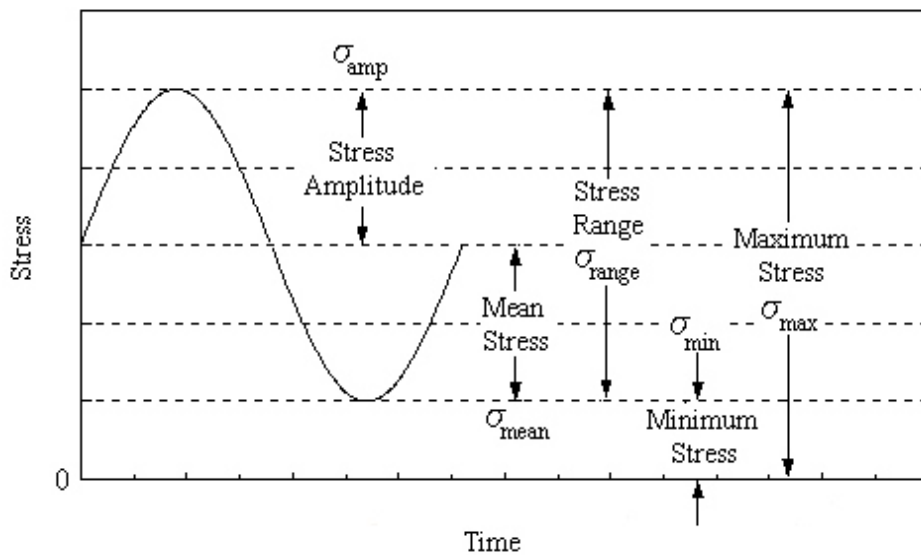
Figure 4. Cyclic Loading Test Parameters.

Displayed in Figure 5 are a grouping of typical R-values as well as an identification of the primary loading regimes.

Figure 5. Load Regimes and R-Values.

Constant amplitude testing of a material at a constant R-value, but at a family of maximum stress levels is typically summarized in stress-cycle (S-N) diagrams. The information displayed on an S-N diagram is usually the maximum stress level as a function of the number of cycles to failure on a semi-log plot. Figure 6 [4] is a typical S-N diagram and for 7075-T6 aluminum.

Constant amplitude testing at a variety of R-values can be summarized within a Goodman diagram, see Figure 7, relating the alternating stress to the mean stress. Each set of tests at a constant R-value is represented by a straight line as defined in Equation 2. Small amplitude and consequently, longer tests are closer to the origin on any selected radial line of constant R-value.

$$\sigma_{alt} = \left[\frac{1 - R}{1 + R} \right] \sigma_{mean} \tag{2}$$

where σ_{alt} is the alternating stress value = σ_{amp}
    R = R-value
    σ_{mean} = mean stress level

A slope of zero represents the ultimate tensile strength test, while a slope of 180° represents an ultimate compressive strength test.

11

Figure 6. S-N Curve for 7075-T6 Aluminum Alloy, Fully Reversed
(R-value = -1) Axial Loading [4].
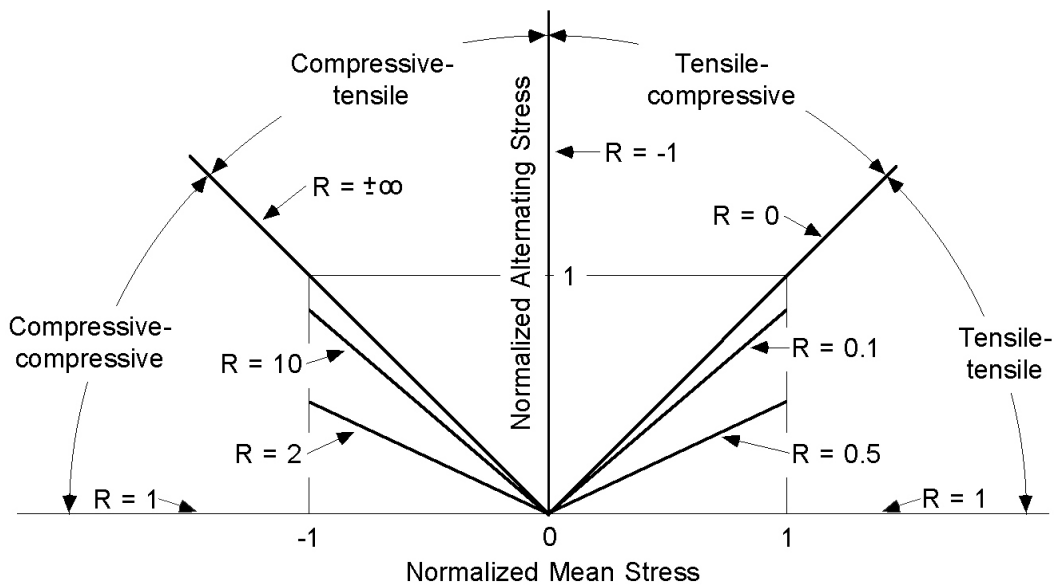
Figure 7. Goodman Diagram.

Historically, the first serious concern for fatigue failure in metals came with the expansion of the railway industry in the mid 19th century. Early investigations by Wöhler led to the summary of constant amplitude fatigue in diagrams relating stress and life (S-N diagrams). These diagrams can be considered a means for life prediction for metals subjected to constant amplitude loading. Estimates of S-N diagrams can be developed from fundamental material properties, thereby speeding the design process by minimizing laboratory fatigue testing. Other investigators, Gerber and Goodman [2], researched the effects of the mean and range of stresses upon lifetimes. For a given maximum stress level, the greater the stress range the greater the cyclic damage. Diagrams relating the mean and alternating stresses bear the names of these gentlemen.

Palmgren proposed [22] and Miner developed [6] the first cumulative damage rule in attempts to account for variable amplitude cyclic loading. Frequently, the "Miner's rule" is called a linear model, relating to the linear addition of damage contributions of each cycle of loading. Each cycle is considered to contribute damage in the amount of the fractional amount of life expended at that cycle's constant amplitude equivalent.

$$ Miner's \ Sum \ = \ \sum_i \ \frac{n_i}{N_i} \tag{3} $$

where i is the cycle sequential index
n_i is the number of cycles at stress level σ_i
N_i is the number of constant amplitude cycles to failure at stress level σ_i

Miner's work in aluminum revealed a wide variation in the predictive capability of this linear damage rule. The rule is incapable of accounting for any sequence effects for a variable amplitude load spectrum. Sequencing effects or load interactions such as work hardening and "over stressing" are not addressed by this rule [6]. Over stressing is the loading sequence of first applying high loads and then cycling the material to failure at lower loads. The rule also cannot satisfy the consequences of a single large cycle that can cause catastrophic failure with little contribution to the damage rule.

Irwin can be considered the father of linear elastic fracture mechanics (LEFM) and fatigue crack growth lifetime predictions. During the last half of the 20th century, failure of aircraft and bridges due to crack growth led to the development and acceptance of fracture mechanics for lifetime predictions [2, 3, 23, 24].

It is generally understood and approximated that the crack growth rate is a function of the stress intensity factor as the Paris law [3, 23, 24].

$$ \frac{da}{dN} \ = \ C\Delta K^{-m} \tag{4} $$

where a is the crack size
N is the number of cycles of loading

13

ΔK is the stress intensity factor range
C and m are constants for the material

This equation is valid over a portion of the lifetime or crack growth history. The relationship fits the middle range of the overall S-shaped crack growth rate versus ΔK curve on a double logarithmic plot as shown in Figure 8 [26]. At the low stress intensity factors of region I, crack growth is extremely slow, leading to the postulate that crack growth does not occur below some threshold value, K_{th}. Region II covers a major portion of the crack growth and is modeled as the Paris law, equation 4. Rapid crack growth occurs in region III, as the maximum stress intensity factor approaches some critical stress intensity factor K_c.

The stress intensity factor, K, is approximated with Equation 5 [3, 23, 24].

$$K = S_a \, Y\sqrt{\pi \, A} \qquad\qquad (5)$$

where S_a is the applied stress
Y is a geometric factor
a is the crack length
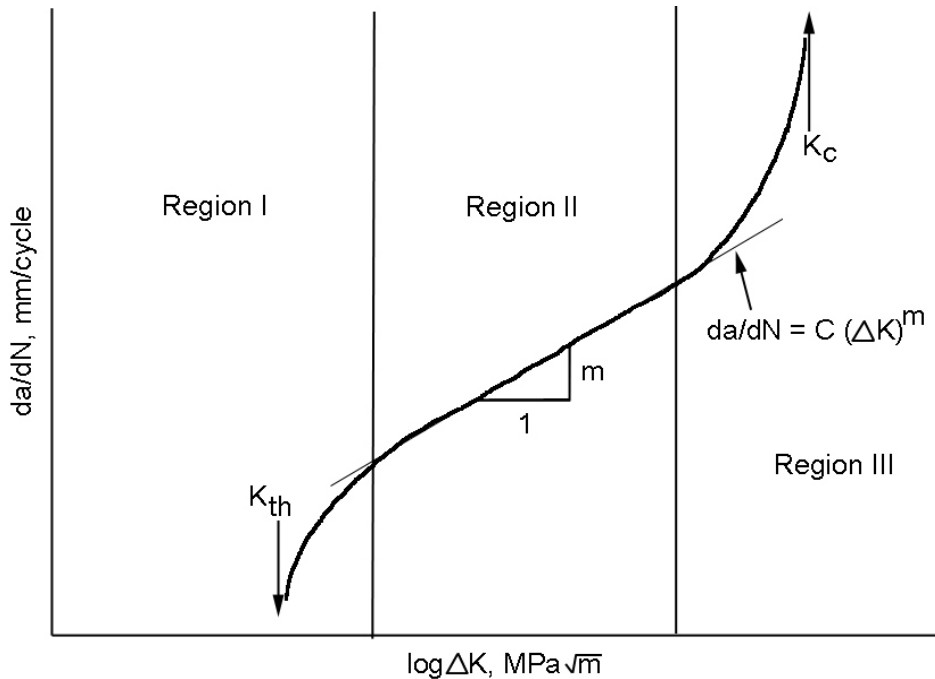
Figure 8. Stress Intensity Factor and Crack Growth Rate Trends.

Substitutions, rearrangement and integration of the above two equations results in an expression

14

relating the number of cycles required to grow a crack between two sizes (Y is taken as 1.0):

$$N = \frac{1}{CS_a^m \; \pi^{m/2}} \left(\frac{2}{-m+2}\right) a^{\frac{-m+2}{2}} \Bigg|_{a_i}^{a_d} \quad ,(m \neq 2) \tag{6}$$

where a_d is the minimum detectable crack size
a_i is some increased crack size
N represents the number of required cycles
S_a is the applied stress
C and m are constants for the material

Load sequencing effects can be important in the fatigue of metals. Crack growth in constant amplitude fatigue has been found to be slowed by a high load cycle or overload [23]. The type of overload has a great effect on the crack growth rate or retardation. Tensile overloads can retard crack growth whereas compressive overloads will offer little effect by themselves or will cause a reduction of the beneficial retardation of a prior tensile overload. The amount of retardation is dependent upon the size of the plastic zone created at the crack tip during a tensile high load cycle. Upon relaxation of the high load, the material in the plastic zone will be in compression. The following "normal" cycles must cause the crack to progress through this compressed zone before continuing at the faster rate.

Fiberglass Laminates

The damage metric of metals is chiefly that of crack growth, whereas for laminates there is no clear, dominant metric. Damage can be attributed to a variety of contributors, such as fiber breakage, matrix cracking, fiber debonding and pullout and delamination.

The laminate under consideration in this research was comprised of E-glass (electrical grade) reinforcement and a thermoset matrix. Each of these constituents play roles in the strength and fatigue resistance of the laminate. The tensile properties for loading in the fiber direction are fiber dominated, while compressive properties are matrix dominated [25].

Laminate Fatigue Description

The following description of the progression of fatigue damage of laminates is summarized from References 25 and 26. Reifsnider [25] provided a detailed analysis of the progression of fatigue damage in laminates as shown in Figure 9. This analysis considers both tensile and compressive loads as well as a variety of laminate ply orientations. Upon initial tensile cyclic loading, at levels below the ultimate strength, matrix cracks in the off-axis plies occur first. This cracking will continue until a pattern or spacing of the matrix cracking becomes saturated. This spacing is dictated by the ability of the laminate to redistribute the loads to the material between cracks. This degree of damage has

15

been termed a characteristic damage state, which also signals a transition from one stage of damage development to another.
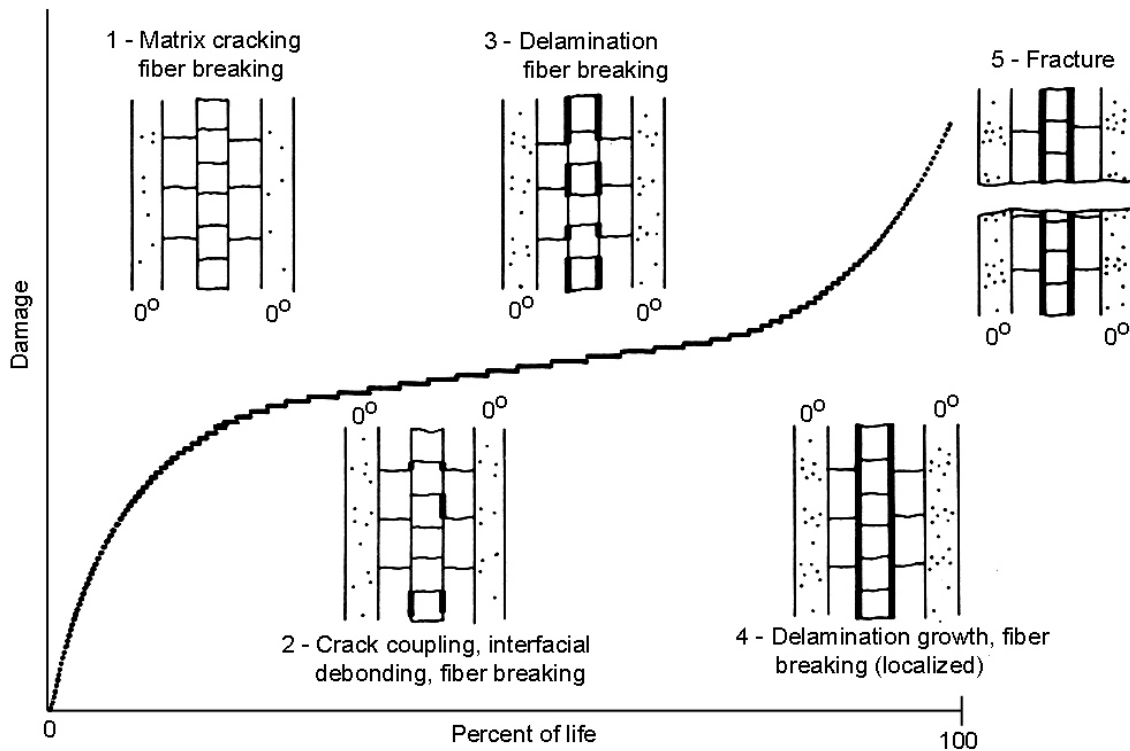
Figure 9. Schematic representation of the development of damage during the fatigue life of a composite laminate [25].

Upon continued cyclic loading, matrix cracking continues, but may develop in interlaminar areas and along axial fibers, causing a coalescing and interdependence of cracking, ultimately leading to localized delamination. Compressive excursions will promote this delamination process, not providing a damage retardation as was discussed for fatigue in metals.

Continued cycling will cause a spreading of and interaction of localized damage. Loads will be redistributed causing some fiber damage, breakage, debonding and delamination growth. With continuation of cycling, the load carrying capacity will be reduced to levels that can no longer support the applied load. The failure is sudden and catastrophic, with fiber breakage and pull out described as "brooming".

The damage manifests itself in changes of bulk properties such as stiffness and residual or remaining strength of the laminate. After initiation of damage (analogous to loading metals at stresses that produce a stress intensity factor above its threshold) the damage accumulates rapidly at first and then accumulates more slowly. This acceleration and deceleration of damage is not consistent with the continual increase of damage accumulation (crack length) in metals. The damage accumulation

16

in laminates is consistent with the initial rapid loss of stiffness and then a slowing of the stiffness reduction [27, 28]. This is also proposed in the lifetime prediction models for composite materials section as related to the loss of residual strength of laminates.

Fatigue Trends of Fiberglass Laminates

Constant amplitude fatigue testing of laminates is generally summarized in stress-cycle (S-N) diagrams and represented in models as either linear on semi-log (equation 7) or log-log (equation 8) plots for exponential or power law trends, respectively.

$$\frac{\sigma}{\sigma_0} = C_1 - b \log (N) \tag{7}$$

$$\frac{\sigma}{\sigma_0} = C_2 N^{-\frac{1}{m}} \tag{8}$$

where σ is the maximum applied stress
σ_0 the ultimate strength
N the number of cycles to failure
C_1, C_2, b and m are regression parameters

Rearrangement of equations 7 and 8 to solve for N, led to equations 9 and 10. Equation 9 is exponential in form, while equation 10 is of the power law form.

$$N = 10^A , \quad where \quad A = \left[\frac{C_1 - \dfrac{\sigma}{\sigma_0}}{b} \right] \tag{9}$$

$$N = \left[\frac{\sigma}{C_2 \, \sigma_0} \right]^{-m} \tag{10}$$

Typical S-N curves for these fatigue regression analyses are shown in Figure 10.
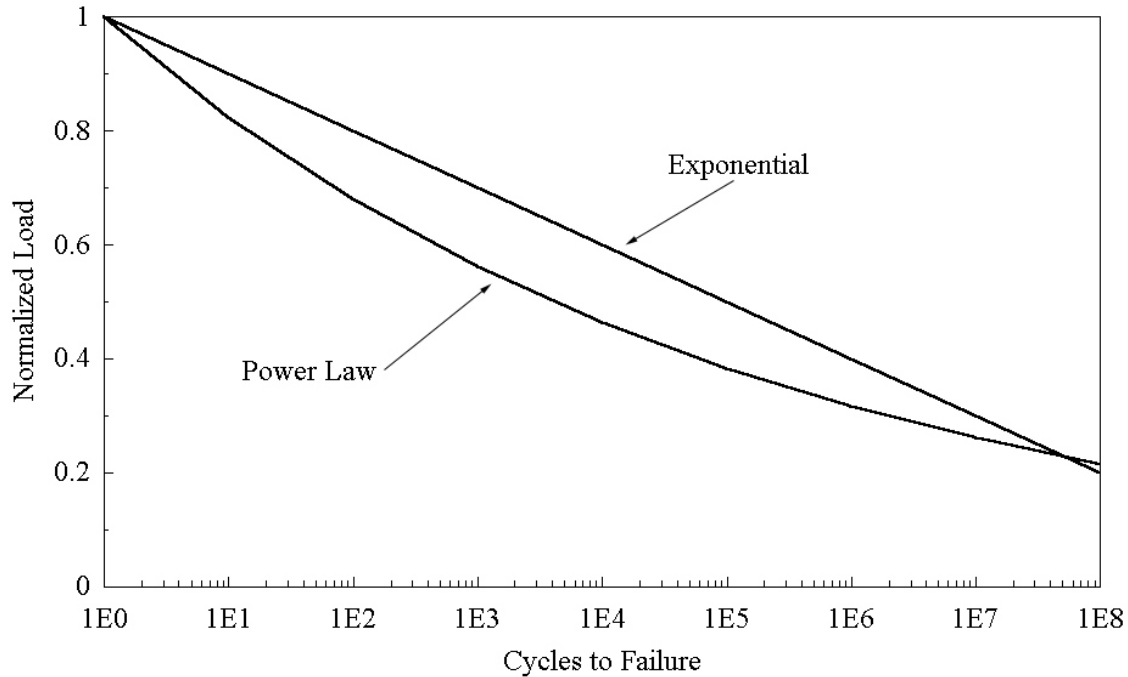
Figure 10. Comparison of Exponential and Power Law Constant Amplitude Laminate Fatigue Trends on Semi-Log Plot.

Much of the early work used exponential fits and semi-log plots, with the power law representation and log-log plots becoming popular with the advent of high cycle testing. Questions have arisen as to which is the better fatigue model (regression equation) for use in lifetime prediction methods involving extrapolation to higher cycles [5, 10, 29-33]. The selection of the "best" fit may be the cause of a shift in the failure prediction at some fraction of the laminate's life [34]. This seems somewhat subject to the material, type of loading and the fraction of life expended.

A general rule has been promoted for quick comparison of the fatigue sensitivity of various laminates comprised of 0° and off axis plies. The stress or strain normalized slope, b, of the exponential regression has frequently been touted as 0.1 (10 percent per decade) for "good" fiberglass laminates in tension (R = 0.1), while a slope of 0.14 has been considered a "poor" material response [14, 35]. The general trend for the better laminates in compression (R = 10) is 0.07 (7 percent per decade), while the poorer laminates follow a fatigue trend of 0.11 (11 percent per decade) [35]. Reversing load (R = -1) fatigue response ranges from 0.12 to 0.18 (12 to 18 percent per decade). These fatigue trends are summarized in Figure 11.

Sutherland and Mandell [10] compiled a Goodman diagram, Figure 12, based upon the data of Reference 14. Note the asymmetry, relating to the differences in the tensile and compressive fatigue properties.

18
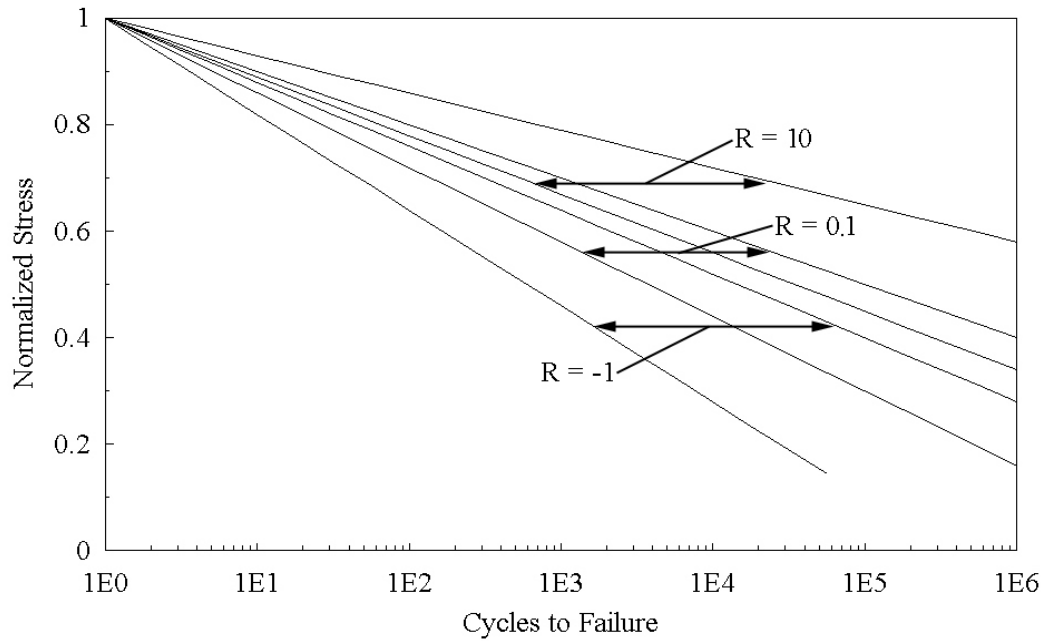
Figure 11. Laminate Fatigue Trends for Tensile, Compressive and Reversing Constant Amplitude Loads.
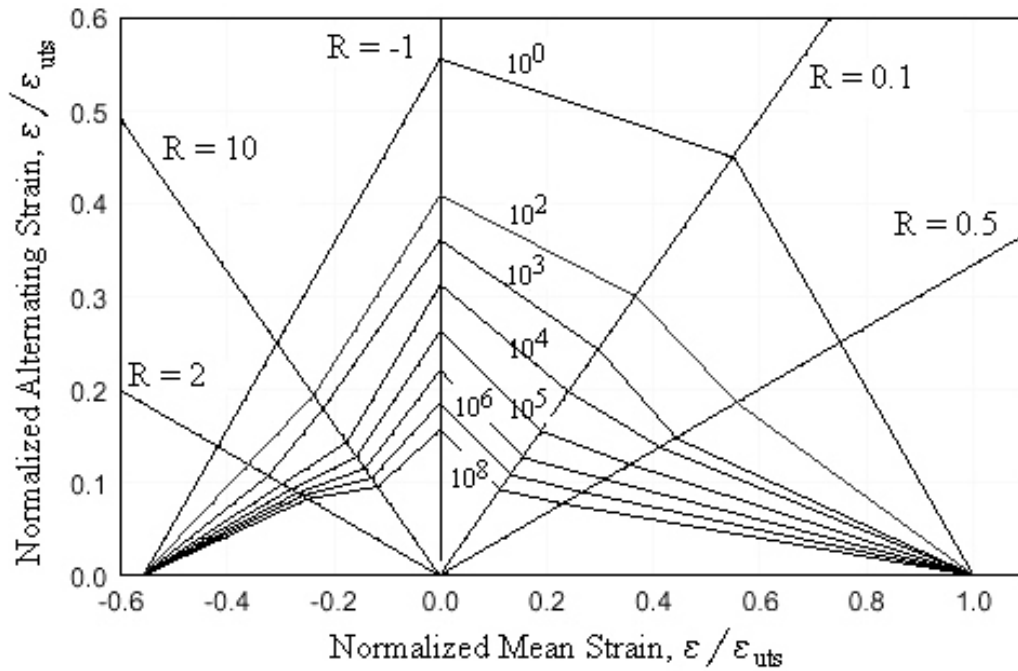
Figure 12. Normalized Goodman Diagram for Fiberglass Laminates Based on the MSU/DOE Data Base [10].

The fatigue sensitivity of unidirectional laminates does vary with fiber volume fraction, with the increase in fiber volume fraction resulting in increased magnitudes for the exponential regression parameter b. This is ostensibly due to the increased likelihood of fiber-to-fiber contact damage with the increased fiber volume. The fiber volume range summarized in Reference 35 was from 0.3 to approximately 0.6.

The effect of the content of 0° plies of the laminate is summarized in Table 1 [14]. The tensile fatigue trend is poorer in the laminates containing combinations of 0° and ±45° plies and improves at the extremes of contents of these orientations. The compressive fatigue trend improves with greater 0° ply content.

Table 1. Summary of Ply Orientation Effect on Fatigue Trends

Percent 0° Plies	b, R = 10	b, R = 0.1
0, (±45° only)	0.106	0.113
16	0.114	0.116
24	0.115	0.128
28	0.088	0.124
39	0.095	0.128
50	0.089	0.128
55-63	-	0.121
69-85	0.072	0.118
100 (0° only)	0.073	0.111

The laminate studied in this research will be compared to the above laminate fatigue trends in constant amplitude fatigue testing and results section.

LIFETIME PREDICTION MODELS FOR COMPOSITE MATERIALS

Lifetime prediction models for laminates have been developed from the basis of nearly every conceivable property of the materials. Engineering mechanical properties such as stiffness and/or compliance [36-38], natural frequency [39], damping [39, 40], and residual strength [41-47] as well as micromechanical properties such as crack density [25], fiber-matrix debonding and pullout, and delamination [48] have been applied towards development of lifetime prediction models. Other models are based upon properties determined by simple fatigue tests of laminates and more evolved statistical analyses [41] of the material. Some researchers have applied linear elastic fracture mechanics, a method considered appropriate for isotropic materials such as metals, to the analysis of fatigue in composites. Regardless of the efforts expended upon the development of reliable models, and of the model's complexity, most researchers still compare the results of their work to the simple, linear model proposed by Miner [6]. The leap from the theoretical, advanced models to their practical use seems to be daunting. Computer codes that have been developed for the fatigue lifetime analysis for wind turbine blade design still use the first model, Miner's linear damage rule [8, 9, 41, 49], and have not applied the newer, and reportedly more reliable models. Practicing engineers prefer simple, easy to apply models, for their use in the design of components.

Miner's Linear Damage Rule

The early work on aluminum by Miner [6] resulted in a simple linear damage accumulation rule that was based upon constant amplitude fatigue test results. The basis of this rule is that the damage contribution of each load level is equal to its cycle ratio, which is the number of cycles experienced at that load level divided by the number of constant amplitude cycles to failure at that same load level. The damage contributions of each load level are algebraically added to allow determining an overall damage level. Symbolically this can be represented as

$$D = \sum Cycle\ Ratios = \sum_i \frac{n_i}{N_i} \qquad (11)$$

where   D is a quantified damage accumulation parameter previously termed Miner's sum in
   equation 3
   i is the indexing parameter related to the number of different load levels
   n_i is the number of cycles experienced at a σ_i maximum stress level
   N_i is the number of constant amplitude cycles to failure at the stress level σ_i.

Typically, failure is taken to occur when D reaches unity, as originally proposed by Miner. The crack growth model discussed earlier for metals used Miner's rule to accumulate crack extension, but failure was considered from the point of view of reaching a critical stress intensity factor. For future reference and comparison to other lifetime prediction models, D_R is defined as the residual Miner's sum.

$$D_R = 1 - D \qquad (12)$$

Miner's original work with aluminum exhibited a range of values for D from 0.61 to 1.49, but with an average of 1.0 and a standard deviation of 0.25. Miner reported that his model did not include any provisions to account for the possibility of load interactions such as related to work hardening. The Miner's rule has limitations in that it does not account for any possible sequencing effects or the fact that the component may fail upon a significant large event that does not numerically contribute greatly to D. The latter is sometimes referred to as a "sudden death behavior," such as reaching K_c in the metals crack growth example.

Several researchers have proposed modifications to Miner's rule to coax the damage parameter, D, closer to unity. Performing a square root, or for that matter any other root, forces the damage parameter closer to unity [13, 21, 41, 50]. Others merely acknowledge that the damage parameter may not be unity, and propose values other than one, such as 0.1 [49]. Any superiority of these modifications is often due to fitting of model constants to particular experimental data [4].

Graphically, Miner's rule can be viewed as shown in Figure 13. The straight line relationship represents the Miner's original linear rule, whereas the line lying below represents a prediction based upon applying a square root to the linear rule. The upper line represents the prediction should an exponent greater than one be applied.

This model has been tested by application of a two stress level spectrum of loads [11, 42]. The first set of cycles at a constant stress level constitutes a loading block. The second block of cycles at a second stress level was run to specimen failure. Empirical results for testing of fiberglass laminate (13 plies of 0° and 90° oriented E-glass fibers in an epoxy matrix) indicated a range of 0.29 to 1.62 for Miner's sum [42]. The general observation was that for a block of high amplitude cycles followed by a block of low amplitude cycles would result in Miner's sums greater than one. The opposite sequencing of a low amplitude block followed by a high amplitude block resulted in Miner's sum less than one.
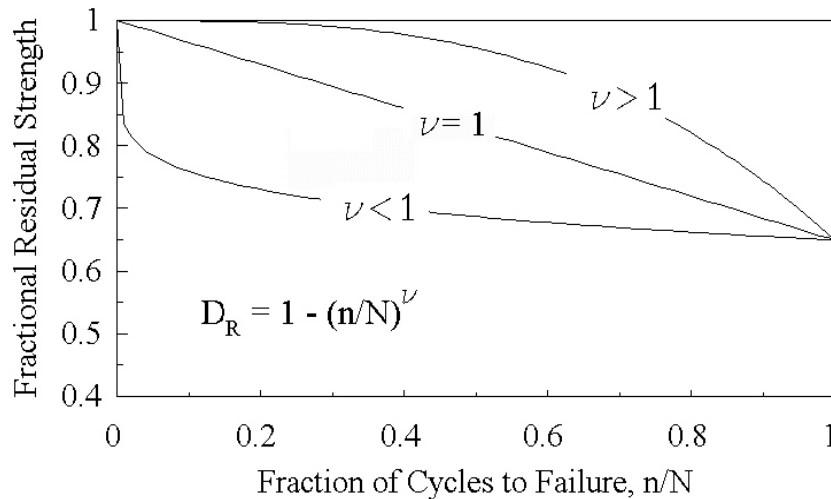
Figure 13. Effect of Exponent on Residual Miner's Sum Model (Constant Amplitude Fatigue).

Residual Strength Based Models

A concept of a material's progressive loss of strength during fatigue has led several researchers to investigate models with this basis [11, 20, 39, 42-47]. In a sense, this parallels the crack growth model for metals with failure when K reaches K_c. Broutman and Sahu [41] were one of the earliest to develop a model founded upon residual strength changes during fatigue. Their model was based upon a linear loss of strength with cycles of fatigue, as represented by:

$$\sigma_R = \sigma_0 + \frac{\sigma_i - \sigma_0}{N} n \qquad (13)$$

where σ_R is the residual strength
σ_i is the maximum applied stress level
σ_0 is the static strength of the specimen
N is the number of constant amplitude cycles to failure at the stress level of σ_i
n is the number of cycles experienced at stress level σ_i

Broutman and Sahu [42] reported the residual strength lifetime prediction rule also satisfies the sequencing effects of high/low and low/high blocks of constant amplitude cycles. Spectra of a high amplitude block followed by a low amplitude block exhibited Miner's sums greater than one if the second block is run to failure. The opposite spectrum of a low followed by a high amplitude block yielded Miner's sums less than one.

Many investigators of residual strength and/or residual stiffness have argued that the residual strength is not a linear function of the number of cycles, but rather non-linear [11, 20, 43-45, 47]. This prompted a modification of the residual strength model to include non-linear possibilities:

$$\sigma_R = \sigma_0 + \left[\sigma_i - \sigma_0\right] \left[\frac{n}{N}\right]^\nu \qquad (14)$$

where the parameter, ν, is termed the strength degradation parameter [43-45]. Strength degradation parameters greater than one define laminates that exhibit little loss of strength throughout most of their life and suffer a sudden failure at the end of life. Parameters less than one represent laminates that suffer the greater damage in their early life. A value of unity for ν reduces equation 14 to the linear model of equation 13.

The general shape of the residual strength curve, Figure 14, is uncertain. Upon considering a simple link between residual stiffness and residual strength, researchers have shown all possible ranges of the strength degradation parameter. This variation leads one to consider that the strength degradation parameter is a material property and hence variable from laminate to laminate.
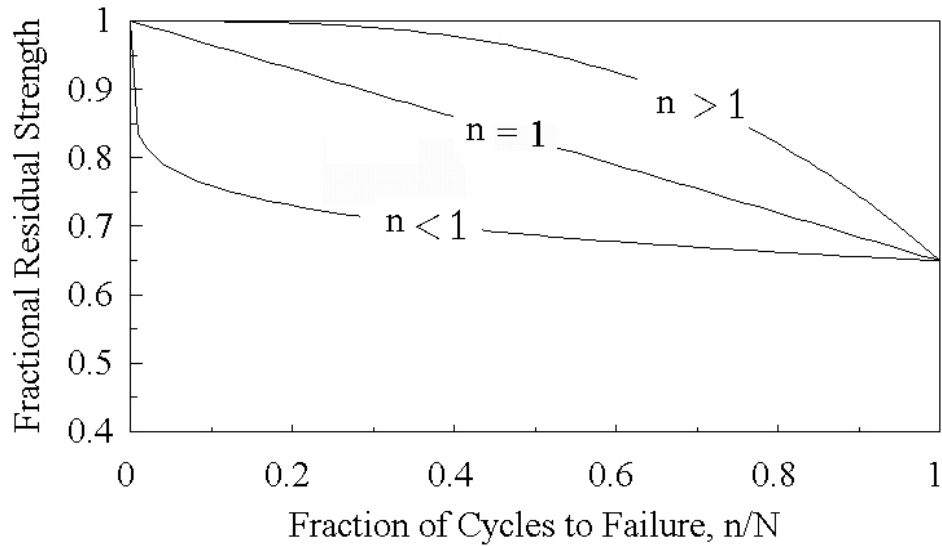
Figure 14. Effect of Exponent on Residual Strength Model (Constant Amplitude Fatigue).

<u>Residual Stiffness Based Models</u>

Another proposed model, similar to the residual strength model, is one based upon the change in stiffness, E, of a material undergoing fatigue [20, 36-38, 46, 51]. The residual stiffness prediction model represented by Equation 15 was proposed by Yang, et. al. [36] and is similar to the nonlinear residual strength model proposed by Schaff and Davidson [43-45]

$$E(n) = E(0) - \left[E(0) - E(n_k)\right]\left[\frac{n}{n_k}\right]^{v(k)} \tag{15}$$

where $E(n)$ and $E(n_k)$ are the stiffnesses at cycles n and n_k respectively
$E(0)$ is the initial stiffness
$v(k)$ is the fitting parameter.

The fitting parameter is considered to be a function of the applied stress level and perhaps even the number of cycles experienced. Experimental results for a graphite laminate of $[90/\pm45/0]_s$ layup were $E(0) = 53.8$ GPa, $E(10,000) = 42$ GPa, and $v(10,000) = 0.162$ (dimensionless). These data were used to generate a graphical representation, Figure 15, of the change in the normalized stiffness over a normalized life.

Note the similarities of the graphs, Figures 14 and 15. The nonlinear residual strength model based upon a strength degradation parameter less than one presents a similar trend as the results of residual stiffness testing by Yang, et. al. [36] and Bach [37].

24
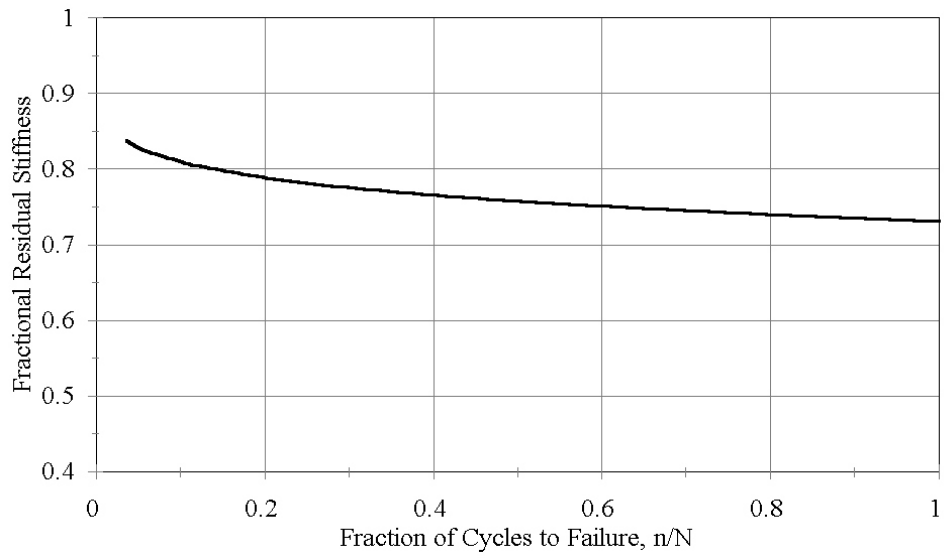
Figure 15. Laminate Residual Stiffness Experimental Trend (Constant Amplitude Fatigue, Carbon/Epoxy).

EXPERIMENTAL PROGRAM

A laboratory test program was developed in attempts to ensure the performance of meaningful fatigue tests. This program included the selection of a typical wind turbine blade fiberglass laminate, design of test specimens, test of laboratory equipment capability, and the execution of planned fatigue tests. The underlying goal was to first perform constant amplitude tests that could be compared with the results of other investigators and then methodically increase the complexity of the loading spectrum.

Investigation of variable amplitude fatigue, including that of two-block load levels can be hampered by the scatter of the testing results. The scatter in constant amplitude fatigue data can be due to testing techniques, specimen preparation, variation in the material itself and the variability of fatigue mechanisms. For data presented in References 1 and 3 there appears to be less scatter at the higher stress tests than at the lower stress tests; this may be due to a "flattening" of the S-N trend. With large scatter of data, the fatigue contribution of each load level in multi-load level testing becomes indistinguishable. Effects of several of these contributing factors can be minimized with proper design of test procedures and fabrication techniques.

Laminate Selection

The choice of the fiberglass laminate was to be one that would be typical of those used in wind turbine blade construction and one that would yield meaningful fatigue test results. The laminate materials and configuration or lay-up can have an effect on the statistical results of fatigue testing. Three different laminates were considered for testing; DD5, DD11 and DD16. The laminate designations are described in References 14 and 35 and in Table 2.

Table 2. Fiberglass Laminates

Material	Percent Fiber Volume	Ply Configuration	Matrix	Fabric Description
DD5	38	$[0/\pm45/0]_s$	P	0's - D155 45's - DB120
DD11	31	$[0/\pm45/0]_s$	P	0's - A130 45's - DB120
DD16	36	$[90/0/\pm45/0]_s$	P	0's & 90's - D155 45's - DB120
P - orthopolyester matrix, CoRezyn 63-AX-051 by Interplastics Corp. A130, D155 & DB120 - Owens Corning Fabrics				

Since this research was to consider spectrum loading effects on the fatigue life of fiberglass laminates, the statistical scatter of constant amplitude load testing was to be minimized. A related factor, the tendency of some coupons to fail near the grip, was also to be minimized under various loading conditions; the addition of 90º outside plies helped in this respect. Of the three laminates listed in Table 2, upon testing, the DD16 was chosen to be best suited for variable amplitude testing. Summarized in Figure 16 are preliminary constant amplitude fatigue test results for the material DD11. Note the unacceptable scatter in the life for the material when loaded to a maximum stress level of slightly greater than 400 MPa. The life for the material when subjected to fatigue at a stress level of 414 MPa was indistinguishable from that at the higher stress level of 475 MPa. The nearly two decades of scatter in the cycles to failure at the 414 MPa load level were deemed unacceptable, and would have been undoubtedly even greater for lower stress tests. Similar, but not as pronounced results were also observed for test results of the DD5 material fatigue. In retrospect, the scatter has since been found to also depend on the variations in the particular reinforcing fabric [35].
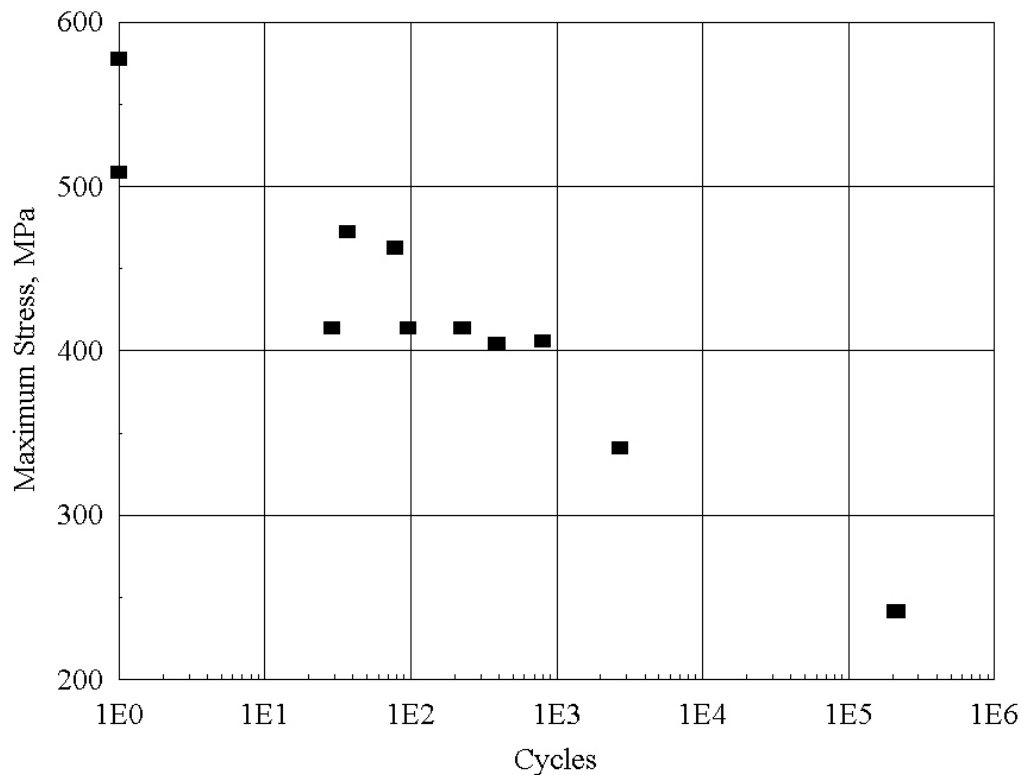
Figure 16. DD11 Constant Amplitude Fatigue, Preliminary Tests for Scatter, R = 0.1.

The material that produced acceptable scatter results was termed DD16 in the database of Reference 14. DD16 was comprised of Owens Corning D155 (stitched unidirectional) and DB120 (stitched ± 45º) fabrics in a $[90/0/\pm45/0]_S$ lay-up for a total of ten plies and eight layers of fabric. The 90º plies on the outside were thought to produce more reliable gage-section failures, as noted earlier.

27

Photographs of the fabrics are shown in Figure 17. Plates of this material were fabricated by a resin transfer molding (RTM) process with Interplastics Corporation CoRezyn 63-AX-051 orthopolyester matrix to an average fiber volume of 0.36. Details can be found in References 14 and 35.
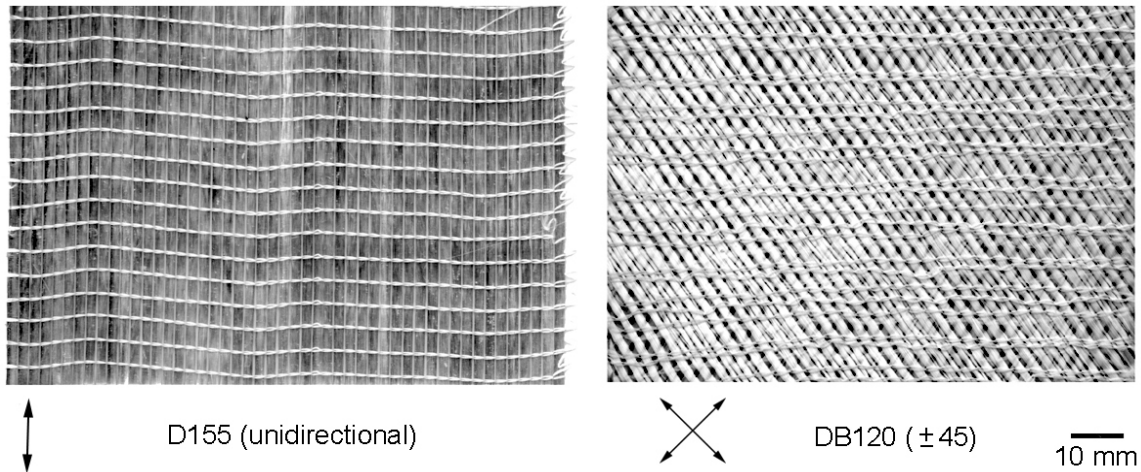
Figure 17. DD16 Laminate Dry Fabrics.

Coupon Design

Coupons were designed for the type of load testing to be fulfilled, whether for tensile-tensile (T-T), compressive-compressive (C-C), or reverse loading. These regimes of loading and their respective R-values are detailed in Figure 5. The location and mode of failure was the factor used to determine the acceptability of the specimen design. The failure mode was to be attributed to the fatigue loading, and not to other factors such as thermal degradation, elastic buckling or gripping effects. Similarly, the location of the failure should be in the gage section as opposed to in or adjacent to the grips. The long history of test coupon geometry development for various fiberglass materials can be found in References 14 and 35.

Tension-Tension Coupons

Tensile-tensile specimen blanks were rectangular in shape, typically 12.7 mm wide by 4 mm thick and 64 to 75 mm long. These blanks were then individually machined to a dog-bone style with a pin router, clamping jig, and master pattern as shown in Figure 18. The profile of each edge was machined sequentially. Machined surfaces were then cleaned with sanding screen to remove any fiber "burrs". Sanding screen was also used to roughen the grip areas in preparation for the addition of tab material. G10 fiberglass tab material, manufactured by International Paper, Inc., was attached to facilitate distribution of testing machine gripping forces. The tabs were 1.6 mm thick with length and width varying dependent upon the test type, as shown in Figure 19. Attempts to perform tensile tests without tabs were not successful, due to laminate failure in the grips of the testing machine. Specimens with straight sides, with or without tabs, were also deemed not acceptable; failures occurred in the grips.
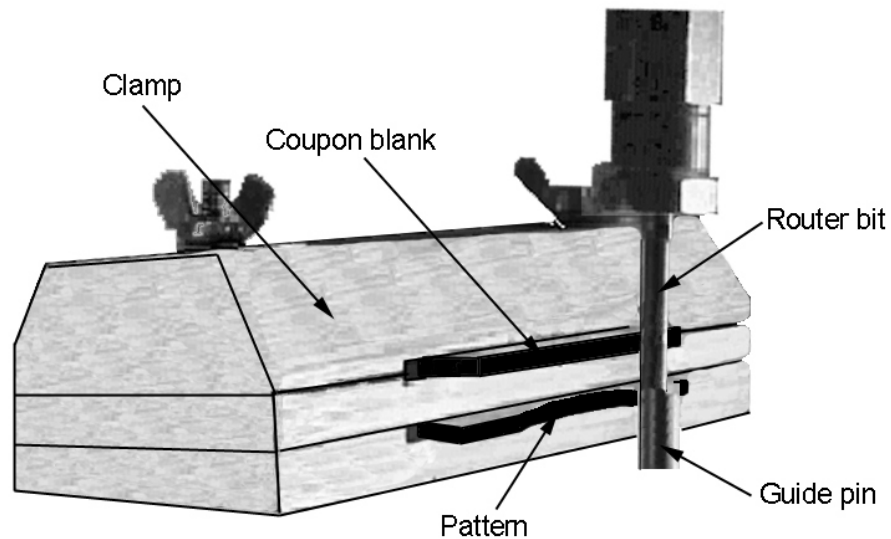
Figure 18. Pin Router.

Specimens with a gage section and tabs, Figure 19, were tested and found to be a successful coupon design. Typical examples of fatigue failures of these tensile specimen are shown in Figure 20. Failures occurred in the gage section and were typical of laminate tensile fatigue failures; the matrix material was severely fractured, fibers were pulled out, broken and "brooming" at the failure. This final design for a tensile test specimen is similar to that for metal-matrix specimen as per ASTM Standard D 3552, rather than the ASTM Standard D 3039 for polymeric-matrix specimens [52].

Coupon number 555 in Figure 20 was a tensile fatigue test performed at an R-value of 0.1 and a constant amplitude maximum stress level of 207 MPa. Coupon 716 was tested with an R-value of 0.1, but under a variable amplitude loading spectrum and with a maximum stress of 245 MPa. Coupon 773 was subjected to a variable amplitude loading spectrum, but with R-values of both 0.1 and 0.5 and a maximum stress of 245 MPa. The bottom coupon, number 774, was subjected to an ultimate tensile test. All coupons displayed the severe fracturing of the matrix, some even to the point of total wasting of the matrix around the 45 degree plies. All examples also exhibit the "brooming" of the fibers that occurred with this explosive type of failure.
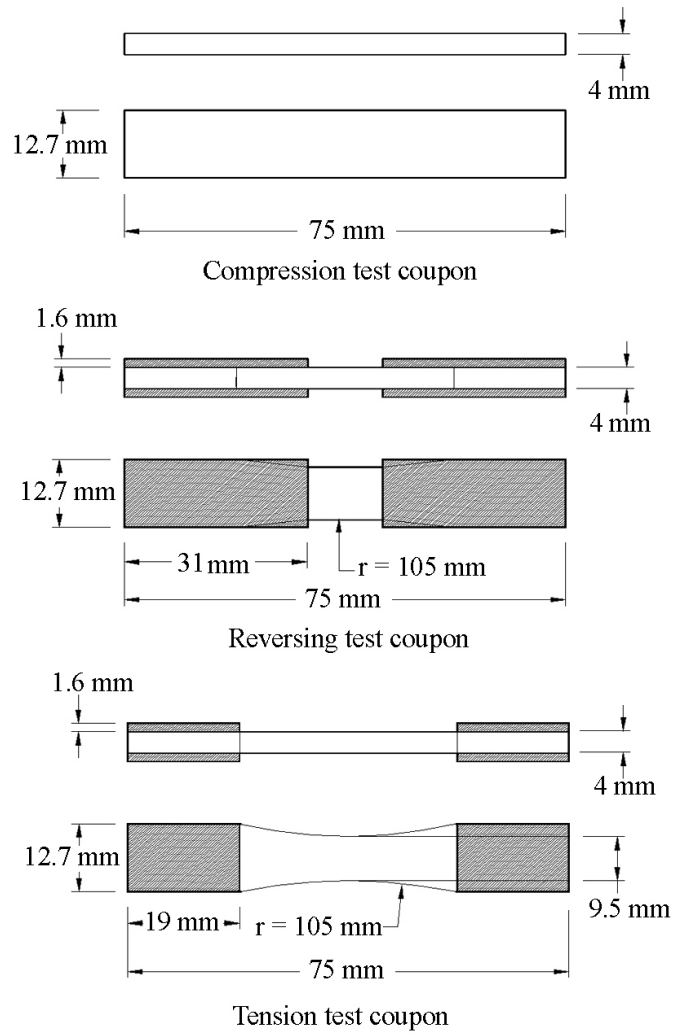
Figure 19. Test Coupon Configurations.
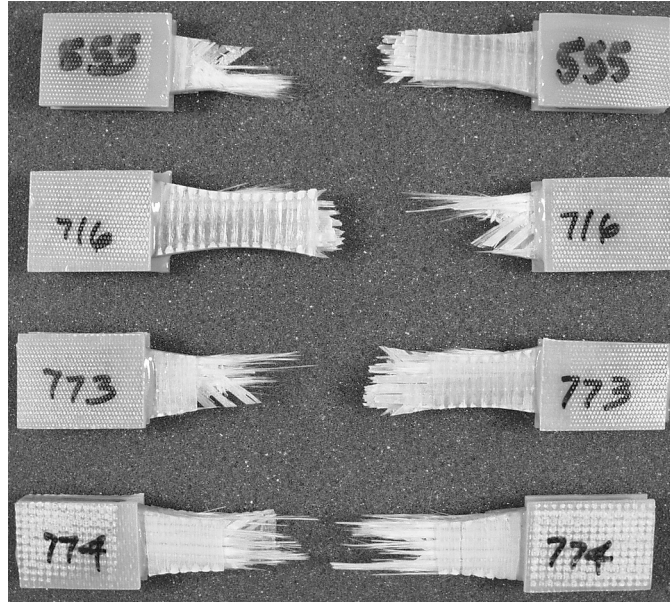
Figure 20. Tensile Coupon Failure Examples.

Compression-Compression Coupons

The specimens designed for the tensile fatigue testing were first considered for compression testing. Unfortunately, buckling was evident due to slight misalignment caused by the variation in tab material thicknesses and also due to the length of the gage section. A workable compression specimen was a simple rectangularly shaped laminate without any tab material. The gage section was held to 12.7 mm by the grips, to preclude buckling. The overall dimensions were the same as those of the tensile specimen blanks. The failure mode of the compression specimen tests was matrix fracture and destruction, resultant fiber debonding, delamination and crushing or buckling of the fibers, Figure 21. Final crushing was relatively symmetrical on each face in the thickness direction, indicating an absence of elastic buckling or misalignment [14, 35].

Coupon number 860 in Figure 21 was subjected to constant amplitude loading spectrum at an R-value of 10 and with a minimum (maximum negative) stress of -207 MPa. Number 915 was subjected to a constant amplitude loading spectrum at an R-value of 2 and a minimum stress of -325 MPa. The bottom example in Figure 21 was subjected to a two-block spectrum with minimum stress levels of -325 and -207 MPa and at an R-value of 10. Each of these examples exhibited the failure mode of matrix cracking, delamination, and final buckling of the fibers due to loss of lateral support with the disintegration of the matrix material.

Figure 22 depicts the delamination that occurred during the compressive cyclic loading of coupons 906, 908 and 893 top to bottom respectively. All three tests were performed at an R-value of 10, with tests 906 and 908 at a maximum compressive stress of 245 MPa and test 898 at 275 MPa. The lower stress tests were terminated at approximately ten million cycles and were considered run-out, or cases that could run for a longer period of time. Coupon 893 was terminated at roughly 60,000 cycles as

an example of delamination response. All three coupons display signs of delamination growth from the edges. Had the cycling continued until failure, undoubtedly, the delamination would have progressed from each side, eventually joining. The weakened laminate would have had reduced buckling resistance and failed similarly to the examples shown in Figure 21.
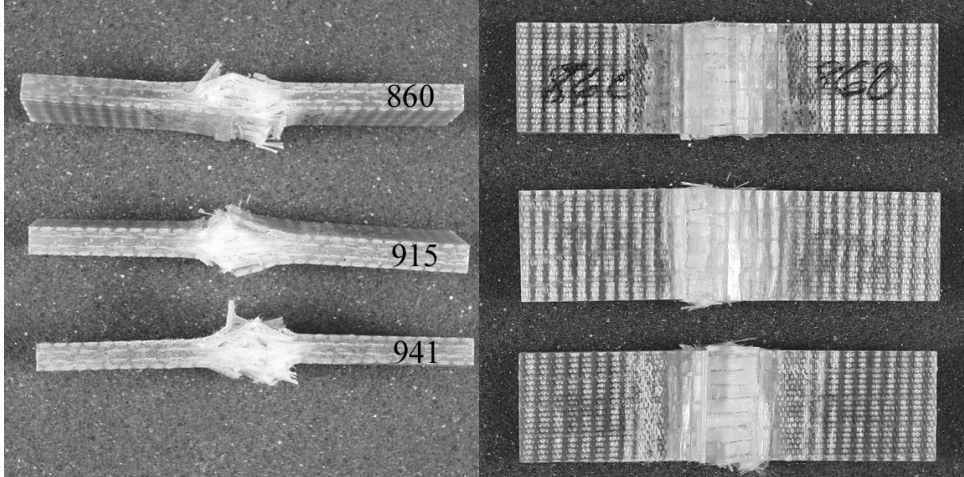
Figure 21. Compressive Coupon Failure Examples.
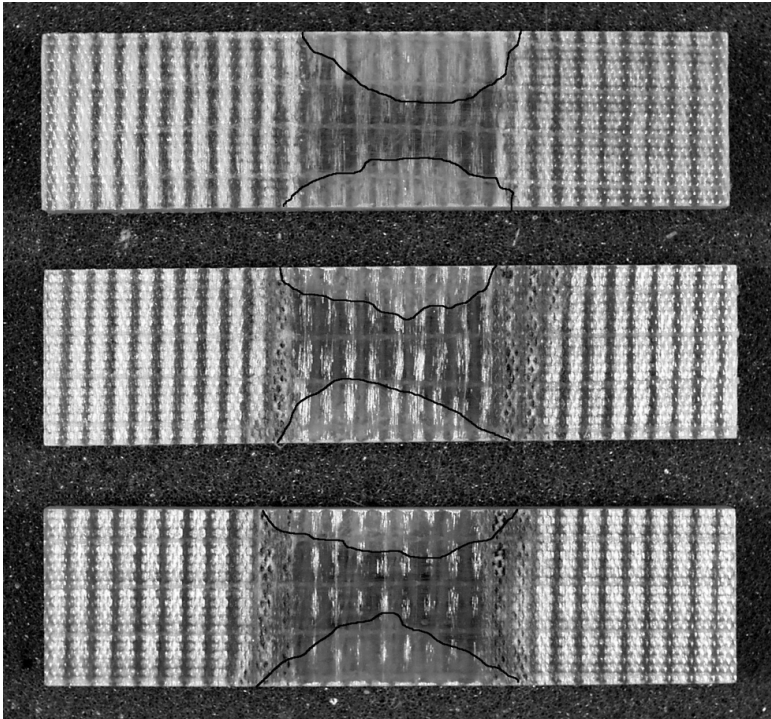
Figure 22. Compressive Coupons at Runout.

Reverse Loading Coupons

Specimens for reverse loading, R-value of -1, are subjected to both tensile and compressive loads and consequently show diverse and complex failure modes. Static tensile and compressive ultimate strengths are considerably different due to the different failure modes and mechanisms. Also, for a given maximum stress level, the reversing load case may be more detrimental to a laminate than either the tensile-tensile or compressive-compressive cases [14]. As a result, both the tensile-tensile and compressive-compressive coupon designs were considered for the reversing coupon design. A slightly modified tensile-tensile specimen proved successful in use for reverse loading fatigue tests. The elongated tabs aided in buckling resistance while providing a 12.7 mm gage section. The compressive-compressive design could not withstand the tensile loading portion of the reversing cycle due to grip failures.

Failure of these specimens were similar to that observed for the tensile only case. Figure 23 is a representation of failures of coupons subjected to reversing load spectra. Coupon number 1041 in Figure 23 was subjected to a constant amplitude reversing spectrum with a maximum and minimum stresses of ±103 MPa. The remaining three examples were specimens subjected to two-block reversing spectra; with the two maximum stress levels of 172 and 103 MPa for the two blocks. The top specimen could have possibly been a compressive failure, yet was separated upon failure reaction of the testing machine. The bottom three examples exhibit similar failure characteristics of the tensile examples of Figure 20. None of the reversing failures were similar in appearance to the compressive failures of Figure 21.
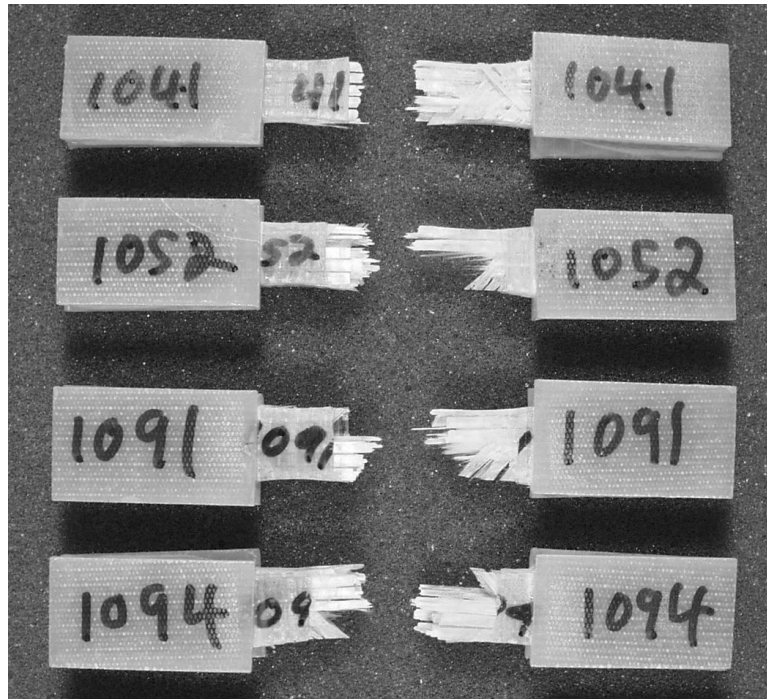
Figure 23. Reversing Coupon Failure Examples.

Testing Equipment

An Instron 8872 hydraulic testing machine with an Instron800 controller was used to subject the specimen to the spectrum loads. This testing machine, shown in Figure 24, was capable of producing ±20 kN of force over a displacement of ± 51 mm, with a 0.64 L/s servo-valve operating at 21 MPa. Specimens were affixed vertically between a stationary grip at the bottom and a moveable one at the top. These hydraulically actuated grips retain the specimen by wedging paired knurled grip faces towards each other, trapping the specimen. The upper set of grips could be moved vertically by means of varying hydraulic pressures within a cylinder. Pressure, in turn, was varied by regulating the flow of hydraulic fluid into and out of the cylinder by means of a servo valve. The servo valve received control signals from a microprocessor based controller of typical linear proportional, integral, and derivative design. Either position or load can be controlled. A variable differential transformer, LVDT, was used to measure position and a load cell to measure the force. Tuning or selection of the proportional, integral and derivative controller gains, was performed manually for different testing campaigns. A tuning method developed by Ziegler and Nichols [53] was used and resulted in the values shown in Table 3.
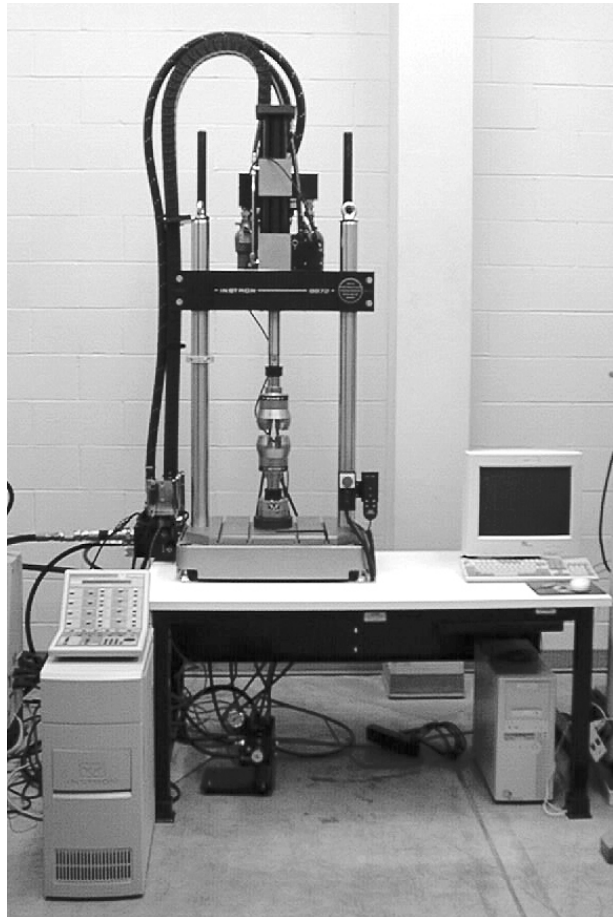
Figure 24. Instron 8872.

Table 3. Instron 8800 Controller Tuning Parameters

Testing Regime	Proportional Gain, dB	Integral Gain, s^{-1}	Derivative Gain, s	Lag, s
Tensile-tensile	-0.25	1.0	0.0	0.8
Compressive-compressive	+2.5	30.0	0.0	0.8
Reversing	+2.5	30.0	0.0	0.8
Amplitude control was not used.				

Performance of the hydraulic machine was dependent upon the frequency of cyclic motion or loading, as well as to the tuning of the controller, the material being tested, and the type of test. As with most systems, the greater the frequency of operation, the lower the amplitude capability.

Frequency response capability of the machine, along with concern for thermal degradation of the laminate under fatigue, led to performing tests at ten Hertz and less. Secondary measurement and recording of the actual loading waveforms, as shown in Figure 25, were favorably compared to that available from the Instron testing equipment.
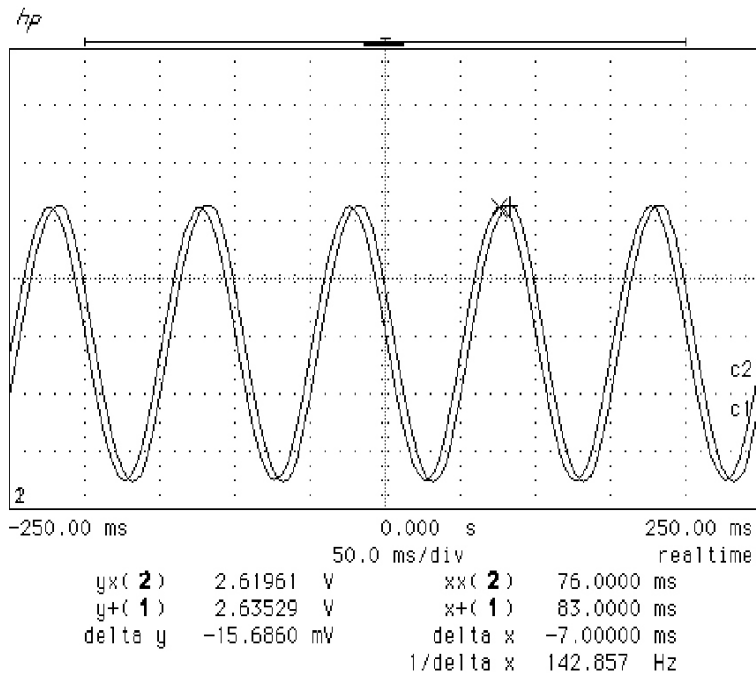
Figure 25. Load Demand and Feedback Signals.

35

The maximum variation of the constant amplitude peak stress for R-values of 0.5, was within 1.5 percent of the mean, whereas the maximum variation of the constant amplitude valley stress was within 0.2 percent. Typical maximum stress and standard deviation for a 241 MPa constant amplitude fatigue test was 239.4 MPa and 0.338 MPa respectively. The maximum stress level generally decreased with time, due to the increased compliance of the specimen; consequently, greater motion was required to attain the loads.

The two-block tests performed with the block loading software exhibited a low error in the maximum stress upon a change from a low amplitude cycle to a high amplitude cycle. Upon a change from a low stress level block to a high stress level block, the typical maximum variation of the peak value of stress was 0.2 percent. This relatively low error was probably achieved by the fact a ramp from one cycle mean to the next cycle mean was used to progress from one block to the next. Two-block testing performed with the random loading software exhibited a higher error upon a change from a low amplitude stress cycle to a high amplitude stress level. The maximum error was 4 percent and occurred at the initiation of the test with the first cycle. Following errors were typically on the order of 2 percent.

Analysis of random spectrum loading revealed the greatest error (difference between demand and feedback) was upon start-up of the test; well removed from the maximum applied stress. The maximum error was less than 4 percent. The difference between the demand and feedback at the maximum stress cycle was less than 2 percent. Based upon the machine performance analysis, the Instron hydraulic testing apparatus was deemed acceptable for spectrum fatigue testing.

Control Software

Instron WaveEditor[©] (Version 6.2.00) and WaveRunner[©] (Version 6.4.0) software packages were primarily developed for block loading type of fatigue testing. The WaveEditor program was used to create the loading files that were subsequently used by the WaveRunner program for control of the hydraulic test machine.

Blocks of loading profiles could be defined as either ramps or sinusoids via WaveEditor. A ramp block was one in which a change in load from one level to another was specified to occur in a user entered amount of time. A sinusoidal block was one that was sinusoidal in shape, where the frequency, number of cycles, load mean and load amplitude were defined. Blocks could be specified to control either position or load. A constant amplitude test was prepared by the use of only one sinusoidal block, that was repeated until specimen failure. A spectrum of more than one sinusoidal loading block was prepared by a sequence of blocks, typically:

a) block one was a ramp from zero load to the mean of the first sinusoidal
   loading block; this was taken as a starter block
b) block two was a sinusoidal block
c) block three was a ramp from the mean load level of the block two to a
   mean load of the upcoming block four

d) block four was a second sinusoidal block
e) block five was a ramp from the mean of the fourth block to the mean
of the second block.

Blocks two through five were then repeated until specimen failure. Additional blocks could be added when more than two load levels were desired. Once loading files were specified by the use of WaveEditor, actual control was accomplished by the use of WaveRunner.

The Instron software package, RANDOM$^{©}$, was used to subject specimens to, as the name implies, random loading spectra. The function of the software was to sinusoidally load a specimen to a random spectrum when given a succession of peak and valley reversal points. A file containing the succession of peaks and valleys was created by use of a BASIC language program. Each line of the file contained a single reversal point. The contents of the file were scaled to a maximum (or minimum) value of one and signed for tension or compression. The entries format was "+#.####", signed and four significant digits. Block loading could therefore easily be accomplished by the use of the RANDOM software package.

Early in fatigue testing, use of the WaveEditor and WaveRunner was discontinued since the RANDOM package would be required for the random spectrum fatigue testing and could also accomplish block fatigue testing. This was done to help preclude any anomalies that might be introduced by differences in software execution.

CONSTANT AMPLITUDE FATIGUE TESTING AND RESULTS

The fatigue testing in this research program, outlined previously, began with constant amplitude testing and progressed towards the implementation of more complex spectra. This first round of testing provided a set of baseline data that was compared to the results of other researchers and was used in the implementation of various life prediction models. Constant amplitude testing was performed at R-values of 0.1, 0.5, -1, 1, 2 and 10 to reasonably cover the significant regions of a Goodman diagram (Figure 7). The results of the constant amplitude fatigue tests were reduced to stress-cycle (S-N) diagrams. Regression analysis was performed for each data set assuming either an exponential (equation 7) or power law (equation 8) trend. The regression equations are hereafter referred to as the fatigue models.

Constant Amplitude Test Results

The results of constant amplitude testing are recorded in raw and reduced form in Appendix B. Results at each R-value are summarized in a graphical form of stress-cycle (S-N) diagrams; Figures 26 through 30 are representations (on semi-log plots) of the constant amplitude fatigue of the laminate coupons for R-values of 0.1, 0.5, -1, 10 and 2.

Each S-N diagram was reduced to two fatigue models by performing both an exponential and power law regression of the respective data sets. The fatigue models were used in subsequent lifetime prediction rules or laws. These fatigue models take on the generic forms of equations 7 and 8, which are repeated here for convenience, for the exponential and power law models, respectively

$$\frac{\sigma}{\sigma_0} = C_1 - b \log (N) \tag{7}$$

where σ = maximum applied stress, MPa
σ_0 = static strength, MPa
C_1 = regression parameter, typically forced through unity
N = number of cycles to failure
b = regression parameter related to th reduction in maximum applied stress for each decade increase in cycles

$$\frac{\sigma}{\sigma_0} = C_2 \, N^{-\frac{1}{m}} \tag{8}$$

Where C_2 = regression parameter

      m = regression parameter, similar [30, 33] to the exponent in equation 4

    Table 4 contains the exponential regression parameters for each R-value as well as a comparison to the work of Samborsky [35] with the same laminate construction, yet from a different batch and specimen geometry.

Table 4. Exponential Regression Analysis Parameters for Constant Amplitude Fatigue

MPa	Range of Applicability	Regression Coefficients	R-Value, Equation 1				
			0.1	0.5	-1	10	2
Present Work UTS=632 UCS=400	1 to 10^7 Cycles	C_1	0.955	0.990	0.994	0.994	1.000
		b	0.120	0.107	0.125	0.081	0.062
		Correlation	0.938	0.942	0.975	0.955	0.927
	10 to 10^7 Cycles	C_1	0.849	0.920	0.722	0.963	1.006
		b	0.096	0.092	0.072	0.074	0.063
		Correlation	0.921	0.860	0.959	0.889	0.624
Reference [34] UTS=672 UCS=418	1 to 10^6 Cycles	C_1	1	-	-	-	-
		b	0.12	-	-	-	-
	-	-	-	-	-	-	-
	-	-	-	-	-	-	-

    Comparison of the work reported in Reference [35] and this present work revealed no significant difference for the fatigue trend, b, for tests at R-values of 0.1. The ultimate tensile strengths were within 5.5 percent and the ultimate compressive strengths were within 4 percent.

    The DD16 laminate used in this research may be considered to have an average fatigue sensitivity when compared to a family of similar laminates [14] comprised of E-glass and a polyester matrix and with a lay-up of zero and off-axis plies, reference Table 1, Chapter 2. The fatigue sensitivity (regression parameter b of equation 9) in tension was reported in Chapter 2, to range from 0.1 to 0.14. The tension fatigue sensitivity of the DD16 material was 0.12 as shown in Table 4. The compression fatigue sensitivity of 0.08 falls in the range of 0.07 to 0.11 for the family of similar laminates. The DD16 reversing load fatigue sensitivity of 0.125 again falls in the range of 0.12 to 0.18 for similar cross-ply laminates.
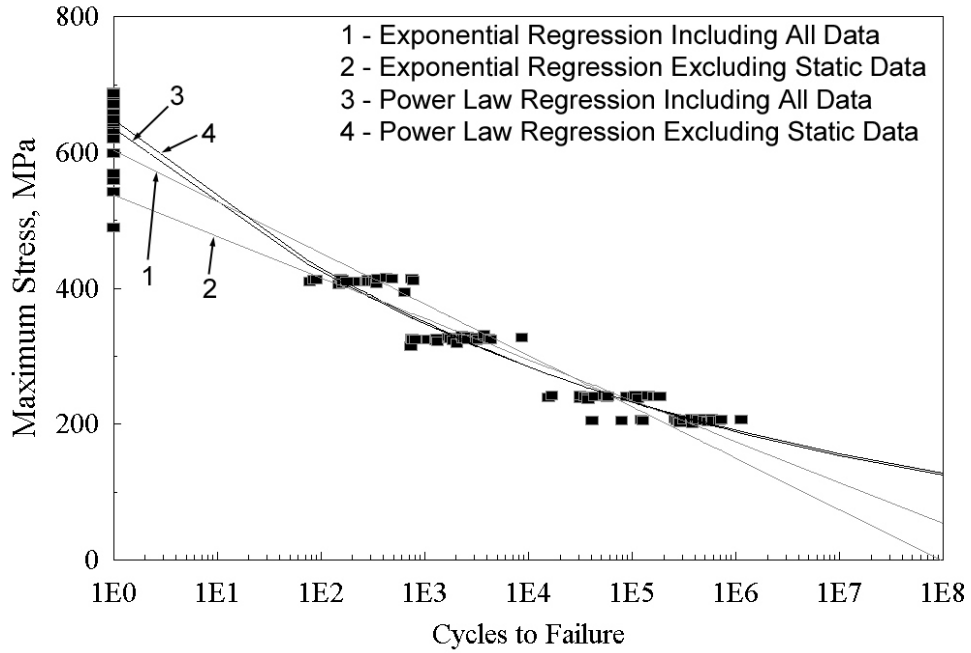
Figure 26. Constant Amplitude Fatigue for R = 0.1.
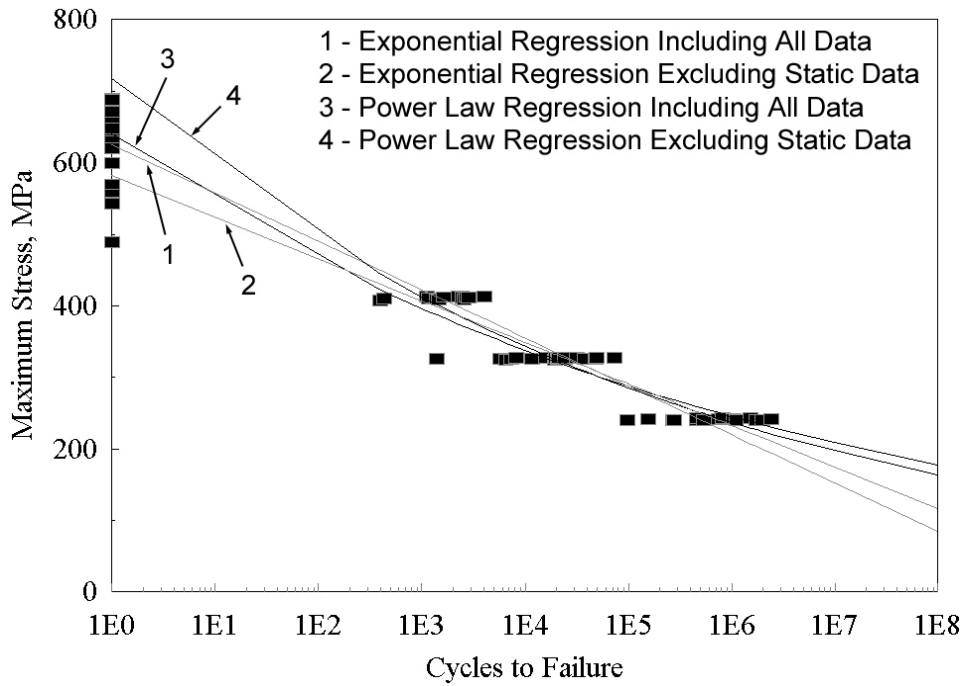
Figure 27. Constant Amplitude Fatigue for R = 0.5.

40
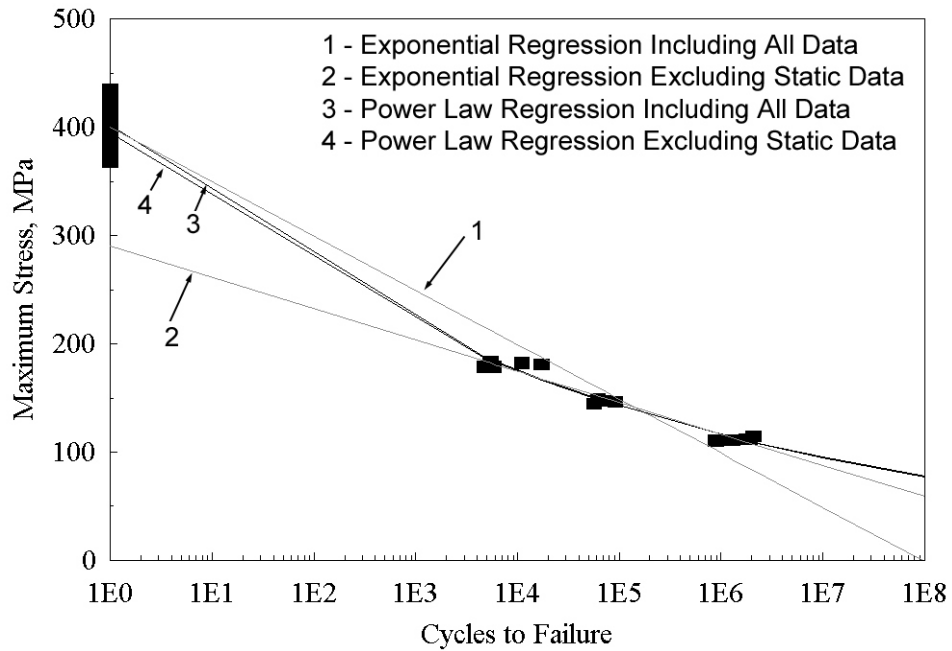
Figure 28. Constant Amplitude Fatigue for R = -1.
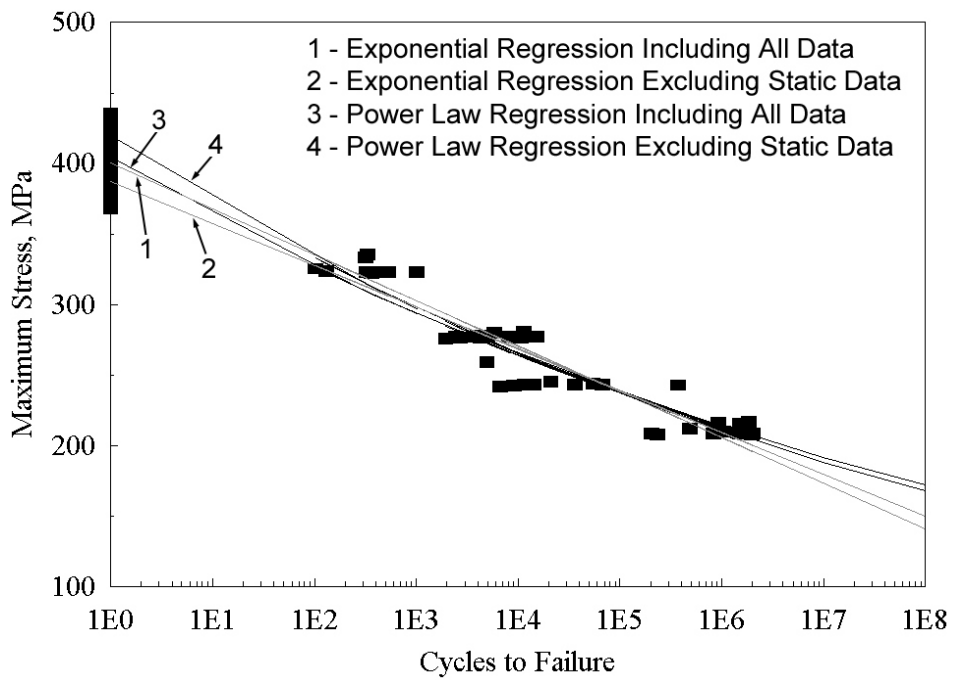
Figure 29. Constant Amplitude Fatigue for R = 10.
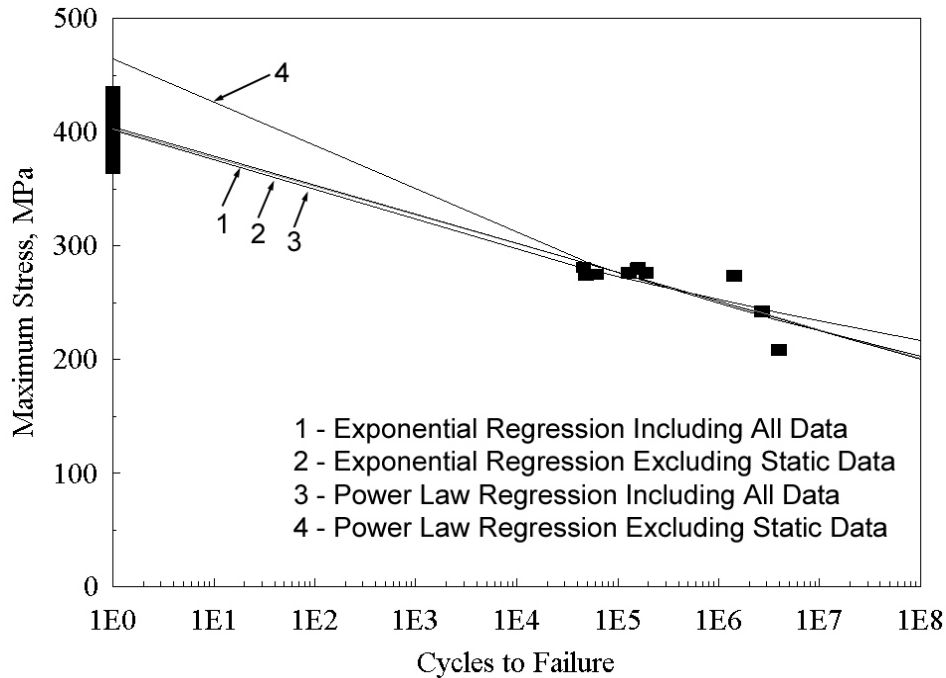
Figure 30. Constant Amplitude Fatigue for R = 2.

The fiber volume fraction of the DD16 laminate was 36 percent, placing this laminate in the class of better laminates' fatigue performance for this fiber volume fraction. The surface 90° plies of the DD16 laminate offered little in the material properties; their main purpose was aiding in mitigating grip effects. Discounting these surface plies places this laminate in the region of high 0° ply content (69 - 85 percent) where the fatigue trends of this laminate are in good agreement with that of similar laminates summarized in Table 1.

Table 5 contains the results of power law regressions at each R-value and comparisons to results of tests of uniaxial fiber lay-up material as reported by Sutherland [29]. Due to the difference in material, direct comparisons are not possible, yet trends can be compared and are similar.

The data of Tables 4 and 5 were also reduced to the graphical form of Goodman diagrams, Figures 31 through 34, and to the graphical form of regression lines, Figures 35 through 42. Note, in Figure 35, the relative order of the R-values, with the reversing condition being the more damaging (more rapid loss of life), followed by the tensile and lastly by the compressive load cases. This is consistent with the information displayed in the Goodman diagrams; note the closer spacing of the constant cycle lines for the compressive case, with the spacing increasing first for the tensile and lastly for the reversing.

Table 5. Power Law Regression Analysis Parameters for Constant Amplitude Fatigue

MPa	Range of Applicability	Regression Coefficients	R-Value, Equation 1				
			0.1	0.5	-1	10	2
Present Work UTS=632 UCS=400	1 to 10^7 Cycles	C_2	1.005	1.013	0.998	1.005	1.000
		m	11.478	14.400	11.158	21.550	29.820
		Correlation	0.966	0.946	0.993	0.961	0.933
	10 to 10^7 Cycles	C_2	1.026	1.135	0.981	1.043	1.155
		m	11.214	12.490	11.343	20.089	22.249
		Correlation	0.936	0.872	0.964	0.906	0.61
Reference [28] UTS=1422 UCS=720	1 to 10^8 Cycles	C_2	1	1	1	1	1
		m	11.3	15.4	14.9	18.0	31.2
	10^3 to 10^8 Cycles	C_2	0.969	0.977	1.124	0.862	0.859
		m	11.6	16.0	13.2	22.5	47.8
	10^5 to 10^8 Cycles	C_2	0.740	0.977	1.124	0.802	0.802
		m	14.3	16.0	13.2	24.9	61.7
Reference [53] UTS=392 UCS=298	10^3 to 10^8 Cycles	C_2	1.30	-	1.64	-	1.26
		m	10.5	-	9.34	-	21.7
	-	-	-	-	-	-	-
	-	-	-	-	-	-	-

Important information can be gleaned from a regression of the fatigue models, but not in a normalized format. Notice in Figures 39 through 42, that for moderate stress levels, there is a crossing of the curves for the tensile and compressive cases. At a given high absolute stress, compression is more damaging, while at low stresses, tension is more damaging.
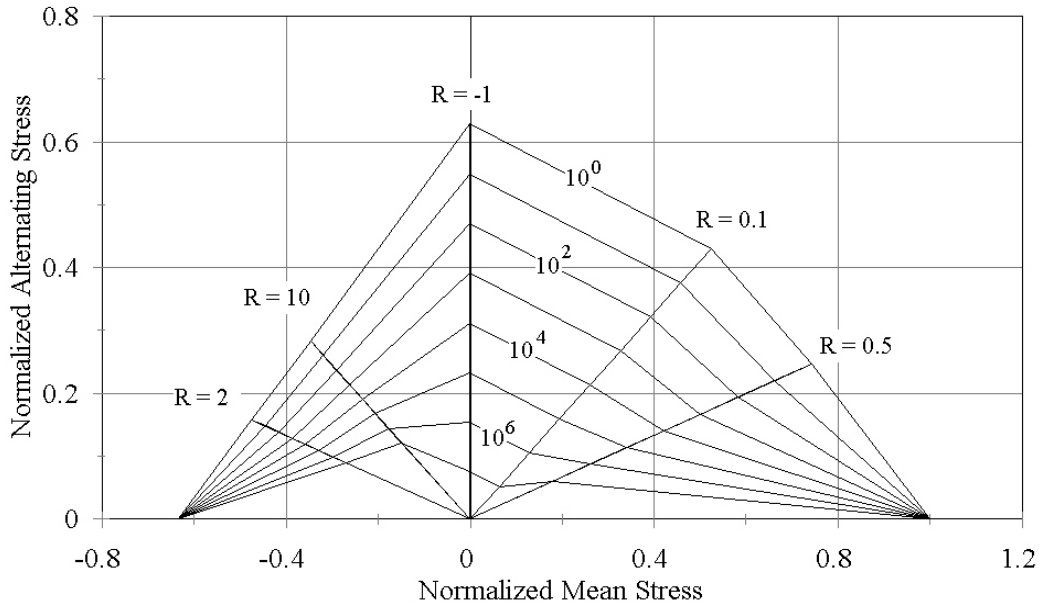
Figure 31. Goodman Diagram Based Upon Exponential Regression Analysis, Including All Data.
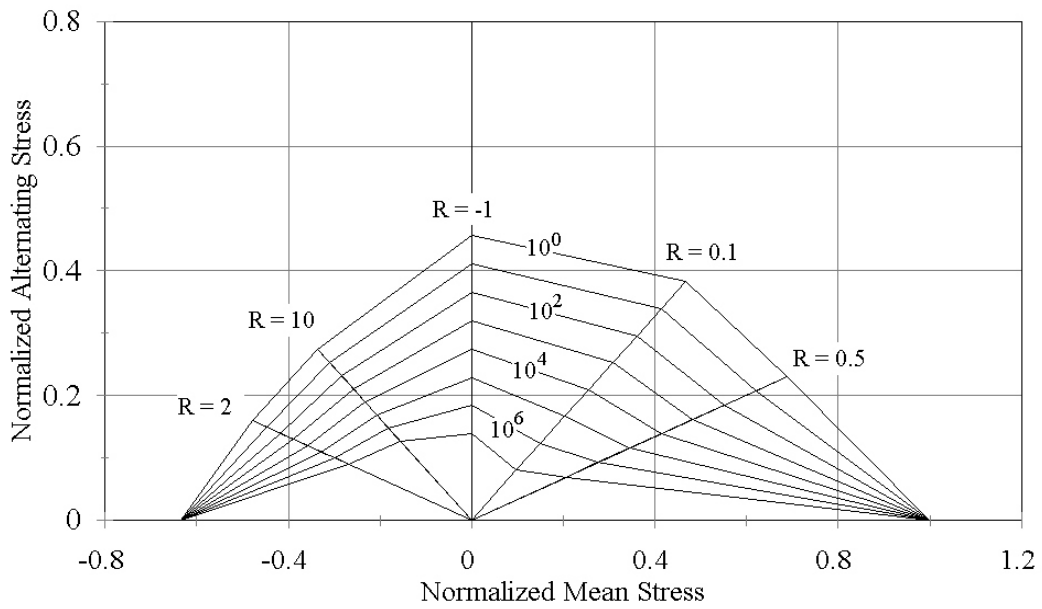
Figure 32. Goodman Diagram Based Upon Exponential Regression Analysis, Excluding Static Data.
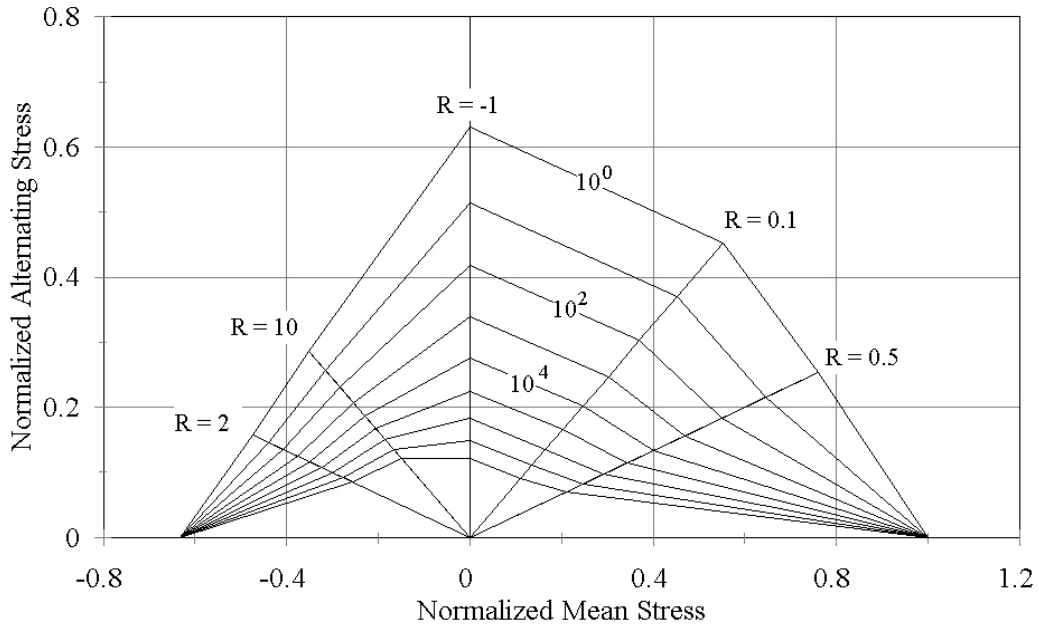
Figure 33. Goodman Diagram Based Upon Power Law Regression Analysis, Including All Data.
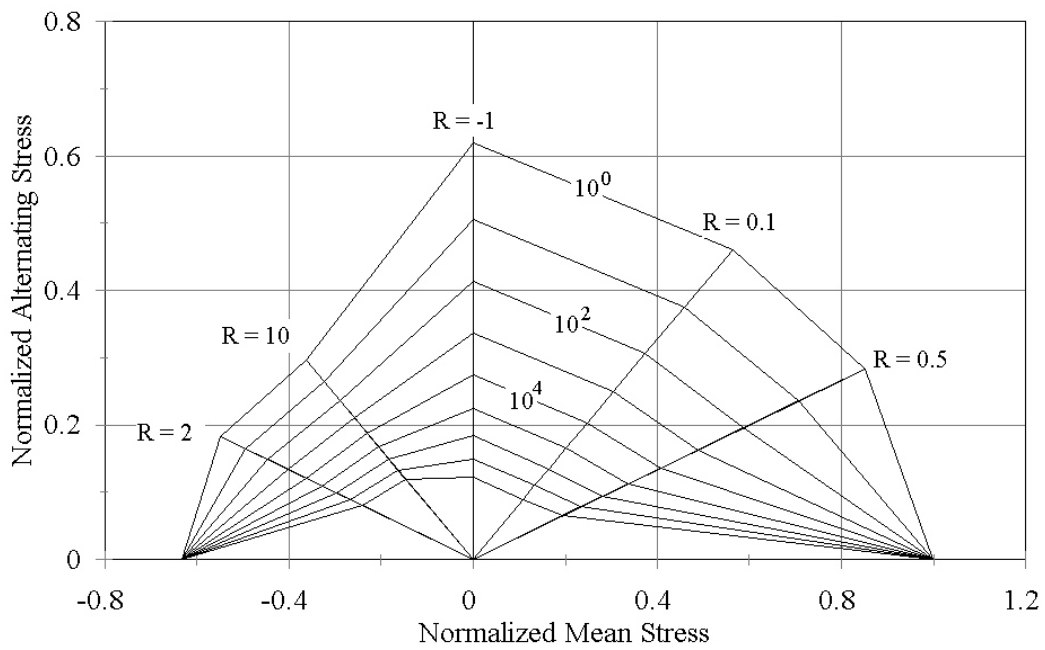
Figure 34. Goodman Diagram Based Upon Power Law Regression Analysis, Excluding Static Data.
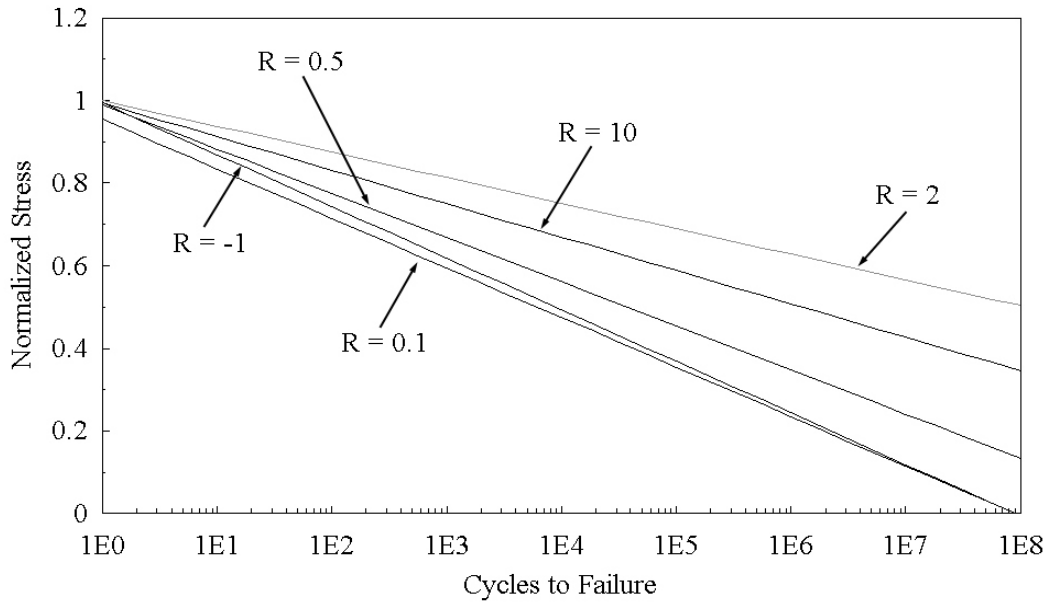
Figure 35. Normalized Fatigue Models, Exponential Regression Including All Data.
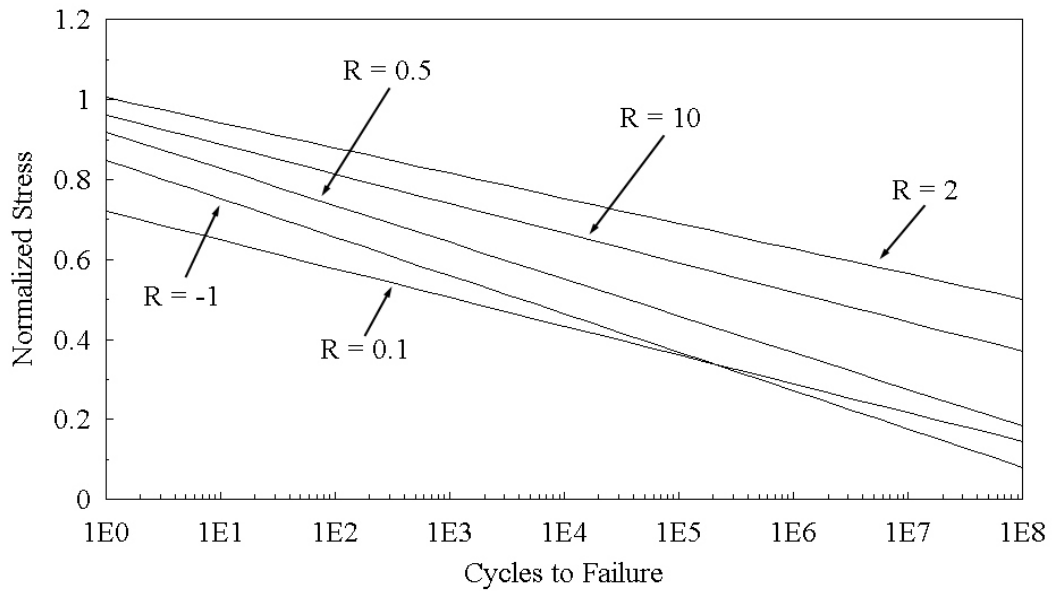
Figure 36. Normalized Fatigue Models, Exponential Regression Excluding Static Data.
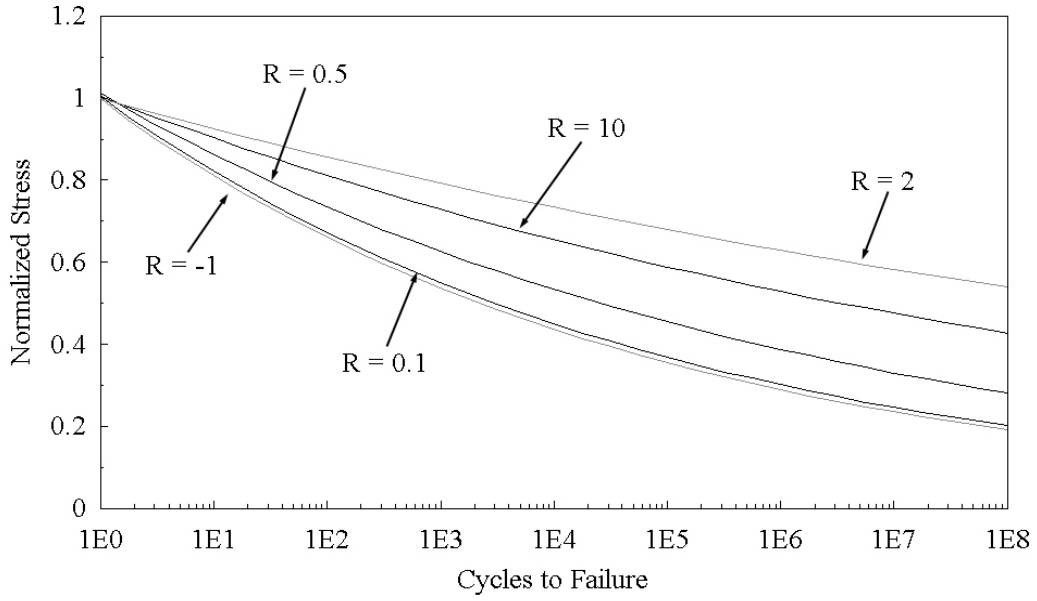
Figure 37. Normalized Fatigue Models, Power Law Regression Including All Data.
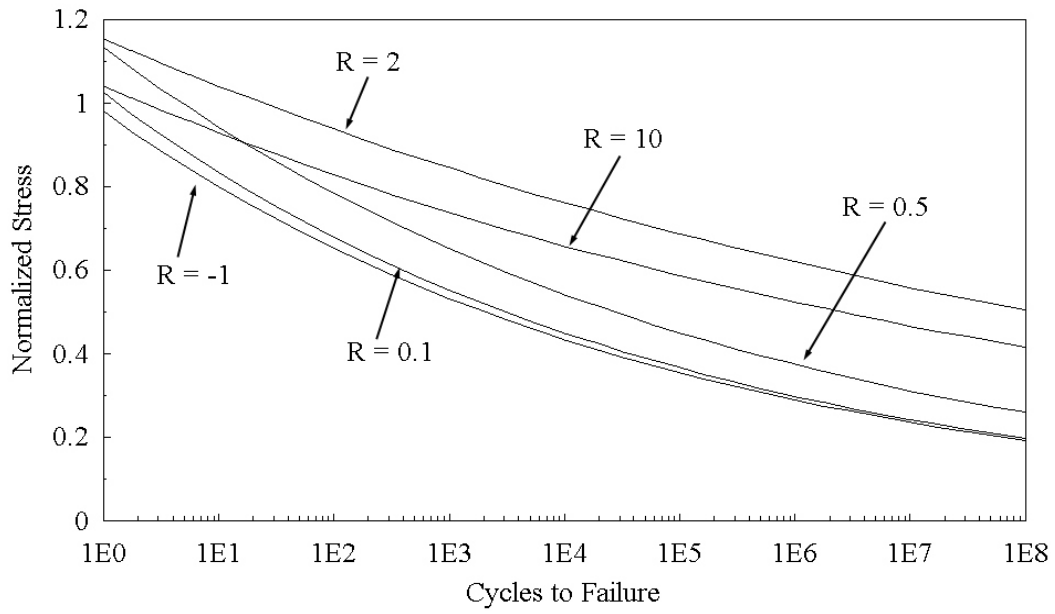
Figure 38. Normalized Fatigue Models, Power Law Regression Excluding Static Data.

47
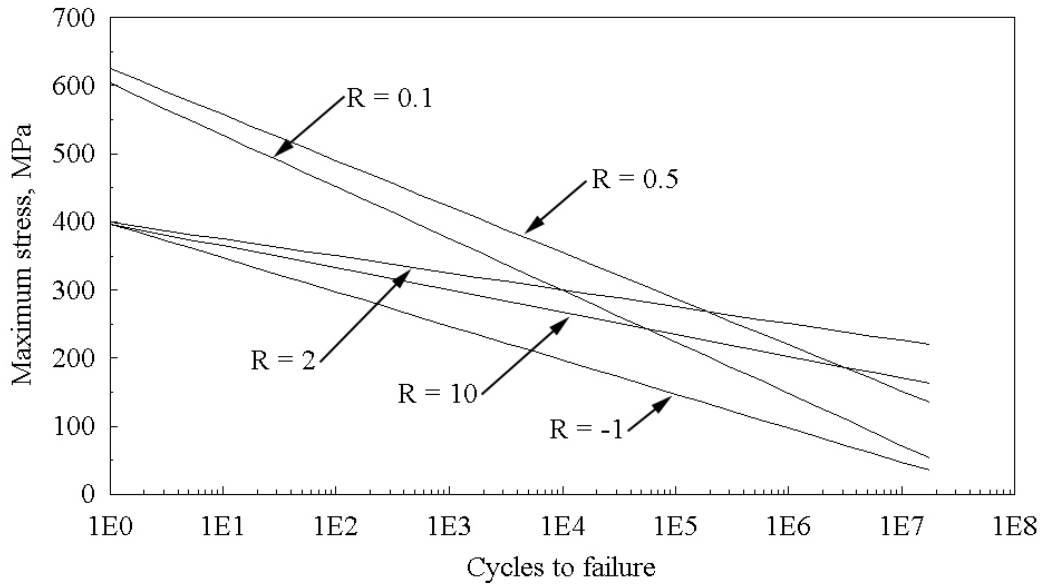
Figure 39. Exponential Fatigue Regression Models For All R-Values Including All Data.
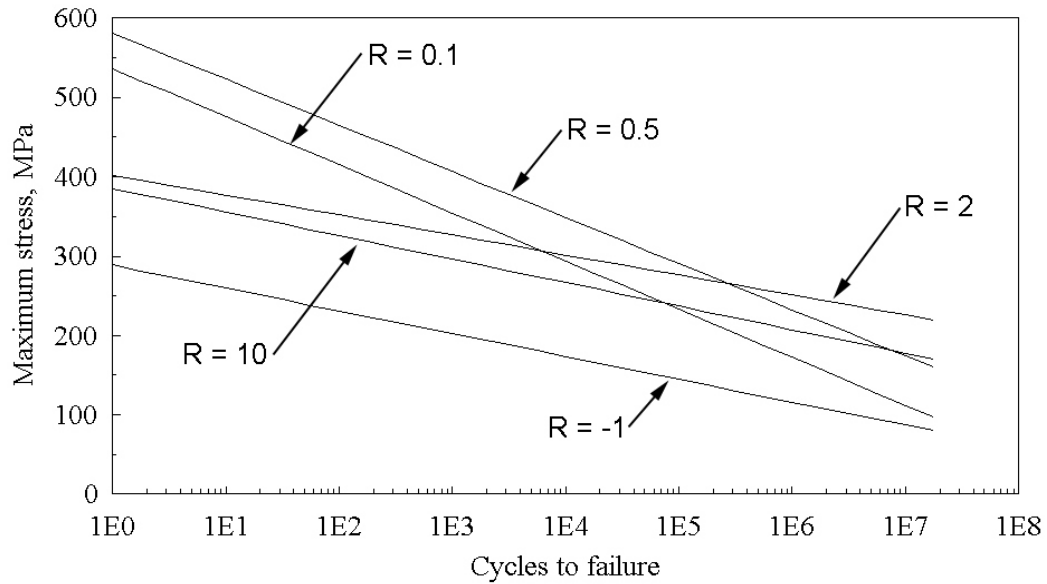
Figure 40. Exponential Fatigue Regression Models For All R-Values Excluding Static Data.
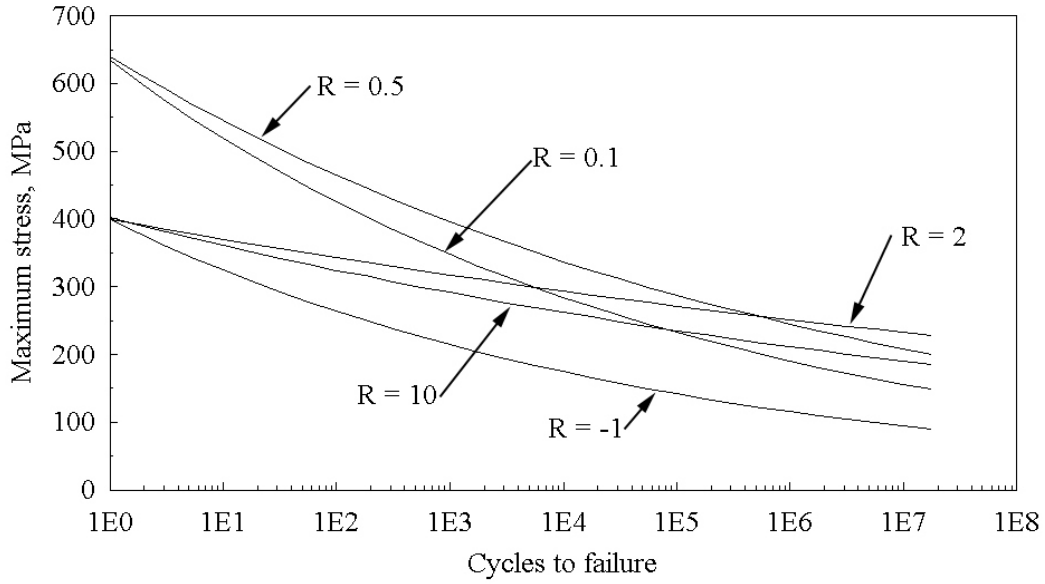
Figure 41. Power Law Fatigue Regression Models For All R-Values Including All Data.
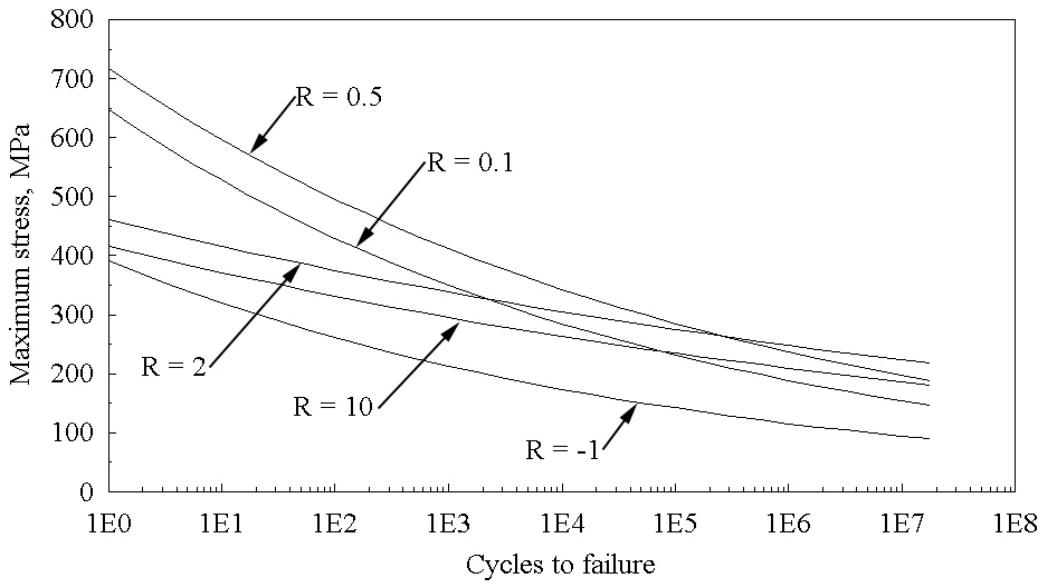
Figure 42. Power Law Fatigue Regression Models For All R-Values Excluding Static Data.

Residual Strength of Laminate Under Fatigue

The general trend of the residual strength of a laminate over its life was previously discussed. Recall that the shape of the strength curve, as related to the number of cycles experienced, can drastically affect lifetime predictions. Attempts were made to perform partial fatigue tests in order to ascertain the residual strength parameter, ν. Specimens were subjected to selected constant amplitude stress levels for a fixed number of cycles. The ultimate strengths of the cycled specimens were measured and compared with the ultimate strength of virgin, un-fatigued, specimens. Residual strength tests have been run for specimens subjected to fatigue at R-values of 0.1 and 0.5.

Figure 43 presents the residual strength results for the laminate subjected to 241 MPa with an R-value of 0.1. Tabulated data were taken from Reference [35] and placed into the graphical form of Figure 43. Specimens were fatigued to cycle accumulations at three different levels, 50,000, 100,000, and 200,000 cycles. Some specimens failed prior to achieving the desired cycle level and are so noted. Also shown and labeled as S-N fatigue, are the results of specimens cycled until failure as well as the virgin material ultimate tensile strength test results. It is evident from the residual strength data collected, that the residual strength parameter, ν, is not greater than unity. The premature failure of specimens before reaching the desired number of cycles complicates the analysis of a reasonable value for ν. Regardless, upon investigating the residual strength results for both R-values of 0.1 and of 0.5, a factor of less than one was considered appropriate. The residual strength tests, summarized in Figure 44, were performed at a maximum stress level of 325 MPa and at an R-value of 0.5.

The general shape of the residual strength lifetime curves (equations 13 and 14) is uncertain. An error analysis of the residual strength data shown in Figure 43 indicates the nonlinear strength degradation curve yields a mean absolute minimum error of 23 percent with a degradation parameter, ν, of 0.265. The linear residual strength curve analysis indicated a mean absolute error of 37 percent. The results of this work and that of Reference [35] indicate that the nonlinear parameter, ν, is not greater than one. Broutman and Sahu [42] data seems to indicate that a linear residual strength degradation is valid; while Yang and Jones [36] indicate (without data) that a nonlinear strength degradation parameter greater than one is reasonable. This parameter may be a function of the laminate as well as the stage of life of the material.
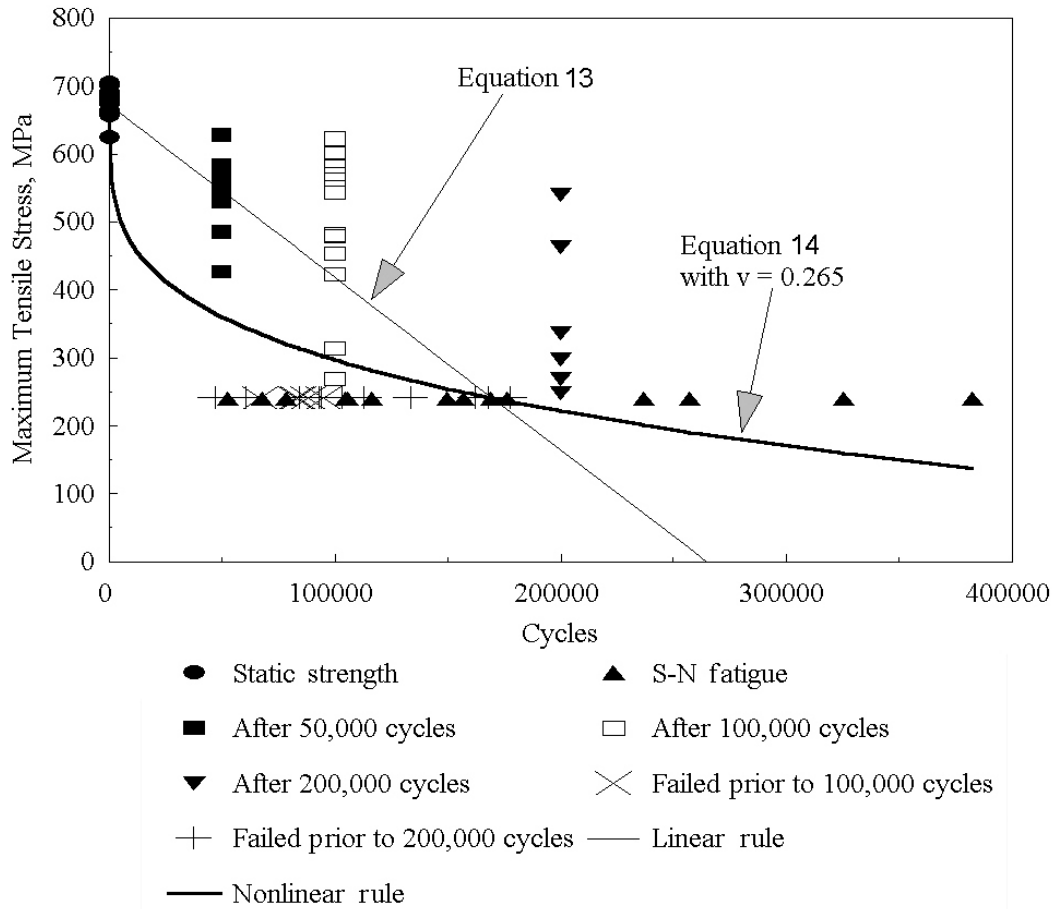
Figure 43. Residual Strength Data For R = 0.1 [35].
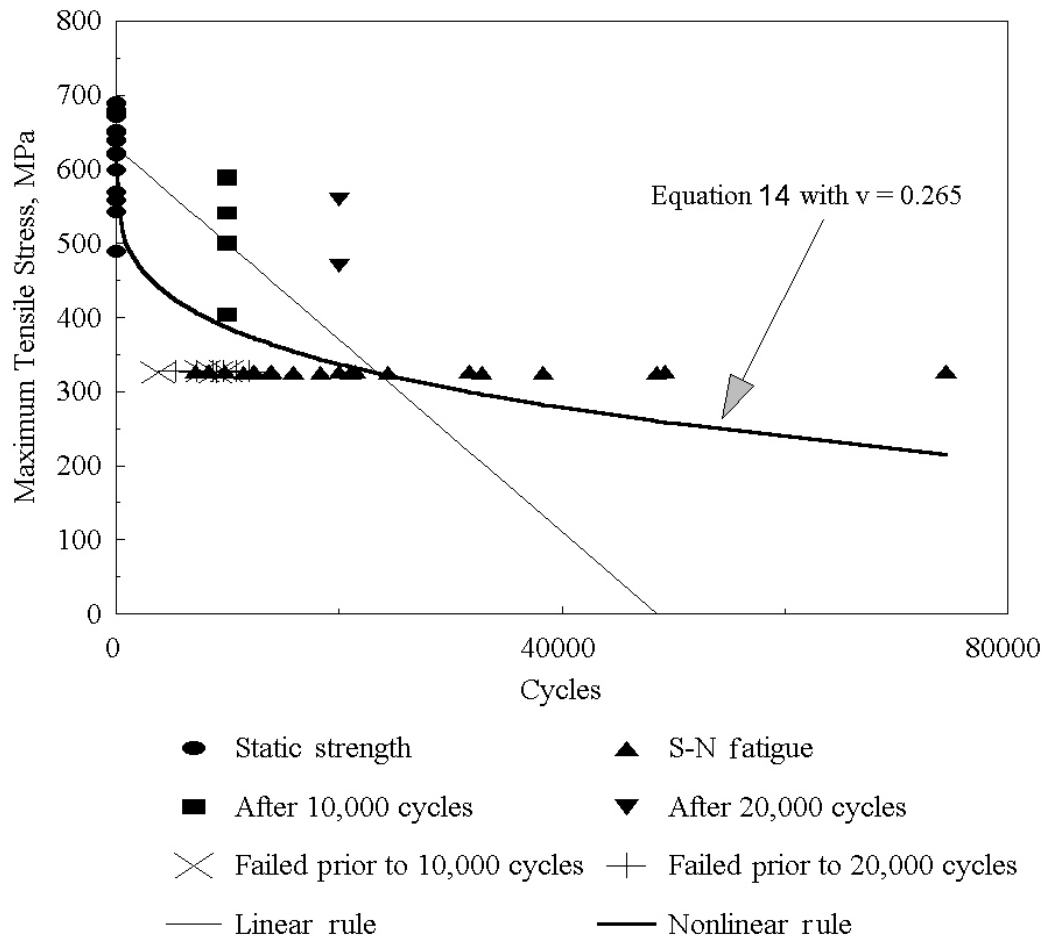
Figure 44. Residual Strength Data For R = 0.5.

An investigation into variable amplitude fatigue testing logically begins with two amplitudes or stress levels before considering more complex spectra. Other researchers have also taken this approach, implementing a spectrum of one block of constant amplitude cycles followed by a second block of different constant amplitude cycles. The second block was run until specimen failure in tests by Yang, et. al. [11].

Testing in this format is not considered representative of a realistic spectrum; consequently, an alternate application of two-block testing was considered for this research. Upon considering a standard European spectrum for wind turbine blades, it is evident that a repetition of blocks would be more appropriate. Note the obvious repetitions in the time-compressed European spectrum WISPER [16, 17] shown in Figure 45.
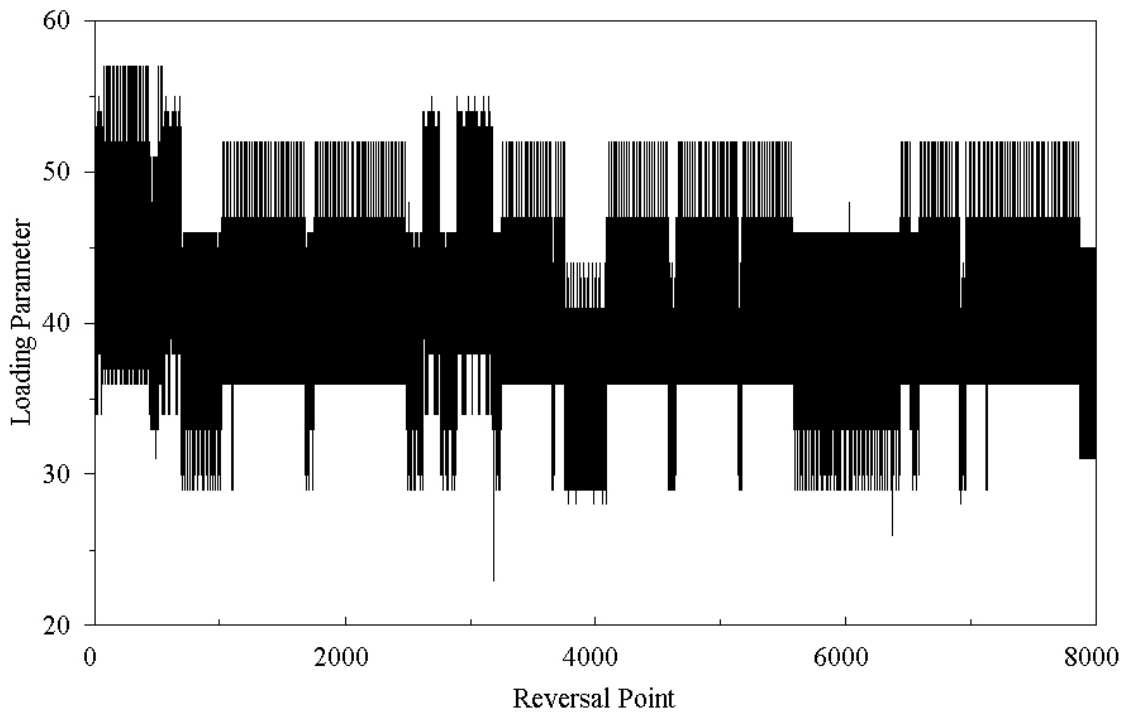
Figure 45. Excerpt of WISPER Spectrum.

Sequence Effects

When entering into studies of fatigue at two different load levels, thought must be given to possible effects of the sequencing of the cycles. This is prompted by the result of fatigue analysis in metals by linear elastic fracture mechanics [23]. In metals, a high load can create a compressed region at the crack tip, thereby retarding crack growth at lower loads, and consequently extending fatigue life.

Three separate spectra containing the same number of cycles at each stress level were developed for investigation of possible sequence effects in the fatigue of this laminate. The three spectra are shown in Figure 46. The first contains a block of one high amplitude cycle followed by 100 low amplitude cycles. These two blocks are shown repeated ten times to create a spectrum of 1010 cycles in length. The second spectrum was comprised of ten high amplitude cycles followed by 1000 low amplitude cycles. The third was constructed to contain ten high amplitude cycles randomly interspersed within 1000 low amplitude cycles. The high amplitude cycle fraction is defined as the number of high amplitude cycles divided by the total number of cycles. Each of these spectra, then, had a fraction of approximately 0.01.

High amplitude cycles were set at an R-value of 0.1 and had a maximum stress of 325 MPa. Low amplitude cycles were also set at an R-value of 0.1, but at a maximum stress of 207 MPa. Figure 47 details the results of 120 tests, 82 two-block and 38 reference constant amplitude tests. The fraction of specimen failures is displayed against the total number of cycles experienced. All of the specimens are from the same batch of fabric reinforcement, and tests were randomly interspersed between the different sequences and the constant amplitude cases.
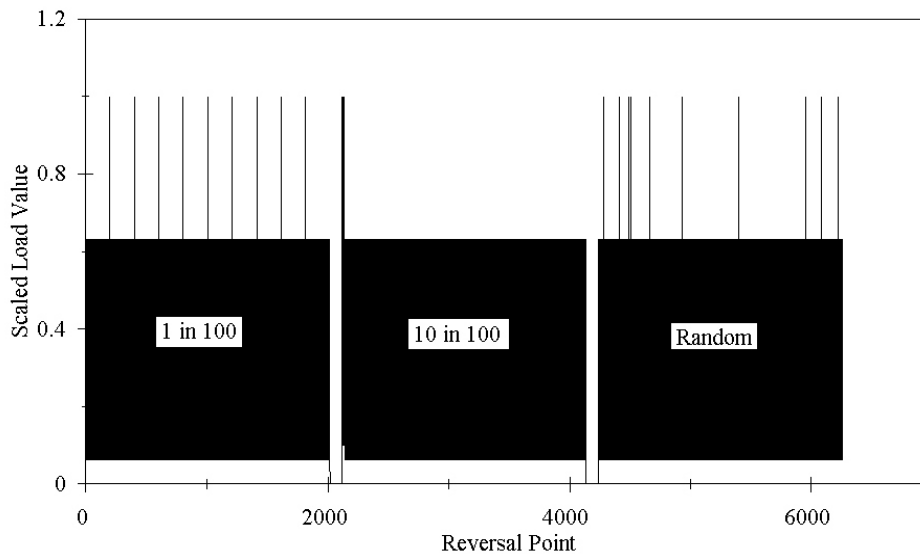
Figure 46. Two-Block Sequences (Blocks Repeated to Failure).
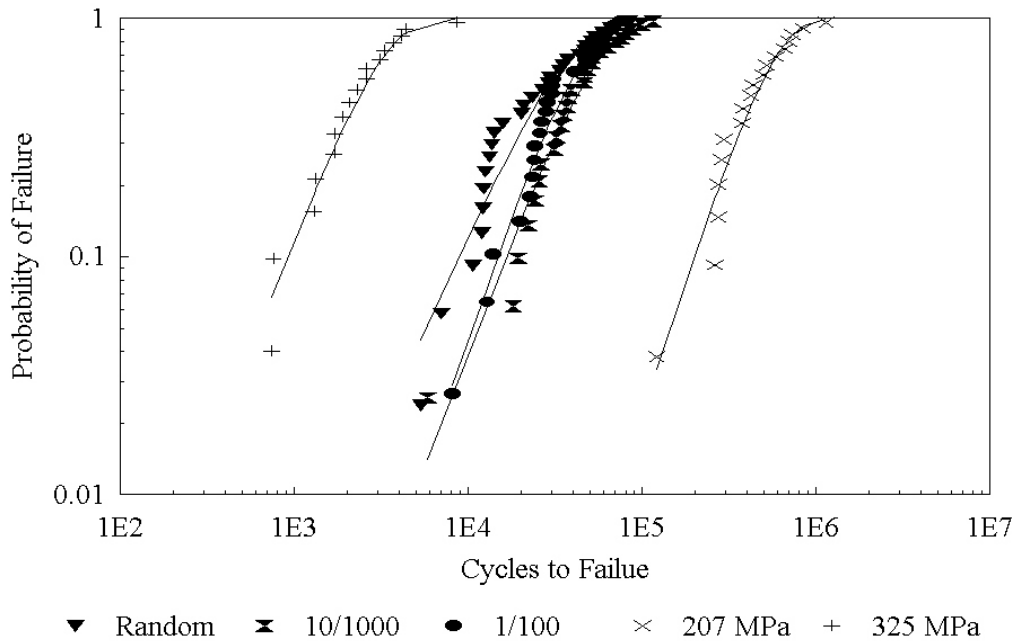
Figure 47. Two-Block Sequence Test.

Within confidence limits of 0.95, there is no statistical difference among the three sequences. Consequently, sequencing was not considered important and ignored for the remainder of the testing.

Only four of the 82 sequencing effect tests achieved Miner's sums greater than unity. In fact the average Miner's sum is slightly less than 0.3, as evident in Figure 48. Compare this against the average Miner's sum of 1.0 for the constant amplitude fatigue tests and it becomes evident that spectral loading does not produce failure at a Miner's sum averaging 1.0. This phenomenon will be investigated later on.
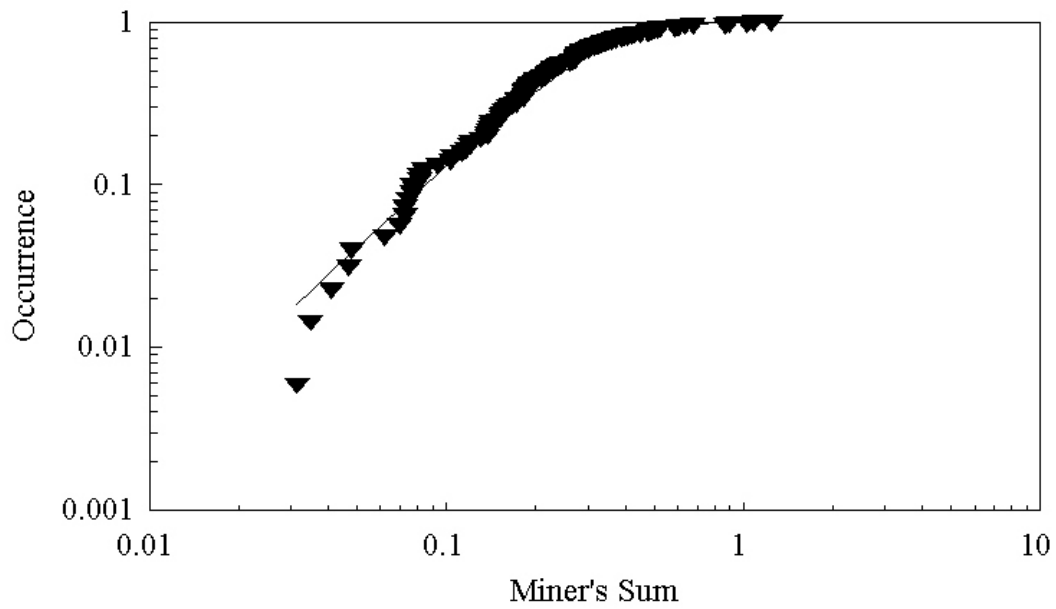
Figure 48. Overall Two-Block Miner's Sum, Stresses 325 and 207 MPa, High Amplitude Cycle Ratio of 0.01.

Two-Block Fatigue Testing

Two-block testing was performed at several combinations of stress levels as well as for different R-values. Testing was performed for cases in which the two stress levels were relatively close as well as distant. Test campaigns are identified in Table 6. The cycles column gives the number of cycles per block; blocks are repeated until failure in all cases.

Table 6. Two-Block Testing Campaigns

High Stress Block			Low Stress Block		
σ_{max}, MPa	R-value	cycles	σ_{max}, MPa	R-value	cycles
414	0.1	10	325	0.1	10, 90, 100, 990, 1K, 9K
414	0.1	10	235	0.1	10, 90, 100, 112, 1K, 10K
325	0.1	10	235	0.1	10, 100, 500, 1K, 3K, 5K
325	0.1	10	207	0.1	10, 50, 90, 100, 1K, 3K, 5K, 10K, 20K, 33K, 50K, 60K
235	0.1	10, 20	207	0.1	10, 90, 100, 990, 1K, 9K, 33K, 50K, 60K
414	0.5	10	325	0.5	10, 50, 100, 1K
414	0.5	10	235	0.5	10, 100, 1K, 10K
325	0.5	10	235	0.5	10, 90, 100, 1K, 10K
235	0.5	10	207	0.5	90
-276	10	10, 1K, 10K	-207	10	10, 100, 1K, 10K
-325	10	10	-207	10	10, 100, 1K, 10K
173	-1	10	104	-1	10, 100, 1K, 10K

One would expect that as the two stress levels approached each other in magnitude, any effects on fatigue would diminish, the limiting case being of constant amplitudes. Tests were arranged to allow investigation of this possibility.

Results of two-block fatigue testing have been summarized into graphical form (Figures 49 - 70) relating the Miner's sum to the fraction of high amplitude cycles. A fraction of high amplitude cycles of zero would, in reality, be a constant amplitude test of the lower stress level. Conversely, a fraction

of one would indicate a constant amplitude test at the higher stress level. In each of the following two-block graphs, the abscissa has been broken into two parts, the extreme left is of a linear scale, allowing the zero fraction to be displayed; the remainder of the scale to the right is logarithmic. Included in each graph are lifetime predictions that will be discussed in a following section. Within the legend of each graph, NRSD and LRSD refer to a nonlinear and linear lifetime residual strength prediction models, respectively the NRSD cases were all run with $\nu = 0.265$). The graphs are presented in pairs, on one page, with the upper displaying the lifetime predictions based upon an exponential fatigue model (equation 7); the lower represents lifetime predictions based upon a power law fatigue model (equation 8).

Note, in most of these figures that the trend of Miner's number varies from one at the left hand margin (low stress level constant amplitude fatigue test) to less than one and finally back towards an average of one at the right hand margin (high stress level constant amplitude fatigue test). There does not appear to be a retardation effect observable in the multi-block fatigue of the tested laminate.

The degrading effect of load interaction (Miner's sums below 1.0) was most prevalent in the tensile tests at R-values of 0.1 and 0.5, with the effect greater for the larger spread of the applied maximum stress levels. The effect was also observed in the reversing load cases, and R-value of -1; and to a much lesser extent in the compressive cases of the R-values of 2 and 10.

A tabulated form of the test results and calculations for all two-block testing campaigns can be found in Appendix C.
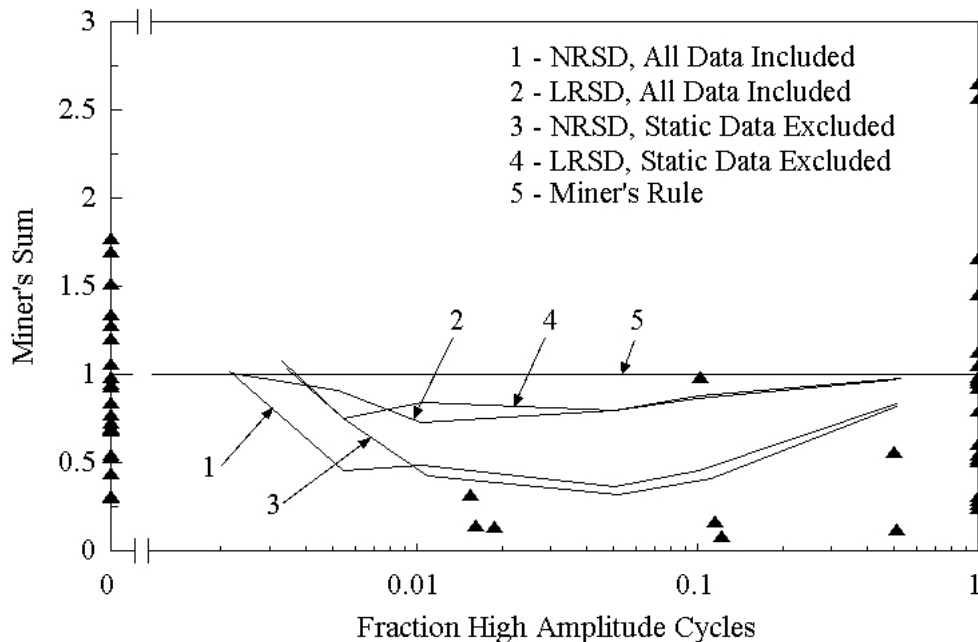
Figure 49. Two-Block Test Results for R = 0.1, 414 & 325 MPa; Exponential Fatigue Model With Linear and Nonlinear Residual Strength and Miner's Rule Lifetime Predictions.
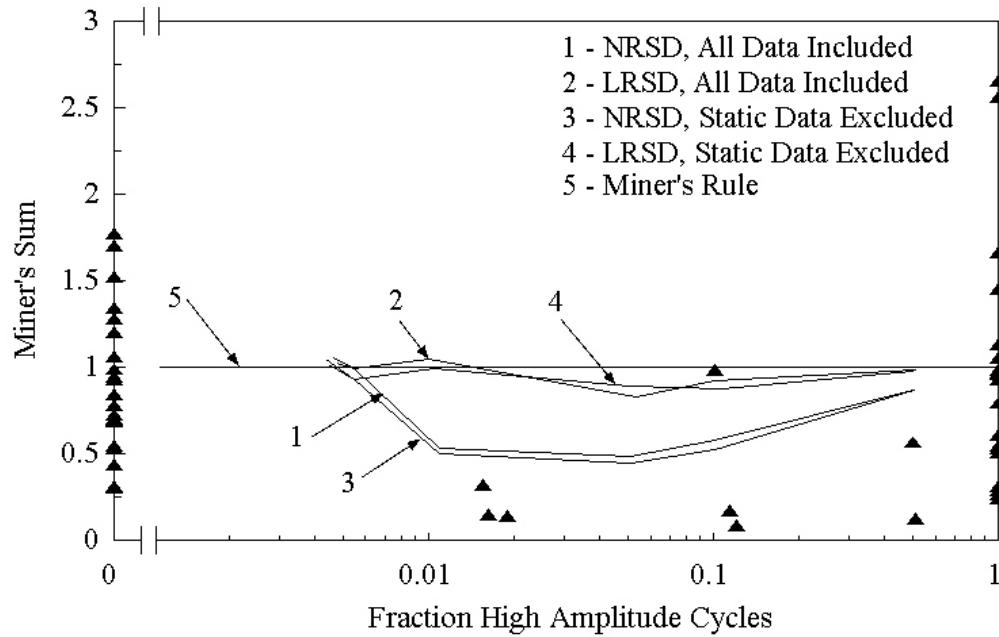
Figure 50. Two-Block Test Results for R = 0.1, 414 & 325 MPa; Power Law Fatigue Model With Linear and Nonlinear Residual Strength and Miner's Rule Lifetime Predictions.
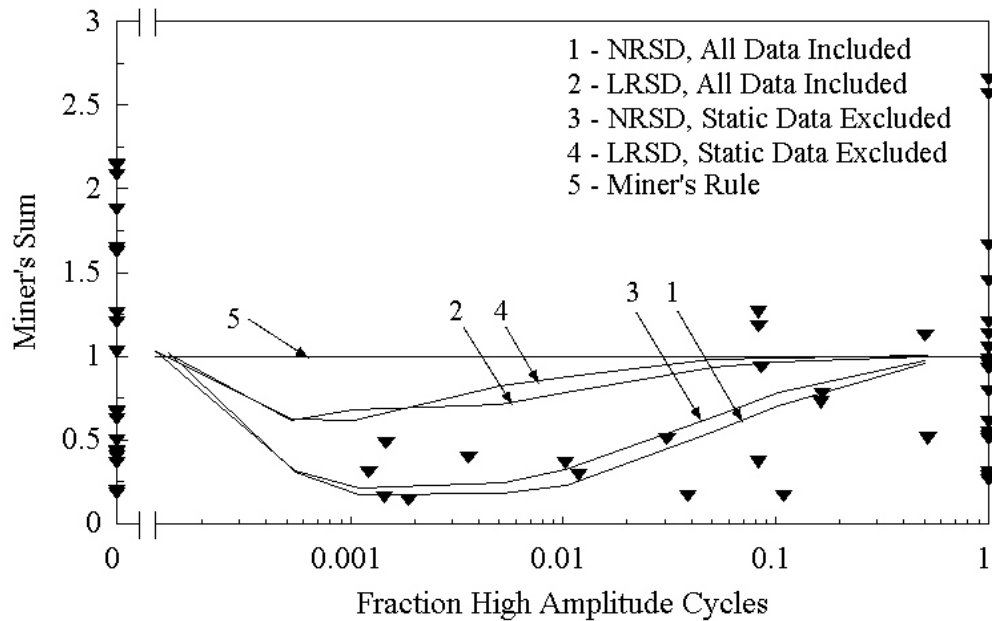
Figure 51. Two-Block Test Results for R = 0.1, 414 & 235 MPa; Exponential Fatigue Model With Linear and Nonlinear Residual Strength and Miner's Rule Lifetime Predictions.
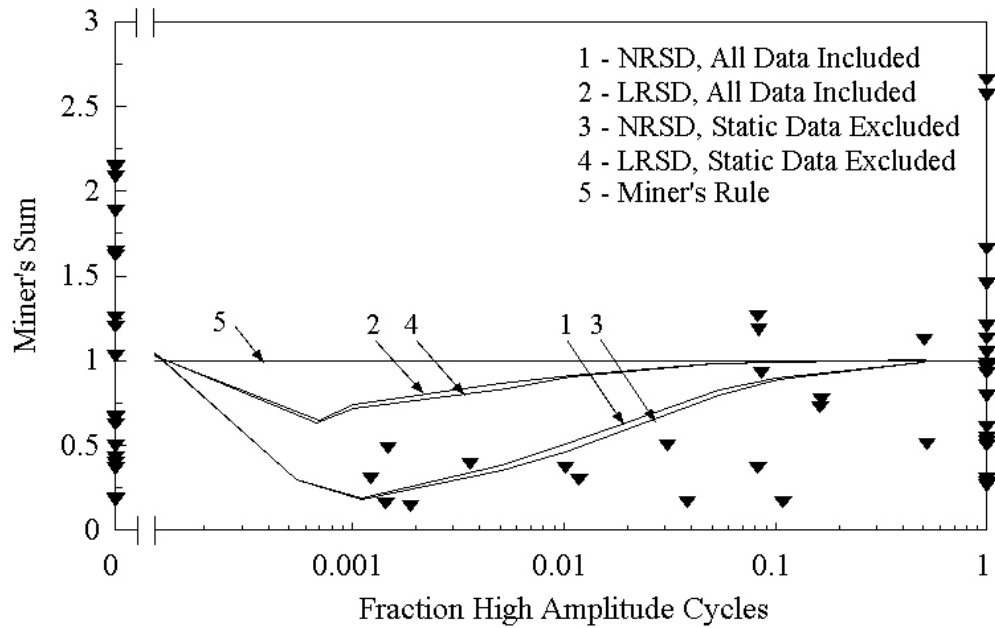
Figure 52. Two-Block Test Results for R = 0.1, 414 & 235 MPa; Power Law Fatigue Model With Linear and Nonlinear Residual Strength and Miner's Rule Lifetime Predictions.
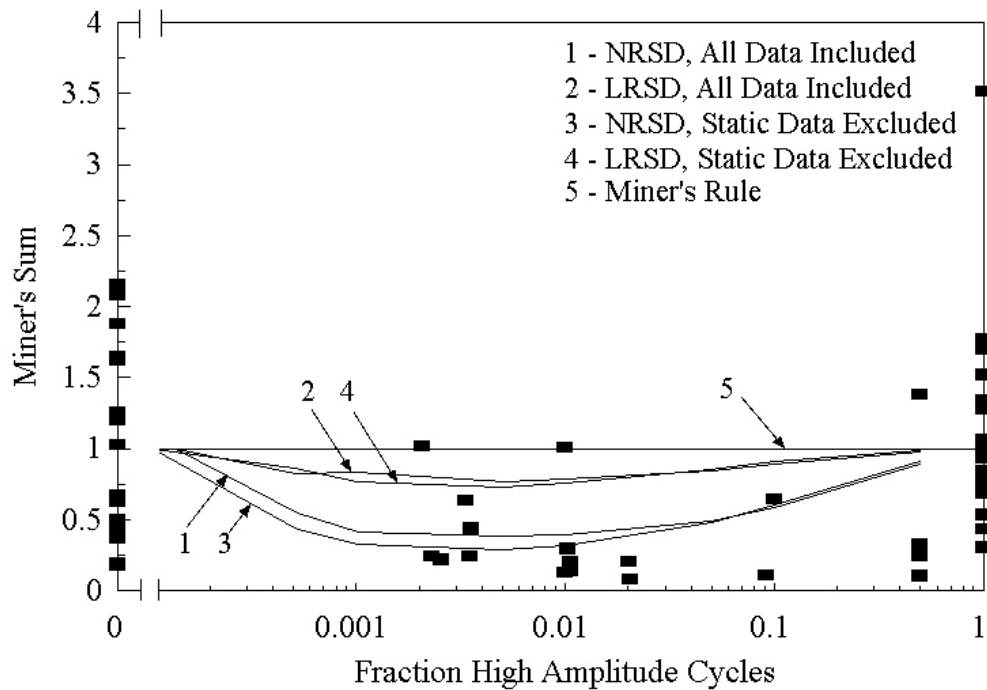
Figure 53. Two-Block Test Results for R = 0.1, 325 & 235 MPa; Exponential Fatigue Model With Linear and Nonlinear Residual Strength and Miner's Rule Lifetime Predictions.
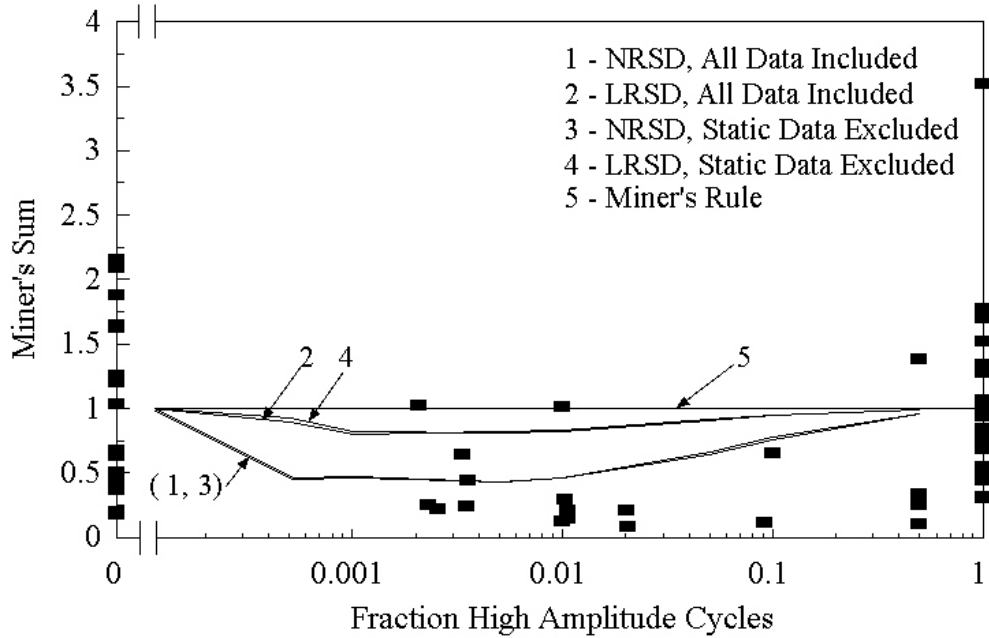
Figure 54. Two-Block Test Results for R = 0.1, 325 & 235 MPa; Power Law Fatigue Model With Linear and Nonlinear Residual Strength and Miner's Rule Lifetime Predictions.
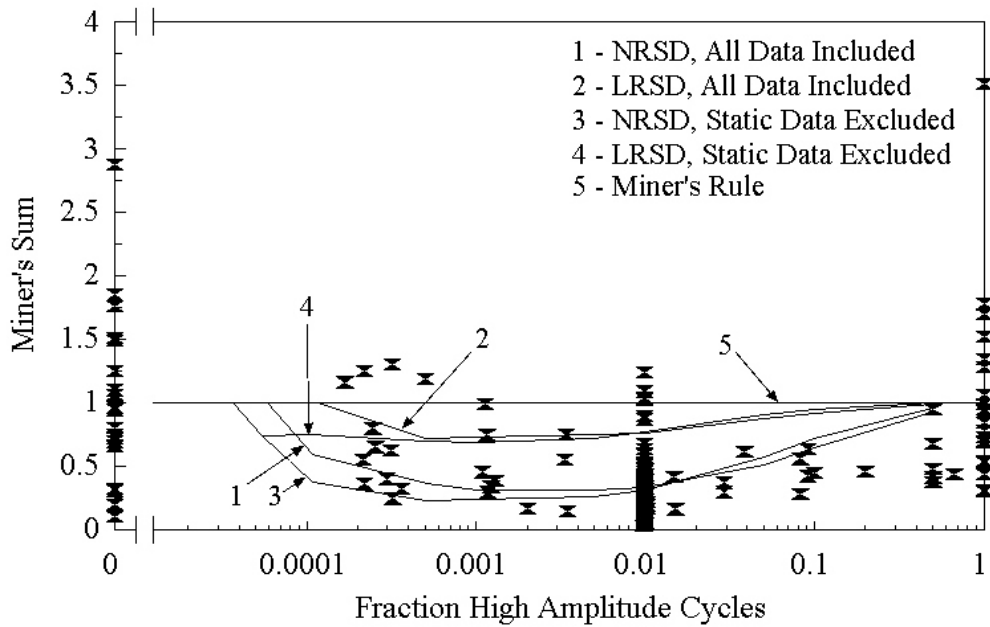
Figure 55. Two-Block Test Results for R = 0.1, 325 & 207 MPa; Exponential Fatigue Model With Linear and Nonlinear Residual Strength and Miner's Rule Lifetime Predictions.

61
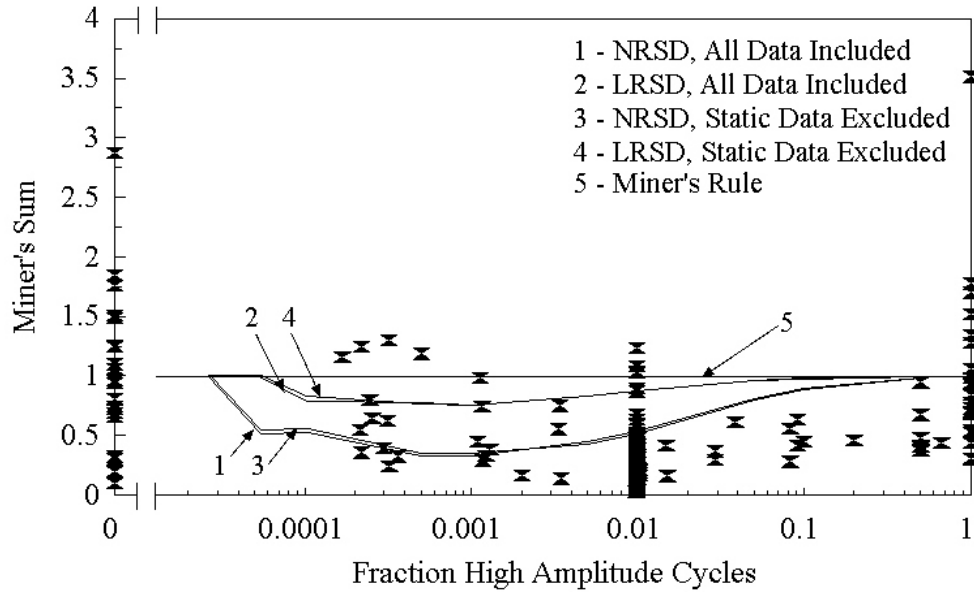
Figure 56. Two-Block Test Results for R = 0.1, 325 & 207 MPa; Power Law Fatigue Model With Linear and Nonlinear Residual Strength and Miner's Rule Lifetime Predictions.
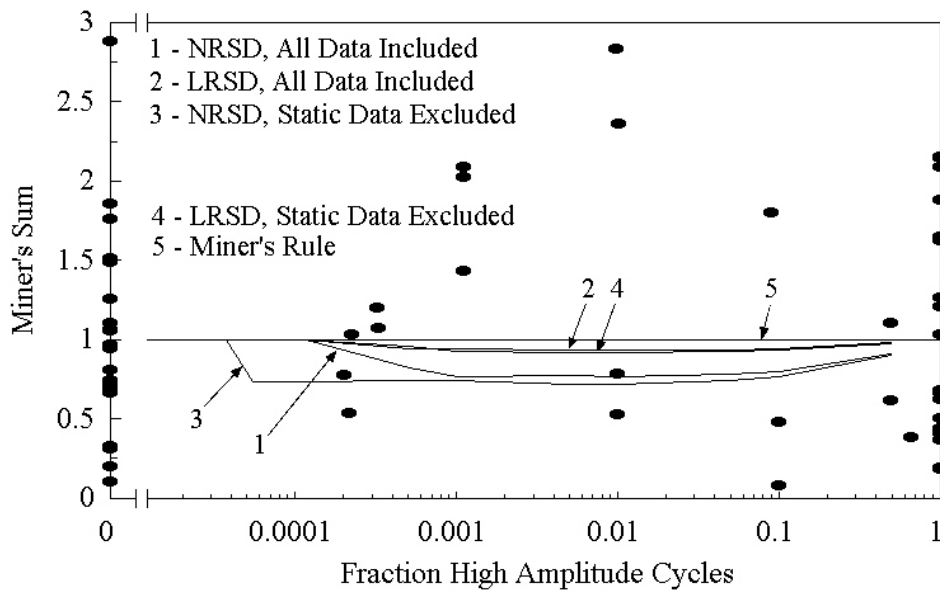
Figure 57. Two-Block Test Results for R = 0.1, 235 & 207 MPa; Exponential Fatigue Model With Linear and Nonlinear Residual Strength and Miner's Rule Lifetime Predictions.
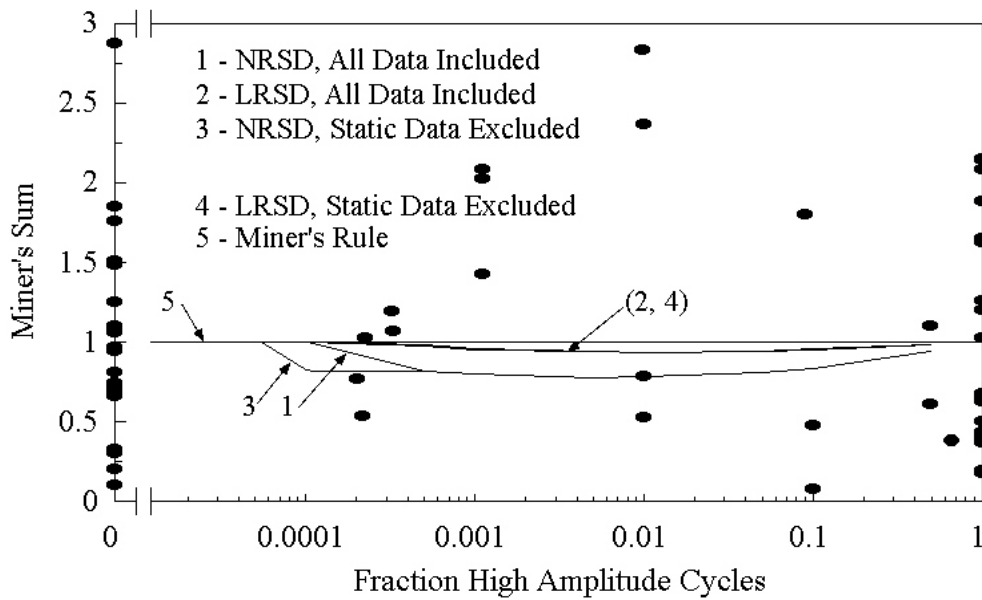
Figure 58. Two-Block Test Results for R = 0.1, 235 & 207 MPa; Power Law Fatigue Model With Linear and Nonlinear Residual Strength and Miner's Rule Lifetime Predictions.
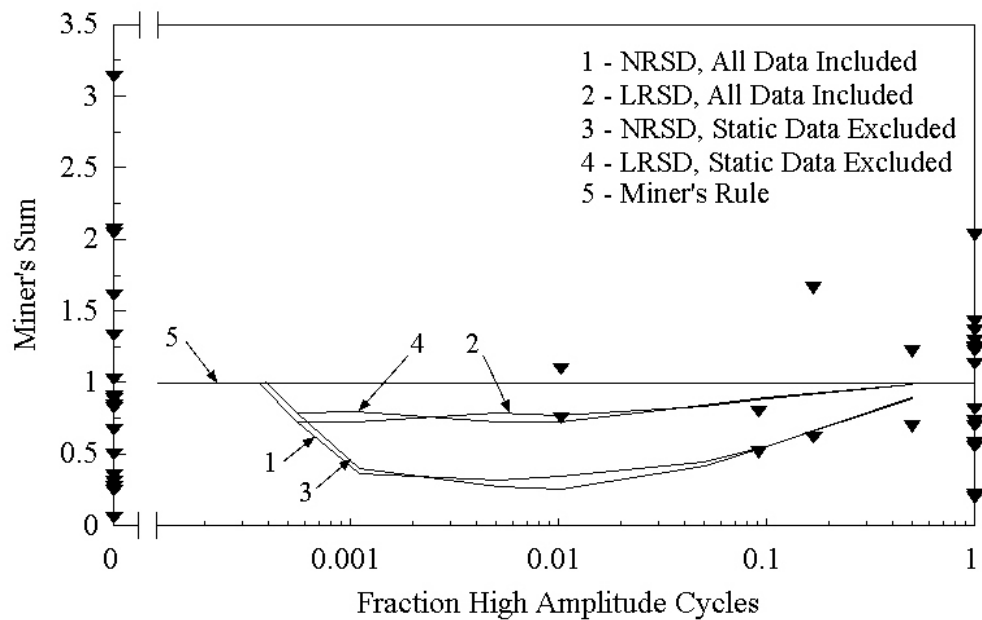
Figure 59. Two-Block Test Results for R = 0.5, 414 & 325 MPa; Exponential Fatigue Model With Linear and Nonlinear Residual Strength and Miner's Rule Lifetime Predictions.
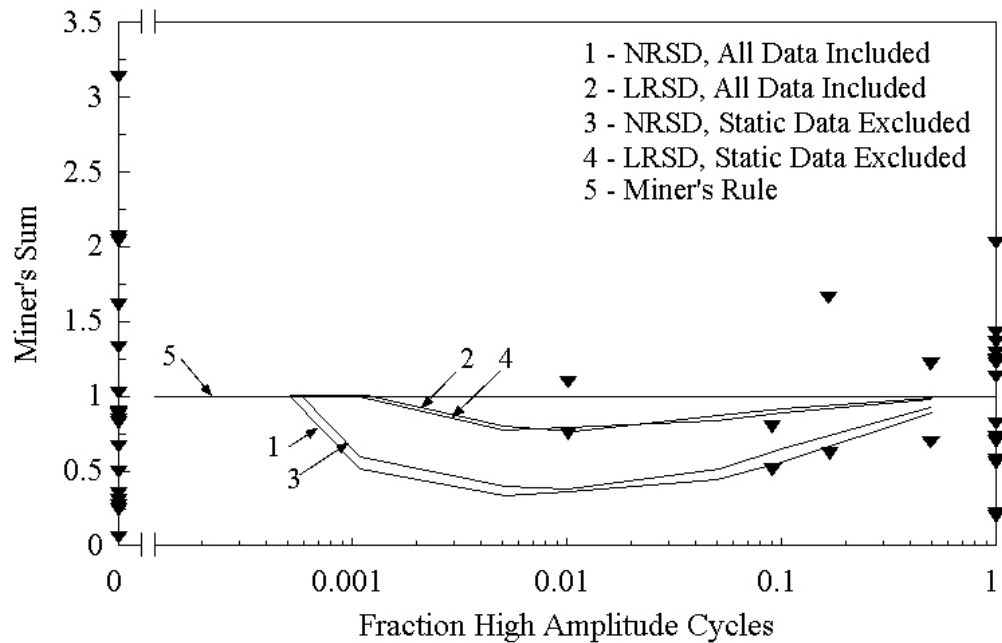
Figure 60. Two-Block Test Results for R = 0.5, 414 & 325 MPa; Power Law Fatigue Model With Linear and Nonlinear Residual Strength and Miner's Rule Lifetime Predictions.
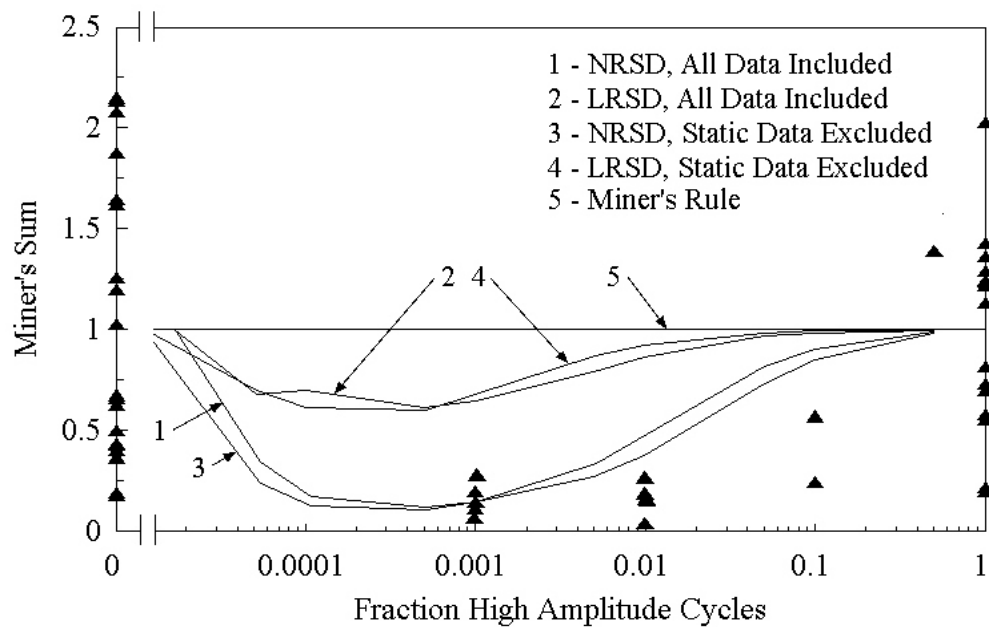
Figure 61. Two-Block Test Results for R = 0.5, 414 & 235 MPa; Exponential Fatigue Model With Linear and Nonlinear Residual Strength and Miner's Rule Lifetime Predictions.
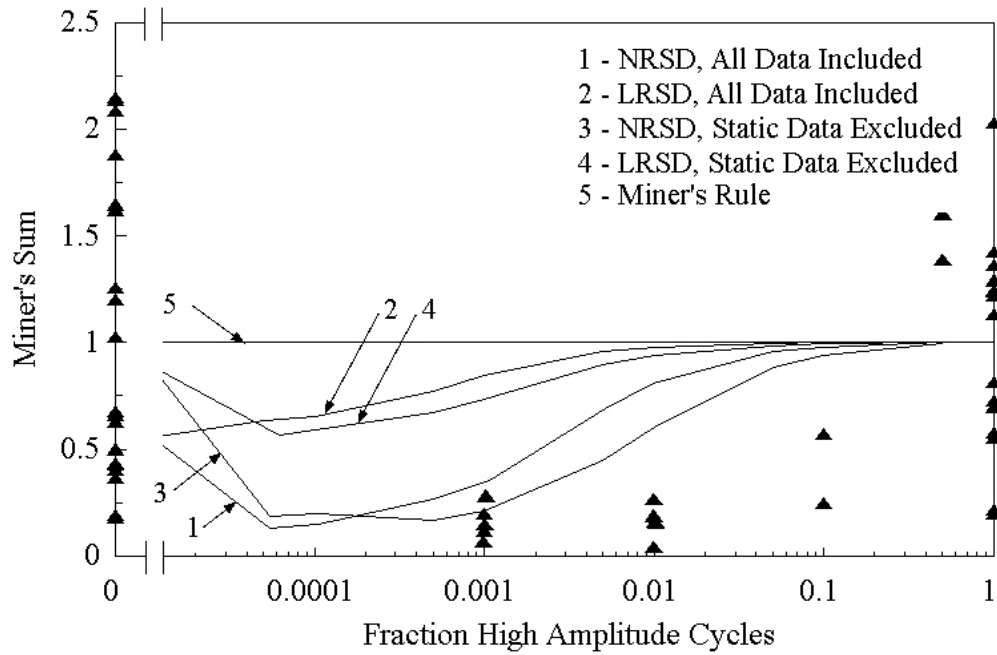
Figure 62. Two-Block Test Results for R = 0.5, 414 & 235 MPa; Power Law Fatigue Model With Linear and Nonlinear Residual Strength and Miner's Rule Lifetime Predictions.
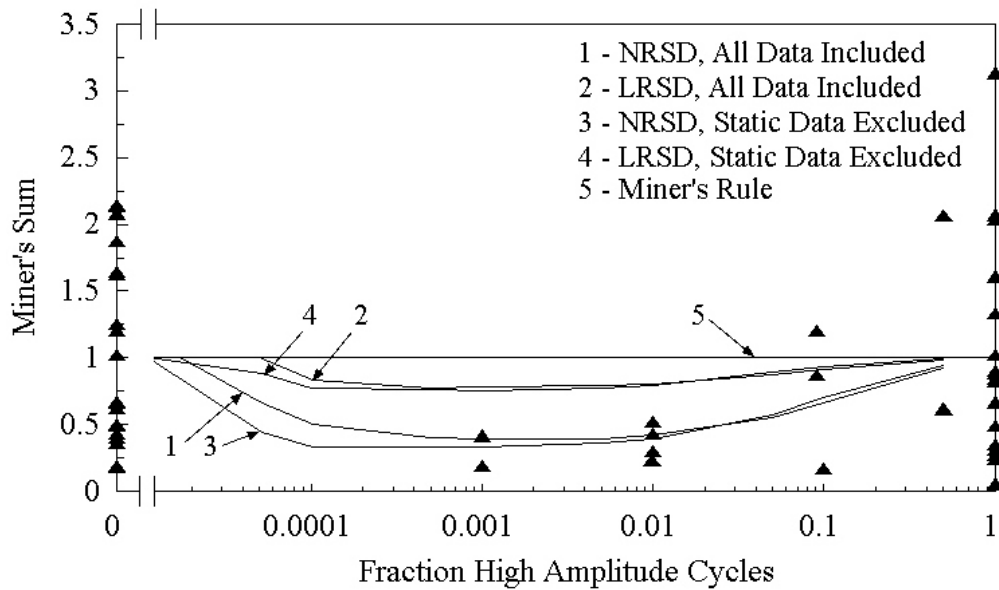
Figure 63. Two-Block Test Results for R = 0.5, 325 & 235 MPa; Exponential Fatigue Model With Linear and Nonlinear Residual Strength and Miner's Rule Lifetime Predictions.
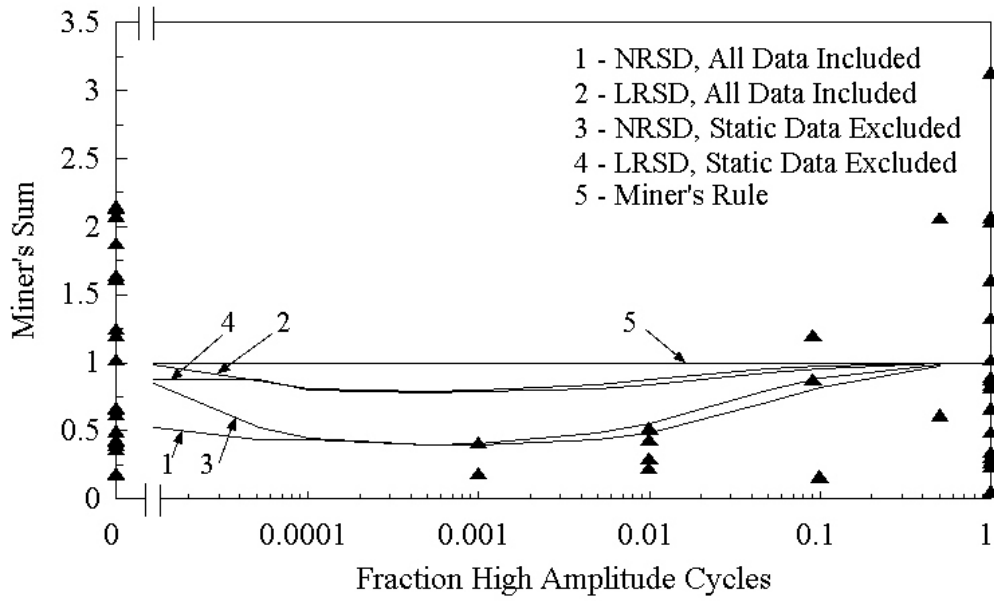
Figure 64. Two-Block Test Results for R = 0.5, 325 & 235 MPa; Power Law Fatigue Model With Linear and Nonlinear Residual Strength and Miner's Rule Lifetime Predictions.
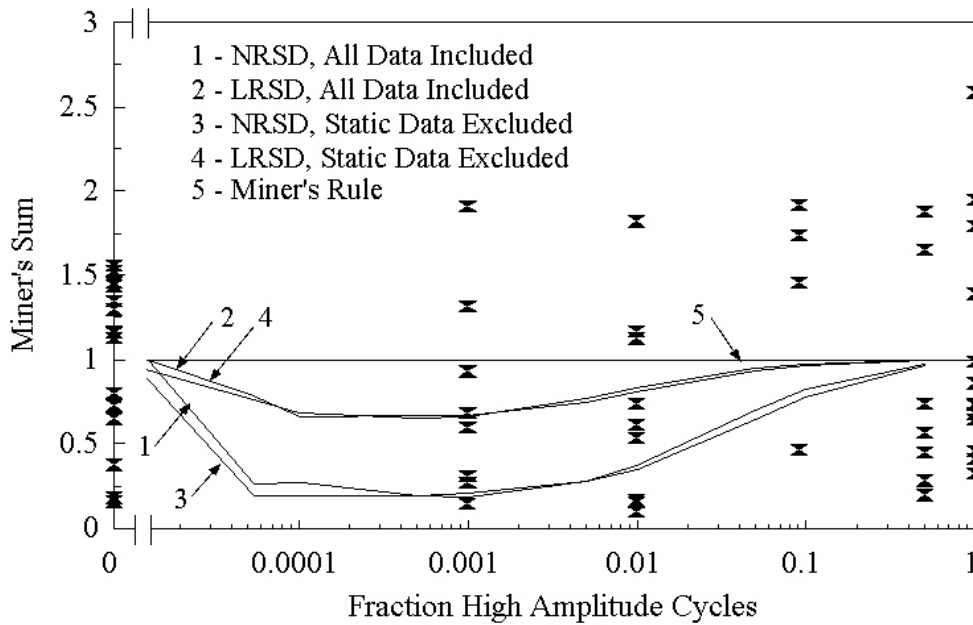
Figure 65. Two-Block Test Results for R = 10, -275 & -207 MPa; Exponential Fatigue Model With Linear and Nonlinear Residual Strength and Miner's Rule Lifetime Predictions.
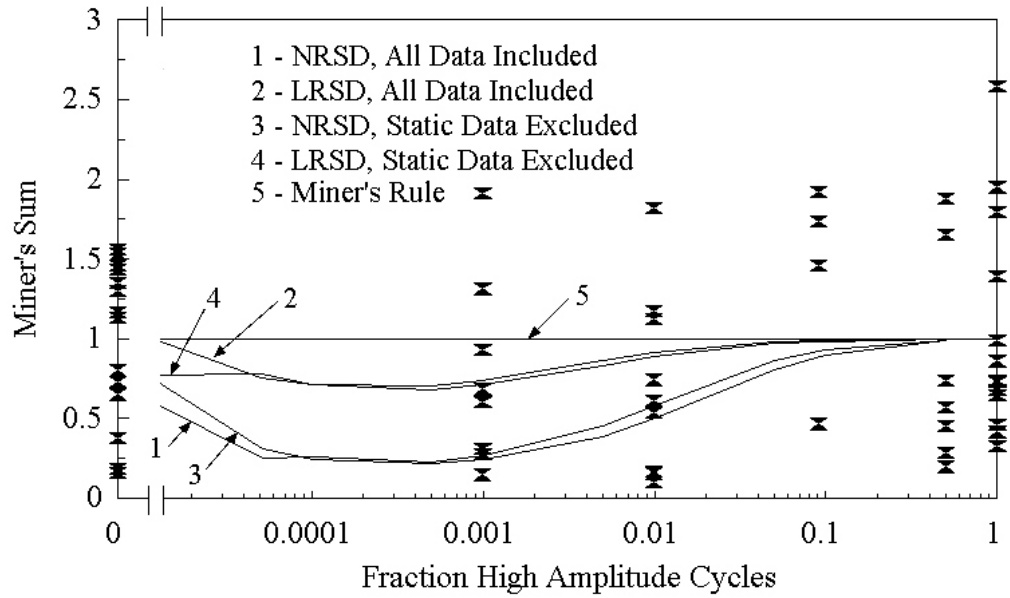
Figure 66. Two-Block Test Results for R = 10, -275 & -207 MPa; Power Law Fatigue Model With Linear and Nonlinear Residual Strength and Miner's Rule Lifetime Predictions.
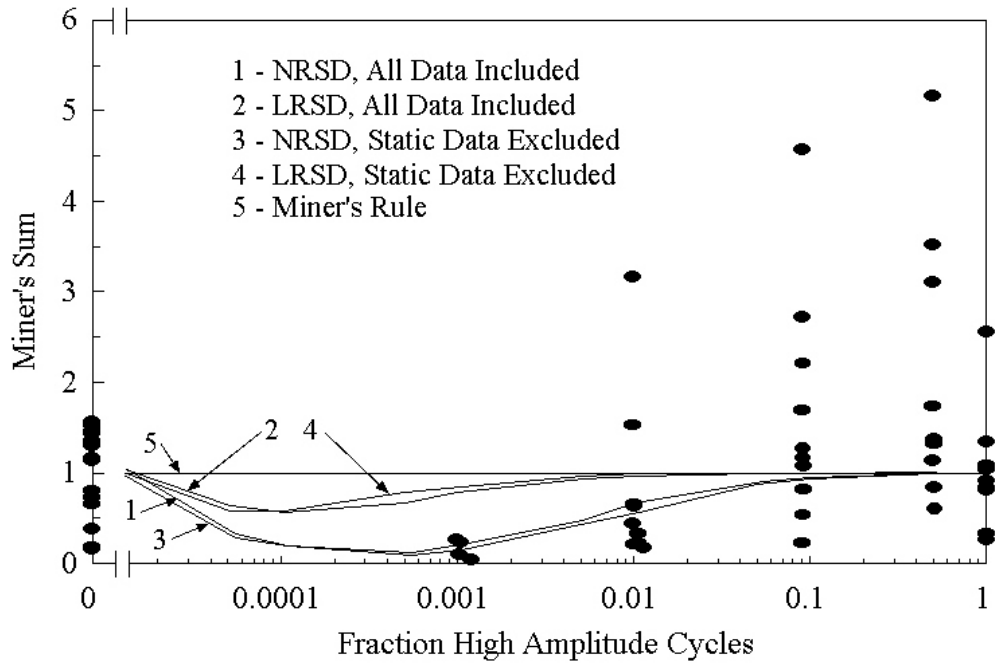
Figure 67. Two-Block Test Results for R = 10, -325 & -207 MPa; Exponential Fatigue Model With Linear and Nonlinear Residual Strength and Miner's Rule Lifetime Predictions.
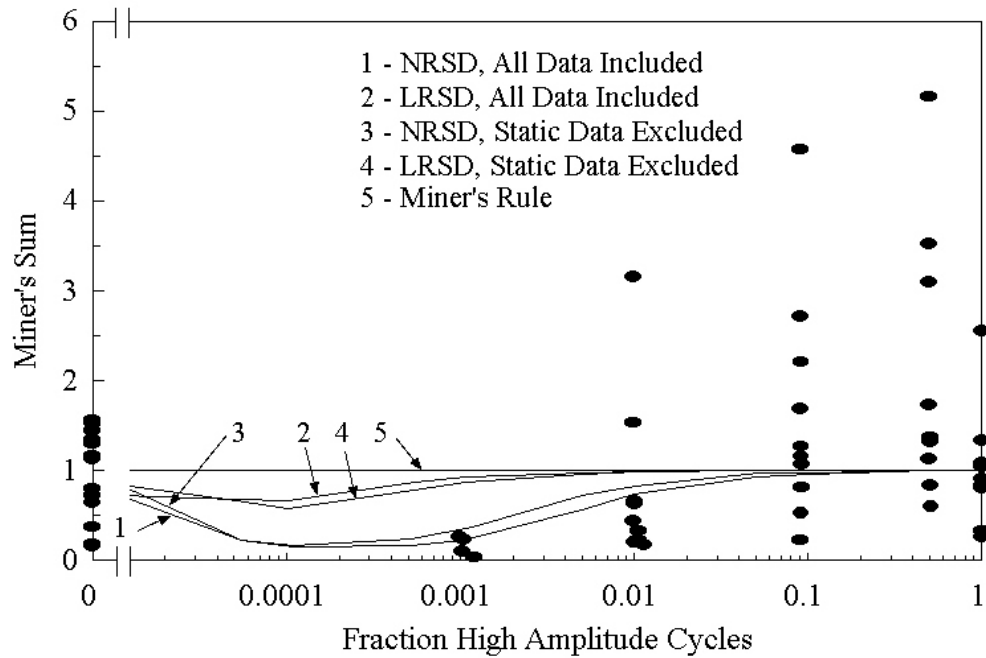
Figure 68. Two-Block Test Results for R = 10, -325 & -207 MPa; Power Law Fatigue Model With Linear and Nonlinear Residual Strength and Miner's Rule Lifetime Predictions.
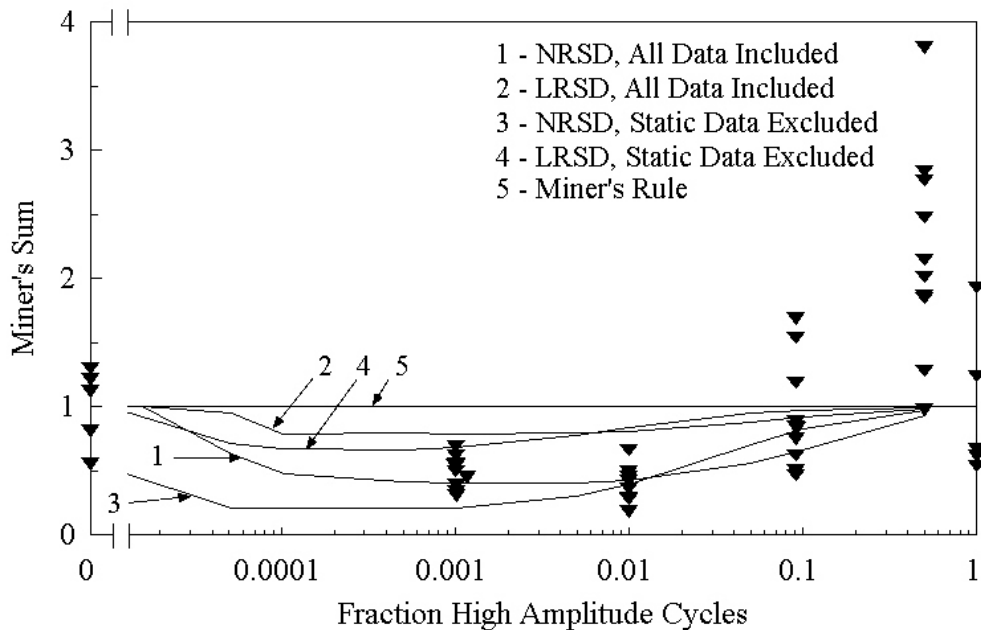
Figure 69. Two-Block Test Results for R = -1, 173 & 104 MPa; Exponential Fatigue Model With Linear and Nonlinear Residual Strength and Miner's Sum Lifetime Predictions.
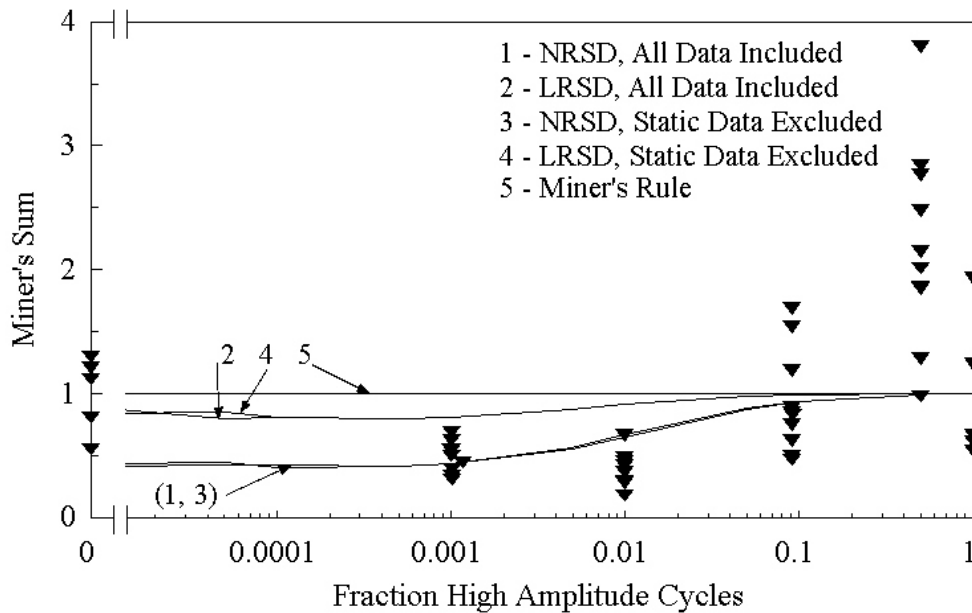
Figure 70. Two-Block Test Results for R = -1, 173 & 104 MPa; Power Law Fatigue Model With Linear and Nonlinear Residual Strength and Miner's Sum Lifetime Predictions.

Multi-Block Fatigue Testing

Additional blocks were added to increase the complexity of the spectrum used in fatigue testing of the selected laminate. Testing of three and six blocks was performed. The three block test spectrum was generally comprised of ten cycles of 414 MPa maximum stress, ten cycles of 325 MPa, and 100 cycles of 235 MPa, all at an R-value of 0.1. The sequencing of the blocks was varied. Testing results were summarized and are shown in Table 7.

The six block spectrum was arranged to the same format as that used by Echtermeyer, et. al., [49] and summarized in Table 8. Results of the six block testing are summarized in Table 9. Note, not all tests were conducted at the same maximum stress level.

The actual lifetime for each of the two, three and six block fatigue tests will be compared to the results of lifetime prediction models in a following section. The actual Miner's sums for each of these multi-block tests were less than one.

69

Table 7. Three-Block Test Results

Test Number	Block Cycles	Stress MPa	Actual Cycles to Specimen Failure	Miner's Sum at Failure
179	10	414	62	0.520
	100	325	600	
	1000	235	6000	
489	10	414	113	0.421
	10	325	110	
	100	235	1100	
490	10	325	180	0.653
	10	414	174	
	100	235	1700	
491	100	235	1600	0.576
	10	325	160	
	10	414	153	
492	10	414	123	0.458
	10	325	120	
	100	235	1200	
493	100	235	1634	0.599
	10	325	160	
	10	414	160	

Table 8. Six-Block Spectrum

Block #	Block Cycles	% Maximum Stress
1	1000	30
2	1000	50
3	400	75
4	10	100
5	400	75
6	1000	50

Table 9. Six-Block Test Results

Test Number	Block Cycles	Stress MPa	Actual Cycles to Specimen Failure	Miner's Sum at Failure
220	1000	97.5	26000	0.397
	1000	162.5	26000	
	400	243.75	10400	
	10	325	260	
	400	243.75	10337	
	1000	162.5	25000	
221	1000	103.5	8000	0.773
	1000	172.5	8000	
	400	258.75	3044	
	10	345	70	
	400	258.75	2800	
	1000	172.5	7000	
222	1000	124.2	2000	0.181
	1000	207	2000	
	400	310.5	654	
	10	414	10	
	400	310.5	400	
	1000	207	1000	
225	1000	103.5	5000	0.115
	1000	172.5	5000	
	400	258.75	2000	
	10	345	50	
	400	258.75	1857	
	1000	172.5	4000	
226	1000	82.8	48000	0.203
	1000	138	48000	
	400	207	19200	
	10	276	480	
	400	207	18968	
	1000	138	47000	

RANDOM SPECTRUM FATIGUE TESTING AND RESULTS

Fatigue testing of the selected laminate has covered constant amplitude and block spectra in the preceding sections. As loading of wind turbine blades is more random in nature, more random spectra also must be considered. Researchers in various industries have developed standard spectra for testing [16, 17]. The European wind research community developed WISPER (WInd turbine reference SPEctRum), a standardized variable amplitude loading history for wind turbine blades. Variations of this spectrum were created for use in this research.

WISPER and WISPERX

WISPER was developed from loading data collected from the root area of blades for wind turbines. The out-of-plane, or flap, loading was collected from nine horizontal axis wind turbines located in western Europe. The data were distilled into a sequence of 265,423 loading reversal points, or approximately 130,000 cycles. The reversal data are normalized to a maximum of 64 and a minimum of 1. In this form, the zero load level occurs at 25.

Analysis of WISPER revealed the spectrum has an average R-value of 0.4. The single largest peak and the single most extreme valley have an R-value of -0.67. The R-value for the adjacent largest spread between the peak and valley was -2.0.

Since the application of the WISPER spectrum at 10 Hertz would take nearly four hours to make one pass, the authors of WISPER derived a shortened version to speed fatigue testing. The shortened version was created by filtering the smaller amplitude cycles, which resulted in one-tenth of the number of cycles, see Figure 71. Consequently the name applied to the new spectrum was WISPERX, the X representing the significance of the one-tenth size. Of the approximately 13,000 cycles in the WISPERX spectrum, only 143 are reversing.

The WISPER authors list several purposes [17] for the standard spectrum, including the evaluation of component design and the "assessment of models for the prediction of fatigue and crack propagation life by calculation, like Miner's Rule." The latter of these purposes was applied in this research.

WISPERX Modifications

WISPERX was re-scaled from its normalized form to a form compatible with the Instron software, RANDOM. The results are shown in Figure 72. The scaling followed the equation:

$$y = \frac{[x - 25]}{[64 - 25]} \qquad \textbf{(18)}$$

where x are the published values for the reversal points and y is the scaled version. The convenience

of forcing the spectrum reversal points to a maximum of one allowed the application of any maximum stress level by a simple multiplier of value equal to the maximum stress level. Each value was saved in a format of sign (±) and the value to four significant figures (+#.####).
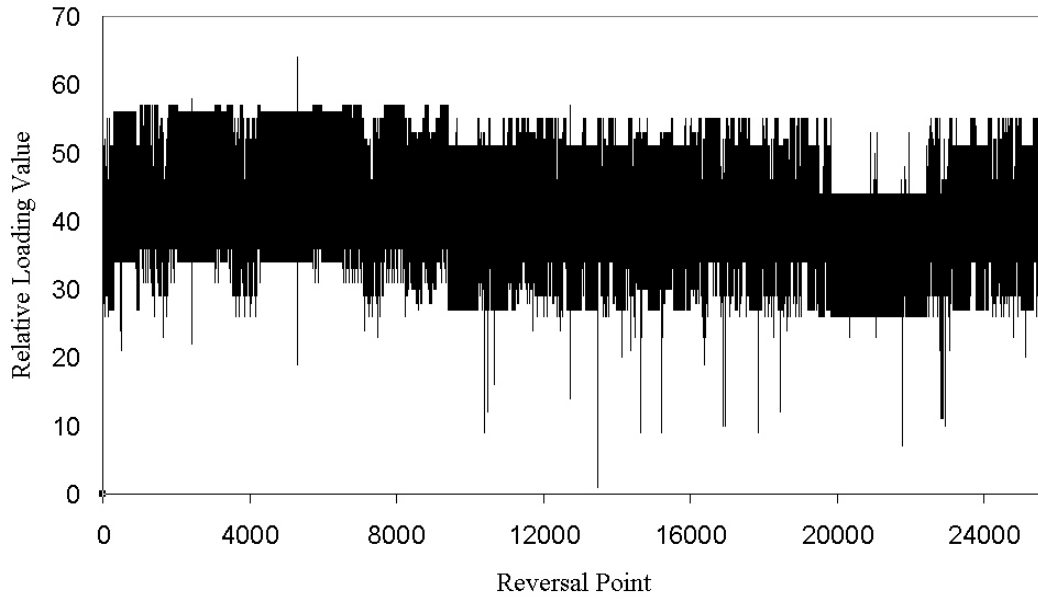
Figure 71. WISPERX Spectrum.
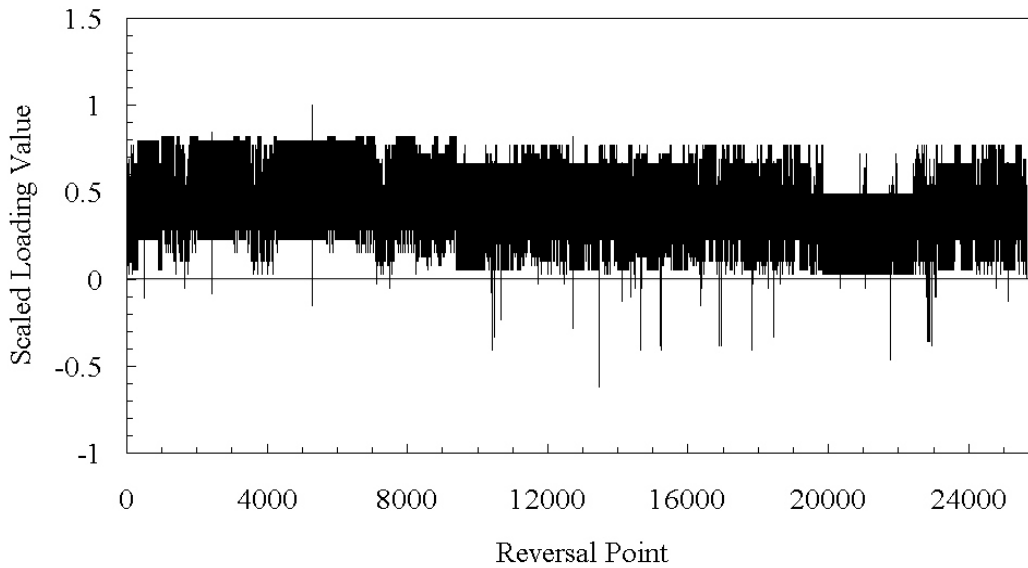
Figure 72. Scaled WISPERX Spectrum.

A wide range of R-values are present in WISPERX, yet only five R-values, other than the ultimate strengths, were tested in preparation of the base-line data. As a first step in applying this type of complex spectrum, it was decided to modify WISPERX to a constant R-value, thus avoiding both complex failure mode interactions and the need to interpolate between different R-values in the Goodman diagram. Two spectra were prepared, one for an R-value of 0.1 and one for 0.5. These modifications were accomplished by noting the peak reversal point and forcing the following valley (or trough) value to be either 0.1 or 0.5 times the peak value. A graphical version of these modifications is shown in Figure 73.
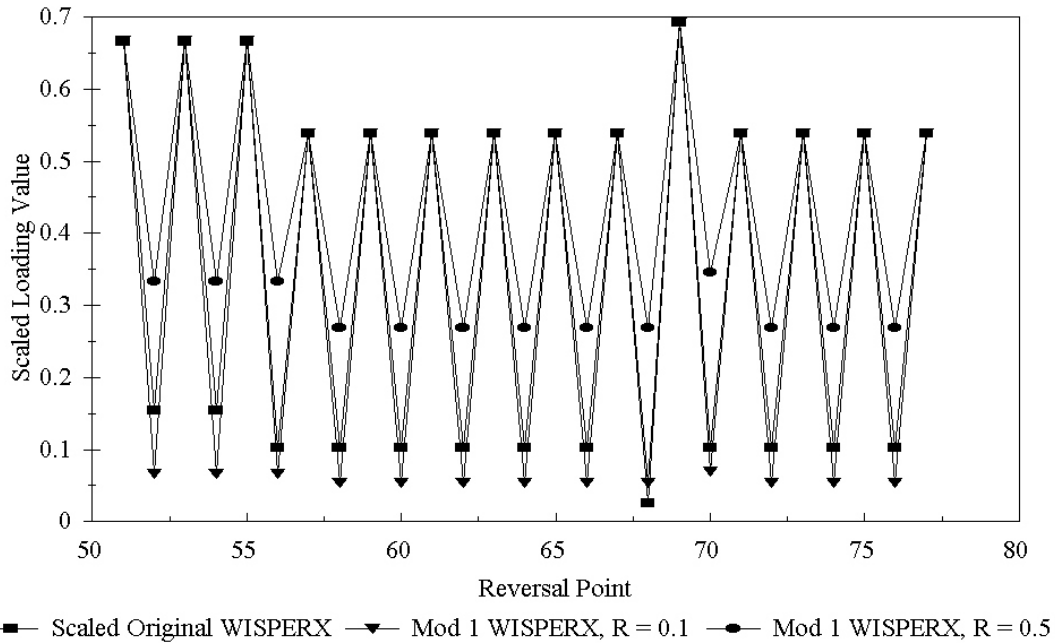
Figure 73. Modified WISPERX Spectrum Example.

Two forms of the modified spectrum were created, both forced the constant R-values, but the first, termed Mod 1, retained only the tension-tension peak-valley reversal points, while the second, Mod 2, retained all reversal points. The first spectrum did not contain the one time extreme condition that was in the original WISPER and WISPERX spectra, while Mod 2 retained this one-time high-load event. Visual appreciation of these spectra can be gained from Figures 74, 75 and 76. Note the single relatively large event occurring at approximately the 5000th reversal point in the Mod 2 spectrum, Figure 76.
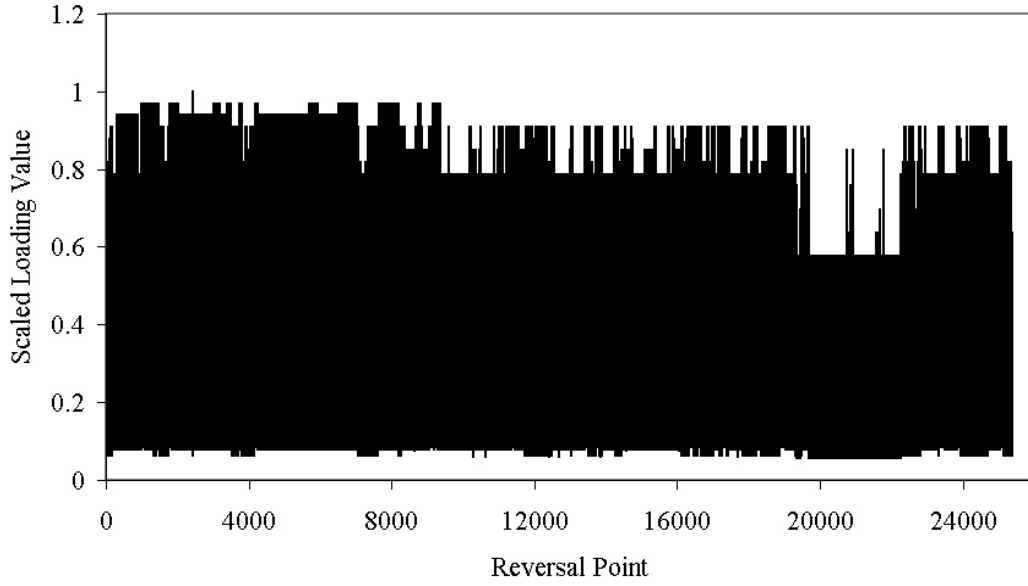
Figure 74. Mod 1 Spectrum for R = 0.1.
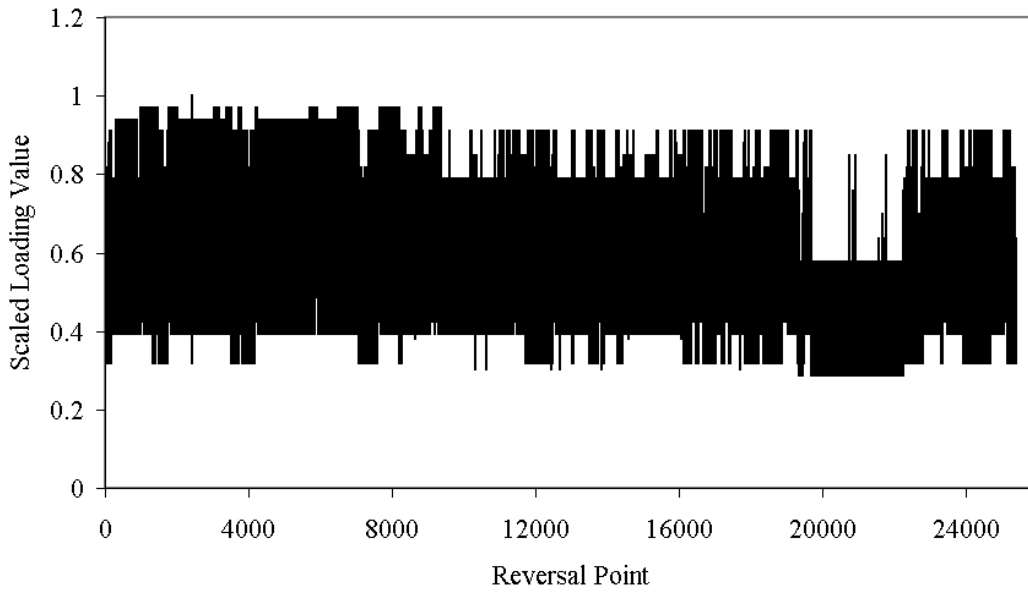
Figure 75. Mod 1 Spectrum for R = 0.5.
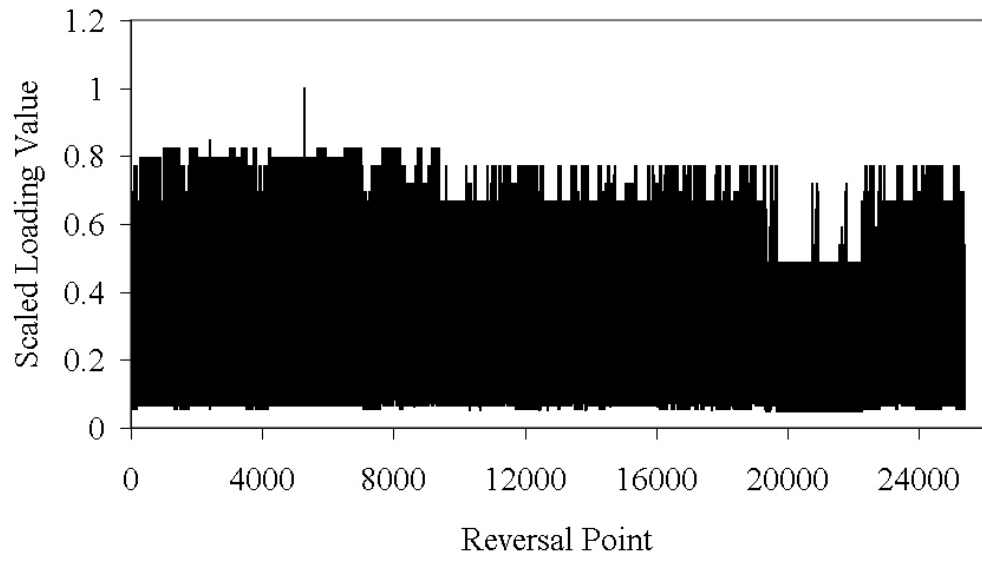
Figure 76. Mod 2 Spectrum for R = 0.1.

Modified WISPERX Spectrum Test Results

Tests were run for these spectra with the loads taken as a multiples of the scaled values. The data are then represented in conventional S-N format where the stress coordinate is the maximum stress in the spectrum. The multiplier is varied to achieve relatively higher or lower stress cases having shorter or longer lifetimes, respectively.

The results for the Mod 1 and 2 spectra are summarized in Figures 77, 78 and 79. The trend of longer lifetimes for the R-value case of 0.5 were also experienced in the constant amplitude testing. Some high stress cases fail prior to completing one full pass through the spectrum. Tables 10 and 11 include a summary of the regression parameters for WISPERX test results for the exponential and power law regression analyses, respectively. These can be compared to the constant amplitude regression results presented in Tables 4 and 5. Reference equations 7 and 8 for definition of the terms C_1, b, C_2 and m. For reference, approximately 13,000 cycles is equivalent to one block of the WISPERX spectra.

Table 10. Exponential Regression Analysis Parameters for WISPERX Fatigue

Range of Applicability	Regression Coefficients	Spectrum			
		Mod 1, R=0.1	Mod 1, R =0.5	Mod 2, R = 0.1	WISPERX
1 to 10^7 Cycles	C_1	1.007	1.019	1.015	1.029
	b	0.121	0.107	0.106	0.107
10 to 10^7 Cycles	C_1	0.879	0.941	0.891	0.872
	b	0.094	0.091	0.093	0.079

Table 11. Power Law Regression Analysis Parameters for WISPERX Fatigue

Range of Applicability	Regression Coefficients	Spectrum			
		Mod 1, R=0.1	Mod 1, R =0.5	Mod 2, R = 0.1	WISPERX
1 to 10^7 Cycles	C_2	1.048	1.056	1.075	1.041
	m	12.02	14.52	13.9	14.2
10 to 10^7 Cycles	C_2	1.111	1.179	1.126	1.21
	m	11.28	12.72	13.1	12.2
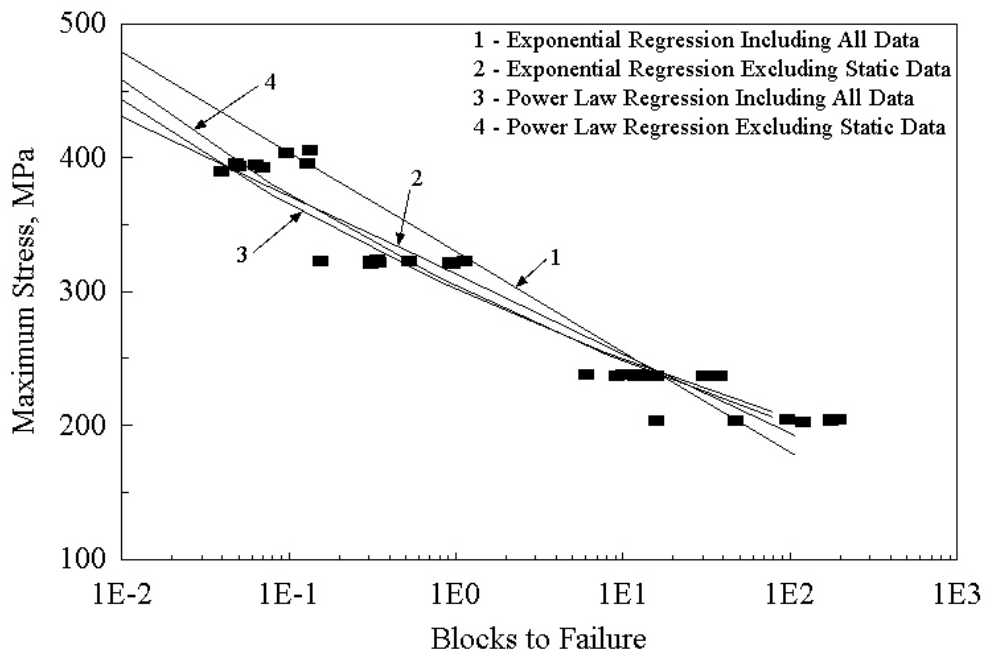
Figure 77. Mod 1 Spectrum Fatigue S-N Curve, R = 0.1.
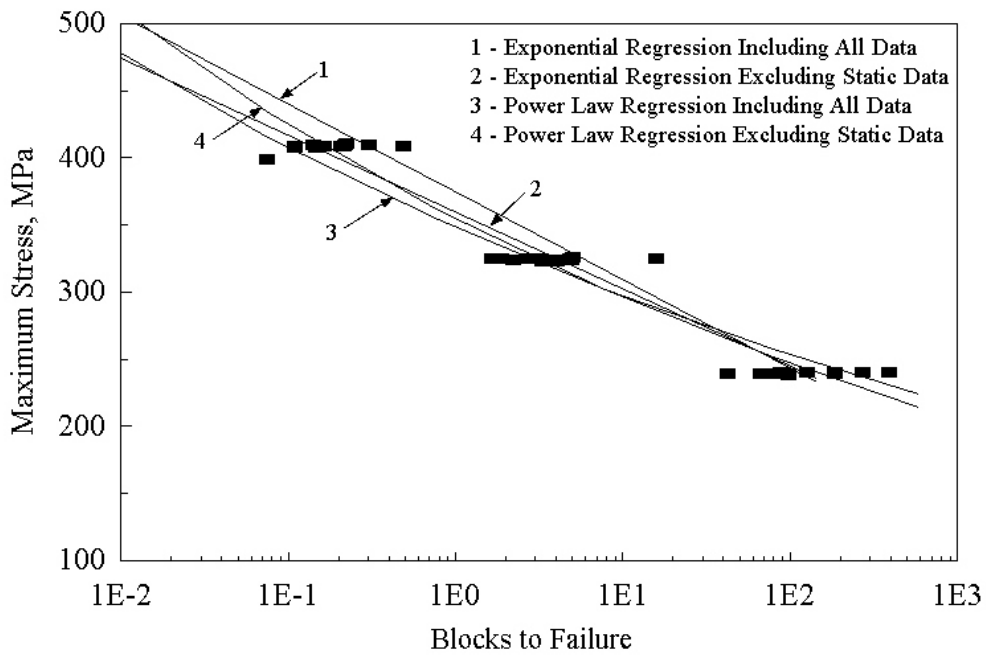
Figure 78. Mod 1 Spectrum Fatigue S-N Curve, R = 0.5.
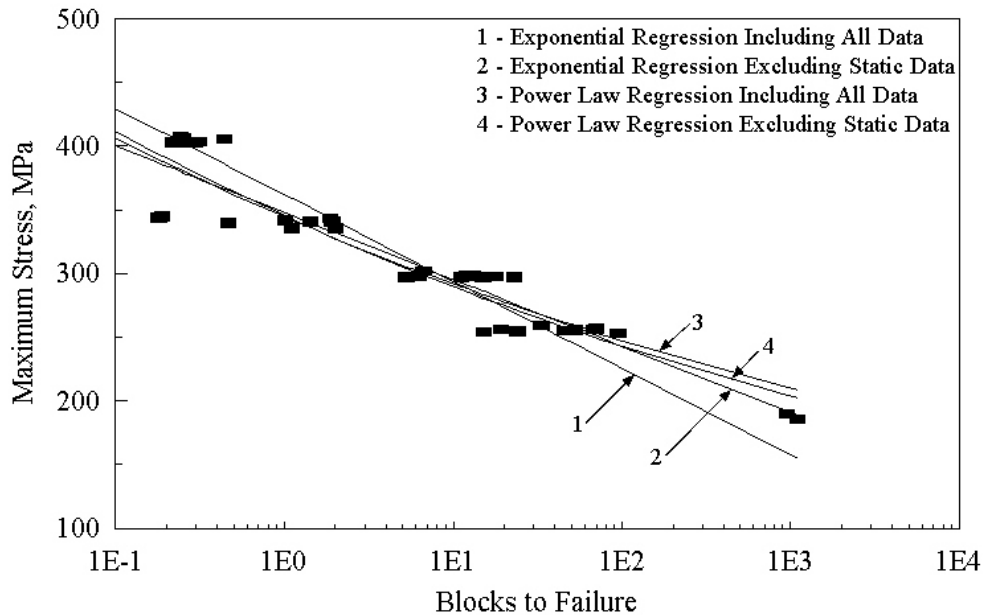
Figure 79. Mod 2 Spectrum Fatigue S-N Curve, R = 0.1.

The slope or trend of the S-N curve in the Mod 2 case is less than that of the comparable case for the Mod 1 spectrum results. The maximum stress incurred in the Mod 2 spectrum tests was a once per pass event, while the maximum stress incurred in the Mod 1 spectrum tests was experienced several times per pass.

Unmodified WISPERX Spectrum Test Results

Testing of coupons that were subjected to the original WISPERX spectrum, without modification for R-value, was also accomplished and summarized as exponential and power law S-N curves, Figure 80. The power law regression gives only slightly better correlation than the exponential regression. The regression analysis may be reviewed in Appendix D.

The actual lifetime for the random tests will be compared to the results of lifetime prediction models in the next section.
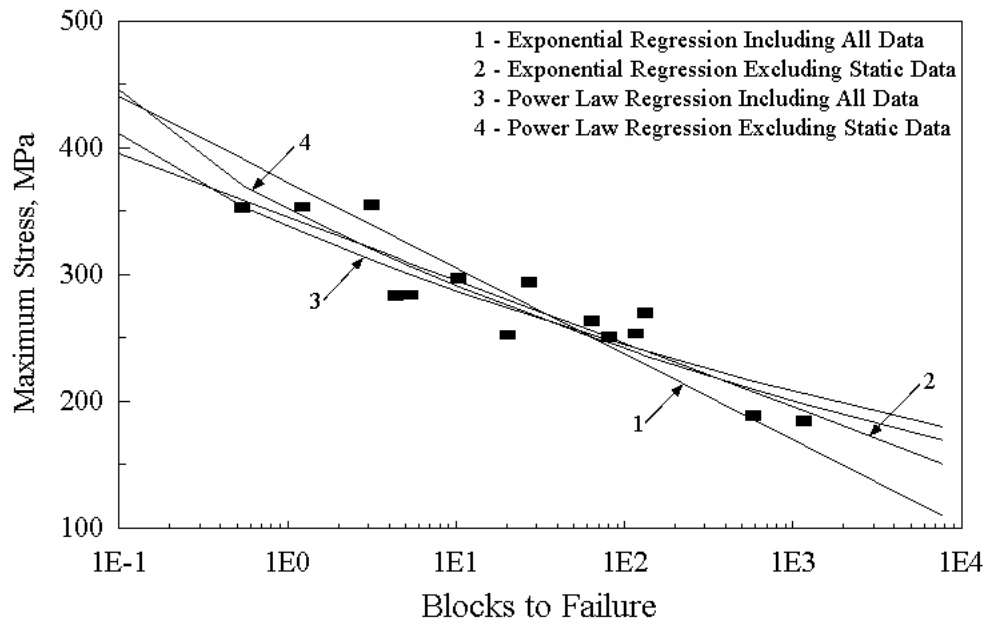
Figure 80. Unmodified WISPERX Spectrum Fatigue S-N Curve.

LIFETIME PREDICTIONS

An accurate cumulative damage law is essential to efficient component design under fatigue loading. The fundamental and most widely applied damage law is that established by Palmgren [22] and Miner [6]. Under this law, damage is considered to develop linearly as a function of the number of cycles encountered at specific load levels. As reported earlier, Miner's sum is consistently less than unity, often on the order of 0.1, for tests using a spectrum of loads.

A component or specimen is considered to have failed when it can no longer support the load intended. One clear deficiency in Miner's sum is that it only accumulates damage and does not consider that the current strength may be exceeded by a particular high stress cycle, whereas residual strength based models inherently consider this event. Three models have been applied to lifetime predictions for theoretical specimens subjected to the various block and modified WISPERX spectra. Results of these predictions are compared to the actual lifetimes encountered during the testing. The three models considered are, 1) Miner's Rule, 2) linear residual strength degradation, and 3) nonlinear residual strength degradation. Constant amplitude fatigue models based upon exponential and power law regression analyses as well as the retention and omission of the static data were used in the residual strength based lifetime prediction rules. All results of predictions are reported in Miner's sum and compared to the actual Miner's sums from test results.

Constant Amplitude Fatigue Life Predictions

The base-line data of the constant amplitude testing was the starting point for the creation of lifetime predictions. The mean number of cycles to failure at each constant amplitude load level was used in all subsequent lifetime predictions; this would force the constant amplitude test Miner's sums to an average value of one. Therefore, the Miner's rule would reasonably accurately predict the lifetime for constant amplitude fatigue tests. Using either the linear or nonlinear residual strength lifetime prediction models for a constant amplitude test would reveal the same results as Miner's rule. Note the equations for the two residual strength degradation prediction methods, equations 13 and 14. Failure would be predicted by either of these equations when the residual strength was reduced to a level equivalent to the applied stress. This would happen when the number of cycles experienced, n, was equal to the number of cycles to failure, N, at that stress level. The constant amplitude test Miner's sum results are presented in Table 12. The "scatter" of Miner's sum for constant amplitude fatigue tests is greater than that experienced with metals.

81

Table 12. Descriptive Statistics for Constant Amplitude Miner's Sum

Case	Mean	Standard Deviation
414 MPa, R = 0.1	1	0.631
327 MPa, R = 0.1	1	0.692
245 MPa, r = 0.1	1	0.682
207 MPa, R = 0.1	1	0.644
414 MPa, R = 0.5	1	0.486
327 MPa, R = 0.5	1	0.820
25 MPa, R = 0.5	1	0.840
-325 MPa, R = 10	1	0.638
-275 MPa, R = 10	1	0.681
-245 MPa, R = 10	1	1.942
-207 MPa, R = 10	1	0.484
-275 MPa, R = 2	1	1.686
173 MPa, R = -1	1	0.591
145 MPa, R = -1	1	0.281
104 MPa, R = -1	1	0.309

Block Spectrum Fatigue Life Prediction Mechanics

Miner's Rule Lifetime Prediction Methodology

Miner's rule predictions are easily accomplished by accumulating the sums of each cycle ratio for each cycle of each block and repeating the sequence of blocks until this sum reaches unity. The cycle ratio for each cycle would be one (i.e. the single cycle) divided by the average number of cycles to failure at that cycle's stress level. This method is summarized in Figure 81.

```
          ┌─────────────────────────┐
          │  Set Miner's sum = zero │
          └─────────────────────────┘
                      │
                      ▼
          ┌─────────────────────────┐
          │   Read next cycle's     │◄──────┐
          │   stress level from file│       │
          └─────────────────────────┘       │
                      │                      │
                      ▼                      │
          ┌─────────────────────────┐       │
          │  Determine N based upon │       │
          │ current cycle's stress  │       │
          │         level           │       │
          └─────────────────────────┘       │
                      │                      │
                      ▼                      │
          ┌─────────────────────────┐       │
          │  Add 1/N to Miner's sum │       │
          └─────────────────────────┘       │
                      │                      │
                      ▼                      │
                   ◇                         │
              Miner's            No          │
              sum = 1  ──────────────────────┘
                   ◇
                   │
                  Yes
                   │
                   ▼
          ┌─────────────────────────┐
          │    Record number        │
          │     of cycles           │
          └─────────────────────────┘
```
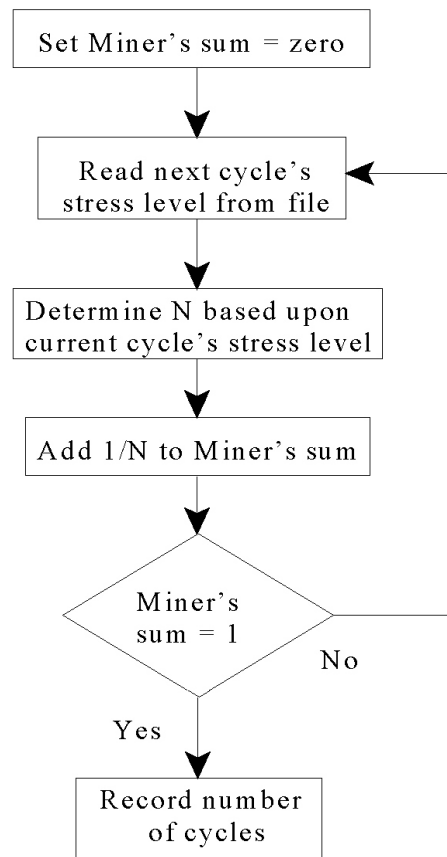
Figure 81.Miner's Sum Lifetime Prediction Methodology.

Residual Strength Rule Based Lifetime Prediction Methodology

Consider a life prediction based upon the linear residual strength model for a two block fatigue spectrum where the first block is n_1 cycles long at a high stress level. The second block at a lower stress level is n_2 cycles long. Trace the strength through the application of a succession of blocks as shown in Figure 82.

Starting with the ultimate strength, the strength decreases monotonically with each cycle in the first block until strength, s_1, is reached after n_1 cycles of high stress. The residual strength s_1 would be the starting strength for fatigue at the stress level of the second block. The corresponding number of cycles theoretically experienced at this strength, s_1, would be n_2'. Fatigue for n_2 cycles in the second block would extend the theoretically experienced cycles from n_2' to n_2'' where $n_2'' - n_2' = n_2$, the number of cycles in the second block. The residual strength at this point in life is s_2, which would be the starting point for the next block, a repeat of the high stress cycle block. The corresponding number of theoretical cycles for at this stress level is n_3'. Fatigue at the high stress cycles would extend the number of cycles to n_3''. Since n_1 is the number of cycles in the first high stress block, then $n_3'' - n_3' = n_1 = n_3$. This process would continue until the residual strength reduces to a value equal to the applied stress.

The calculation process is identical for both the linear and nonlinear residual strength degradation prediction models. The process is valid for blocks as short as one cycle; hence, it is easily applied to random spectra as well as block spectra. The mechanics of these calculations were reduced to a computer algorithm to ease and speed data reduction.
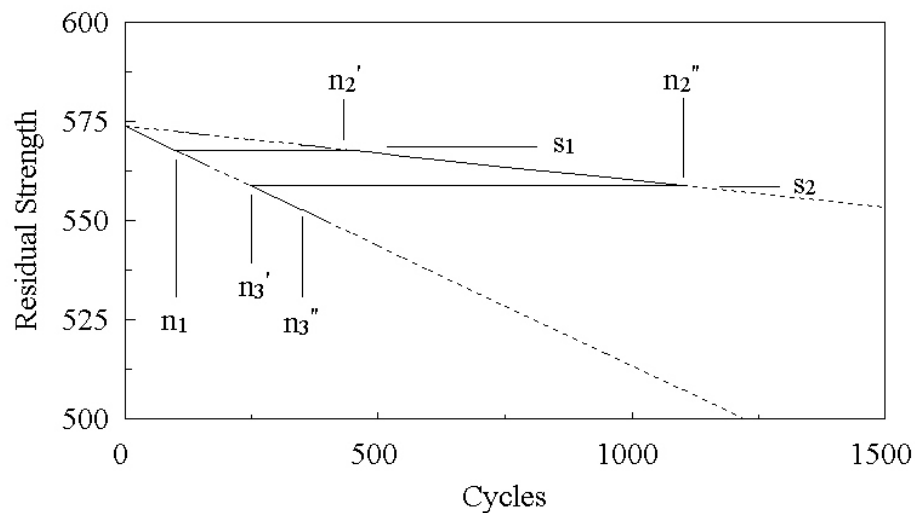
Figure 82. Lifetime Prediction Cycle Trace, Residual Strength Models.

<u>Two-Block Spectrum Fatigue Life Predictions</u>

The results of two-block spectrum fatigue tests were summarized in Figures 49 through 70 as a comparison of the Miner's sum related to the fraction of the high amplitude cycles experienced. The results of various lifetime prediction calculations were also shown on those figures. All but one of the multi-block fatigue test campaigns were performed in specific R-value regions where the mode of failure, tensile or compressive, was expected. This precluded the problem of lifetime predictions for mixed failure mode fatigue. The three prediction methods were applied in nine various configurations which are identified in Table 13 and applied for each load case.

Table 13. Lifetime Prediction Methods

1) Miner's linear rule
2) linear residual strength based with exponential fatigue model of all data
3) linear residual strength based with exponential fatigue model excluding static data
4) linear residual strength based with power law fatigue model of all data
5) linear residual strength based with power law fatigue model excluding static data
6) nonlinear* residual strength based with exponential fatigue model of all data
7) nonlinear* residual strength based with exponential fatigue model excluding static data
8) nonlinear* residual strength based with power law fatigue model of all data
9) nonlinear* residual strength based with power law fatigue model excluding static data
* all nonlinear residual strength predictions assumed $\nu = 0.265$.

<u>General Observations</u>

The limit values for the fraction of high amplitude cycles for the two-block tests are zero and one. A zero fraction represents a constant amplitude fatigue test conducted at the lower stress level while a fraction of one represents the results of a constant amplitude fatigue test at the higher stress level. Consequently, the average of the Miner's sums at the limits must be one, as summarized in Table 12.

A general trend of Miner's sums of less than one is noted in the region between fractions of zero and one. The Miner's rule prediction is a constant value of 1.0 throughout the entire range of high amplitude cycle fractions, indicating the Miner's rule generally predicted a longer life than observed.

The relative magnitudes of the two stress levels had an effect on the variation of the Miner's sum over the range of the high cycle fraction. Test cases that had relatively close stress levels responded

with a lesser variation in the Miner's sum whereas cases with a large difference in stress levels indicated a greater variation or dip in the Miner's sum. The former observation is logical when considering the limiting case of equal stress levels for each block. This would be a constant amplitude fatigue case for which the Miner's sum would be 1.0.

Comparison of Residual Strength Based Lifetime Prediction Rules

The nonlinear rule with $\nu = 0.265$ consistently provided Miner's sums less than those predicted by the linear residual strength degradation rule. This was assured by choosing the nonlinear parameter to be less than one, thereby forcing the predictions to more closely follow test results. Choosing a nonlinear parameter greater than unity would have caused the nonlinear Miner's sums to be greater than those calculated by the linear residual strength degradation method. Both methods trend towards unity at the limits of the high cycle fraction as shown in all Figures 49 through 70. In some cases such as that of Figures 55 and 59, the prediction stabilizes at unity for a range of cycle fractions above zero. In these cases, reducing the high cycle fraction below some value was not possible in that the predicted failure was always in the second low amplitude stress block, and the first high amplitude stress block was never repeated.

The linear and nonlinear methods produce converging Miner's sum predictions when the two block stress levels become closer. Typical examples of this latter observation are those in Figures 49 and 57 for R-values of 0.1 and Figures 65 and 67 for R-values of 10.

Fatigue Model Selection Effect on Predictions

The fatigue models (equations 7 and 8) were based upon the regression analyses of the constant amplitude fatigue test results. There were four basic models prepared: 1) exponential regression analysis that included all fatigue data for each R-value; 2) exponential regression analysis that excluded the static data; 3) power law regression analysis that included all fatigue data; and 4) power law regression analysis that excluded the static data. As there is some concern of possible differences in damage metrics that occur in high stress fatigue, including static tests, and the fatigue at lower stress levels, two fatigue models were prepared for consideration. This also allows breaking the regression results that represent the S-N fatigue data into a series of curves, each considered valid over a range of component life.

Generally, the nonlinear residual strength degradation based prediction models are sensitive to which of the four fatigue models is chosen, whereas the linear strength degradation based predictions models are insensitive. Consider Figure 26, the S-N diagram for constant amplitude fatigue at R-values of 0.1. The power law regression models for both cases of including and excluding the static data are nearly identical. This can also be seen in Figure 50 for the nonlinear lifetime predictions for the two-block case of block stresses of 414 and 325 MPa with R-values of 0.1. The exponential regression models represented in Figure 30 are quite different for the cases of including and excluding the static data. At the higher cycles, an equivalent higher stress is required to cause failure for the exponential fatigue model that excludes the static data than that which includes the static data. Again, this is borne out in the predictions summarized in Figure 49, where the Miner's sums at the low cycle

fractions are greater for the exponential fatigue model that excluded the static data than for that which included the static data.

The nonlinear residual strength based prediction rules provided better agreement with test results than did the linear based rule. Generally, the selection of the fatigue model had little influence in the predictions, at least for the cases of two-block spectra.

Three and Six-Block Spectrum Fatigue Life Predictions

The actual Miner's sums for the three and six block tests (spectra shown in Tables 7 and 8) were consistently less than one, as summarized in Tables 14 and 15. The linear residual strength model predictions of the Miner's sum were always higher than the actual Miner's sums. The nonlinear residual strength model predictions of the Miner's sum were mostly higher than the actual.

Note the predictions for the both linear and nonlinear models are closer to the actual than what would have been predicted by Miner's rule. The nonlinear prediction is closer to the experimental value than the linear prediction in every case.

Modified WISPERX Spectra Fatigue Life Predictions

Predictions for the modified WISPERX spectra were made along the same lines as for block spectra. Predictions based on the three models were reduced to a graphical form of the S-N curve type as in Figures 83 through 88 based upon the exponential and power law fatigue models. The shape of the curves in the higher stress region has abrupt changes in slope that occur at identifiable cycles in the spectrum. The incremental stress level used in the calculation of the lifetimes has an effect on the overall shape of these curves, yet the general trend can be ascertained from the presented figures. In general, the Miner's rule and the linear residual strength degradation models produce similar predictions, while the nonlinear residual strength degradation model is more conservative.

Figures 83 and 84 include the lifetime predictions for the Mod 1 WISPERX spectrum at an R-value of 0.1 for the exponential and power law fatigue models, respectively. The trend of this spectrum, shown in Figure 74, has a change in the average maximum stress level at around the 9,000th reversal point (4,500th cycle) and another at approximately the 19,000th reversal point (9,500th cycle). These are consistent with the changes in the slope in Figures 83 and 84. The scale compression of the logarithm prevents the observation of these slope changes for the higher cycle (greater number of blocks) regime. The power law fatigue model appears to provide a better correlation with the experimental data than the exponential fatigue model for the high cycle regime and for any of the three prediction models.

Table 14. Three-Block Spectrum Fatigue Life Predictions

Test Number	Sequence Cycles	Load	Actual Cycles	Miner's Sum		
				Actual	Linear Prediction	Non-Linear Prediction
179	10	414	62	0.520	0.770	0.282
	100	325	600			
	1000	235	6000			
489	10	414	113	0.421	0.920	0.657
	10	325	110			
	100	235	1100			
490	10	325	180	0.653	0.918	0.651
	10	414	174			
	100	235	1700			
491	100	235	1600	0.576	0.916	0.648
	10	325	160			
	10	414	153			
492	10	414	123	0.458	0.920	0.657
	10	325	120			
	100	235	1200			
493	100	235	1634	0.599	0.916	0.648
	10	325	160			
	10	414	160			

Table 15. Six-Block Spectrum Fatigue Life Predictions

Test No.	Sequence Cycles	Load	Actual Cycles	Miner's Sum		
				Actual	Linear Prediction	Non-Linear Prediction
220	1000	97.5	26000	0.397	0.758	0.335
	1000	162.5	26000			
	400	243.75	10400			
	10	325	260			
	400	243.75	10337			
	1000	162.5	25000			
221	1000	103.5	8000	0.173	0.747	0.296
	1000	172.5	8000			
	400	258.75	3044			
	10	345	70			
	400	258.75	2800			
	1000	172.5	7000			
222	1000	124.2	2000	0.181	0.677	0.203
	1000	207	2000			
	400	310.5	654			
	10	414	10			
	400	310.5	400			
	1000	207	1000			
225	1000	103.5	5000	0.115	0.747	0.296
	1000	172.5	5000			
	400	258.75	2000			
	10	345	50			
	400	258.75	1857			
	1000	172.5	4000			
226	1000	82.8	48000	0.203	0.814	0.406
	1000	138	48000			
	400	207	19200			
	10	276	480			
	400	207	18968			
	1000	138	47000			

Figures 85 and 86 are a summary of the lifetime predictions for the Mod 1 WISPERX spectrum at an R-value of 0.5. The general slope of these prediction curves are less than those of the same spectrum at an R-value of 0.1, as might be expected based upon the results of the constant amplitude fatigue testing. The changes in slope of the predictions are again due to changes in the load values, as evident in Figure 75 for this spectrum. There is little difference among the results for the three prediction models, although the power law fatigue model may provide a better overall correlation with the data at the high stress level. The exponential model appears to provide a better correlation at the low stress level, yet the trend at the lowest stress levels does require further investigation.

Figures 87 and 88 are the results of lifetime predictions for the Mod 2 WISPERX spectrum. The much more dramatic change in slope evident in these figures is a result of the single high load cycle present in this spectrum at approximately the 5,000th reversal point (2,500th cycle) as evident in Figure 76. In general, the lifetime predictions based upon the power law fatigue model provide better correlation with the experimental data than does the exponential fatigue model. The nonlinear strength degradation lifetime prediction method provides a closer correlation to the data than does the other two models. The greater differences in the stress levels created by the presence of the single high load cycle, seems to cause greater variability of the prediction produced by the three models.
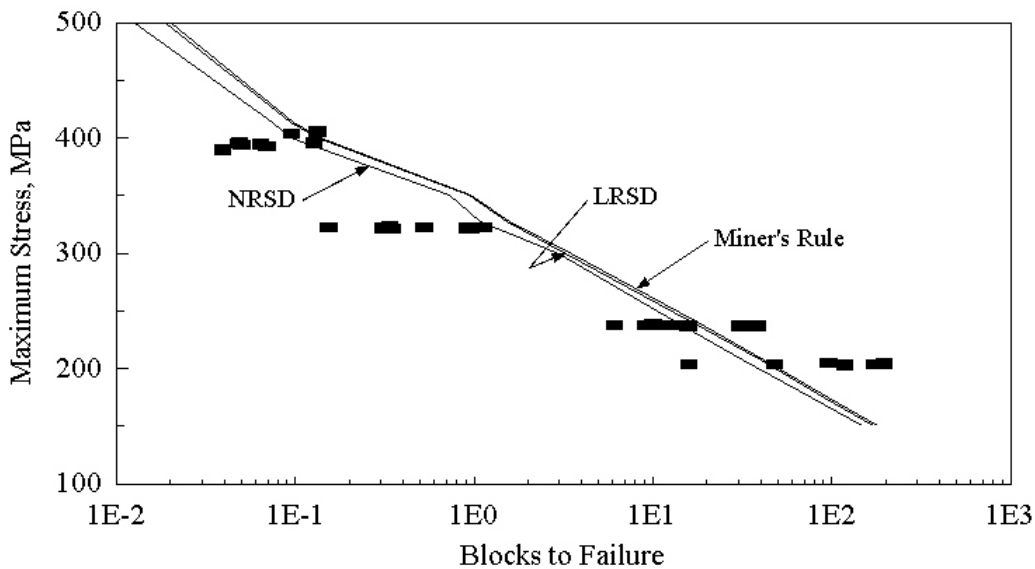
Figure 83. Mod 1 Spectrum Lifetime Predictions, R = 0.1 Exponential Fatigue Model Including All Data.
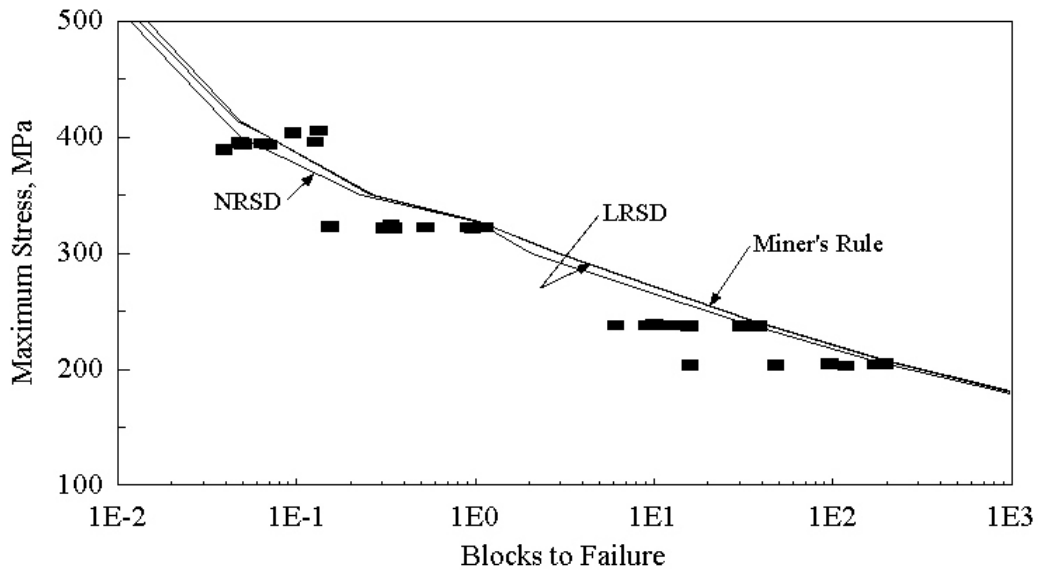
Figure 84. Mod 1 Spectrum Lifetime Predictions, R = 0.1 Power Law Fatigue Model Including All Data.
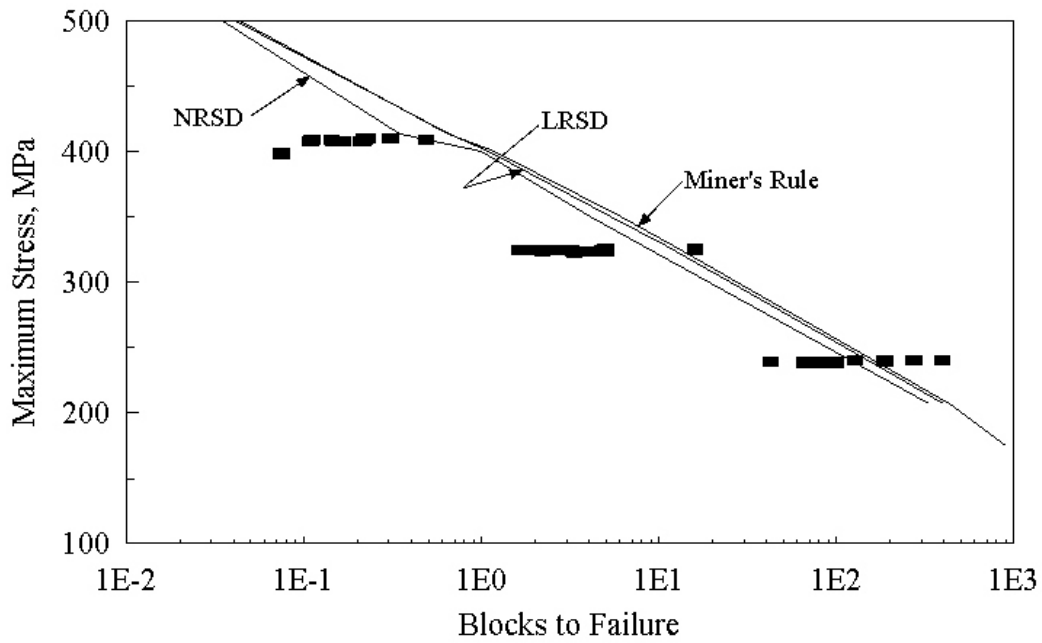
Figure 85. Mod 1 Spectrum Lifetime Predictions, R = 0.5 Exponential Fatigue Model Including All Data.
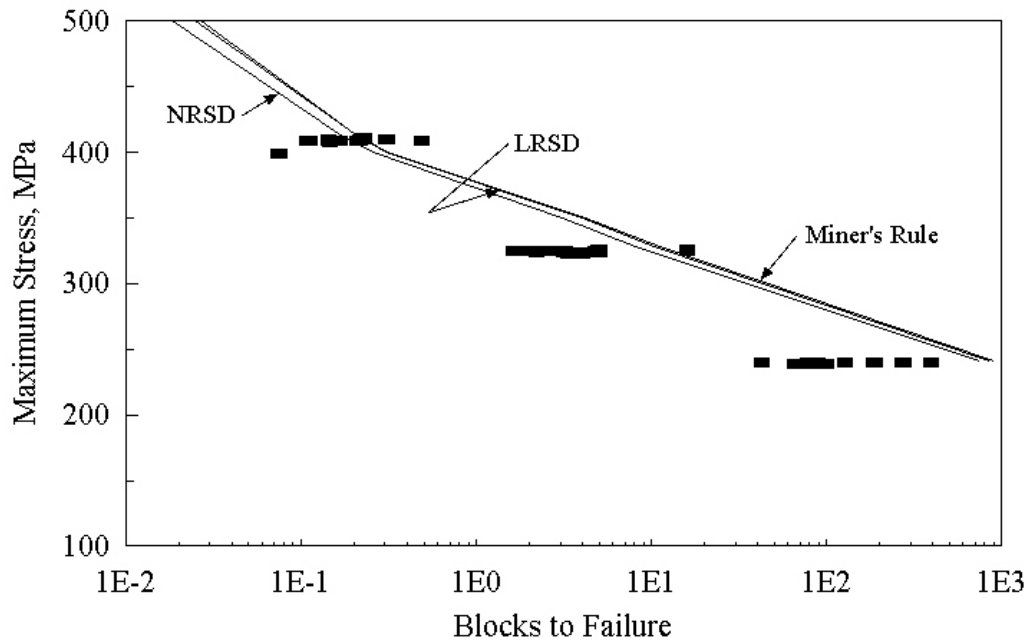
Figure 86. Mod 1 Spectrum Lifetime Predictions, R = 0.5 Power Law Fatigue Model Including All Data.
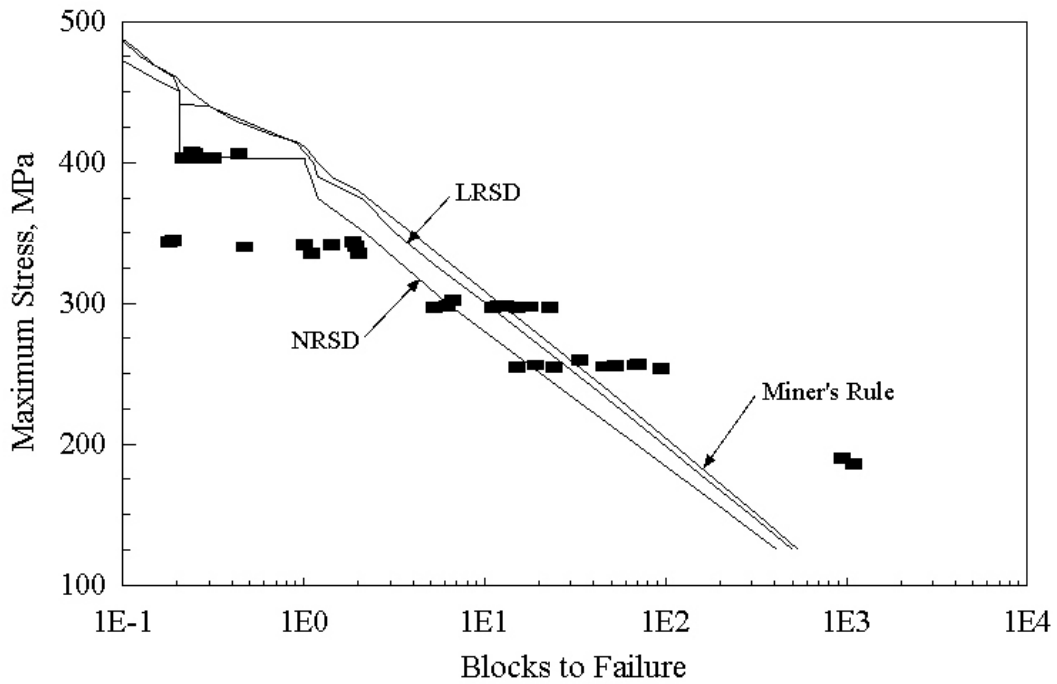
Figure 87. Mod 2 Spectrum Lifetime Predictions Exponential Fatigue Model Including All Data.
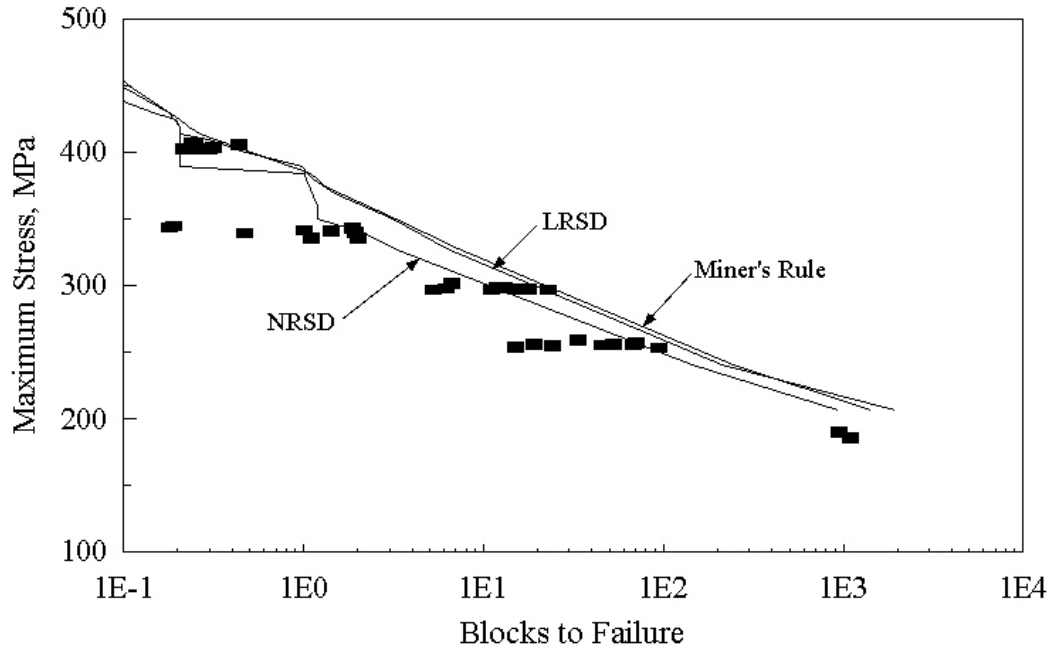
Figure 88. Mod 2 Spectrum Lifetime Predictions Power Law Fatigue Model
Including All Data.

It, therefore, seems that the selection of the prediction model becomes important when the variability of the stress levels in the spectrum becomes greater, as was the case in the Mod 2 spectrum.

The choice of the fatigue model becomes important for the case of a modified WISPERX spectrum fatigue predictions at the low stress/high cycle regime, where more of the cycles are at stress levels where the constant amplitude data must be extrapolated beyond the experimental data. The power law fatigue model provides a better correlation to data.

Block or Cycle Damage Contributions

Are all stress levels important in the fatigue of the laminate, or is one set of levels more damaging than others, to the point that all other stress cycles can be ignored? If the cycle ratio (the ratio of cycles experienced to cycles to failure, equation 3) is an indication of the damage contribution at each level, which is the premise of all three models investigated herein, then comparisons of the cycle ratio at each stress level can answer this question.

Consider the heavily tested two-block case of R = 0.1 with the two maximum stress levels of 325 and 207 MPa. There were over 100 tests performed at the approximate high amplitude cycle fractional ratio of 0.01 (reference Figure 62, Chapter 6). The average tested Miner's sum for this case was 0.287, with a standard deviation of 0.222. Compare these statistics to the constant amplitude test results of Miner's sums of one. The average two-block Miner's sum was considerably less than one, while the standard deviation was also less, indicating less scatter for the

93

block testing. The average calculated damage contribution based on Miner's sum due to the higher stress cycles was 36 percent, with the remaining 64 percent due to the low amplitude cycles. This can better be summarized graphically, Figure 89, for this cycle fraction along with the other fractions. For a spectrum with 15 percent high amplitude stress cycles, the damage contribution is split equally between the two load levels. Notice, when the high amplitude stress spectrum content was roughly 50 percent or greater, all the damage essentially could be attributed to the high amplitude cycles. As the number of high amplitude cycles was reduced, the damage contribution from the low stress cycles was significant, greater than 10 percent, to 0.3 percent for the high amplitude cycles.
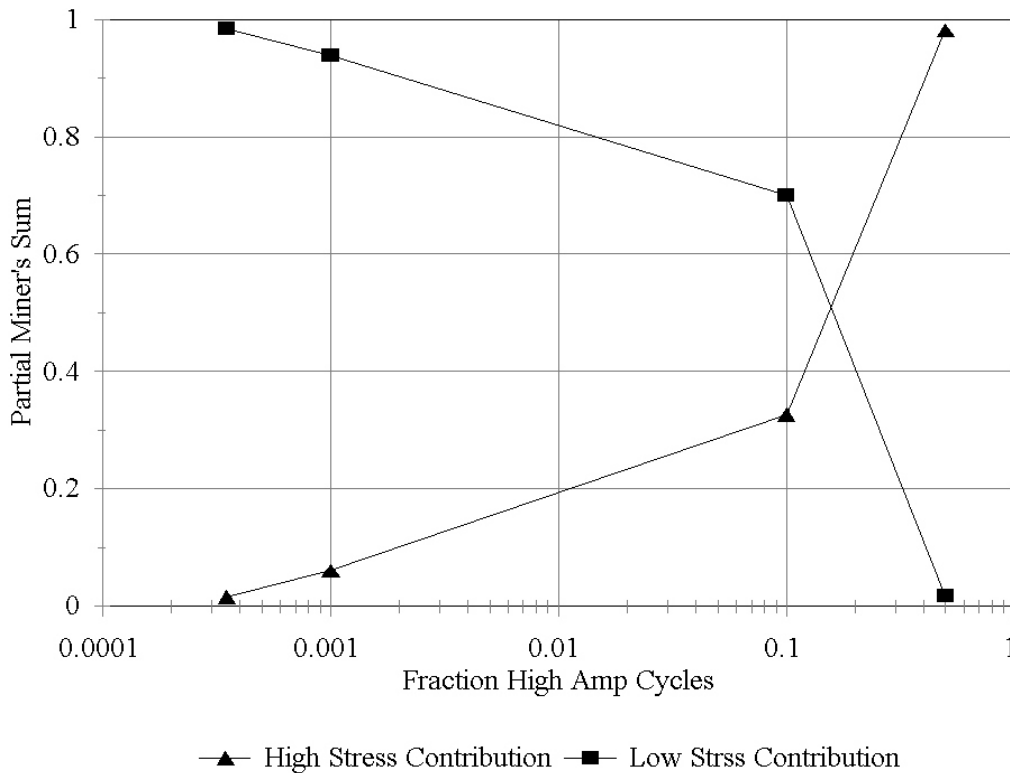
Figure 89. Two-Block Stress Level Damage Contributions.

Analysis of the damage contribution for the more random spectra, such as the various modified WISPERX cases, can be done similarly, provided the stress levels are properly handled. Since there is a multitude of stress levels in the WISPERX spectrum, segregating the levels into a series of increasing groups would produce a set of manageable size. Traditionally, this grouping is accomplished by rainflow counting methods [55, 56]. Here, each stress cycle is isolated, from which the range and mean values for that cycle are calculated. A matrix of bins for each of the groupings for range and mean is filled with the count of the number of cycles in each. A computer algorithm, was developed to perform the necessary calculations to rainflow count a spectrum. Figure 90, is a

three dimensional representation of a rainflow count of the published WISPERX spectrum. For comparison, a rainflow count of a constant amplitude test would have a single peak at a unique bin. A rainflow count of a two-block test would display two peaks at two unique bins representative of the two stress levels. The Mod 1 or Mod 2 spectrum would appear as a series of peaks formed along a straight line on the plane of a rainflow count matrix. The slope of this line would be in accordance with that of equation 2, $(1 - R)/(1 + R)$.
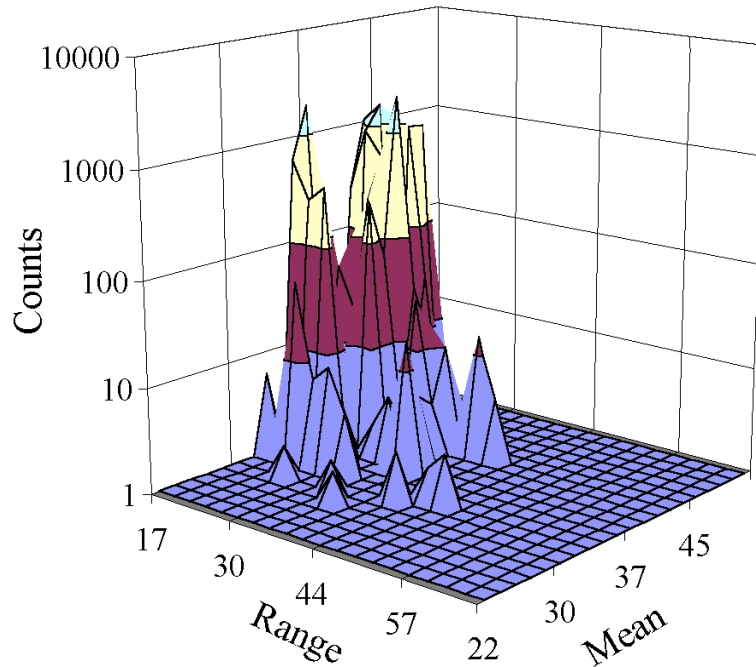
Figure 90. WISPERX Spectrum Cycle Count.

Information from a matrix such as that in Figure 90 can be used along with the fatigue models, Tables 4 or 5, to develop a Miner's sum for theoretical tests performed with the spectrum represented. The comparisons in Figures 91 and 92 use the exponential fatigue model with static data included. The damage caused by each bin of stress cycles can also be calculated, such as that shown in Figure 91. For the case shown in Figure 91, Mod 1 spectrum, R = 0.5, 414 MPa maximum stress, the relatively low number of high amplitude cycles caused the greatest amount of damage to the laminate. As the maximum stress level was decreased, the significance of the high amplitude cycles, although still significant, became less. Figure 92 displays results for a test similar to that of Figure 91, but with the maximum stress reduced.

Generally, as a spectrum includes a greater difference in load levels, the life prediction model becomes more important. This is illustrated in Figure 93, which shows predictions for two-block repeated spectra with different ratios of low to high block amplitude. When the damage is mostly caused by low stresses, but occasional high stresses occur, then the residual strength models are more accurate and differ strongly from Miner's rule [57]. The 24 percent ratio is less than half of the any tested stress ratios shown in the two-block figures, discussed earlier. Continuing the fraction of high

amplitude cycles to zero would cause the Miner's sum to trend to one, the low amplitude constant amplitude mean Miner's sum.
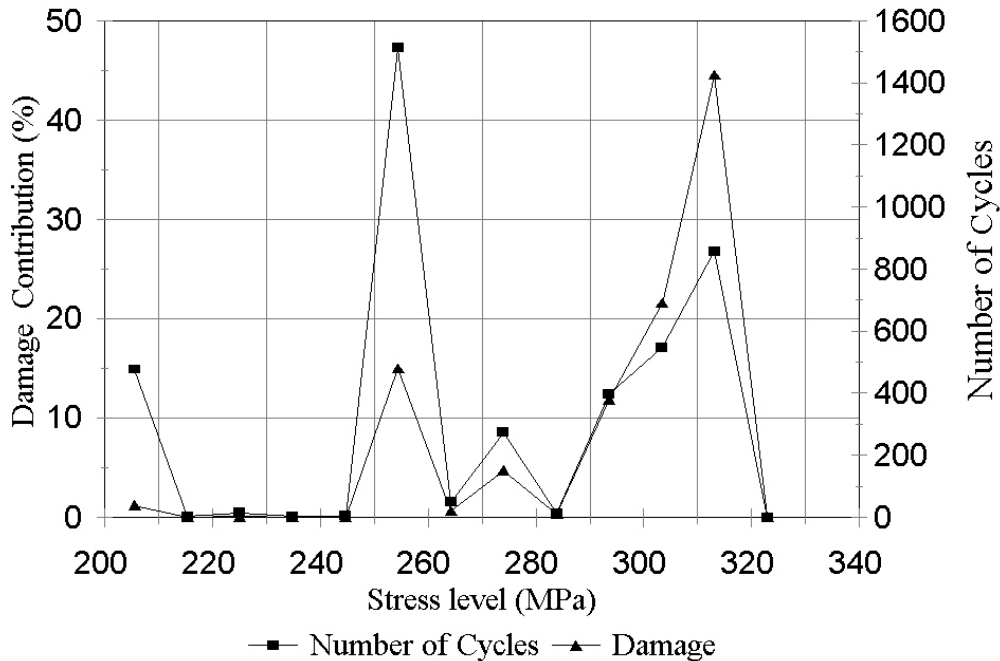
Figure 91. Stress Level Damage Contributions, Mod 1 Spectrum, R = 0.5, 414 MPa Maximum Stress.

Unmodified WISPERX Spectrum Fatigue Life Predictions

Fatigue lifetime predictions for a spectrum that contains a wide variety of R-values such that cycles of loading may be tensile, compressive or reversing require a consideration of the mode of failure. All previous discussions were restricted to tests and calculations that avoided this problem by forcing a consistent, known failure mode.

Consider that the failure mode must change from one that is tension dominated to one that is compression dominated as the R-value changes from 0.1 to -1 [9]. The R-values of 0.1 and -1 are listed, since they are the values for which tests have been conducted. Depending upon the laminate, the transition could occur between R-values of 0 and ∞, as is shown in Figure 94 (Figure 94 is a modification of Figure 5 to better illustrate the transition region). The fact of this transition is evident in analysis of the stress (y-axis) intercept for the S-N curves for the constant amplitude fatigue tests, such as Figures 33 through 37.
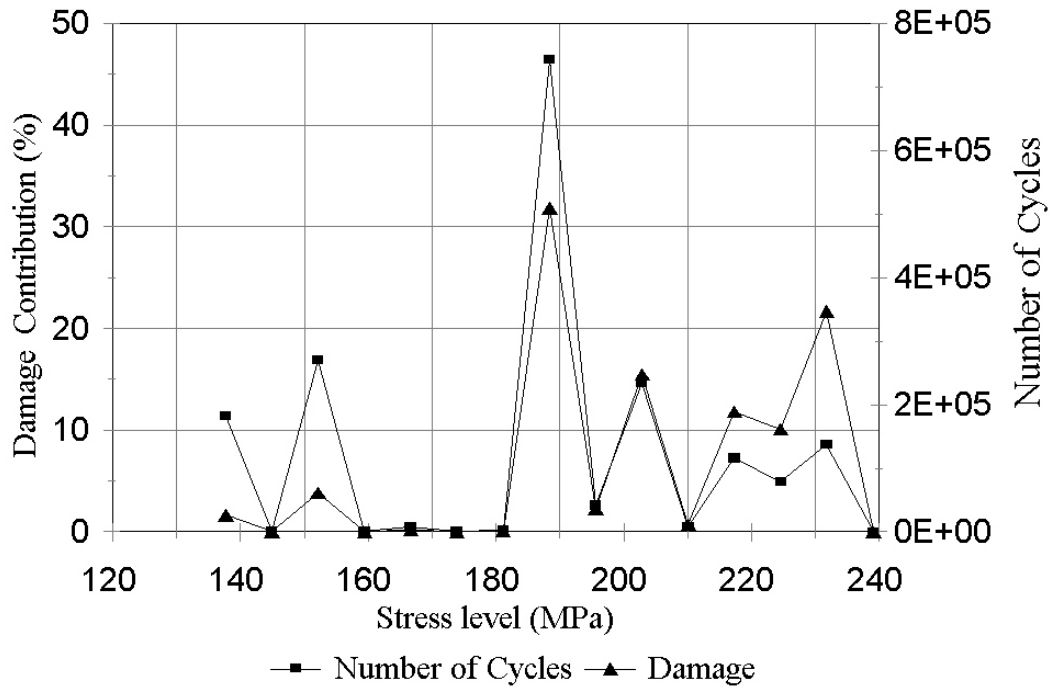
Figure 92. Stress Level Damage Contributions, Mod 1 Spectrum, R = 0.5, 241 MPa Maximum Stress.
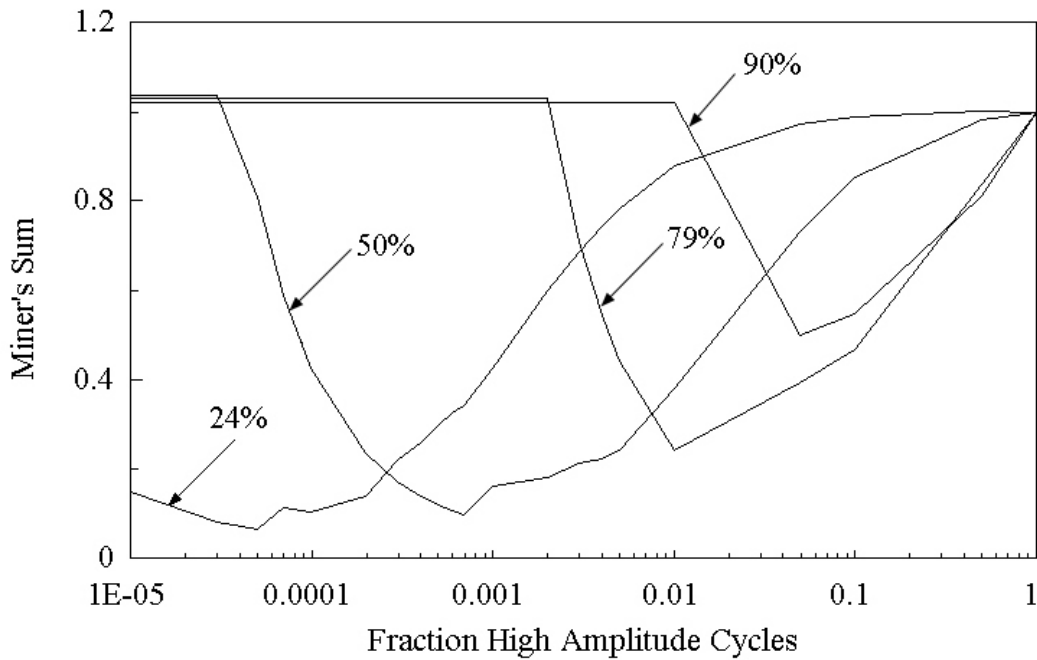
Figure 93. Two-Block Load Level Sensitivity, Low-Block Amplitude as Percent of High-Block Amplitude (nonlinear residual strength model prediction with v = 0.265, exponential fatigue model).
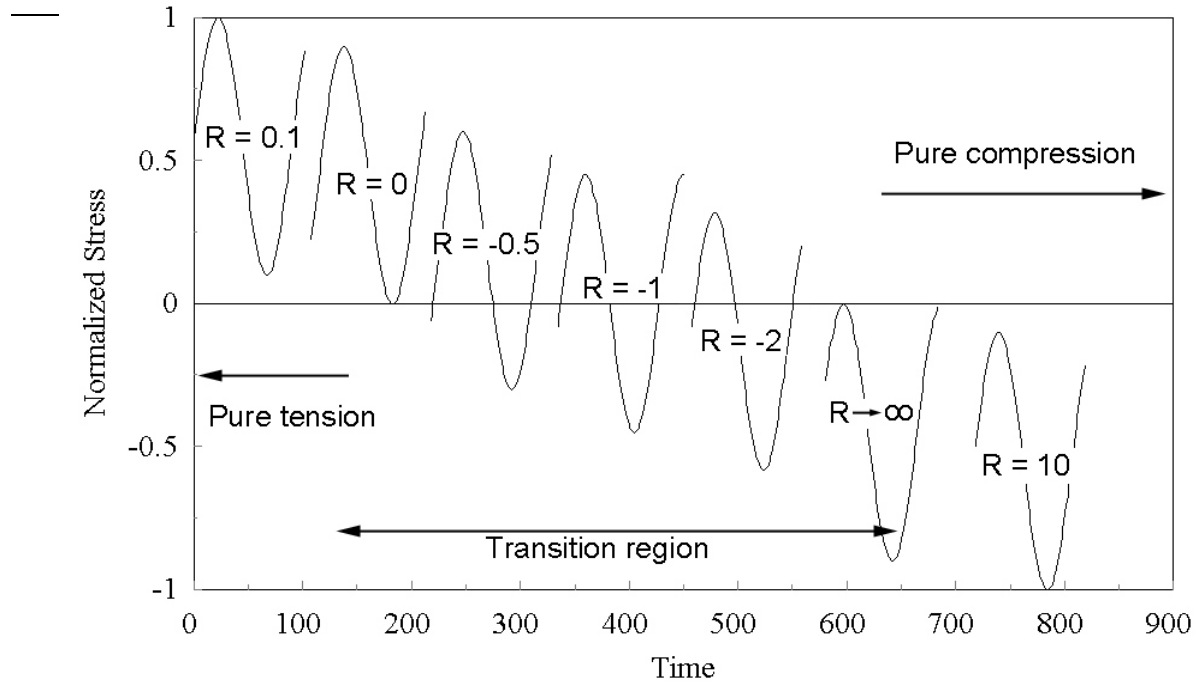
Figure 94. Transition From Tensile to Compressive Failure Mode, Constant Amplitude.

In order to apply the residual strength lifetime prediction models for this type of variable amplitude spectrum, the demarcation R-value must be known, as there are two distinct residual strength curves for compression and tension loading. This is not the case for application of Miner's rule in that the accepted interpolations from a Goodman diagram circumvent this need.

Lacking test information to allow determining this demarcation R-value, some logically developed value must be used. Hypothesize that the damage a laminate may suffer is dependent upon the ratio of the maximum stress to the ultimate strength for either tension or compression loading. If this were the case consider that the R-value that allows equal ratios of the tension maximum stress to the ultimate tensile stress and the compression minimum stress to the ultimate compressive stress would be the transition R-value. For equivalent damage from either the maximum tensile or compressive load then based upon the above hypothesis,

$$\frac{\sigma_{min}}{\sigma_{ucs}} = \frac{\sigma_{max}}{\sigma_{uts}} \qquad (17)$$

Upon considering the same stress range (alternating stress), as shown in Figure 94, equation 18 reduces to:

98

$$R = \frac{\sigma_{ucs}}{\sigma_{uts}} \qquad (18)$$

This R-value, for the tested laminate, was -0.63. This was then used as the demarcation R-value for the selection of the residual strength curve to be applied for any given cycle in a variable amplitude spectrum containing tensile, compressive and reversing loading cycles.

The lifetime predictions based upon this method of failure mode demarcation are shown in Figures 95 and 96 for the exponential and power law fatigue models, respectively. Only the two lifetime prediction rules of NRSD and Miner's rule were employed as the LRSD and Miner's rule have yielded very similar results. The incremental value for the stress level was held coarse and hence any spectrum effects at the low cycles are not as evident as in previous Figures 83 through 88. The nonlinear residual strength rule was much more conservative than the Miner's rule. The prediction rules based upon the exponential fatigue model do not seem to follow the general slope of the experimental data. The predictions based upon the exponential fatigue model over-predict life at the low cycles and under-predict life at the high cycles. The rule predictions based upon the power law fatigue model over-predict life throughout the life, yet seem to follow the general slope much better.
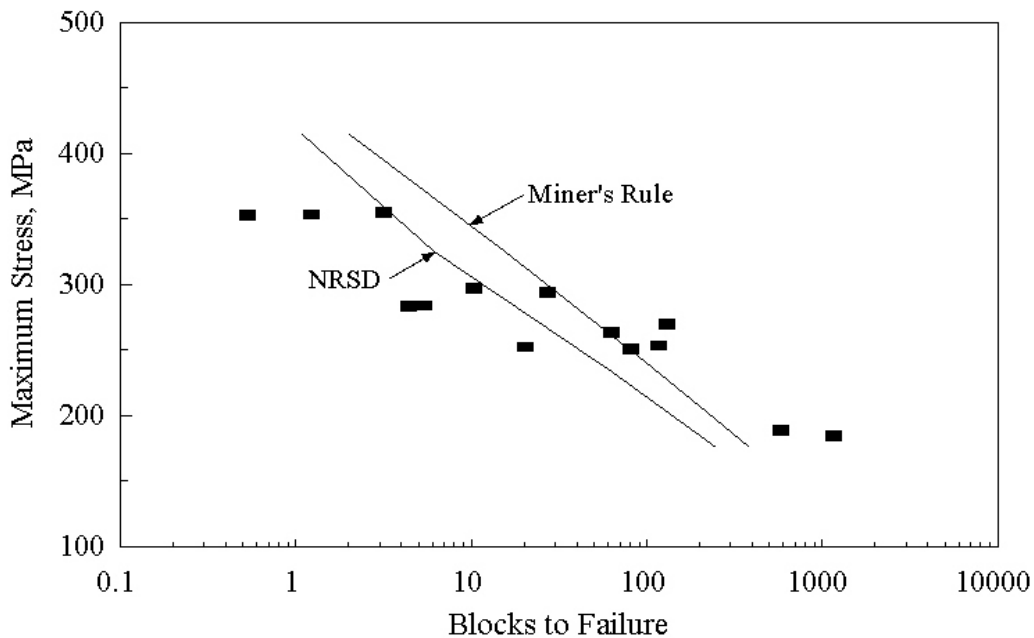
Figure 95. Unmodified WISPERX Spectrum Lifetime Predictions, Exponential Fatigue Model Including All Data.
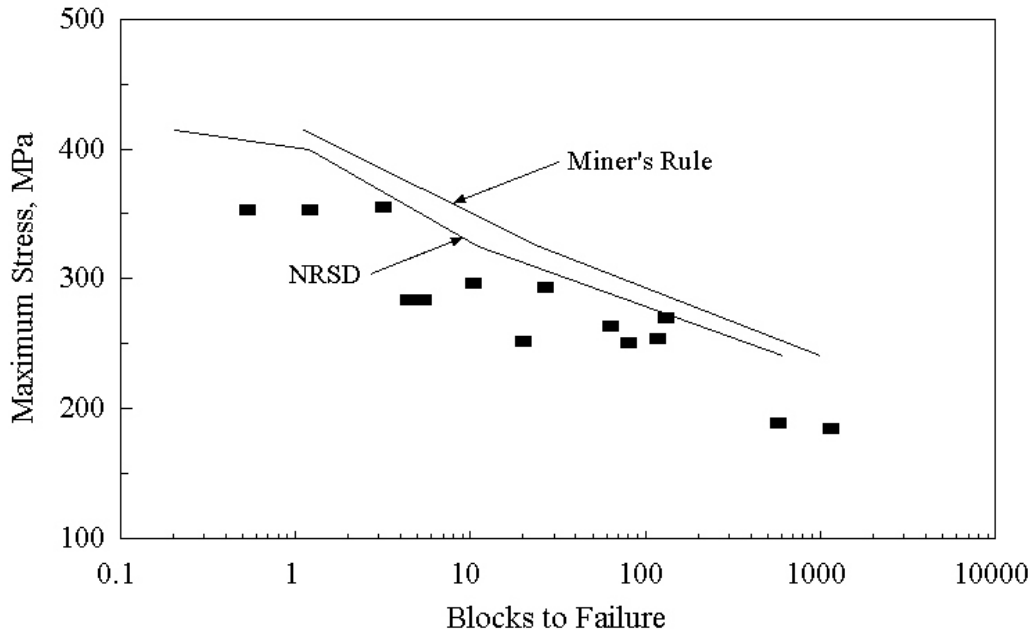
Figure 96. Unmodified WISPERX Spectrum Lifetime Predictions, Power Law Fatigue Model Including All Data.

Comparisons between the WISPERX results of van Delft [5] and the present fatigue results for the WISPERX spectrum are shown in Figure 97. The lifetimes predicted by van Delft are much greater than those of the present research, similar to the results presented by Sutherland and Mandell [10]. Prediction rules employed by van Delft and during this present research over-predict the actual lifetimes.
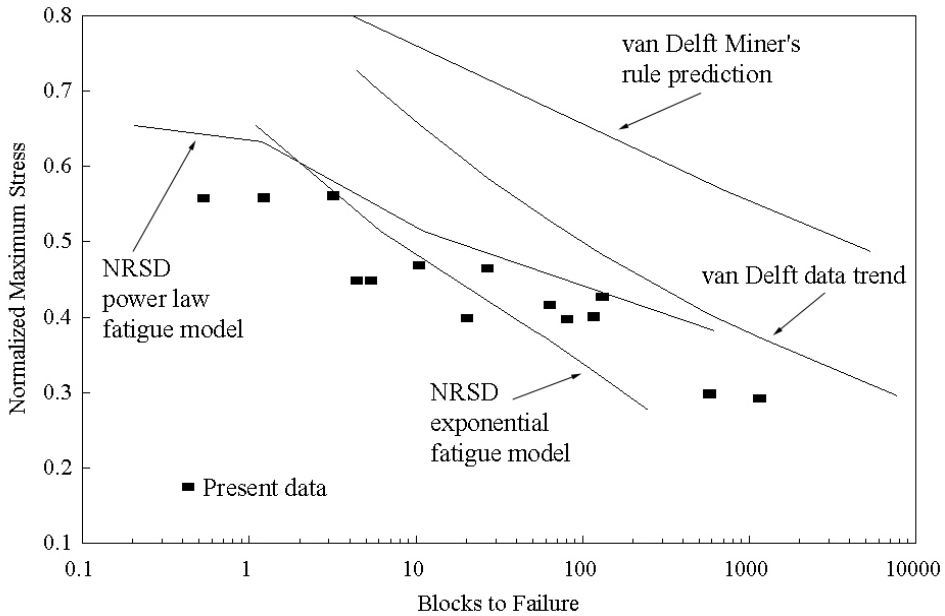
Figure 97. Comparison of WISPERX Lifetime Predictions.

SUMMARY, CONCLUSIONS AND RECOMMENDATIONS

The research conducted and reported here involved the development of an experimental program that, when implemented, generated a substantial quantity of fatigue data. Test methodologies, including material selection, test specimen geometry, data acquisition, and testing machine performance, were all held to unusually high standards, so that meaningful conclusions could be rendered relative to the accuracy of theoretical predictions in this and future studies. The data are those of the fatigue of specimens of the selected laminate, subjected to a variety of loads spectra and cycled until the specimens were sufficiently failed that they could not support loads. Other researchers have primarily investigated the response of laminates to either constant amplitude or simple two-block spectra. The present work extends the complexity to multi-block and random spectra.

Three fatigue life prediction models were employed to estimate the life of laminates subjected to a variety of loading spectra. Comparisons are made between the prediction models and the experimental data. While additional work with other models and loads spectra may be necessary to definitively prove the superiority of one prediction scheme over others, these results do allow limited conclusions to be drawn as to: (1.) the preferred methods of extrapolating the baseline constant amplitude S-N trends to higher cycles and (2.) the accuracy of cumulative damage models for particular spectrum characteristics.

Lifetime Observations and Application to Blade Design

Spectra involving two or more different stress levels generally resulted in lifetimes less than predicted by Miner's rule. This was not entirely expected. Other researchers [41] have reported that, for the application of two blocks of stress levels, with the second block run to specimen failure, the actual lifetimes may be greater or lesser than predicted by Miner's rule. The conclusion that Miner's rule is non-conservative for nearly all spectra tested raised questions as to the current status of wind turbine blades designed using this method. Fortunately, blades appear to be generally over-designed in terms of strength and fatigue lifetime, with designs often driven by stiffness related factors.

Better agreement between predictions and data was found by the application of residual strength based rules than by the use of the linear Miner's rule. This was particularly notable where the spectra (repeated block spectra) had sufficient variations in stress levels to separate the prediction rules. Although the nonlinear residual strength degradation rule introduces an unknown parameter that must be determined experimentally, it does provide a better prediction of lifetimes than the linear residual strength rule. The exponential parameter in equation 16 has not been optimized; in fact the parameter may be a function of several factors, such as stress level, fatigue age and laminate selection. Presently the parameter has been given a value of 0.265, the result of a rudimentary error analysis of residual strength data and a mere visual fitting of the prediction results to experimental data. The choice of a nonlinear exponential parameter less than 1.0 indicates a relatively rapid decrease in residual strength early in the specimen or blade lifetime. This choice is supported by all of the different types of spectra as well as direct residual strength measurements. Thus, not only is it practical to predict changes in

material and blade strength at different fractions of test or service lifetime, it may be essential in designing against the occurrence of "hurricane" extreme load conditions.

Comments on Spectrum Effects

The Mod 1, Mod 2 and WISPERX spectra are rather benign and as such fatigue results for these spectra, do not differ greatly from the similar constant amplitude fatigue results. Regression results of the Mod 1 spectrum test results at an R-value of 0.1 produced a log-log inverse slope, regression parameter m, of 12.0, whereas, the constant amplitude equivalent was 11.5. Similarly for the Mod 1 spectrum at an R-value of 0.5, the inverse slope was 14.5 compared to the constant amplitude value of 14.4. The Mod 2 spectrum, which included the one large cycle, and was forced to an R-value of 0.1, produced an inverse slope of 13.9; compare this to the constant amplitude value of 11.5. It appears that for the case of the random spectrum of limited stress variation, such as the Mod 1 spectrum, the fatigue sensitivity of the laminate is little different from that achieved by a constant amplitude spectrum. The single large cycle of the Mod 2 spectrum does cause some effect and deviate the fatigue sensitivity of this spectrum from the constant amplitude equivalent.

The WISPERX spectrum has an average R-value of approximately 0.4. The fatigue inverse slope for these tests was 14.2, not much removed from the 14.4 of the constant amplitude (R-value = 0.5) fatigue results.

Spectra such as the two-block spectra reported, have a greater variation in the cyclic load levels and have a greater effect on the fatigue lifetime predictions. This is born out by the difference seen in the lifetime predictions of the two-block as shown in the previous figures. The differences among the Miner's rule, linear residual strength degradation rule and the nonlinear residual strength rule are more pronounced than those seen in the WISPERX spectra results. One may presume, and wish to investigate, that the greater variation in stress levels that a spectrum contains, the more important the selection of the fatigue lifetime prediction rule.

Stress Level Sequencing Effects

An investigation into the possibility of any stress level sequencing effects on lifetimes has not shown this to be a significant factor, at least for the sequences selected. The spectra of different sequences of cycles in repeated blocks did not have an effect on the life of the specimens. Yet, when the blocks are not repeated (the second block continued until failure), the sequencing does produce significantly different results. Upon comparing the results of the residual strength degradation lifetime predictions to the experimental results of other investigators [42], the fact that sequencing is important for this special case was confirmed both experimentally and theoretically. Consequently, it is believed that sequencing effects of the cycles experienced during the actual service of components subjected to realistic random spectra, is not significant. This observation allows for the possibility that relatively simple cumulative damage rules may be used (although load conditions where compressive and tensile failure modes interact significantly may prove to cause complications).

Fatigue Model Selection

The results of the constant amplitude fatigue testing were summarized into two fatigue models based upon exponential and power law regression curves representing the data. Generally, for the two-block fatigue testing, the selection of the fatigue model is immaterial. Application of either the exponential or the power law fatigue models caused little difference in the lifetime predictions for the two-block loading spectra. This appears to be due to a limit of the number of cycles that are placed within each of the two blocks. These tests were typically extending over a range of a few thousand to a million cycles, a range over which the two fatigue models differ only slightly, and extrapolation to lower stresses using the models is unnecessary. Testing at lower stress levels for each block would force the testing into greater numbers of cycles, at which point, the selection of the fatigue model may become significant if the constant amplitude input trends require extrapolation beyond the range of experimental data.

The significance of the higher number of cycles was evident in the modified and unmodified WISPERX fatigue testing. In fact, the power law fatigue model provided a better lifetime prediction than the exponential model when the number of cycles was extended by an order of magnitude to 10 million.

Recommendations for Future Work

Many questions are still unanswered in regards to laminate response to spectrum loading; in fact work is still in progress in this research area. Items of ongoing work and areas of potential work are discussed below.

Spectrum Considerations

Upon studying the relatively benign WISPERX spectrum as compared to some of the two-block spectra, and the various rule prediction accuracies for those spectra, testing of other more robust spectra may provide more insight into rule selection. Other random spectra have been collected; wind turbine start/stop sequences, WISPER, FALSTAFF, as well as spectrum based upon data collected from operational wind turbines in Montana. Lifetimes of the laminate when subjected to these varied spectra may provide more insight into fatigue prediction, since loads often are more variable than WISPERX.

Compressive Residual Strength

There appears to be some differences in the response of the laminate to tensile and compressive loading as evidenced in the two-block testing. Residual strength testing of laminates was performed only for tensile loading case. This indicated the residual strength degradation lifetime prediction rule warrants use. Testing of the residual strength of the laminate subjected to compressive loading would be of interest.

Failure Mode Transition

At some loading condition, the failure mode transitions from tensile to compressive. The application of the residual strength degradation lifetime prediction model is somewhat dependent upon this transition point for the selection of the proper strength degradation path. This warrants an investigation into the failure mode and the breakpoint between these two fundamental loading conditions. Testing at a finer grid of R-values in the region surrounding R = -1 would be of interest.

Residual Strength Model Refinement

The nonlinear residual strength model was somewhat calibrated to the experimental data by selection of the exponent, ν, in equation 14. Adjustment of this single parameter causes a shifting of the predictions, in a manner similar to offset adjustment in instrumentation calibration. The introduction of a second variable of, as yet an unknown function, may allow better calibration of the model to fit the experimental data.

Simple magnitude shifting of the exponent can provide a better correlation with the experimental data for the unmodified WISPERX case that used the power law fatigue model. Unfortunately, this would not correct the lack of fit as observed in some of the two-block fatigue cases wherein the model is under-conservative for a spectrum of large high-amplitude cycle fractions and over-conservative for a spectrum with a smaller fraction. The second parameter may achieve a better calibration.

High Cycle Spectrum Fatigue Testing

Since the desired life of wind turbine blades can exceed 30 years or over 10^9 cycles, investigation of lifetimes of this magnitude, for laminates subjected to spectrum loading needs to be performed. It appears upon observation of the data in Figures 77 through 80, 83 through 88 and 95 and 96, the power law fatigue model provides a better correlation to the data than does the exponential fatigue model. Additional testing in the higher cycle region may provide more confidence for this conclusion.

REFERENCES

1. Wahl, N.K., "Spectrum Fatigue Lifetime and Residual Strength for Fiberglass Laminates," Department of Mechanical Engineering, Montana State University, Doctoral Thesis, August 2001.

2. Fuchs, H. O., Stephens, R. I., *Metal Fatigue in Engineering,* John Wiley & Sons publishers, 1980, pp. 1-5.

3. Anderson. T. L., *Fracture Mechanics, Fundamentals and Applications,* CRC Press, Inc. publishers, 1991, pp. 597-629.

4. Grover, H. J., *Fatigue of Aircraft Structures,* U.S. Government Printing Office, Washington, D.C., 1966, pp. 95-103.

5. Delft, D. R. V. van, de Winkel, G. D., Joosse, P. A., "Fatigue Behaviour of Fibreglass Wind Turbine Blade Material Under Variable Amplitude Loading," *Wind Energy 1997,* AIAA-97-0951, ASME/AIAA, (1997).

6. Miner, M. A., "Cumulative Damage in Fatigue," *Journal of Applied Mechanics,* Sept., 1945, pp. A-159 - A-164.

7. Kensche, Christoph, W., *High Cycle Fatigue of Glass Fibre Reinforced Epoxy Materials for Wind Turbines,* Institut für Bauweisen- und Konstruktionsforschung, DLR-Fb 92-17, 1992, pp. 14-15.

8. Schluter, L. L., Sutherland, H. J., *Reference Manual for the LIFE2 Computer Code,* Sandia National Laboratories, 1989, pp. 7-1.

9. Sutherland, H. J., Veers, P. S., Ashwill, T. D., "Fatigue Life Prediction for Wind Turbines: A Case Study on Loading Spectra and Parameter Sensitivity," American Society for Testing and Materials, 1995, pp.174-206.

10. Sutherland, H. J., Mandell, J. F., "Application of the U.S. High Cycle Fatigue Data Base to Wind Turbine Blade Lifetime Predictions," *Energy week 1996,* ASME, 1996.

11. Yang, J. N., Jones, D. L., "Effect of Load Sequence on the Statistical Fatigue of Composites," *AIAA Journal,* Vol. 18, No. 12, Dec, 1980, pp. 1525-1531.

12. Yang, J. N., Jones, D. L., "Load Sequence Effects on the Fatigue of Unnotched Composite Materials," *Fatigue of Fibrous Composite Materials, ASTM STP 723,* American Society for Testing and Materials, 1981, pp. 213-232.

13. Hwang, W., Han, K. S., "Cumulative Damage Models and Multi-Stress Fatigue Life Prediction," *Journal of Composite Materials,* Vol. 20, March, 1986, pp. 125-153.

14.   Mandell, J. F., Samborsky, D. D., "DOE/MSU Composite Material Fatigue Database: Test Methods, Materials and Analysis," Contractor Report SAND97-3002, Sandia National Laboratories, Albuquerque, NM, 1997.

15.   de Smet, B. J., Bach, P. W., *DATABASE FACT, FAtigue of Composites for wind Turbines,* Netherlands Energy Research Foundation ECN, ECN-C--94-045, 1994.

16.   ten Have, A. A., "WISPER and WISPERX: A Summary Paper Describing Their Backgrounds, Derivation and Statistics," *Wind Energy 1993,* SED-Vol. 14, ASME, (1993), pp. 169-178.

17.   ten Have, A. A., "WISPER and WISPERX, Final Definition of Two Standardised Fatigue Loading Sequences for Wind Turbine Blades," NLR TP 91476 U, National Aerospace Laboratory NLR, the Netherlands.

18.   Kelley, N. D., National Wind Technology Center, Golden, CO, Personal Communication, 2000.

19.   National Research Council, *Assessment of Research Needs for Wind Turbine Rotor Materials Technology,* National Academy Press, pp. 59-60, (1991).

20.   Sendeckyj, G. P. "Life Prediction for Resin-Matrix Composite Materials," *Fatigue of Composite Materials,* K. L. Reifsnider, Ed., Elsevier Sciences Publishers, 1990, pp. 431-483.

21.   Bond, I. P., "Fatigue life prediction for GRP subjected to variable amplitude loading," *Composites, Part A: Applied Science and Manufacturing,* 1999, pp. 961-970.

22.   Palmgren, A., "Die Lebensdauer von Kugellagern," ZDVDI, Vol. 68, No. 14, 1924, pp. 339.

23.   Broek, David, *Elementary Engineering Fracture Mechanics,* Martinus Nijhoff Publishers, 1982, pp. 13, 434-452.

24.   Hertzberg, Richard, W., *Deformation and Fracture Mechanics of Engineering Materials,* John Wiley & Sons publishers, 1996, pp. 591-641.

25.   Reifsnider, K. L., "Damage and Damage Mechanics (Chapter 2)," *The Fatigue Behavior of Composite Materials,* K. L. Reifsnider, Ed., Elsevier (1990), pp. 11-77.

26.   Hertzberg, Richard W., Manson, John A., *Fatigue of Engineering Plastics,* Academic Press, Inc. publishers, 1980, pp. 239-256, 268-271.

27.   Chawla, K. K., *Composite Materials Science and Engineering,* Springer-Verlag Publishers, New York, 1987, pp. 249-250.

28.   Reed, Robert Michael, "Long Term Fatigue of Glass Fiber Reinforced Composite Materials for Wind Turbine Blades," Masters Thesis, Department of Chemical Engineering, Montana State University, 1991.

29.   Sutherland, Herbert, J., "Damage Estimates for European and U.S. Sites Using the U.S. High-Cycle Fatigue Data Base," *IEA R&D Wind Annex XI, Symposium on Wind Turbine Fatigue,* DLR, Stuttgart, February 1-2, 1996.

30.   Joosse, P. A., Delft, D. R. V. van, Bach, P. W., *Fatigue Design Curves Compared to Test Data of Fibreglass Blade Material,* Netherlands Energy Research Foundation ECN, ECN-RX-94-108, 1994, pp. 7.

31.   Mandell, John F., Samborsky, Daniel, D., Sutherland, Herbert, J., "Effects of Materials Parameters and Design Details on the Fatigue of Composite Materials for Wind Turbine Blades," European Wind Energy Conference, 1999.

32.   Sutherland, Herbert J., Carlin, Palmer W., "Damage Measurements on the NWTC Direct-Drive, Variable-Speed Test Bed," American Institute of Aeronautics and Astronautics, 1998.

33.   Delft, D. R. V. van, Rink, H. D., Joosse, P. A., Bach, P. W., *Fatigue Behaviour of Fibreglass Wind Turbine Blade Material at the Very High Cycle Range,* Netherlands Energy Research Foundation ECN, ECN-RX-94-111, 1994.

34.   Mandell, J. F., "Fatigue Behavior of Short Fiber Composite Materials," *The Fatigue Behavior of Composite Materials,* K. L. Reifsnider, Ed. Elsevier (1990), pp. 241-254.

35.   Samborsky, Daniel, D., "Fatigue of E-Glass fiber Reinforced Composite Materials and Substructures," Masters Thesis, Department of Civil Engr. Montana State University, 1999.

36.   Yang, J. N., Jones, D. L., Yang, S. H., Meskini, A., "A Stiffness Degradation Model for Graphite/Epoxy Laminates," *Journal of Composite Materials,* Vol. 24, July, 1990, pp. 753-769.

37.   Bach, P. W., *High Cycle Fatigue Testing of Glass Fibre Reinforced Polyester and Welded Structural Details*, Netherlands Energy Research Foundation ECN, ECN-C--91-010, 1991, pp. 34.

38.   Subramanian, S., Reifsnider, K. L., Stinchcomb, W. W., "A cumulative damage model to predict the fatigue life of composite laminates including the effect of a fibre-matrix interphase," *Int. J. Fatigue*, Vol. 17, No. 5, 1995, pp. 343-351.

39.   Kung, D. N., Qi, G. Z., Yang, J. C. S., "Fatigue Life Prediction of Composite Materials," *Recent Advances in Structural Mechanics,* PVP-Vol. 225/NE-Vol. 7, American Society of Mechanical Engineers, 1991, pp. 41-50.

40.   Rivière, A., "Damping Characterization of Composite Materials by Mechanical Spectrometry," Laboratoire de Mécanique et de Physique des Matériaux - URA CNRS nº 863 ENSMA, Rue Guillaume VII, 86034 Poitiers (France), pp. 316-322.

41.   Revuelta, D., Cuartero, J., Miravele, A., Clemente, R., "A new approach to fatigue analysis in composites based on residual strength degradation," *Composite Structures 48,* Elsevier Science Ltd., 1999, pp. 183-186.

42.   Broutman, L. J., Sahu, S., "A New Theory to Predict Cumulative Fatigue Damage in Fiberglass Reinforced Plastics," *Composite Materials: Testing and Design (Second Conference), ASTM STP 497,* American Society for Testing and Materials, 1972, pp. 170-188.

43.   Schaff, J. R., Davidson, B. D., "Life Prediction Methodology for Composite Structures. Part I - Constant Amplitude and Two-Stress Level Fatigue," *Journal of Composite Materials,* Vol. 31, No. 2, 1997, pp. 128-157.

44.   Schaff, J. R., Davidson, B. D., "Life Prediction Methodology for Composite Structures. Part II - Spectrum Fatigue," *Journal of Composite Materials,* Vol. 31, No. 2, 1997, pp. 158-181.

45.   Schaff, J. R., Davidson, B. D., "A Strength-Based Wearout Model for Predicting the Life of Composite Structures," *Composite Materials: Fatigue and Fracture (Sixth Volume), ASTM STP 1285,* E. A. Armanious, Ed., American Society for Testing and Materials, 1997, pp. 179-200.

46.   Whitworth, H. A., "Evaluation of the residual strength degradation in composite laminates under fatigue loading," *Composite Structures 48,* Elsevier Science Ltd., 2000, pp. 261-264.

47.   Reifsnider, K. L., "Interpretation of Laboratory Test Information for Residual Strength and Life Prediction of Composite Systems," *Cyclic Deformation, Fracture and Nondestructive Evaluation of Advanced Materials, ASTM STP 1157,* M. R. Mitchell and O. Buck, Eds., American Society for Testing and Materials, Philadelphia, 1992, pp. 205-223.

48.   O'Brien, T. K., "Characterization of Delamination Onset and Growth in a Composite Laminate," *Damage in Composite Materials, ASTM STP 775,* K. L. Reifsnider, Ed., American Society for Testing and Materials, 1982, pp. 140-167.

49.   Echtermeyer, A. T., Kensche, C., Bach, P., Poppen, M., Lilholt, H., Andersen, S. I., Brøndsted, P., "Method to Predict Fatigue Lifetimes of GRP Wind Turbine Blades and Comparison With Experiments," *European Union Wind Energy Conference,* 1996, pp. 907-913.

50.   Solin, J., "Methods for comparing fatigue lives for spectrum loading," *Int. J. Fatigue*, Vol., 12, No. 1, 1990, pp. 35-42.

51. Lee, L. J., Yang, J. N., Sheu, D. Y., "Prediction of Fatigue Life for Matrix-Dominated Composite Laminates," *Composites Science and Technology,* Elsevier Science Publishers Ltd., 1992, pp. 21-28.

52. Han, Patricia, Editor, *Tensile Testing,* ASM International, 1992, pp. 187-191.

53. Nichols, N. B., Ziegler, J. G., "Optimum Settings for Automatic Controllers," *ASME Transactions*, Vol. 64, No. 8, 1942, pp. 759-768.

54. Joosse, P. A., Delft, D. R. V. van, Bach, P. W., *Fatigue Design Curves Compared to Test Data of Fibreglass Blade Material,* Netherlands Energy Research Foundation ECN, ECN-RX-94-108, 1994, pp. 2.

55. Downing, S. D., Socie, D. F., "Simple Rainflow Counting Algorithms," *International Journal of Fatigue,* Vol. 4, No. 1, 1982, pp. 31-40.

56. Kelley, N. D., National Wind Technology Center, Golden, CO, Personal Communication, 1996.

57. Wahl, Neil. Samborsky, Daniel, Mandell, John, Cairns, Douglas, "Spectrum Fatigue Lifetime and Residual Strength for Fiberglass Laminates in Tension," *A Collection of the 2001 ASME Wind Energy Symposium,* American Institute of Aeronautics and Astronautics, Inc. and American Society of Mechanical Engineers, 2001, pp. 49- 59.

APPENDICES

APPENDIX A

SPECTRUM FATIGUE DATABASE

<u>Nomenclature</u>

Column 1:   Test # is the unique identifying number for each test. Coupons were manufactured sequentially from plates and randomly selected from the stock and sequentially numbered. The tests were not conducted in this sequential number, but randomly in batches. An asterisk in this column indicates the test was not successful.

Residual strength tests are represented by two successive entries of the same identifying number. The first entry indicates the cyclic fatigue portion of the test, while the second entry with the letter "r" appended to the test number indicates the static test of the coupon.

Column 2:   The comments for each test provide some insight as to the type of test or the success of the test.

DNF represents did not finish. Other entries such as tab or grip failure are self descriptive of the success of the test.

Dh/Dt is two-block spectrum test comment. This is an estimate of the expected ratio of the damage contribution of the high stress cycles and the total number of cycles expectected. A Dh/Dt of unity would represent a constant amplitude test at the higher stress level. Tests identified with the Dh/Dt were conducted with the higher amplitude maximum stress of 414 MPa while the lower amplitude maximum stress was 235 MPa. These were based upon initial estimates of the constant amplitude cycles to failure of 10^4 and 10^6 for the two stress levels respectively.

An entry such as that of test number 154, "47.5/30-0.5" indicates that this test was conducted with a two-block spectrum with the first block's maximum stress equal to 47.5 ksi (325 MPa) and the second block's, 30 ksi (207 MPa). The damage contribution of the higher stress block was expected to be 50% (0.5).

Test 176 is listed as "47.5/30-10/1000" which represents a two-block test with stress levels of 47.5 and 30 ksi. The number of cycles in the first block, the high cyclic amplitude block is 10, while the second block contains 1000 cycles. Tests with the character(s) "r" or "r#" or "rand#"appended to the cycle numbers indicates the cycles were randomly ordered rather than in separate blocks; here the cycle numbers indicate an overall proportioning of the cycle numbers.

1 cycle indicates that this particular test was an ultimate strength test.

A listed stress, such as the "500 MPa" of test number 11 indicates the test is a constant amplitude test with the maximum stress equal to 500 MPa.

An entry such as "R=0.5" indicates the test was performed at a R-value of 0.5. The lack of an R-value implies the default value of 0.1 was used.

The descriptor "wvrnr" implies the Instron WaveRunner software package was used to control the hydraulic system. Descriptors such as "load#" indicate the Instron RANDOM software package was used for control.

Entries such as "Wisperx", "WisxR05", "WisxR01", "Wisxmix", or "Wispk" indicate that a modified WISPERX or original WISPERX spectrum was used to load the specimen.

Column 3:	The entries in this column indicate the type of coupon used and the material and batch used for the laminate.
Column 4:	The frequency of the test is documented in column six. Ultimate strength tests were conducted at the same rate as the cyclic tests. These tests are indicated by the entry "1 cycle".
Column 5:	This column lists the number of cycles conducted at the high amplitude stress level.
Column 6:	The number of cycles conducted at the low amplitude stress level. Tests of more than two-blocks are summarized in Tables 6 and 7 of the text.
Column 7:	The total number of cycles of the test is listed in this column.
Column 8:	The maximum load encountered during the test is listed in pounds.

Test #	Comment	Coupon Style/Material	Freq Hz	# High Cycles	# Low Cycles	Total Cycles	Hi Block Max
2	Dh/Dt=1	1/DD5	10	4717		4717	1949
3	Dh/Dt=1	1/DD5	10	2711		2711	2037
4	Dh/Dt=1	1/DD5	10	1812		1812	2160
6	1 cycle	1/DD5	1 cycle	1		1	3844
7	1 cycle	1/DD5	1 cycle	1		1	3854
8	1 cycle	1/DD5	1 cycle	1		1	3899
9	Dh/Dt=1	1/DD5		3711		3711	2072
11	500 MPa	1/DD5	10	877		877	2353
13	500 MPa	1/DD5	10	584		584	2389
14	690 MPa	1/DD5	10	28		28	3367
17	Dh/Dt=0	1/DD5	10		3096821	3096821	1196
18	Dh/Dt=0	1/DD5	30		1709382	1709382	1142
19	Dh/Dt=0.1	1/DD5	10	670	594000	594670	1976
20	Dh/Dt=0.9	1/DD5	10	7950	88928	96878	2001
22	Dh/Dt=0.1	1/DD5	10	1600	1435500	1437100	2001
23	Dh/Dt=0.25	1/DD5	10	2025	607500	609525	1957
24	Dh/Dt=0.25	1/DD5	10	3090	925500	928590	1949
25	Dh/Dt=0.75	1/DD5	10	6880	226061	232941	1984
26	Dh/Dt=0.75	1/DD5	10	6415	211530	217945	1984
27	Dh/Dt=0.5	1/DD5	10	2850	285000	287850	2019
28	Dh/Dt=0.9	1/DD5	10	7855	87808	95663	2028
29	Dh/Dt=0.1	1/DD5	10	400	1800000	1800400	1900
31	Dh/Dt=0	1/DD5	10		4501339	4501339	1177
32	Dh/Dt=1	1/DD5	10	4221		4221	1976
33	690 Mpa	1/DD5	10	67		67	3162
34	500 MPa	1/DD5	10	1113		1113	2316
35	690 MPa	1/DD5	10	39		39	3335
36	Dh/Dt=0.5	1/DD5	10	3270	327000	330270	2008
37	Dh/Dt=0.6	1/DD5	10	2860	189428	192288	2063
38	Dh/Dt=0.95	1/DD5	10	10100	52468	62568	2045
39	Dh/Dt=0.75	1/DD5	10	4340	144622	148962	1984
40	Dh/Dt=0.9	1/DD5	10	5040	56336	61376	2003
41	Dh/Dt=0.6	1/DD5	10	1727	114057	115784	2010
42	Dh/Dt=0.5	1/DD5	10	3670	366000	369670	1975
43	Dh/Dt=0.25	1/DD5	10	1960	588000	589960	1975
44	Dh/Dt=0.9	1/DD5	10	6440	72016	78456	2035
45	Dh/Dt=0.5	1/DD5	10	2780	277000	279780	1981
46	Dh/Dt=0.75	1/DD5	10	3920	130594	134514	2026
47	Dh/Dt=0.25	1/DD5	10	1330	399000	400330	2027
48	Dh/Dt=0.95	1/DD5	10	8610	44720	53330	1984
70	Dh/Dt=1	2t/DD5	10	1743		1743	3267
71	Dh/Dt=1	2t/DD5	10	1767		1767	3302
72	Dh/Dt=1	2t/DD5	10	1017		1017	3337

Test #	Comment	Coupon Style/Material	Freq Hz	# High Cycles	# Low Cycles	Total Cycles	Hi Block Max
73	Dh/Dt=0.95	2t/DD5	10	1130	5824	6954	3337
74	Dh/Dt=0.95	2t/DD5	10	1980	10244	12224	3302
75	Dh/Dt=1	2t/DD5	10	1515		1515	3125
76	Dh/Dt=0.95	2t/DD5	10	1190	6188	7378	3196
77	Dh/Dt=0.9	2t/DD5	10	1080	11984	13064	2775
78	Dh/Dt=0.75	2t/DD5	10	1150	38076	39226	2880
79	Dh/Dt=0.5	2t/DD5	10	470	46000	46470	3021
81	Dh/Dt=0.1	2t/DD5	10	30	25918	25948	2851
82	Dh/Dt=0.6	2t/DD5	10	520	34017	34537	2978
83	Dh/Dt=0	2t/DD5	10		628444	628444	1642
84	Dh/Dt=1	2m/DD5	10	1697		1697	2555
85	1 cycle	2m/DD5	1 cycle	1		1	4507
86	500 MPa	2m/DD5	10	463		463	3056
87	500 MPa	2m/DD5	10	527		527	3091
89	Dh/Dt=0.5	2m/DD5	10	293	28527	28820	3111
90	Dh/Dt=0.9	2m/DD5	10	720	7952	8672	2852
91	Dh/Dt=0.1	2m/DD5	10	50	45000	45050	3228
92	Dh/Dt=0.25	2m/DD5	10	1102	330000	331102	2593
93	Dh/Dt=0.0	2m/DD5	10		1407916	1407916	1463
94	Dh/Dt=0.75	2m/DD5	10	782	26052	26834	2579
95	Dh/Dt=0.6	2m/DD5	10	903	60030	60933	2728
96	Dh/Dt=0.25	2m/DD5	10	710	213000	213710	2622
97	Dh/Dt=0.99	2m/DD5	10	4024	4020	8044	2606
98	Dh/Dt=0	2m/DD5	10		3403091	3403091	1427
99	Dh/Dt=0.99	2m/DD5	10	5956	5950	11906	2489
100	Dh/Dt=0.5	2m/DD5	10	2416	241000	243416	2314
101	Dh/Dt=0.9	2m/DD5	10	5337	59696	65033	2510
102	Dh/Dt=0.1	2m/DD5	10	795	711000	711795	2583
103	Dh/Dt=1.0	2m/DD5	10	1496		1496	2406
104	Dh/Dt=0.9	2m/DD5	10	2380	26544	28924	2606
105	1 cycle	2m/DD5	1 cycle	1		1	4744
106	Dh/Dt=1.0	2m/DD5	10	5660		5660	2523
107	Dh/Dt=0.1	2m/DD5	10	680	609298	609978	2645
108	Dh/Dt=1	2m/DD11B	10	97		97	3149
109	Dh/Dt=0	2m/DD11B	10		217518	217518	1798
110	Dh/Dt=0	2m/DD11B	10		208911	208911	1911
111	Dh/Dt=1	2m/DD11B	10	226		226	3144
112	Dh/Dt=0.75	2m/DD11B	10	21	668	689	3352
113	Dh/Dt=0.25	2m/DD11B	10	104	30000	30104	3187
114	1 cycle	2m/DD11B	1 cycle	1		1	4195
115	1 cycle	2m/DD11B	1 cycle	1		1	4358
116	475MPa	2m/DD11B	10	37		37	3683
117	350MPa	2m/DD11B	10	2729		2729	2716

Test #	Comment	Coupon Style/Material	Freq Hz	# High Cycles	# Low Cycles	Total Cycles	Hi Block Max
118	475MPa	2m/DD11B	10	78		78	3685
119	Dh/Dt=1	2m/DD11B	10	29		29	3232
120	Dh/Dt=0.9	2m/DD11B	10	576	6384	6960	3052
121	Dh/Dt=0.5	2m/DD11B	10	88	8000	8088	3165
122	Dh/Dt=0.99	2m/DD11B	10	368	360	728	3071
123	Dh/Dt=1.0	2m/DD11B	10	801		801	3274
124	Dh/Dt=1.0	2m/DD11B	10	392		392	3032
125	56ksi/32.6ksi	2m/DD11B	10	1228	13664	14892	3043
126	Dh/Dt=0.9	2m/DD11B	10	237	2576	2813	3213
127	Dh/Dt=0.0	2m/DD11B	10		107287	107287	
128	1 cycle	2m/DD16A	1 cycle	1		1	4438
129	Dh/Dt=1	2m/DD16A	10	78		78	3722
130	Dh/Dt=1	2m/DD16A	10	149		149	3765
131	Dh/Dt=0	2m/DD16A	10		141377	141377	1875
132	Dh/Dt=0.5	2m/DD16A	10	72	7000	7072	3707
133	Dh/Dt=0.75	2m/DD16A	10	40	1002	1042	3765
134	Dh/Dt=0.25	2m/DD16A	10	54	15000	15054	3480
135	Dh/Dt=0.9	2m/DD16A	10	230	2464	2694	3804
136	Dh/Dt=0.1	2m/DD16A	10	13	9000	9013	3782
137	Dh/Dt=0.99	2m/DD16A	10	130	120	250	3732
138	Dh/Dt=0	2m/DD16A	10		143456	143456	1999
139	328 MPa	2m/DD16A	10	2297		2297	2800
140	328 MPa	2m/DD16A	10	1914		1914	2690
141	1 cycle	2m/DD16A	1 cycle	1		1	4812
142	Dh/Dt=0.1	2m/DD16A	10	22	18000	18022	3476
143	Dh/Dt=0.5	2m/DD16A	10	60	5000	5060	3489
144	Dh/Dt=0.75	2m/DD16A	10	117	3674	3791	3431
145	Dh/Dt=0.9	2m/DD16A	10	91	1008	1099	3638
146	Dh/Dt=0.99	2m/DD16A	10	286	280	566	3768
147	Dh/Dt=0.0	2m/DD16A	10		31943	31943	3704
148	Dh/Dt=1	2m/DD16A	10	155		155	3861
149	Dh/Dt=0.95	2m/DD16A	10	182	936	1118	3542
150	Dh/DT=0.95	2m/DD16A	10	195	988	1183	3834
151	207 MPa	2m/DD16A	10	274271		274271	1923
152	207 MPa	2m/DD16A	10	294549		294549	1902
153	207 MPa	2m/DD16A	10	382826		382826	1738
154	47.5/30-0.5	2m/DD16A	10	432	43000	43432	2856
155	47.5/30-0.9	2m/DD16A	10	1077	11984	13061	2991
156	47.5/30-0.1	2m/DD16A	10	120	92379	92499	2916
157	47.5/30-0.25	2m/DD16A	10	554	162287	162841	2602
158	47.5/30-0.99	2m/DD16A	10	1840	1830	3670	2746
159	47.5/30-0.75	2m/DD16A	10	1062	35404	36466	2721
160	30 ksi - 0.0	2m/DD16A	10		495397	495397	1770

Test #	Comment	Coupon Style/Material	Freq Hz	# High Cycles	# Low Cycles	Total Cycles	Hi Block Max
161	47.5 ksi - 1.0	2m/DD16A	10	1722		1722	2906
162	47.5/30-0.5	2m/DD16A	10	1432	143000	144432	2538
163	47.5/30-0.9	2m/DD16A	10	2119	23632	25751	2696
164	47.5/30-0.1	2m/DD16A	10	270	239206	239476	2786
165	47.5/30-0.25	2m/DD16A	10	406	120000	120406	2799
166	47.5/30-0.99	2m/DD16A	10	4249	4240	8489	2972
167	47.5/30-0.75	2m/DD16A	10	932	31062	31994	2679
168	47.5 ksi - 1.0	2m/DD16A	10	744		744	2850
169	30 ksi - 0.0	2m/DD16A	10		588371	588371	
170	47.5/30-0.99	2m/DD16A	10	3552	3550	7102	2776
171	47.5ksi - 1.0	2m/DD16A	10	3152		3152	2439
172	60 ksi - 1.0	2m/DD16A	10	162		162	3367
173	1 cycle	2m/DD16A	1 cycle	1		1	4329
174	35ksi - 1.0	2m/DD16A	10		37855	37855	2097
175	47.5/30-10/667	2m/DD16A	10	987	65366	66353	2669
176	47.5/30-10/1000	2m/DD16A	10	349	34000	34349	2860
177	47.5/35-10/1000	2m/DD16A	10	656	65000	65656	2468
178	47.5/35-10/1000	2m/DD16A	10	197	19000	19197	2504
179	60/47.5/35	2m/DD16A	10	62	600	6662	3010
180	47.5/30-20/10	2m/DD16A	10	2418	1200	3618	2814
181	47.5/30-10/250	2m/DD16A	10	2207	54750	56957	2706
182	47.5/30-10/40	2m/DD16A	10	2419	9640	12059	2654
183	47.5/30-10/1000	2m/DD16A	10	510	50906	51416	3086
184	47.5/30-10/667	2m/DD16A	10	359	23345	23704	2871
186	47.5/30-10/33000	2m/DD16A	10	106	330000	330106	2747
187	47.5/30-10/33000	2m/DD16A	10	42	165000	165042	2917
188	47.5/30-10/50000	2m/DD16A	10	30	139982	140012	2950
189	47.5/30-10/60000	2m/DD16A	10	50	295894	295944	2462
190	47.5/30-10/20000	2m/DD16A	10	150	297672	297822	2372
191	47.5/30-10/50000	2m/DD16A	10	30	101013	101043	2867
192	47.5/30-10/33000	2m/DD16A	10	50	158561	158611	2841
193	47.5/30-10/60000	2m/DD16A	10	20	91339	91359	2925
194	47.5/35-10/1000	2m/DD16A	10	140	13016	13156	2589
195	47.5/35-10/3000	2m/DD16A	10	150	44460	44610	2371
196	47.5/35-10/5000	2m/DD16A	10	40	17361	17401	2805
198	47.5/35-10/500	2m/DD16A	10	250	12114	12364	2314
199	47.5/35-10/100	2m/DD16A	10	364	3600	3964	2761
200	47.5/35-10/10	2m/DD16A	10	1357	1350	2707	2446
201	47.5/35-10/500	2m/DD16A	10	100	4774	4874	2782
202	47.5/35-10/1000	2m/DD16A	10	100	9359	9459	2872
203	47.5/35-10/5000	2m/DD16A	10	40	15564	15604	2835
204	47.5/35-10/3000	2m/DD16A	10	110	30522	30632	2285
205	35-0/100	2m/DD16A	10		15680	15680	1847

Test #	Comment	Coupon Style/Material	Freq Hz	# High Cycles	# Low Cycles	Total Cycles	Hi Block Max
206	47.5-10/0	2m/DD16A	10	1339		1339	2440
207	47.5/30-10/10-N	2m/DD16A	10	2163	2160	4323	2541
208	47.5/30-10/10-D	2m/DD16A	10	2326	2320	4646	2679
209	47.5/35-10/10-N	2m/DD16A	10	583	580	1163	2721
210	47.5/35-10/10-D	2m/DD16A	10	1815	1810	3625	2441
211	60/35-10/10-N	2m/DD16A	10	98	90	188	3257
212	60/35-10/10-D	2m/DD16A	10	72	70	142	3178
213	47.5-10-N	2m/DD16A	10	3306		3306	2534
214	47.5-10-D	2m/DD16A	10	2078		2078	2496
215	60/35-10/9000	2m/DD16A	10	17	9000	9017	3329
216	47.5/30-10/9000	2m/DD16A	10	85	72000	72085	2705
217	47.5/35-10/3000	2m/DD16A	10	60	17063	17123	2666
218	47.5/30-10/3000	2m/DD16A	10	110	31739	31849	2635
219	47.5/30-10/5000	2m/DD16A	10	80	39441	39521	2800
220	6block-47.5 max	2m/DD16A	10			97997	2679
221	6block-50ksi max	2m/DD16A	10			28915	2924
222	6block-60ksi max	2m/DD16A	10			6064	3249
225	6block-50ksi max	2m/DD16A	10			20907	2907
226	6block-40ksi max	2m/DD16A	10			181648	2256
229	47.5/30-10/60000	2m/DD16A	10	20	61684	61704	2761
230	47.5/30-10/50000	2m/DD16A	10	70	319095	319165	2531
232	47.5/30-10/9000	2m/DD16A	10	100	81000	81100	2747
233	47.5/30-10/50000	2m/DD16A	10	50	202625	202675	2630
234	47.5/30-10/9000	2m/DD16A	10	210	180000	180210	2543
235	47.5/30-10/33000	2m/DD16A	10	30	82555	82585	2707
236	30 ksi residual/failed	2m/DD16A	10		446342	446342	1648
237	30 ksi residual	2m/DD16A	10		200016	200016	1608
237r	30 ksi residual	2m/DD16A	1 cycle				3240
238	30 ksi residual	2m/DD16A	10		100009	100009	1624
238r	30 ksi residual	2m/DD16A	1 cycle				3544
239	30 ksi residual/failed	2m/DD16A	10		111838	111838	1826
240	30 ksi residual	2m/DD16A	10		300010	300010	
240r	30 ksi residual	2m/DD16A	1 cycle				3381
241	30 ksi residual/failed	2m/DD16A	10		130521	130521	1670
242	30 ksi residual/failed	2m/DD16A	10		133659	133659	1588
243	30 ksi residual	2m/DD16A	10		100010	100010	1739
243r	30 ksi residual	2m/DD16A	1 cycle				3382
244	30 ksi residual/failed	2m/DD16A	10		38964	38964	1876
245	30 ksi residual	2m/DD16A			50008	50008	
245r	30 ksi residual	2m/DD16A	1 cycle				4244
246	35/30 - 10/10	2m/DD16A	10	67370	67365	134735	1977
247	35/30 - 10/9000	2m/DD16A	10	600	535083	535683	1864
248	35/30 - 10/33000	2m/DD16A	10	100	307196	307296	1953

Test #	Comment	Coupon Style/Material	Freq Hz	# High Cycles	# Low Cycles	Total Cycles	Hi Block Max
249	35/30 - 10/60000	2m/DD16A	10	30	137575	137605	1977
250	35/30 - 10/9000	2m/DD16A	10	580	518806	519386	1965
251	35/30 - 10/60000	2m/DD16A	10	40	198456	198496	1779
252	35/30 - 10/10	2m/DD16A	10	37306	37300	74606	1989
253	35/30 - 10/9000	2m/DD16A	10	410	366273	366683	1857
254	35/30 - 10/33000	2m/DD16A	10	90	274261	274351	1956
255	35/30 - 20/10	2m/DD16A	10	26342	13170	39512	1987
256	60/47.5 - 10/10	2m/DD16A	10	42	40	82	3288
257	60/47.5 - 10/1000	2m/DD16A	10	10	603	613	3361
258	60/47.5 - 10/100	2m/DD16A	10	20	145	165	3314
259	60/47.5 - 10/100	2m/DD16A	10	39	300	339	3281
260	60/47.5 - 1/1000	2m/DD16A	01/10	20	1268	1288	3235
261	47.5/30 - 10/10	2m/DD16A	10	519	510	1029	2545
263	47.5/30 - 1/100r	2m/DD16A	10	942	94100	95042	2483
264	47.5/30 - 1/100r	2m/DD16A	10	90	8900	8990	2785
265	47.5/30 - 10/10000	2m/DD16A	10	120	110187	110307	2673
267	47.5/30 - 10/1000r	2m/DD16A	10	340	33037	33377	2469
268	1 cycle	2m/DD16A	1 cycle	1		1	4038
269	1 cycle	2m/DD16A	1 cycle	1		1	4203
270	1 cycle	2m/DD16A	1 cycle	1		1	3807
271	1 cycle	2m/DD16A	1 cycle	1		1	3894
272	1 cycle	2m/DD16A	1 cycle	1		1	3895
273	1 cycle	2m/DD16B	1 cycle	1		1	5607
274	1 cycle	2m/DD16B	1 cycle	1		1	5581
275	60/35 - 10/112	2m/DD16B	10	274	3024	3298	2977
276	47.5/30 - 10/1000	2m/DD16B	10	359	35000	35359	2585
277	35/30 - 10/1000	2m/DD16B	10	1320	131237	132557	2043
278	35/30 - 10/100	2m/DD16B	10	34940	349366	384306	2062
279	47.5/35 - 10/5000	2m/DD16B	10	150	71692	71842	2539
280	47.5/35 - 10/1000	2m/DD16B	10	80	7892	7972	3039
281	47.5/30 - 10/100	2m/DD16B	10	2543	25400	27943	2496
282	60 ksi	2m/DD16B	10	85		85	3521
283	1 cycle	2m/DD16B	1 cycle	1		1	5771
284	35	2m/DD16B	10	109547		109547	2111
285	35/30 - 10/1000	2m/DD16B	10	7060	706997	714057	1952
287	47.5/30 - 10/1000r	2m/DD16B	10	408	40800	41208	2796
288	47.5/30 - 10/1000r	2m/DD16B	10	288	28840	29128	2865
289	47.5/30 - 1/100r	2m/DD16B	10	81	8100	8181	2845
290	47.5/30 - 10/1000r	2m/DD16B	10	175	17448	17623	2894
291	47.5/30 - 10/1000	2m/DD16B	10	610	60710	61320	2888
294	47.5/30 - 10/1000	2m/DD16B	10	540	53027	53567	2522
295	47.5/30 - 10/1000r	2m/DD16B	10	442	44166	44608	2986
296	1 cycle	2m/DD16B	1 cycle	1		1	4566

Test #	Comment	Coupon Style/Material	Freq Hz	# High Cycles	# Low Cycles	Total Cycles	Hi Block Max
297	60 ksi	2m/DD16B	10	491		491	3381
298	60 ksi	2m/DD16B	10	356		356	3689
299	35/30 - 10/990	2m/DD16B	10	5970	590898	596868	2056
300	60/35 - 10/9000	2m/DD16B	10	40	27155	27195	3482
301	35/30 - 10/90	2m/DD16B	10	10170	91462	101632	2124
302	35 ksi	2m/DD16B	10	54487		54487	2096
303	35/30 - 10/49990	2m/DD16B	10	60	264911	264971	2226
304	60/35 - 10/112	2m/DD16B	10	312	3472	3784	3622
305	30 ksi	2m/DD16B	10		121190	121190	1810
306	1 cycle	2m/DD16B	1 cycle	1		1	5823
307	60/35 - 10/90	2m/DD16B	10	44	360	404	4109
308	60 ksi	2m/DD16B	10	91		91	3545
309	30 ksi	2m/DD16B	10		373306	373306	1713
310	60/47.5 - 10/10	2m/DD16B	10	141	140	281	3164
311	60/47.5 - 10/90	2m/DD16B	10	173	1530	1703	3524
312	60/47.5 - 10/990	2m/DD16B	10	10	517	527	3715
313	60 ksi	2m/DD16B	10	429		429	3396
314	47.5/30 - 10/1000r	2m/DD16B	10	335	33528	33863	2643
315	47.5/30 - 10/10	2m/DD16B	10	2174	2170	4344	2929
316	47.5/30 - 10/90	2m/DD16B	10	1762	15840	17602	2837
317	47.5/30 - 10/1000r	2m/DD16B	10	464	46400	46864	2842
318	35/30 - 10/90	2m/DD16B	10	1610	14403	16013	2244
319	35/30 - 10/990	2m/DD16B	10	1980	195842	197822	2086
320	47.5/30 - 1/100r	2m/DD16B	10	301	30100	30401	2993
321	47.5	2m/DD16B	10	2611		2611	2717
322	47.5/30 - 10/1000r	2m/DD16B	10	441	44103	44544	2764
323	35	2m/DD16B	10	16884		16884	2246
324	47.5/30 - 1/100r	2m/DD16B	10	127	12700	12827	3052
325	47.5	2m/DD16B	10	8653		8653	2701
326	35	2m/DD16B	10	104679		104679	2045
327	47.5/30 - 10/1000r	2m/DD16B	10	480	48211	48691	2790
328	47.5/30 - 10/1000	2m/DD16B	10	799	79000	79799	2807
329	1 cycle	2m/DD16B	1 cycle	1		1	4665
330	47.5/30 - 10/1000r	2m/DD16B	10	379	37932	38311	2770
331	47.5/30 - 10/1000r3	2m/DD16B	10	980	98000	98980	2803
332	47.5/30 - 1/100r	2m/DD16B	10	278	27800	28078	3054
333	47.5/30 - 10/1000r3	2m/DD16B	10	510	51000	51510	3042
334	47.5/30 - 10/1000r2	2m/DD16B	10	591	59082	59673	2718
335	60 ksi - R=0.5	2m/DD16B	10	4701		4701	3542
336	47.5 ksi - R=0.5	2m/DD16B	10	32173		32173	2755
337	35 ksi - R=0.5	2m/DD16B	10	1469317		1469317	2119
339	47.5/30 - 10/1000 R=0.5	2m/DD16B	10	1630	16200	17830	2817
343	35 ksi - R=0.5	2m/DD16B	10	350682		350682	2087

Test #	Comment	Coupon Style/Material	Freq Hz	# High Cycles	# Low Cycles	Total Cycles	Hi Block Max
344	30 ksi	2m/DD16B	10		run out		1785
345	35/30 ksi - 10/90 R=0.5	2m/DD16B	10	80180	721620	801800	2189
346	60 ksi R=0.5	2m/DD16B	10	3836		3836	3479
347	47.5 ksi R=0.5	2m/DD16B	10	20006		20006	2955
348	47.5/30 ksi - 10/1000 R=0.5	2m/DD16B	10	1790	179000	180790	2912
349	1 cycle	2m/DD16B	1 cycle	1		1	4454
350	47.5/35 - 10/10	2m/DD16B	10	5749	5740	11489	2802
351	47.5/35 - 10/90	2m/DD16B	10	1899	17010	18909	2814
352	47.5/30 - 10/1000 R=0.5	2m/DD16B	10	1710	171000	172710	2809
353	47.5/30 - 10/1000r3	2m/DD16B	10	350	35002	35352	2872
354	47.5/30 - 10/1000r2	2m/DD16B	10	832	83248	84080	2800
363	47.5	2m/DD16C	10	3139		3139	2898
368	47.5/30 - 10/1000r	2m/DD16C	10	551	55063	55614	2886
369	47.5/30 - 10/1000	2m/DD16C	10	312	31000	31312	2840
370	47.5/30 - 1/100r	2m/DD16C	10	584	58400	58984	2775
371	47.5/30 - 1/100r	2m/DD16C	10	257	25700	25957	2916
372	47.5/30 - 10/1000r3	2m/DD16C	10	750	75006	75756	2974
373	47.5/30 - 10/1000r3	2m/DD16C	10	479	47874	48353	2807
374	47.5/30 - 10/1000	2m/DD16C	10	1470	146350	147820	2758
375	47.5/30 - 10/1000r3	2m/DD16C	10	561	56122	56683	2889
376	47.5	2m/DD16C	10	1706		1706	2978
377	47.5/30 - 1/100r	2m/DD16C	10	670	67000	67670	2857
378	30	2m/DD16C	10		261287	261287	1829
379	47.5/30 - 1/100r	2m/DD16C	10	606	60600	61206	2913
380	47.5/30 - 10/1000r3	2m/DD16C	10	699	69875	70574	2794
381	47.5/30 - 10/1000r3	2m/DD16C	10	630	63002	63632	2815
382	47.5/30 - 1/100r	2m/DD16C	10	301	30100	30401	2841
383	1 cycle	2m/DD16C	1 cycle	1		1	5525
384	47.5/30 - 1/100r	2m/DD16C	10	681	68100	68781	2797
385	47.5/30 - 10/1000r3	2m/DD16C	10	364	36388	36752	2983
386	47.5/30 - 10/1000	2m/DD16C	10	454	45000	45454	2882
387	47.5/30 - 10/1000 random3	2m/DD16C	10	460	46001	46461	2909
388	47.5/30 - 1/100 onecycle	2m/DD16C	10	1698	169800	171498	2877
389	47.5/30 - 10/1000 random3	2m/DD16C	10	510	51005	51515	2897
390	47.5/30 - 10/1000 random3	2m/DD16C	10	869	86907	87776	2902
391	30 ksi	2m/DD16C	10		421272	421272	1827
392	47.5/30 - 1/100 onecycle	2m/DD16C	10	755	75500	76255	2860
393	47.5/30 - 1/100 onecycle	2m/DD16C	10	407	40700	41107	2934
394	47.5/30 - 10/1000	2m/DD16C	10	720	71039	71759	2824

Test #	Comment	Coupon Style/Material	Freq Hz	# High Cycles	# Low Cycles	Total Cycles	Hi Block Max
395	47.5/30 - 1/100 onecycle	2m/DD16C	10	306	30600	30906	2878
396	47.5/30 - 10/1000 random3	2m/DD16C	10	800	80004	80804	2760
397	47.5/30 - 10/1000	2m/DD16C	10	993	99000	99993	3009
398	47.5/30 - 10/1000 random3	2m/DD16C	10	369	36860	37229	2811
399	47.5/30 - 1/100 onecycle	2m/DD16C	10	598	59800	60398	2898
400	60/47.5 - 10/10 R=0.5	2m/DD16C	10	1292	1290	2582	3353
401	60/47.5 - 10/50 R=0.5	2m/DD16C	10	879	4350	5229	3204
402	60/47.5 - 10/100 R=0.5	2m/DD16C	10	560	5576	6136	3193
403	60/47.5 - 10/1000 R=0.5	2m/DD16C	10	165	16000	16165	3281
404	60/47.5 - 10/10 R=0.5	2m/DD16C	10	2266	2260	4526	3451
405	60/47.5 - 10/50 R=0.5	2m/DD16C	10	2352	11750	14102	3252
406	60/47.5 - 10/100 R=0.5	2m/DD16C	10	872	8700	9572	3435
407	60/47.5 - 10/1000 R=0.5	2m/DD16C	10	240	23256	23496	3353
408	60 ksi R=0.5	2m/DD16C	10	2290		2290	3456
409	47.5 ksi R=0.5	2m/DD16C	10		49288	49288	2586
410	1 cycle	2m/DD16C	1 cycle	1		1	5174
411	47.5/30 - 10/1000 random3	2m/DD16C	10	460	46000	46460	2588
412	35 ksi R=0.5	2m/DD16C	10	829489		829489	1933
413	60/35 - 10/10 R=0.5	2m/DD16C	10	3233	3230	6463	3242
414	60/35 - 10/1000 R=0.5	2m/DD16C	10	267	26000	26267	3444
415	60/35 - 10/10000 R=0.5	2m/DD16C	10	175	170000	170175	3197
416	47.5 ksi R=0.5	2m/DD16C	10	74500		74500	2492
417	60 ksi R=0.5	2m/DD16C	10	4100		4100	3294
418	35 ksi R=0.5	2m/DD16C	10	1559097		1559097	1874
419	60/35 - 10/10000 R=0.5	2m/DD16C	10	91	90000	90091	3419
420	60/35 - 10/1000 R=0.5	2m/DD16C	10	258	25000	25258	3456
421	60/35 - 10/10 R=0.5	2m/DD16C	10	2800	2800	5600	3330
422	47.5/35 - 10/10 R=0.5	2m/DD16C	10	14325	14320	28645	2620
423	47.5/35 - 10/100 R=0.5	2m/DD16C	10	22439	224300	246739	2632
424	47.5/35 - 10/1000 R=0.5	2m/DD16C	10	1939	193000	194939	2567
425	47.5/35 - 10/1000 R=0.5	2m/DD16C	10	1481	148000	149481	2579
426	35 ksi R=0.5	2m/DD16C	10	808064		808064	1925
427	47.5/35 - 10/100 R=0.5	2m/DD16C	10	16397	163900	180297	2563
428	47.5/35 - 10/10 R=0.5	2m/DD16C	10	47833	47830	95663	2600
429	47.5 ksi R=0.5	2m/DD16C	10	33362		33362	2617
430	1 cycle	2m/DD16C	1 cycle	1		1	4531
431	60 ksi R=0.5	2m/DD16C	10	2469		2469	3303
432	47.5/30 - 1/100 R=0.1	2m/DD16C	01/10	447	44600	45047	2608
433	60 R=0.1	2m/DD16C	10	757		757	3274
434	47.5 R=0.1	2m/DD16C	10	3744		3744	2559

Test #	Comment	Coupon Style/Material	Freq Hz	# High Cycles	# Low Cycles	Total Cycles	Hi Block Max
435	35 R=0.1	2m/DD16C	10	181518		181518	1940
436	30 R=0.1	2m/DD16C	10	1137595		1137595	1637
437	47.5/30 - 10/1000	2m/DD16C	10	1282	128000	129282	2572
438	47.5/30 - 10/1000 random2	2m/DD16C	10	432	43206	43638	2600
439	60/47.5/35 - 10/10/100	2m/DD16C	10	394	390	4684	3291
440	47.5/60/35 - 10/10/100	2m/DD16C	10	820	811	9731	3195
441	60/35/47.5 - 10/100/10	2m/DD16C	10	219	2100	2529	3314
442	60/47.5/35 - 10/10/100	2m/DD16C	10	270	260	3130	3591
443	35/47.5/60 - 100/10/10	2m/DD16C	10	4200	420	5037	3282
444	60/37.9 - 10/1000 rand5	2m/DD16C	10	24	2383	2407	3357
445	47.5/30 - 10/1000 rand5	2m/DD16C	10	156	15629	15785	2658
446	47.5/30 - 10/1000 rand5	2m/DD16C	10	291	29134	29425	2625
447	47.5/30 - 10/1000 rand5	2m/DD16C	10	810	81086	81896	2549
448	47.5/30 - 10/1000 rand5	2m/DD16C	10	231	23134	23365	2603
449	47.5/30 - 10/1000 rand5	2m/DD16C	10	331	33134	33465	2660
450	47.5/30 - 10/1000 rand5	2m/DD16C	10	201	20127	20328	2646
451	47.5/30 - 10/1000 rand5	2m/DD16C	10	136	13576	13712	2615
452	47.5/30 - 10/1000 rand5	2m/DD16C	10	369	36851	37220	2576
453	47.5/30 - 10/1000 rand5	2m/DD16C	10	125	12469	12594	2613
454	47.5/30 - 10/1000 rand5	2m/DD16C	10	509	50912	51421	2570
455	47.5/30 - 10/1000 rand5	2m/DD16C	10	289	28912	29201	2760
456	47.5/30 - 10/1000 rand5	2m/DD16C	10	269	26851	27120	2615
457	47.5/30 - 10/1000 rand5	2m/DD16C	10	122	12209	12331	2559
459	60 ksi residual	2m/DD16C	10	100		100	3232
459r	60 ksi residual	2m/DD16C	1 cycle				5112
460	60 ksi residual	2m/DD16C	10	478		100	3382
461	60 ksi residual	2m/DD16C	10	810		100	3342
462	60 ksi residual	2m/DD16C	10	100		100	3332
462r	60 ksi residual	2m/DD16C	1 cycle				5324
463	60 ksi residual	2m/DD16C	10	100		100	3313
462r	60 ksi residual	2m/DD16C	1cycle				5289
464	47.5 ksi residual	2m/DD16C	10	1000		100	2890
464r	47.5 ksi residual	2m/DD16C	1 cycle				5830
465	47.5 ksi residual	2m/DD16C	10	7752		100	2717
466	47.5 ksi residual	2m/DD16C	10	1000		100	2756
466r	47.5 ksi residual	2m/DD16C	1 cycle				4960
467	47.5 ksi residual	2m/DD16C	10	9811		100	2580
468	47.5 ksi residual	2m/DD16C	10	1000		100	2597
468r	47.5 ksi residual	2m/DD16C	1 cycle				4525
469	35 ksi residual	2m/DD16C	10	10000		100	1906
469r	35 ksi residual	2m/DD16C	1 cycle				5133
470	35 ksi residual	2m/DD16C	10	100000		100	2016

Test #	Comment	Coupon Style/Material	Freq Hz	# High Cycles	# Low Cycles	Total Cycles	Hi Block Max
470r	35 ksi residual	2m/DD16C	1 cycle				4929
471	35 ksi residual	2m/DD16C	10	100000		100	1922
471r	35 ksi residual	2m/DD16C	1 cycle				5091
472	35 ksi residual	2m/DD16C	10	10000		100	2007
472r	35 ksi residual	2m/DD16C	1 cycle				5402
473	35 ksi residual	2m/DD16C	10	10000		100	1878
473r	35 ksi residual	2m/DD16C	1 cycle				5088
474	1 cycle	2m/DD16C	1 cycle	1		1	5558
475	47.5 ksi residual	2m/DD16C	10	10000			2732
475r	47.5 ksi residual	2m/DD16C	1 cycle				5282
476	35 ksi residual	2m/DD16C	10	100000			1922
476r	35 ksi residual	2m/DD16C	1 cycle				4772
477	60 ksi residual	2m/DD16C	10	1000			3243
477r	60 ksi residual	2m/DD16C	1 cycle				5189
479	1 cycle	2m/DD16C	1 cycle	1		1	5146
480	47.5/30 - 1/100 onecycle	2m/DD16C	10	469	46900	47369	2710
481	47.5/30 - 10/1000 random2	2m/DD16C	10	528	52876	53404	2589
482	47.5/30 - 10/1000 block	2m/DD16C	10	320	32007	32327	2613
483	47.5/30 - 10/1000 rand5	2m/DD16C	10	349	34949	35298	2624
484	47.5 ksi	2m/DD16C	10	936		936	2580
485	30 ksi, R=0.1	2m/DD16C	10	286613		286613	1664
486	60 ksi	2m/DD16C	10	1119		1119	3281
487	47.5 ksi, R=0.5	2m/DD16C	10	21452		21452	2800
488	35 ksi, R=0.5	2m/DD16C	10	156860		156860	1891
489	60/47.5/35 - 10/10/100	2m/DD16C	10	113	110		3241
490	47.5/60/35 - 10/10/100	2m/DD16C	10	180	174		3359
491	35/47.5/60 - 100/10/10	2m/DD16C	10	1600	160		3329
492	60/47.5/35 - 10/10/100	2m/DD16C	10	123	120		3377
493	35/47.5/60 - 100/10/10	2m/DD16C	10	1634	160		3316
494	47.5 ksi residual - R=0.5	2m/DD16C	10	9596		9596	2621
495	47.5 ksi residual - R=0.5	2m/DD16C	10	9872		9872	2650
496	47.5 ksi residual - R=0.5	2m/DD16C	10	12289		12289	2773
497	47.5 ksi residual - R=0.5	2m/DD16C	10	8981		8981	2479
498	47.5 ksi residual - R=0.5	2m/DD16C	10	8899		8899	2708
499	47.5 ksi residual - R=0.5	2m/DD16C	10	32810		32810	2304
500	47.5 ksi residual - R=0.5	2m/DD16C	10	20000		20000	2417
500r	47.5 ksi residual - R=0.5	2m/DD16C	1 cycle				4149
501	47.5 ksi residual - R=0.5	2m/DD16C	10	10000		10000	2583
501r	47.5 ksi residual - R=0.5	2m/DD16C	1 cycle				3969
502	47.5 ksi residual - R=0.5	2m/DD16C	10	12442		12442	2492
503	47.5 ksi residual - R=0.5	2m/DD16C	10	5336		5336	2517
504	47.5 ksi residual - R=0.5	2m/DD16C	10	10000		10000	2503

Test #	Comment	Coupon Style/Material	Freq Hz	# High Cycles	# Low Cycles	Total Cycles	Hi Block Max
504r	47.5 ksi residual - R=0.5	2m/DD16C	1 cycle				4464
505	47.5 ksi residual - R=0.5	2m/DD16C	10	9800		9800	2572
506	47.5 ksi residual - R=0.5	2m/DD16C	10	11920		11920	2608
507	47.5 ksi residual - R=0.5	2m/DD16C	10	3769		3769	2843
508	47.5 ksi residual - R=0.5	2m/DD16C	10	8254		8254	2656
509	47.5 ksi residual - R-0.5	2m/DD16C	10	20000		20000	2543
509r	47.5 ksi residual - R=0.5	2m/DD16C	1 cycle				3659
510	47.5 ksi residual - R=0.5	2m/DD16C	10	10000		10000	2685
510r	47.5 ksi residual - R=0.5	2m/DD16C	1 cycle				4100
511	47.5 ksi residual - R=0.5	2m/DD16C	10	18330		18330	2559
512	47.5 ksi residual - R=0.5	2m/DD16C	10	8643		8643	2659
513	47.5 ksi residual - R=0.5	2m/DD16C	10	10000		10000	2529
513r	47.5 ksi residual - R=0.5	2m/DD16C	1 cycle				4570
514	47.5 ksi residual - R=0.5	2m/DD16C	10	11418		11418	2537
515	47.5 ksi residual - R=0.5	2m/DD16C	10	10814		10814	2536
516	47.5 ksi residual - R=0.5	2m/DD16C	10	7732		7732	2755
517	47.5 ksi residual - R=0.5	2m/DD16C	10	13968		13968	2741
518	47.5 ksi residual - R=0.5	2m/DD16C	10	8684		8684	2588
519	47.5 ksi residual - R=0.5	2m/DD16C	10	10000		10000	2892
519r	47.5 ksi residual - R=0.5	2m/DD16C	1 cycle				4793
520	47.5 ksi residual - R=0.5	2m/DD16C	10	7107		7107	2629
521	47.5 ksi residual - R=0.5	2m/DD16C	10	7189		7189	2530
522	47.5 ksi residual - R=0.5	2m/DD16C	10	10000		10000	2549
522r	47.5 ksi residual - R=0.5	2m/DD16C	1 cycle				3149
523	47.5 ksi residual - R=0.5	2m/DD16C	10	13784		13784	2619
524	47.5/30 ksi 1/100 block	2m/DD16C	10	227	22674	22901	2597
525	47.5/30 ksi 10/1000 block	2m/DD16C	10	340	34008	34348	2555
526	47.5/30 ksi 10/1000 rand5	2m/DD16C	10	470	46982	47452	2541
527	47.5/30 ksi 1/100 block	2m/DD16C	10	393	39300	39693	2545
528	47.5/30 ksi 10/1000 block	2m/DD16C	10	192	19209	19401	2506
529	47.5/30 ksi 10/1000 rand5	2m/DD16C	10	119	11851	11970	2537
530	47.5/30 ksi 1/100 block	2m/DD16C	10	233	23300	23533	2691
531	47.5/30 ksi 10/1000 block	2m/DD16C	10	1150	115005	116155	2545
532	47.5/30 ksi 10/1000 rand5	2m/DD16C	10	131	13134	13265	2544
533	47.5/30 ksi 1/100 block	2m/DD16C	10	550	55019	55569	2619
534	47.5/30 ksi 10/1000 block	2m/DD16C	10	240	24008	24248	2460

Test #	Comment	Coupon Style/Material	Freq Hz	# High Cycles	# Low Cycles	Total Cycles	Hi Block Max
535	47.5/30 ksi 10/1000 rand5	2m/DD16C	10	105	10548	10653	2652
536	47.5/30 ksi 1/100 block	2m/DD16C	10	261	26153	26414	2657
537	47.5/30 ksi 10/1000 block	2m/DD16C	10	220	22001	22221	2476
538	47.5/30 ksi 10/1000 rand5	2m/DD16C	10	141	14087	14228	2499
539	47.5/30 ksi 1/100 block	2m/DD16C	10	469	46900	47369	2436
540	47.5/30 ksi 10/1000 block	2m/DD16C	10	58	5834	5892	2693
541	47.5/30 ksi 10/1000 rand5	2m/DD16C	10	122	12209	12331	2596
542	47.5/30 ksi 1/100 block	2m/DD16C	10	239	23900	24139	2622
543	47.5/30 ksi 10/1000 block	2m/DD16C	10	260	25951	26211	2882
544	47.5/30 ksi 10/1000 rand5	2m/DD16C	10	53	5342	5395	2685
545	47.5/30 ksi 1/100 block	2m/DD16C	10	241	24060	24301	2525
546	47.5/30 ksi 10/1000 block	2m/DD16C	10	179	17908	18087	2672
547	47.5/30 ksi 10/1000 rand5	2m/DD16C	10	463	46342	46805	2565
548	47.5/30 ksi 1/100 block	2m/DD16C	10	198	19800	19998	2527
549	47.5/30 ksi 10/1000 block	2m/DD16C	10	310	31007	31317	2406
550	47.5/30 ksi 10/1000 rand5	2m/DD16C	10	70	6982	7052	2740
551	47.5/30 ksi 1/100 block	2m/DD16C	10	138	13767	13905	2599
552	47.5/30 ksi 10/1000 block	2m/DD16C	10	254	25393	25647	2543
553	47.5/30 ksi 10/1000 rand5	2m/DD16C	10	206	20576	20782	2467
554	47.5 ksi, R=0.1	2m/DD16C	10	763		763	2595
556	47.5 ksi, R=0.5	2m/DD16C	10	15905		15905	2540
557	47.5 ksi,R=0.5	2m/DD16C	10	38319		38319	2317
558	47.5 ksi, R=0.5	2m/DD16C	10	8357		8357	2276
559	47.5 ksi, R=0.5	2m/DD16C	10	31685		31685	2551
560	47.5 ksi, R=0.5	2m/DD16C	10	21025		21025	2448
561	47.5 ksi, R=0.5	2m/DD16C	10	48516		48516	2460
562	47.5 ksi, R=0.5	2m/DD16C	10	24391		24391	2456
563	35 ksi, R=0.5	2m/DD16C	10	1051280		1051280	1731
564	35 ksi, R=0.5	2m/DD16C	10	1988538		1988538	2016
565	35 ksi, R=0.5	2m/DD16C	10	1119777		1119777	1698
566	35 ksi, R=0.5	2m/DD16C	10	280171		280171	1761
568	35 ksi, R=0.5	2m/DD16C	10	1749635		1749635	1750

Test #	Comment	Coupon Style/Material	Freq Hz	# High Cycles	# Low Cycles	Total Cycles	Hi Block Max
569	35 ksi, R=0.5	2m/DD16C	10	763276		763276	1737
570	35 ksi, R=0.5	2m/DD16C	10	2470072			1678
571	60 ksi, R=0.5	2m/DD16C	10	1652		1652	3211
572	60 ksi, R=0.5	2m/DD16C	10	2513		2513	2864
573	60 ksi, R=0.5	2m/DD16C	10	2519		2519	3038
576	60 ksi, R=0.5	2m/DD16C	10	2755		2755	2941
577	60 ksi, R=0.1	2m/DD16C	10	310		310	3072
578	60 ksi, R=0.1	2m/DD16C	10	274		274	3006
579	60 ksi, R=0.1	2m/DD16C	10	283		283	3133
580	60 ksi, R=0.1	2m/DD16C	10	334		334	3154
581	47.5 ksi, R=0.1	2m/DD16C	10	4375		4375	2430
582	47.5 ksi, R=0.1	2m/DD16C	10	4190		4190	2414
583	47.5 ksi, R=0.1	2m/DD16C	10	2620		2620	2350
584	47.5 ksi, R=0.1	2m/DD16C	10	1306		1306	2376
585	35 ksi, R=0.1	2m/DD16C	10	186268		186268	1782
586	35 ksi, R=0.1	2m/DD16C	10	89527		89527	1755
587	35 ksi, R=0.1	2m/DD16C	10	35109		35109	1796
588	35 ksi, R=0.1	2m/DD16C	10	187293		187293	1787
589	30 ksi, R=0.1	2m/DD16C	10	697446		697446	1624
590	30 ksi, R=0.1	2m/DD16C	10	436185		436185	1475
591	30 ksi, R=0.1	2m/DD16C	10	732874		732874	1476
592	30 ksi, R=0.1	2m/DD16C	10	366748		366748	1587
593	47.5/30 ksi, R=0.1, load5	2m/DD16D	10	1020	102006	103026	2196
594	47.5/30 ksi, R=0.1, wvrnr	2m/DD16D	01/10	379	37000	37379	2362
595	47.5/30 ksi, R=0.1, load5	2m/DD16D	10	410	41006	41416	2368
596	47.5/30 ksi, R=0.1,wvrnr	2m/DD16D	10	310	30570	30880	2453
597	47.5/30 ksi, R=0.1, load5	2m/DD16D	10	1850	185004	186854	2627
598	47.5/30 ksi, R=0.1, wvrnr	2m/DD16D	01/10	324	32000	32324	2317
599	47.5/30 ksi, R=0.1, load5	2m/DD16D	10	2120	212007	214127	2493
600	47.5/30 ksi, R=0.1, wvrnr	2m/DD16D	01/10	853	85000	85853	2373
601	47.5/30 ksi, R=0.1, load5	2m/DD16D	10	490	49001	49491	2157
602	47.5/30 ksi, R=0.1, wvrnr	2m/DD16D	10	310	30952	31262	2858
603	47.5/30 ksi, R=0.1, load5	2m/DD16D	10	500	50008	50508	2222

Test #	Comment	Coupon Style/Material	Freq Hz	# High Cycles	# Low Cycles	Total Cycles	Hi Block Max
604	47.5/30 ksi, R=0.1, wvrnr	2m/DD16D	10	390	38919	39309	2747
605	60 ksi, R=0.1, wvrnr	2m/DD16D	10	783		783	3332
606	60 ksi, R=0.1, load10	2m/DD16D	10	286		286	3425
607	47.5 ksi, R=0.1	2m/DD16D	10	1690		1690	3020
608	47.5 ksi, R=0.1, load10	2m/DD16D	10	1794		1794	3016
609	35 ksi, R=0.1	2m/DD16D	10	58826		58826	2072
610	35 ksi, R=0.1, load10	2m/DD16D	10	43618		43618	2064
611	30 ksi, R=0.1	2m/DD16D	10	318890		318890	1646
612	30 ksi, R=0.1, load10	2m/DD16D	10	418886		418886	1875
616	47.5 ksi, R=0.1, wvrnr	2m/DD16D	10	1081		1081	2783
617	47.5 ksi, R=0.1, load10	2m/DD16D	10	2433		2433	2802
618	47.5 ksi, R=0.1, wvrnr, ??	2m/DD16D	10	769		769	3052
619	47.5 ksi, R=0.1, load10	2m/DD16D	10	2329		2329	2771
620	60 ksi, R=0.1, wvrnr	2m/DD16D	10	234		234	3574
621	60 ksi, R=0.1, load10	2m/DD16D	10	180		180	3698
622	60 ksi, R=0.1, wvrnr	2m/DD16D	10	290		290	3690
623	60 ksi, R=0.1, load10	2m/DD16D	10	311		311	3495
624	60 ksi, R=0.1, wvrnr	2m/DD16D	10	161		161	3756
625	30 ksi, R=0.1, load10	2m/DD16D	10	41493		41493	1870
626	30 ksi, R=0.1, wvrnr	2m/DD16D	10	496355		496355	1831
627	30 ksi, R=0.1, load10	2m/DD16D	10	598609		598609	1744
628	30 ksi, R=0.1, wvrnr	2m/DD16D	10	129134		129134	1756
629	30 ksi, R=0.1, load10	2m/DD16D	10	78888		78888	1807
630	35 ksi, R=0.1, wvrnr	2m/DD16D	10	57742		57742	2217
632	35 ksi, R=0.1, load10	2m/DD16D	10	37576			2262
633	35 ksi, R=0.1, wvrnr	2m/DD16D	10	43491			2080
634	35 ksi, R=0.1, load10	2m/DD16D	10	163745			2031
635	1 cycle	2m/DD16D	1 cycle	1		1	5901
636	35 ksi, R=0.5, wvrnr	2m/DD16D	10	464516			2074
638	35 ksi, R=0.5, wvrnr	2m/DD16D	10	460884			1973
640	35 ksi, R=0.5, wvrnr	2m/DD16D	10	98521			2041
641	47.5 ksi, R=0.5, load11	2m/DD16D	10	7421			2768
642	47.5 ksi, R=0.5, wvrnr	2m/DD16D	10	5801			2784
643	47.5 ksi, R=0.5, load11	2m/DD16D	10	6548			2787
644	47.5 ksi, R=0.5, wvrnr	2m/DD16D	10	24381			3158
645	47.5 ksi, R=0.5, load11	2m/DD16D	10	19568			2775
646	1 cycle	2m/DD16D	1 cycle	1		1	4953
647	60 ksi, R=0.5, load11	2m/DD16D	10	2609			3615
648	60 ksi, R=0.5, wvrnr	2m/DD16D	10	438			3428
649	60 ksi, R=0.5, load11	2m/DD16D	10	2507			3607
650	60 ksi, R=0.5, wvrnr	2m/DD16D	10	1169			3559

Test #	Comment	Coupon Style/Material	Freq Hz	# High Cycles	# Low Cycles	Total Cycles	Hi Block Max
651	60 ksi, R=0.5, load11	2m/DD16D	10	1475			3858
652	1 cycle	2m/DD16D	1 cycle	1		1	4285
653	1 cycle	2m/DD16D	1 cycle	1		1	5624
654	60 ksi max, Wisperx	2m/DD16D	10	14090		14090	3656
655	1 cycle	2m/DD16D	1 cycle	1		1	5879
656	60 ksi max, Wisperx	2m/DD16D	10	13404		13404	2981
657	60/35 ksi, R=0.5, load12	2m/DD16D	10	490	4411	4901	3568
658	60/35 ksi, R=0.5, load12	2m/DD16D	10	1130	10178	11308	3462
659	60/35 ksi, R=0.5, load13	2m/DD16D	10	310	30695	31005	3520
660	60/35 ksi, R=0.5, load13	2m/DD16D	10	440	43565	44005	3788
661	47.5 ksi max, Wisperx	2m/DD16D	10	160725		160725	2965
662	47.5/35 ksi, R=0.5, load14	2m/DD16D	10	2800	277206	280006	2719
663	47.5/35 ksi, R=0.5, load14	2m/DD16D	10	3360	332645	336005	2699
665	47.5/35 ksi, R=0.5, load15	2m/DD16D	10	3230	29073	32303	2858
666	1 cycle	2m/DD16D	1 cycle	1		1	5726
667	60/35 ksi, R=0.5, load16	2m/DD16D	10	120	119888	120008	3627
668	60/35 ksi, R=0.5, load16	2m/DD16D	10	41	41388	41429	3885
669	60/35 ksi, R=0.5, load18	2m/DD16D	10	70	6934	7004	3807
670	60/35 ksi, R=0.5, load16	2m/DD16D	10	70	69935	70005	3429
671	1 cycle	2m/DD16D	1 cycle	1		1	5633
672	47.5 ksi, R=0.5, load11	2m/DD16D	10	1400		1400	2799
673	35 ksi, R=0.5, load11	2m/DD16D	10	100193		100193	1977
674	47.5/35 ksi, R=0.5, load17	2m/DD16D	10	350	349656	350006	2837
675	47.5/35 ksi, R=0.5, load17	2m/DD16D	10	160	160773	160933	2724
676	60 ksi max, Wisperx	2m/DD16D	10	12832		12832	3621
677	60 ksi max, WisxR05	2m/DD16D	10	1874		1874	3862
678	60 ksi max, WisxR05	2m/DD16D	10	2812		2812	3660
679	60 ksi max, WisxR05	2m/DD16D	10	6270		6270	3697
680	60 ksi max, WisxR05	2m/DD16D	10	2768		2768	4006
682	60 ksi max, WisxR05	2m/DD16D	10	2680		2680	3584
683	60 ksi max, WisxR05	2m/DD16D	10	2102		2102	3671
684	60 ksi max, WisxR05	2m/DD16D	10	1397		1397	3519
685	60 ksi max, WisxR05	2m/DD16D	10	956		956	3401
686	60 ksi max, WisxR05	2m/DD16D	10	3915		3915	3596
687	47.5 ksi max, WisxR05	2m/DD16D	10	40997		40997	2816
688	47.5 ksi max, WisxR05	2m/DD16D	10	51690		51690	2732
689	47.5 ksi max, WisxR05	2m/DD16D	10	28166		28166	2733
690	47.5 ksi max, WisxR05	2m/DD16D	10	34678		34678	2717

Test #	Comment	Coupon Style/Material	Freq Hz	# High Cycles	# Low Cycles	Total Cycles	Hi Block Max
691	47.5 ksi max, WisxR05	2m/DD16D	10	42728		42728	2831
692	47.5 ksi max, WisxR05	2m/DD16D	10	42077		42077	2842
693	47.5 ksi max, WisxR05	2m/DD16D	10	204617		204617	2825
694	47.5 ksi max, WisxR05	2m/DD16D	10	64030		64030	2819
695	47.5 ksi max, WisxR05	2m/DD16D	10	61941		61941	2989
696	47.5 ksi max, WisxR05	2m/DD16D	10	24102		24102	2888
697	35 ksi max, WisxR05	2m/DD16D	10	1268170		1268170	2072
698	35 ksi max, WisxR05	2m/DD16D	10	851414		851414	2049
700	35 ksi max, WisxR05	2m/DD16D	10	5040003		5040003	2242
701	35 ksi max, WisxR05	2m/DD16D	10	3466288		3466288	2119
702	35 ksi max, WisxR05	2m/DD16D	10	1620900		1620900	2051
703	35 ksi max, WisxR05	2m/DD16D	10	1002695		1002695	1992
704	35 ksi max, WisxR05	2m/DD16D	10	993446		993446	2005
705	35 ksi max, WisxR05	2m/DD16D	10	1130037		1130037	2306
706	35 ksi max, WisxR05	2m/DD16D	10	2387020		2387020	2264
707	30 ksi max, WisxR01	2m/DD16D	10	2502591		2502591	1728
708	30 ksi max, WisxR01	2m/DD16D	10	1523103		1523103	1790
709	35 ksi max, WisxR01	2m/DD16D	10	392963		392963	2110
710	35 ksi max, WisxR01	2m/DD16D	10	77859		77859	2186
711	47.5 ksi max, WisxR01	2m/DD16D	10	3963		3963	2741
712	47.5 ksi max, WisxR01	2m/DD16D	10	4457		4457	2986
713	60 ksi max, WisxR01	2m/DD16D	10	893		893	3356
714	60 ksi max, WisxR01	2m/DD16D	10	504		504	3640
715	30 ksi max, WisxR01	2m/DD16D	10	1231745		1231745	2020
716	35 ksi max, WisxR01	2m/DD16D	10	201697		201697	2103
717	60 ksi max, Load11	2m/DD16D	10	2886		2886	3677
718	60 ksi max, Load11	2m/DD16D	10	1412		1412	3453
719	47.5 ksi max, Load11	2m/DD16D	10	21037		21037	2736
720	47.5 ksi, Load11, R=0.5	2m/DD16D	10	120101		120101	2728
721	35 ksi max, Load11	2m/DD16D	10	272818		272818	2077
722	35 ksi max, Load11	2m/DD16D	10	545546		545546	2121
723	60 ksi max, WisxR01	2m/DD16D	10	1227		1227	3398
724	47.5 ksi max, WisxR01	2m/DD16D	10	4330		4330	3000
725	35 ksi max, WisxR01	2m/DD16D	10	128215		128215	1937
726	47.5 ksi max, WisxR01	2m/DD16D	10	3973		3973	3024
726a	1 cycle	2m/DD16D	1 cycle	1		1	5765
727	35 ksi max, WisxR01	2m/DD16D	10	491135		491135	2089
728	35 ksi max, WisxR01	2m/DD16D	10	116302		116302	2001
729	35 ksi max, WisxR01	2m/DD16D	10	153229		153229	2013
730	35 ksi max, WisxR01	2m/DD16D	10	165568		165568	2170
732	30 ksi max, WisxR01	2m/DD16D	10	609578		609578	1758
733	30 ksi max, WisxR01	2m/DD16D	10	202727		202727	1707
734	30 ksi max, WisxR01	2m/DD16D	10	2231997		2231997	1744

Test #	Comment	Coupon Style/Material	Freq Hz	# High Cycles	# Low Cycles	Total Cycles	Hi Block Max
735	47.5 ksi max, WisxR01	2m/DD16D	10	1977		1977	2960
736	47.5 ksi max, WisxR01	2m/DD16D	10	11721		11721	2684
737	47.5 ksi max, WisxR01	2m/DD16D	10	6742		6742	2655
738	47.5 ksi max, WisxR01	2m/DD16D	10	14445		14445	2673
739	1 cycle	2m/DD16D	1 cycle	1		1	5734
740	60 ksi max, WisxR01	2m/DD16D	10	620		620	3485
741	60 ksi max, WisxR01	2m/DD16D	10	1120		1120	3282
742	60 ksi max, WisxR01	2m/DD16D	10	818		818	3706
743	60 ksi max, WisxR01	2m/DD16D	10	624		624	3661
744	60 ksi max, Load10	2m/DD16D	10	642		642	3339
745	47.5 ksi max, Load10	2m/DD16D	10	1290		1290	2936
746	35 ksi max, Load10	2m/DD16D	10	31733		31733	2012
747	30 ksi max, Load10	2m/DD16D	10	544532		544532	1649
748	60 ksi max, Wisxmix	2m/DD16D	10	2211		2211	3597
749	60 ksi max, Wisxmix	2m/DD16D	10	3313		3313	3437
750	60 ksi max, Wisxmix	2m/DD16D	10	1744		1744	3576
751	60 ksi max, Wisxmix	2m/DD16D	10	2260		2260	3497
752	60 ksi max, Wisxmix	2m/DD16D	10	2058		2058	3405
753	60 ksi max, Wisxmix	2m/DD16D	10	5679		5679	3657
754	60 ksi max, Wisxmix	2m/DD16D	10	3634		3634	3440
755	60 ksi max, Wisxmix	2m/DD16D	10	1705		1705	3488
756	1 cycle	2m/DD16D	1 cycle	1		1	5940
757	47.5 ksi max, Wisxmix	2m/DD16D	10	8425		8425	3057
758	47.5 ksi max, Wisxmix	2m/DD16D	10	17202		17202	2687
759	47.5 ksi max, Wisxmix	2m/DD16D	10	17170		17170	2991
760	47.5 ksi max, Wisxmix	2m/DD16D	10	49795		49795	2732
761	47.5 ksi max, Wisxmix	2m/DD16D	10	15763		15763	2878
762	47.5 ksi max, Wisxmix	2m/DD16D	10	29281		29281	2908
763	47.5 ksi max, Wisxmix	2m/DD16D	10	9075		9075	3075
764	47.5 ksi max, Wisxmix	2m/DD16D	10	45756		45756	2974
765	1 cycle	2m/DD16D	1 cycle	1		1	5849
766	35 ksi max, Wisxmix	2m/DD16D	10	259709		259709	2071
767	35 ksi max, Wisxmix	2m/DD16D	10	625695		625695	2111
768	35 ksi max, Wisxmix	2m/DD16D	10	157203		157203	2022
769	35 ksi max, Wisxmix	2m/DD16D	10	373607		373607	1959
770	35 ksi max, Wisxmix	2m/DD16D	10	477747		477747	2091
771	35 ksi max, Wisxmix	2m/DD16D	10	165811		165811	2156
772	35 ksi max, Wisxmix	2m/DD16D	10	534391		534391	2040
773	35 ksi max, Wisxmix	2m/DD16D	10	763579		763579	1994
774	1 cycle	2m/DD16D	1 cycle	1		1	5893
775	30 ksi max, Wisxmix	2m/DD16D	10	2883840		2883840	1859
776	30 ksi max, Wisxmix	2m/DD16D	10	1085994		1085994	1740
777	30 ksi max, Wisxmix	2m/DD16D	10	1803131		1803131	1757

Test #	Comment	Coupon Style/Material	Freq Hz	# High Cycles	# Low Cycles	Total Cycles	Hi Block Max
778	30 ksi max, Wisxmix	2m/DD16D	10	1005992		1005992	1816
779	30 ksi max, Wisxmix	2m/DD16D	10	496982		496982	1913
780	30 ksi max, Wisxmix	2m/DD16D	10	1701443		1701443	1864
781	30 ksi max, Wisxmix	2m/DD16D	10	2392836		2392836	1889
782	30 ksi max, Wisxmix	2m/DD16D	10	2079241		2079241	1834
783	1 cycle	2m/DD16D	1 cycle	1		1	6086
784	60 ksi max, Load10	2m/DD16D	10	343		343	3445
785	60 ksi max, Load11	2m/DD16D	10	400		400	3809
786	60 ksi max, WisxR01	2m/DD16D	10	1713		1713	3419
787	60 ksi max, WisxR05	2m/DD16D	10	1349		1349	3645
788	47.5 ksi max, Load10	2m/DD16D	10	815		815	2677
789	47.5 ksi max, Load11	2m/DD16D	10	11812		11812	2961
790	47.5 ksi max, WisxR01	2m/DD16D	10	12294		12294	2860
791	47.5 ksi max, WisxR05	2m/DD16D	10	63945		63945	2992
792	35 ksi max, Load10	2m/DD16D	10	115525		115525	2178
793	35 ksi, R = 0.5	2m/DD16D	10	334060		334060	2185
794	35 ksi max, WisxR01	2m/DD16D	10	104636		104636	2032
795	35 ksi max, WisxR05	2m/DD16D	10	862547		862547	2238
796	-40 ksi, R=10	c/DD16D	10	11608		11608	-4041
797	-40 ksi, R=10	c/DD16D	10	2463		2463	-3942
798	-40 ksi, R=10	c/DD16D	10	2727		2727	-4101
799	-40 ksi, R=10	c/DD16D	10	5904		5904	-4024
800	-40 ksi, R=10	c/DD16D	10	5123		5123	-3996
801	-35 ksi, R=10	c/DD16D	10	379064		379064	-3531
802	-35 ksi, R=10	c/DD16D	10	54873		54873	-3636
803	-35 ksi, R=10	c/DD16D	10	11145		11145	-3666
804	-35 ksi, R=10	c/DD16D	10	11738		11738	-3454
805	-35 ksi, R=10	c/DD16D	10	21240		21240	-3746
806	-40 ksi, R=10	c/DD16D	10	5010		5010	-3962
807	-30 ksi, R=10	c/DD16D	10	487946		487946	-3099
808	-30 ksi, R=10	c/DD16D	10	993821		993821	-3045
809	-30 ksi, R=10	c/DD16D	10	1859843		1859843	-2927
810	-30 ksi, R=10	c/DD16D	10	1747111		1747111	-2991
811	-30 ksi, R=10	c/DD16D	10	1464645		1464645	-2949
812	1 cycle	c/DD16D	1 cycle	1		1	-5815
813	-40 ksi, R=10	c/DD16D	10	2469		2469	-4077
814	-40 ksi, R=10	c/DD16D	10	4353		4353	-4002
816	-40 ksi, R=10	c/DD16D	10	3850		3850	-3979
817	-40 ksi, R=10	c/DD16D	10	15393		15393	-3875
818	1 cycle	c/DD16D	1 cycle	1		1	-5626
819	-35 ksi, R=10	c/DD16D	10	14172		14172	-3617
820	-35 ksi, R=10	c/DD16D	10	36657		36657	-3526
821	-35 ksi, R=10	c/DD16D	10	6704		6704	-3692

Test #	Comment	Coupon Style/Material	Freq Hz	# High Cycles	# Low Cycles	Total Cycles	Hi Block Max
822	-35 ksi, R=10	c/DD16D	10	9235		9235	-3448
823	-35 ksi, R=10	c/DD16D	10	67973		67973	-3484
824	1 cycle	c/DD16D	1 cycle	1		1	-5948
825	-30 ksi, R=10	c/DD16D	10	1505733		1505733	-2976
826	-30 ksi, R=10	c/DD16D	10	1980344		1980344	-3017
827	-30 ksi, R=10	c/DD16D	10	1037244		1037244	-3069
828	-30 ksi, R=10	c/DD16D	10	1508674		1508674	-3043
829	-30 ksi, R=10	c/DD16D	10	842537		842537	-3078
830	1 cycle	c/DD16D	1 cycle	1		1	-5560
831	1 cycle	c/DD16D	1 cycle	1		1	-5769
832	1 cycle	c/DD16D	1 cycle	1		1	-5395
833	1 cycle	c/DD16D	1 cycle	1		1	-6103
834	1 cycle	c/DD16D	1 cycle	1		1	-5485
835	1 cycle	c/DD16D	1 cycle	1		1	-6182
836	-40/-30 ksi,10/1000/R=10	c/DD16D	10	3030	303000	306030	-3994
837	-40/-30 ksi,10/1000/R=10	c/DD16D	10	2500	250000	252500	-3917
838	-40/-30 ksi,10/1000/R=10	c/DD16D	10	2200	220005	222205	-4040
839	-40/-30 ksi,10/1000/R=10	c/DD16D	10	4590	459006	463596	-3916
840	-40/-30 ksi,10/100/R=10	c/DD16D	10	2651	26508	29159	-3896
841	-40/-30 ksi,10/100/R=10	c/DD16D	10	8311	83107	91418	-3880
842	-40/-30 ksi,10/100/R=10	c/DD16D	10	9890	98903	108793	-3891
843	-40/-30 ksi,10/100/R=10	c/DD16D	10	10920	109206	120126	-3879
844	-40/-30 ksi,10/10/R=10	c/DD16D	10	1684	1684	3368	-4042
845	-40/-30 ksi,10/10/R=10	c/DD16D	10	11151	11151	22302	-3901
846	-40/-30 ksi,10/10/R=10	c/DD16D	10	4374	4374	8748	-4086
847	-40/-30 ksi,10,000/10/R=10	c/DD16D	10	290	290007	290297	-4066
848	-40/-30 ksi,10,000/10/R=10	c/DD16D	10	330	330003	330333	-4059
849	-40/-30 ksi,10,000/10/R=10	c/DD16D	10	2030	2030002	2032032	-3918
850	-40/-30 ksi,1000/10/R=10	c/DD16D	10	630	63000	63630	-4027
851	-40/-30 ksi,1000/10/R=10	c/DD16D	10	7430	743010	750440	-3937
852	-40/-30 ksi,1000/10/R=10	c/DD16D	10	4780	478000	482780	-3921
853	-40/-30 ksi,1000/10/R=10	c/DD16D	10	400	40007	40407	-4184

Test #	Comment	Coupon Style/Material	Freq Hz	# High Cycles	# Low Cycles	Total Cycles	Hi Block Max
854	-40/-30 ksi,1000/10/R=10	c/DD16D	10	680	68001	68681	-3985
855	-40 ksi, R=10	c/DD16D	10	4063		4063	-3942
856	-40 ksi, R=10	c/DD16D	10	4410		4410	-3909
857	-40 ksi, R=10	c/DD16D	10	1957		1957	-4121
858	-40 ksi, R=10	c/DD16D	10	8288		8288	-3910
859	-40 ksi, R=10	c/DD16D	10	10692		10692	-3949
860	-30 ksi, R=10	c/DD16D	10	2021912		2021912	-2965
861	-30 ksi, R=10	c/DD16D	10	943072		943072	-3077
862	-30 ksi, R=10	c/DD16D	10	205084		205084	-3110
863	-30 ksi, R=10	c/DD16D	10	1884110		1884110	-3131
864	-30 ksi, R=10	c/DD16D	10	235297		235297	-3024
865	1 cycle	c/DD16D	1 cycle	1		1	-6107
866	1 cycle	c/DD16D	1 cycle	1		1	-5727
867	1 cycle	c/DD16D	1 cycle	1		1	-5982
868	1 cycle	c/DD16D	1 cycle	1		1	-5574
869	1 cycle	c/DD16D	1 cycle	1		1	-5941
870	-40/-30 ksi,10/10/R=10	c/DD16D	10	1171	1170	2341	-4084
871	-40/-30 ksi,10/10/R=10	c/DD16D	10	2675	2674	5349	-4061
872	-40/-30 ksi,10/10/R=10	c/DD16D	10	1685	1684	3369	-4070
873	-40/-30 ksi,10/10/R=10	c/DD16D	10	3362	3362	6724	-4038
874	-40/-30 ksi,10/10/R=10	c/DD16D	10	9812	9812	19624	-3893
875	-40/-30 ksi,10,000/10/R=10	c/DD16D	10	990	990000	990990	-3899
876	-40/-30 ksi,10,000/10/R=10	c/DD16D	10	1398	1397653	1399051	-3934
877	-40/-30 ksi,10,000/10/R=10	c/DD16D	10	153	155364	155517	-4056
878	-40/-30 ksi,10,000/10/R=10	c/DD16D	10	728	727806	728534	-3948
879	-40/-30 ksi,10,000/10/R=10	c/DD16D	10	640	640008	640648	-3907
880	1 cycle	c/DD16D	1 cycle	1		1	-5469
881	1 cycle	c/DD16D	1 cycle	1		1	-5689
882	1 cycle	c/DD16D	1 cycle	1		1	-5980
883	1 cycle	c/DD16D	1 cycle	1		1	-5601
884	1 cycle	c/DD16D	1 cycle	1		1	-6011
885	1 cycle	c/DD16D	1 cycle	1		1	-5618
886	1 cycle	c/DD16D	1 cycle	1		1	-5880
887	1 cycle	c/DD16D	1 cycle	1		1	-5380
888	1 cycle	c/DD16D	1 cycle	1		1	-5848
889	1 cycle	c/DD16D	1 cycle	1		1	-5939
892	-40 ksi, R=2	c/DD16D	10	130733		130733	-3973

Test #	Comment	Coupon Style/Material	Freq Hz	# High Cycles	# Low Cycles	Total Cycles	Hi Block Max
893	-40 ksi, R=2, Pwr Failure	c/DD16D	8	62258		62258	-3962
894	-40 ksi, R=2	c/DD16D	10	158396		158396	-3958
895	-40 ksi, R=2	c/DD16D	10	1442932		1442932	-3939
896	-40 ksi, R=2	c/DD16D	10	162400		162400	-4135
897	-40 ksi, R=2	c/DD16D	10	46304		46304	-3988
898	-40 ksi, R=2	c/DD16D	10	192595		192595	-3928
899	-40 ksi, R=2	c/DD16D	10	48990		48990	-4004
905	-35 ksi, R=2	c/DD16D	10	1190152		1190152	-3546
907	-35 ksi, R=2, coupon runout	c/DD16D	10	4950838		4950838	-3498
908	-35 ksi, R=2, load11.prn, runout	cDD16D	10	11829100		11829100	-3435
909	-35 ksi, R=2	c/DD16D	10	2738468		2738468	-3516
910	-47.5, R=2	c/DD16D	10	4297		4297	-4550
919	-30 ksi, R=2, has not failed	c/DD16D	10	4013900		4013900	-3109
920	-47.5 ksi, R=10	c/DD16D	10	131		131	-4534
921	-47.5 ksi, R=10	c/DD16D	10	364		364	-4521
922	-47.5 ksi, R=10	c/DD16D	10	415		415	-4630
923	-47.5 ksi, R=10	c/DD16D	10	334		334	-4783
924	-47.5 ksi, R=10	c/DD16D	10	533		533	-4548
925	-47.5 ksi, R=10	c/DD16D	10	1019		1019	-4621
926	-47.5 ksi, R=10	c/DD16D	10	327		327	-4697
927	-47.5 ksi, R=10	c/DD16D	10	322		322	-4845
928	-47.5 ksi, R=10	c/DD16D	10	433		433	-4634
929	-47.5 ksi, R=10	c/DD16D	10	104		104	-4823
930	-47.5/-30 ksi,10/100/R=10	c/DD16D	8	324	3200	3524	-4715
931	-47.5/-30 ksi,10/100/R=10	c/DD16D	8	1080	10800	11880	-4567
932	-47.5/-30 ksi,10/100/R=10	c/DD16D	8	670	6700	7370	-4569
933	-47.5/-30 ksi,10/100/R=10	c/DD16D	8	212	2100	2312	-4781
934	-47.5/-30 ksi,10/100/R=10	c/DD16D	8	1815	18100	19915	-4502
935	-47.5/-30 ksi,10/100/R=10	c/DD16D	8	427	4200	4627	-4814
936	-47.5/-30 ksi,10/100/R=10	c/DD16D	8	462	4600	5062	-4632
937	-47.5/-30 ksi,10/100/R=10	c/DD16D	8	877	8700	9577	-4575
938	-47.5/-30 ksi,10/100/R=10	c/DD16D	8	90	900	990	-4692

Test #	Comment	Coupon Style/Material	Freq Hz	# High Cycles	# Low Cycles	Total Cycles	Hi Block Max
939	-47.5/-30 ksi,10/100/R=10	c/DD16D	8	505	5000	5505	-4570
940	-47.5/-30 ksi,10/10/R=10	c/DD16D	8	546	540	1086	-4628
941	-47.5/-30 ksi,10/10/R=10	c/DD16D	8	2053	2050	4103	-4556
942	-47.5/-30 ksi,10/10/R=10	c/DD16D	8	1235	1230	2465	-4534
943	-47.5/-30 ksi,10/10/R=10	c/DD16D	8	452	450	902	-4563
944	-47.5/-30 ksi,10/10/R=10	c/DD16D	8	1402	1400	2802	-4707
945	-47.5/-30 ksi,10/10/R=10	c/DD16D	8	334	330	664	-4633
946	-47.5/-30 ksi,10/10/R=10	c/DD16D	8	525	520	1045	-4656
947	-47.5/-30 ksi,10/10/R=10	c/DD16D	8	239	230	469	-4664
948	-47.5/-30 ksi,10/10/R=10	c/DD16D	8	690	690	1380	-4624
950	-47.5/-30 ksi, 10/10K, R = 10	cDD16D	8	21	20000	20021	-4707
951	-47.5/-30 ksi, 10/10K, R = 10	cDD16D	8	139	130000	130139	-4750
952	-47.5/-30 ksi, 10/10K, R = 10	cDD16D	8	688	680000	680688	-4622
953	-47.5/-30 ksi, 10/10K, R = 10	cDD16D	8	272	270000	270272	-4732
956	-47.5/-30 ksi,10/10,000/R=10	c/DD16D	8	73	70000	70073	-4636
957	-47.5/-30 ksi,10/10,000/R=10	c/DD16D	8	12	10000	10012	-4674
958	-47.5/-30 ksi,10/10,000/R=10	c/DD16D	8	31	30000	30031	-4796
959	-47.5/-30 ksi,10/10,000/R=10	c/DD16D	8	80	80004	80084	-4779
960	-47.5/-30 ksi,10/1000/R=10	c/DD16D	8	171	17000	17171	-4719
961	-47.5/-30 ksi,10/1000/R=10	c/DD16D	8	128	12000	12128	-4744
962	-47.5/-30 ksi,10/1000/R=10	c/DD16D	8	84	8000	8084	-4813
963	-47.5/-30 ksi,10/1000/R=10	c/DD16D	8	244	24000	24244	-4644
964	-47.5/-30 ksi,10/1000/R=10	c/DD16D	8	87	8000	8087	-4774

Test #	Comment	Coupon Style/Material	Freq Hz	# High Cycles	# Low Cycles	Total Cycles	Hi Block Max
965	-47.5/-30 ksi,10/1000/R=10	c/DD16D	8	254	25000	25254	-4637
966	-47.5/-30 ksi,10/1000/R=10	c/DD16D	8	69	6000	6069	-4696
967	-47.5/-30 ksi,10/1000/R=10	c/DD16D	8	81	8000	8081	-4648
968	-47.5/-30 ksi,10/1000/R=10	c/DD16D	8	1220	122000	123220	-4609
969	-47.5/-30 ksi,10/1000/R=10	c/DD16D	8	591	590000	590591	-4657
970	Wispk	2m/DD16D	10	3844		3844	2914
971	Wispk	2m/DD16D	10	1276		1276	2875
972	Wispk	2m/DD16D	10	2325		2325	2960
973	Wispk	2m/DD16D	10	2448		2448	2889
974	Wispk	2m/DD16D	10	3130		3130	3352
975	Wispk	2m/DD16D	10	4044		4044	3081
976	Wispk	2m/DD16D	10	2806		2806	3115
977	Wispk	2m/DD16D	10	5722		5722	2716
978	Wispk	2m/DD16D	10	3233		3233	3387
979	Wispk	2m/DD16D	10	3203		3203	3669
980	Wispk	2m/DD16D	10	167885		167885	2233
981	Wispk	2m/DD16D	10	155850		155850	2475
982	Wispk	2m/DD16D	10	195616		195616	2462
983	Wispk	2m/DD16D	10	86293		86293	2669
984	Wispk	2m/DD16D	10	298800		298800	2270
985	Wispk	2m/DD16D	10	169839		169839	2299
986	Wispk	2m/DD16D	10	68426		68426	2524
987	Wispk	2m/DD16D	10	231019		231019	2319
988	Wispk	2m/DD16D	10	144430		144430	2543
989	Wispk	2m/DD16D	10	80980		80980	2458
990	Wispk	2m/DD16D	10	195751		195751	2338
991	Wispk	2m/DD16D	10	598438		598438	2202
992	Wispk	2m/DD16D	10	876955		876955	1878
993	Wispk	2m/DD16D	10	1231928		1231928	1878
995	Wispk	2m/DD16D	10	312744		312744	2222
996	Wispk	2m/DD16D	10	432307		432307	2164
997	Wispk	2m/DD16D	10	912240		912240	1979
998	Wispk	2m/DD16D	10	680774		680774	2175
999	Wispk	2m/DD16D	10	248429		248429	2227
1000	Wispk	2m/DD16D	10	14371		14371	2945
1001	Wispk	2m/DD16D	10	26045		26045	2810
1002	Wispk	2m/DD16D	10	18334		18334	2593
1003	Wispk	2m/DD16D	10	24906		24906	2934

Test #	Comment	Coupon Style/Material	Freq Hz	# High Cycles	# Low Cycles	Total Cycles	Hi Block Max
1004	Wispk	2m/DD16D	10	6048		6048	3026
1005	Wispk	2m/DD16D	10	13058		13058	2613
1006	Wispk	2m/DD16D	10	24196		24196	2698
1007	Wispk	2mDD16C	10	14130978		14130978	1550
1016	Wispk	2mDD16C	10	12289518		12289518	1513
1037	25 ksi, R = -1	2mDD16E	5	11189		11189	1464
1038	25 ksi, R = -1	2mDD16E	5	5556		5556	1474
1039	20 ksi, R = -1	2mDD16E	5	93249		93249	1220
1040	20 ksi, R = -1	2mDD16E	5	74482		74482	1197
1041	15 ksi, R = -1	2mDD16E	5	1313993		1313993	950
1042	15 ksi, R = -1	2mDD16E	5	902103		902103	929
1043	15 ksi, R = -1	2mDD16E	5	1814761		1814761	924
1044	25 ksi, R = -1	2mDD16E	5	4861		4861	1487
1045	20 ksi, R = -1	2mDD16E	5	62837		62837	1222
1046	15 ksi, R = -1	2mDD16E	5	785091		785091	914
1047	20 ksi, R = -1	2mDD16E	5	93636		93636	1199
1048	25 ksi, R = -1	2mDD16E	5	17397		17397	1258
1049	15 ksi, R = -1	2mDD16E	5	2108317		2108317	928
1050	25 ksi, R = -1	2mDD16E	5	6004		6004	1424
1051	20 ksi, R = -1	2mDD16E	5	57737		57737	1225
1087	-25/-15 ksi, 10/10, R=-1	2mDD16E	5	25430	25420	50850	1741
1088	-25/-15 ksi, 10/10, R=-1	2mDD16E	5	16536	16530	33066	1703
1089	-25/-15 ksi, 10/10, R=-1	2mDD16E	5	11467	11460	22927	1722
1090	-25/-15 ksi, 10/10, R=-1	2mDD16E	5	8779	8770	17549	1748
1091	-25/-15 ksi, 10/10, R=-1	2mDD16E	5	18018	18010	36028	1749
1092	-25/-15 ksi, 10/10, R=-1	2mDD16E	5	16674	16670	33344	1697
1093	-25/-15 ksi, 10/10, R=-1	2mDD16E	5	24781	24780	49561	1751
1094	-25/-15 ksi, 10/10, R=-1	2mDD16E	5	34040	34030	68070	1722
1095	-25/-15 ksi, 10/10, R=-1	2mDD16E	5	19245	19240	38485	1657
1096	-25/-15 ksi, 10/10, R=-1	2mDD16E	5	22190	22180	44370	1747
1097	-25/-15, 10 / 100, R=-1	2mDD16E	5	7581	75800	83381	1730
1098	-25/-15, 10 / 100, R=-1	2mDD16E	5	14380	143781	158161	1698
1099	-25/-15, 10 / 100, R=-1	2mDD16E	5	6405	64000	70405	1769
1100	-25/-15, 10 / 100, R=-1	2mDD16E	5	13142	131400	144542	1713
1101	-25/-15, 10 / 100, R=-1	2mDD16E	5	7191	71900	79091	1706
1102	-25/-15, 10 / 100, R=-1	2mDD16E	5	5291	52900	58191	1746
1103	-25/-15, 10 / 100, R=-1	2mDD16E	5	10150	101488	111638	1775
1104	-25/-15, 10 / 100, R=-1	2mDD16E	5	4283	42800	47083	1779
1105	-25/-15, 10 / 100, R=-1	2mDD16E	5	7100	70018	77118	1737
1106	-25/-15, 10 / 100, R=-1	2mDD16E	5	4003	40000	44003	1785
1107	-25/-15, 10/1000, R=-1	2mDD16E	5	1671	167000	168671	1758
1108	-25/-15, 10/1000, R=-1	2mDD16E	5	2470	246518	248988	1716
1109	-25/-15, 10/1000, R=-1	2mDD16E	5	2425	242000	244425	1807

Test #	Comment	Coupon Style/Material	Freq Hz	# High Cycles	# Low Cycles	Total Cycles	Hi Block Max
1110	-25/-15, 10/1000, R=-1	2mDD16E	5	1641	164000	165641	1755
1111	-25/-15, 10/1000, R=-1	2mDD16E	5	2836	283000	285836	1731
1112	-25/-15, 10/1000, R=-1	2mDD16E	5	3848	384000	387848	1779
1113	-25/-15, 10/1000, R=-1	2mDD16E	5	2621	262000	264621	1786
1114	-25/-15, 10/1000, R=-1	2mDD16E	5	2600	259000	261600	1788
1115	-25/-15, 10/1000, R=-1	2mDD16E	5	2110	210319	212429	1825
1116	-25/-15, 10/1000, R=-1	2mDD16E	5	1050	104409	105459	1789
1117	-25/-15 ksi, 10/10K, R=-1	2mDD16E	5	860	853094	853954	1710
1118	-25/-15 ksi, 10/10K, R=-1	2mDD16E	5	430	423228	423658	1743
1119	-25/-15 ksi, 10/10K, R=-1	2mDD16E	5	960	950993	951953	1853
1120	-25/-15 ksi, 10/10K, R=-1	2mDD16E	5	760	750198	750958	1814
1121	-25/-15 ksi, 10/10K, R=-1	2mDD16E	5	770	762262	763032	1728
1122	-25/-15 ksi, 10/10K, R=-1	2mDD16E	5	550	542948	543498	1699
1123	-25/-15 ksi, 10/10K, R=-1	2mDD16E	5	750	749389	750139	1750
1124	-25/-15 ksi, 10/10K, R=-1	2mDD16E	5	690	683831	684521	1771
1125	-25/-15 ksi, 10/10K, R=-1	2mDD16E	5	470	464239	464709	1791
1126	-25/-15 ksi, 10/10K, R=-1	2mDD16E	5	700	600096	600796	1870

Coupon style nt = no tab
Coupon style 2t = rectangular with filed taper
Coupon style 2m = milled dogbone
Coupon style c = compression rectangular w/o tabs
Dh/Dt = damage due to high cycles divided by total damage
eg: 47.5/30 implies a two block test with the first block having a maximum stress of 47.5 ksi and the
        second block, 30 ksi
rand5, load10, load11, WisxR01, WisxR05, Wisxmix, etc impliy random files containing loading spectra.
        Utilizes Instron RANDOM software
wvrnr implies use of Instron WAVERUNNER software.

APPENDIX B

CONSTANT AMPLITUDE FATIGUE TEST SUMMARY

Test #	Total Cycles	Log Cycles	MPa, Max Stress	Log Stress	Exponent All Data	Power All Data	Power -Static	Exponent -Static
R=0.1								
274	1	0.000	680.4	2.833	604.0	635.3	648.6	537.0
283	1	0.000	649.5	2.813	604.0	635.3	648.6	537.0
296	1	0.000	489.1	2.689	604.0	635.3	648.6	537.0
306	1	0.000	673.1	2.828	604.0	635.3	648.6	537.0
329	1	0.000	542.6	2.734	604.0	635.3	648.6	537.0
349	1	0.000	558.5	2.747	604.0	635.3	648.6	537.0
383	1	0.000	652.4	2.815	604.0	635.3	648.6	537.0
410	1	0.000	638.3	2.805	604.0	635.3	648.6	537.0
430	1	0.000	598.9	2.777	604.0	635.3	648.6	537.0
474	1	0.000	629.5	2.799	604.0	635.3	648.6	537.0
479	1	0.000	657.4	2.818	604.0	635.3	648.6	537.0
635	1	0.000	670.1	2.826	604.0	635.3	648.6	537.0
646	1	0.000	569.3	2.755	604.0	635.3	648.6	537.0
652	1	0.000	619.3	2.792	604.0	635.3	648.6	537.0
653	1	0.000	676.4	2.830	604.0	635.3	648.6	537.0
655	1	0.000	688.8	2.838	604.0	635.3	648.6	537.0
666	1	0.000	670.9	2.827	604.0	635.3	648.6	537.0
671	1	0.000	687.3	2.837	604.0	635.3	648.6	537.0
739	1	0.000	644.3	2.809	604.0	635.3	648.6	537.0
726a	1	0.000	647.8	2.811	604.0	635.3	648.6	537.0
129	78	1.892	409.1	2.612	460.7	434.7	439.8	422.7
282	85	1.929	413.3	2.616	457.9	431.4	436.5	420.5
308	91	1.959	412.6	2.616	455.7	428.9	433.8	418.7
130	149	2.173	405.6	2.608	439.5	410.8	415.2	405.7
148	155	2.190	414.0	2.617	438.2	409.4	413.7	404.7
624	161	2.207	411.8	2.615	436.9	408.1	412.3	403.7
172	162	2.210	407.0	2.610	436.7	407.9	412.1	403.5
621	180	2.255	410.5	2.613	433.3	404.1	408.2	400.8
620	234	2.369	410.0	2.613	424.6	395.0	398.8	393.9
578	274	2.438	410.6	2.613	419.4	389.6	393.2	389.7
579	283	2.452	410.2	2.613	418.4	388.5	392.1	388.9
606	286	2.456	412.2	2.615	418.0	388.1	391.7	388.6
622	290	2.462	410.0	2.613	417.6	387.7	391.2	388.3
577	310	2.491	410.2	2.613	415.4	385.4	388.9	386.5
623	311	2.493	410.1	2.613	415.3	385.3	388.8	386.4
580	334	2.524	410.5	2.613	412.9	382.9	386.3	384.6
784	343	2.535	406.6	2.609	412.1	382.1	385.5	383.9
298	356	2.551	414.2	2.617	410.8	380.8	384.1	382.9
313	429	2.632	414.7	2.618	404.7	374.7	377.8	378.0

Test #	Total Cycles	Log Cycles	MPa, Max Stress	Log Stress	Exponent All Data	Power All Data	Power -Static	Exponent -Static
297	491	2.691	413.8	2.617	400.3	370.3	373.3	374.4
744	642	2.807	393.8	2.595	391.5	361.8	364.5	367.4
168	744	2.872	315.1	2.498	386.6	357.1	359.7	363.5
433	757	2.879	414.4	2.617	386.0	356.6	359.1	363.1
554	763	2.883	326.1	2.513	385.8	356.3	358.9	362.9
618	769	2.886	324.9	2.512	385.5	356.1	358.6	362.7
605	783	2.894	411.1	2.614	384.9	355.5	358.1	362.2
788	815	2.911	324.1	2.511	383.6	354.3	356.8	361.2
616	1081	3.034	324.8	2.512	374.3	345.7	347.9	353.7
745	1290	3.110	322.9	2.509	368.5	340.4	342.5	349.1
584	1306	3.116	325.3	2.512	368.1	340.0	342.1	348.8
206	1339	3.127	321.6	2.507	367.3	339.3	341.3	348.1
607	1690	3.228	325.8	2.513	359.6	332.5	334.3	342.0
376	1706	3.232	327.6	2.515	359.3	332.2	334.0	341.8
161	1722	3.236	327.8	2.516	359.0	331.9	333.8	341.5
608	1794	3.254	325.4	2.512	357.7	330.8	332.5	340.5
140	1914	3.282	323.1	2.509	355.6	328.9	330.6	338.8
214	2078	3.318	318.7	2.503	352.9	326.6	328.2	336.6
139	2297	3.361	330.0	2.519	349.6	323.7	325.3	334.0
619	2329	3.367	325.7	2.513	349.1	323.3	324.9	333.6
617	2433	3.386	325.2	2.512	347.7	322.1	323.6	332.5
321	2611	3.417	328.3	2.516	345.3	320.1	321.6	330.6
583	2620	3.418	324.9	2.512	345.2	320.0	321.5	330.5
363	3139	3.497	327.0	2.515	339.3	315.0	316.4	325.8
171	3152	3.499	322.7	2.509	339.2	314.9	316.2	325.7
213	3306	3.519	324.0	2.511	337.6	313.6	314.9	324.4
434	3744	3.573	331.2	2.520	333.5	310.2	311.4	321.2
582	4190	3.622	325.2	2.512	329.8	307.2	308.3	318.2
581	4375	3.641	324.7	2.511	328.4	306.0	307.1	317.1
325	8653	3.937	327.3	2.515	306.0	288.4	289.0	299.2
205	15680	4.195	238.1	2.377	286.4	273.8	274.1	283.6
323	16884	4.227	242.2	2.384	284.0	272.1	272.3	281.6
746	31733	4.502	237.9	2.376	263.3	257.5	257.4	265.1
147	31943	4.504	241.5	2.383	263.0	257.4	257.2	264.9
587	35109	4.545	240.2	2.381	259.9	255.3	255.1	262.4
632	37576	4.575	239.5	2.379	257.7	253.8	253.5	260.7
632	37576	4.575	239.5	2.379	257.7	253.8	253.5	260.7
174	37855	4.578	236.4	2.374	257.5	253.6	253.4	260.5
625	41493	4.618	205.5	2.313	254.4	251.6	251.3	258.1
633	43491	4.638	239.8	2.380	252.9	250.5	250.2	256.8

Test #	Total Cycles	Log Cycles	MPa, Max Stress	Log Stress	Exponent All Data	Power All Data	Power -Static	Exponent -Static
610	43618	4.640	240.1	2.380	252.8	250.5	250.2	256.7
302	54487	4.736	241.6	2.383	245.5	245.7	245.3	250.9
630	57742	4.761	239.3	2.379	243.6	244.4	244.0	249.4
609	58826	4.770	240.5	2.381	243.0	244.0	243.6	248.9
629	78888	4.897	205.7	2.313	233.3	237.9	237.3	241.2
586	89527	4.952	240.0	2.380	229.2	235.3	234.6	237.9
326	104679	5.020	241.3	2.383	224.0	232.1	231.4	233.8
284	109547	5.040	241.7	2.383	222.5	231.2	230.5	232.6
792	115525	5.063	237.6	2.376	220.8	230.1	229.4	231.2
305	121190	5.083	206.7	2.315	219.2	229.1	228.4	229.9
305	121190	5.083	206.7	2.315	219.2	229.1	228.4	229.9
628	129134	5.111	205.4	2.313	217.1	227.9	227.1	228.3
131	141377	5.150	241.3	2.383	214.1	226.1	225.3	225.9
138	143456	5.157	241.6	2.383	213.7	225.8	225.0	225.5
634	163745	5.214	239.8	2.380	209.3	223.2	222.3	222.0
634	163745	5.214	239.8	2.380	209.3	223.2	222.3	222.0
435	181518	5.259	240.8	2.382	205.9	221.2	220.3	219.3
585	186268	5.270	239.8	2.380	205.1	220.7	219.8	218.7
588	187293	5.273	239.9	2.380	204.9	220.6	219.7	218.5
378	261287	5.417	207.2	2.316	194.0	214.3	213.3	209.8
151	274271	5.438	205.0	2.312	192.4	213.4	212.3	208.5
485	286613	5.457	206.6	2.315	190.9	212.6	211.5	207.4
152	294549	5.469	202.4	2.306	190.0	212.1	211.0	206.6
611	318890	5.504	206.2	2.314	187.4	210.6	209.5	204.6
309	373306	5.572	207.4	2.317	182.2	207.8	206.6	200.4
153	382826	5.583	201.1	2.303	181.4	207.3	206.1	199.8
612	418886	5.622	206.1	2.314	178.4	205.7	204.5	197.4
391	421272	5.625	207.0	2.316	178.3	205.6	204.4	197.3
590	436185	5.640	206.2	2.314	177.1	205.0	203.7	196.3
160	495397	5.695	207.0	2.316	172.9	202.7	201.4	193.0
626	496355	5.696	205.6	2.313	172.9	202.7	201.4	192.9
747	544532	5.736	204.0	2.310	169.8	201.0	199.7	190.5
169	588371	5.770	207.0	2.316	167.3	199.7	198.4	188.5
627	598609	5.777	205.6	2.313	166.7	199.4	198.1	188.0
589	697446	5.844	205.8	2.314	161.7	196.7	195.4	184.0
591	732874	5.865	206.2	2.314	160.1	195.9	194.5	182.7
436	1137595	6.056	206.5	2.315	145.6	188.5	187.0	171.2
R=0.5								
274	1	0.000	680.4	2.833	625.8	640.2	717.5	581.5
283	1	0.000	649.5	2.813	625.8	640.2	717.5	581.5

Test #	Total Cycles	Log Cycles	MPa, Max Stress	Log Stress	Exponent All Data	Power All Data	Power -Static	Exponent -Static
296	1	0.000	489.1	2.689	625.8	640.2	717.5	581.5
306	1	0.000	673.1	2.828	625.8	640.2	717.5	581.5
329	1	0.000	542.6	2.734	625.8	640.2	717.5	581.5
349	1	0.000	558.5	2.747	625.8	640.2	717.5	581.5
383	1	0.000	652.4	2.815	625.8	640.2	717.5	581.5
410	1	0.000	638.3	2.805	625.8	640.2	717.5	581.5
430	1	0.000	598.9	2.777	625.8	640.2	717.5	581.5
474	1	0.000	629.5	2.799	625.8	640.2	717.5	581.5
479	1	0.000	657.4	2.818	625.8	640.2	717.5	581.5
635	1	0.000	670.1	2.826	625.8	640.2	717.5	581.5
646	1	0.000	569.3	2.755	625.8	640.2	717.5	581.5
652	1	0.000	619.3	2.792	625.8	640.2	717.5	581.5
653	1	0.000	676.4	2.830	625.8	640.2	717.5	581.5
655	1	0.000	688.8	2.838	625.8	640.2	717.5	581.5
666	1	0.000	670.9	2.827	625.8	640.2	717.5	581.5
671	1	0.000	687.3	2.837	625.8	640.2	717.5	581.5
739	1	0.000	644.3	2.809	625.8	640.2	717.5	581.5
726a	1	0.000	647.8	2.811	625.8	640.2	717.5	581.5
785	400	2.602	407.9	2.611	450.0	422.3	444.2	430.4
648	438	2.641	409.6	2.612	447.3	419.6	440.9	428.1
486	1119	3.049	412.9	2.616	419.8	393.2	409.0	404.4
650	1169	3.068	409.7	2.612	418.5	392.0	407.6	403.3
672	1400	3.146	325.4	2.512	413.2	387.1	401.7	398.8
718	1412	3.150	410.0	2.613	412.9	386.9	401.5	398.6
651	1475	3.169	408.2	2.611	411.7	385.7	400.1	397.5
571	1652	3.218	411.9	2.615	408.3	382.7	396.4	394.6
408	2290	3.360	412.9	2.616	398.7	374.1	386.2	386.4
431	2469	3.393	412.6	2.616	396.5	372.2	383.9	384.5
649	2507	3.399	410.2	2.613	396.1	371.8	383.4	384.1
572	2513	3.400	411.4	2.614	396.0	371.7	383.4	384.0
573	2519	3.401	411.4	2.614	395.9	371.6	383.3	384.0
647	2609	3.416	408.6	2.611	394.9	370.7	382.2	383.1
576	2755	3.440	411.9	2.615	393.3	369.3	380.5	381.7
717	2886	3.460	410.6	2.613	392.0	368.2	379.1	380.5
417	4100	3.613	413.1	2.616	381.6	359.3	368.6	371.7
642	5801	3.764	325.7	2.513	371.5	350.7	358.5	362.9
643	6548	3.816	324.4	2.511	367.9	347.8	355.1	359.9
641	7421	3.870	325.1	2.512	364.2	344.8	351.5	356.7
558	8357	3.922	327.5	2.515	360.7	341.9	348.2	353.7
789	11812	4.072	325.5	2.513	350.6	333.8	338.7	345.0

Test #	Total Cycles	Log Cycles	MPa, Max Stress	Log Stress	Exponent All Data	Power All Data	Power -Static	Exponent -Static
556	15905	4.202	326.6	2.514	341.9	327.0	330.7	337.5
645	19568	4.292	324.2	2.511	335.8	322.3	325.3	332.2
347	20006	4.301	327.6	2.515	335.1	321.8	324.7	331.7
560	21025	4.323	326.2	2.513	333.7	320.7	323.4	330.4
719	21037	4.323	325.5	2.513	333.6	320.7	323.4	330.4
487	21452	4.331	326.7	2.514	333.1	320.3	322.9	329.9
644	24381	4.387	326.0	2.513	329.3	317.4	319.6	326.7
562	24391	4.387	326.5	2.514	329.3	317.4	319.6	326.7
559	31685	4.501	326.6	2.514	321.6	311.7	313.0	320.1
557	38319	4.583	326.1	2.513	316.0	307.6	308.2	315.3
561	48516	4.686	326.1	2.513	309.1	302.6	302.5	309.3
409	49288	4.693	326.8	2.514	308.6	302.3	302.1	308.9
416	74500	4.872	327.7	2.515	296.5	293.7	292.2	298.5
640	98521	4.994	239.9	2.380	288.3	288.1	285.8	291.5
673	100193	5.001	239.8	2.380	287.8	287.8	285.4	291.0
488	156860	5.196	241.3	2.383	274.7	278.9	275.3	279.7
721	272818	5.436	240.0	2.380	258.4	268.4	263.4	265.8
566	280171	5.447	240.7	2.382	257.6	267.9	262.8	265.1
638	460884	5.664	240.8	2.382	243.0	258.8	252.6	252.5
636	464516	5.667	243.0	2.386	242.8	258.7	252.4	252.3
722	545546	5.737	240.2	2.381	238.1	255.8	249.2	248.3
569	763276	5.883	241.0	2.382	228.2	249.9	242.6	239.8
412	829489	5.919	241.9	2.384	225.8	248.5	241.0	237.7
563	1051280	6.022	241.1	2.382	218.8	244.4	236.4	231.7
565	1119777	6.049	240.8	2.382	217.0	243.4	235.2	230.1
418	1559097	6.193	242.0	2.384	207.3	237.8	229.1	221.8
568	1749635	6.243	240.4	2.381	203.9	235.9	227.0	218.9
564	1988538	6.299	240.8	2.382	200.1	233.8	224.7	215.7
570	2470072	6.393	240.9	2.382	193.7	230.3	220.8	210.2
R=-1								
812	1	0.000	399.5	2.601	400.1	401.9	394.9	290.5
818	1	0.000	395.8	2.597	400.1	401.9	394.9	290.5
824	1	0.000	405.5	2.608	400.1	401.9	394.9	290.5
830	1	0.000	368.3	2.566	400.1	401.9	394.9	290.5
831	1	0.000	410.5	2.613	400.1	401.9	394.9	290.5
832	1	0.000	368.2	2.566	400.1	401.9	394.9	290.5
833	1	0.000	416.4	2.620	400.1	401.9	394.9	290.5
834	1	0.000	379.0	2.579	400.1	401.9	394.9	290.5
835	1	0.000	435.1	2.639	400.1	401.9	394.9	290.5

Test #	Total Cycles	Log Cycles	MPa, Max Stress	Log Stress	Exponent All Data	Power All Data	Power -Static	Exponent -Static
865	1	0.000	427.5	2.631	400.1	401.9	394.9	290.5
866	1	0.000	408.6	2.611	400.1	401.9	394.9	290.5
867	1	0.000	406.7	2.609	400.1	401.9	394.9	290.5
868	1	0.000	387.8	2.589	400.1	401.9	394.9	290.5
869	1	0.000	419.8	2.623	400.1	401.9	394.9	290.5
880	1	0.000	370.9	2.569	400.1	401.9	394.9	290.5
881	1	0.000	404.8	2.607	400.1	401.9	394.9	290.5
882	1	0.000	427.0	2.630	400.1	401.9	394.9	290.5
883	1	0.000	397.2	2.599	400.1	401.9	394.9	290.5
884	1	0.000	421.5	2.625	400.1	401.9	394.9	290.5
885	1	0.000	394.6	2.596	400.1	401.9	394.9	290.5
886	1	0.000	411.2	2.614	400.1	401.9	394.9	290.5
887	1	0.000	374.4	2.573	400.1	401.9	394.9	290.5
888	1	0.000	415.7	2.619	400.1	401.9	394.9	290.5
889	1	0.000	413.7	2.617	400.1	401.9	394.9	290.5
1044	4861	3.687	178.4	2.251	215.3	187.8	186.9	183.9
1038	5556	3.745	182.8	2.262	212.4	185.6	184.7	182.2
1050	6004	3.778	178.3	2.251	210.7	184.3	183.4	181.2
1037	11189	4.049	182.1	2.260	197.2	174.3	173.6	173.4
1048	17397	4.240	180.6	2.257	187.5	167.5	167.0	167.9
1051	57737	4.761	144.9	2.161	161.4	150.4	150.2	152.8
1045	62837	4.798	148.5	2.172	159.6	149.3	149.1	151.7
1040	74482	4.872	146.8	2.167	155.9	147.0	146.9	149.6
1039	93249	4.970	146.2	2.165	151.0	144.1	144.0	146.8
1047	93636	4.971	146.3	2.165	150.9	144.1	144.0	146.7
1042	902103	5.955	110.2	2.042	101.6	117.6	117.9	118.3
1041	1313993	6.119	110.9	2.045	93.4	113.7	114.1	113.5
1043	1814761	6.259	111.7	2.048	86.4	110.4	110.9	109.5
1046	1962727	6.293	111.3	2.046	84.7	109.7	110.1	108.5
1049	2108317	6.324	114.5	2.059	83.1	109.0	109.4	107.6
R=10								
812	1	0.000	399.5	2.601	400.2	404.7	419.8	387.4
818	1	0.000	395.8	2.597	400.2	404.7	419.8	387.4
824	1	0.000	405.5	2.608	400.2	404.7	419.8	387.4
830	1	0.000	368.3	2.566	400.2	404.7	419.8	387.4
831	1	0.000	410.5	2.613	400.2	404.7	419.8	387.4
832	1	0.000	368.2	2.566	400.2	404.7	419.8	387.4
833	1	0.000	416.4	2.620	400.2	404.7	419.8	387.4
834	1	0.000	379.0	2.579	400.2	404.7	419.8	387.4
835	1	0.000	435.1	2.639	400.2	404.7	419.8	387.4

Test #	Total Cycles	Log Cycles	MPa, Max Stress	Log Stress	Exponent All Data	Power All Data	Power -Static	Exponent -Static
865	1	0.000	427.5	2.631	400.2	404.7	419.8	387.4
866	1	0.000	408.6	2.611	400.2	404.7	419.8	387.4
867	1	0.000	406.7	2.609	400.2	404.7	419.8	387.4
868	1	0.000	387.8	2.589	400.2	404.7	419.8	387.4
869	1	0.000	419.8	2.623	400.2	404.7	419.8	387.4
880	1	0.000	370.9	2.569	400.2	404.7	419.8	387.4
881	1	0.000	404.8	2.607	400.2	404.7	419.8	387.4
882	1	0.000	427.0	2.630	400.2	404.7	419.8	387.4
883	1	0.000	397.2	2.599	400.2	404.7	419.8	387.4
884	1	0.000	421.5	2.625	400.2	404.7	419.8	387.4
885	1	0.000	394.6	2.596	400.2	404.7	419.8	387.4
886	1	0.000	411.2	2.614	400.2	404.7	419.8	387.4
887	1	0.000	374.4	2.573	400.2	404.7	419.8	387.4
888	1	0.000	415.7	2.619	400.2	404.7	419.8	387.4
889	1	0.000	413.7	2.617	400.2	404.7	419.8	387.4
923	334	2.523	335.4	2.526	318.4	309.1	314.4	312.5
927	322	2.507	333.5	2.523	318.9	309.6	314.9	313.0
929	104	2.015	325.2	2.512	334.9	326.3	333.2	327.6
920	131	2.116	323.8	2.510	331.6	322.8	329.4	324.6
924	533	2.726	322.9	2.509	311.8	302.4	307.1	306.5
922	415	2.618	322.9	2.509	315.4	306.0	311.0	309.7
928	433	2.636	322.8	2.509	314.8	305.4	310.3	309.1
925	1019	3.008	322.7	2.509	302.7	293.5	297.4	298.1
926	327	2.514	322.7	2.509	318.7	309.4	314.7	312.8
921	364	2.561	322.4	2.508	317.2	307.8	313.0	311.4
796	11608	4.065	280.5	2.448	268.5	262.1	263.4	266.7
799	5904	3.771	279.7	2.447	278.0	270.5	272.5	275.4
855	4063	3.609	277.8	2.444	283.2	275.2	277.6	280.3
856	4410	3.644	277.7	2.444	282.1	274.2	276.4	279.2
800	5123	3.709	277.3	2.443	280.0	272.3	274.4	277.3
817	15393	4.187	277.2	2.443	264.5	258.7	259.8	263.1
816	3850	3.585	277.2	2.443	284.0	275.9	278.3	280.9
858	8288	3.918	277.0	2.442	273.2	266.2	267.9	271.1
797	2463	3.391	276.8	2.442	290.3	281.7	284.6	286.7
859	10692	4.029	276.5	2.442	269.6	263.1	264.5	267.8
814	4353	3.639	276.4	2.442	282.3	274.3	276.6	279.4
798	2727	3.436	276.4	2.441	288.8	280.3	283.1	285.4
813	2469	3.392	276.0	2.441	290.2	281.6	284.5	286.7
857	1957	3.291	275.4	2.440	293.5	284.7	287.9	289.7
806	5010	3.700	259.1	2.413	280.3	272.5	274.7	277.5

Test #	Total Cycles	Log Cycles	MPa, Max Stress	Log Stress	Exponent All Data	Power All Data	Power -Static	Exponent -Static
805	21240	4.327	245.3	2.390	260.0	254.9	255.6	258.9
802	54873	4.739	243.9	2.387	246.6	243.9	243.8	246.7
823	67973	4.832	243.1	2.386	243.6	241.5	241.3	243.9
804	11738	4.070	243.1	2.386	268.3	262.0	263.3	266.6
820	36657	4.564	243.0	2.386	252.3	248.5	248.8	251.9
819	14172	4.151	242.9	2.385	265.7	259.7	260.8	264.1
803	11145	4.047	242.8	2.385	269.0	262.6	264.0	267.2
801	379064	5.579	242.6	2.385	219.4	223.0	221.5	221.8
822	9235	3.965	242.5	2.385	271.7	264.9	266.5	269.7
821	6704	3.826	241.4	2.383	276.2	268.9	270.7	273.8
863	1884110	6.275	216.5	2.335	196.8	207.0	204.5	201.1
861	933072	5.970	216.4	2.335	206.7	213.8	211.8	210.1
828	1508674	6.179	215.2	2.333	200.0	209.1	206.8	203.9
808	1680674	6.225	214.5	2.331	198.4	208.1	205.6	202.6
807	487946	5.688	211.5	2.325	215.9	220.4	218.7	218.5
827	1037244	6.016	209.9	2.322	205.2	212.8	210.6	208.8
811	1464645	6.166	209.1	2.320	200.4	209.4	207.1	204.3
829	842537	5.926	208.5	2.319	208.2	214.9	212.8	211.5
825	1505733	6.178	208.2	2.318	200.0	209.1	206.8	204.0
809	1859843	6.269	208.1	2.318	197.0	207.1	204.6	201.3
810	1747111	6.242	208.1	2.318	197.9	207.7	205.2	202.1
860	2021912	6.306	208.0	2.318	195.8	206.3	203.8	200.2
862	205084	5.312	207.9	2.318	228.1	229.4	228.3	229.7
826	1980344	6.297	207.9	2.318	196.1	206.5	204.0	200.4
864	235297	5.372	207.5	2.317	226.1	228.0	226.8	227.9
R=2								
812	1	0.000	399.5	2.601	402.5	402.4	465.0	404.9
818	1	0.000	395.8	2.597	402.5	402.4	465.0	404.9
824	1	0.000	405.5	2.608	402.5	402.4	465.0	404.9
830	1	0.000	368.3	2.566	402.5	402.4	465.0	404.9
831	1	0.000	410.5	2.613	402.5	402.4	465.0	404.9
832	1	0.000	368.2	2.566	402.5	402.4	465.0	404.9
833	1	0.000	416.4	2.620	402.5	402.4	465.0	404.9
834	1	0.000	379.0	2.579	402.5	402.4	465.0	404.9
835	1	0.000	435.1	2.639	402.5	402.4	465.0	404.9
865	1	0.000	427.5	2.631	402.5	402.4	465.0	404.9
866	1	0.000	408.6	2.611	402.5	402.4	465.0	404.9
867	1	0.000	406.7	2.609	402.5	402.4	465.0	404.9

Test #	Total Cycles	Log Cycles	MPa, Max Stress	Log Stress	Exponent All Data	Power All Data	Power -Static	Exponent -Static
868	1	0.000	387.8	2.589	402.5	402.4	465.0	404.9
869	1	0.000	419.8	2.623	402.5	402.4	465.0	404.9
880	1	0.000	370.9	2.569	402.5	402.4	465.0	404.9
881	1	0.000	404.8	2.607	402.5	402.4	465.0	404.9
882	1	0.000	427.0	2.630	402.5	402.4	465.0	404.9
883	1	0.000	397.2	2.599	402.5	402.4	465.0	404.9
884	1	0.000	421.5	2.625	402.5	402.4	465.0	404.9
885	1	0.000	394.6	2.596	402.5	402.4	465.0	404.9
886	1	0.000	411.2	2.614	402.5	402.4	465.0	404.9
887	1	0.000	374.4	2.573	402.5	402.4	465.0	404.9
888	1	0.000	415.7	2.619	402.5	402.4	465.0	404.9
889	1	0.000	413.7	2.617	402.5	402.4	465.0	404.9
897	46304	4.666	280.6	2.448	285.3	280.7	286.9	285.7
899	48990	4.690	273.8	2.438	284.7	280.1	286.2	285.1
893	62258	4.794	274.7	2.439	282.1	277.9	283.1	282.4
892	130733	5.116	275.9	2.441	274.0	271.1	273.8	274.2
894	158396	5.200	279.3	2.446	271.9	269.3	271.5	272.0
896	162400	5.211	280.9	2.449	271.6	269.1	271.2	271.8
898	192595	5.285	275.9	2.441	269.8	267.6	269.1	269.9
895	1442932	6.159	273.4	2.437	247.8	250.1	245.8	247.5
909	2738468	6.438	242.4	2.384	240.8	244.8	238.8	240.4
919	4013900	6.604	208.2	2.318	236.6	241.7	234.8	236.2

APPENDIX C

MULTI-BLOCK FATIGUE TEST SUMMARY

Test #	actual Miner's number	Fraction Hi	NRSD exponent all data	LRSD exponent all data	NRSD exponent -static	LRSD exponent -static	NRSD power all data	LRSD power all data	NRSD power -static	LRSD power -static
				+60/47.5 ksi, R=0.1						
		0.505					0.871			
		0.102					0.579			
		0.052					0.487			
		0.011					0.531			
		0.005					0.987			
		0.005					1.053			
		0.005					1.053			
		0.005					1.053			
		0.005					1.053			
		0.005					1.053			
		0.514						0.985		
		0.101						0.921		
		0.054						0.828		
		0.010						1.043		
		0.005						0.987		
		0.005						1.021		
		0.005						1.021		
		0.005						1.021		
		0.005						1.021		
		0.005						1.021		
		0.510							0.865	
		0.102							0.526	
		0.052							0.447	
		0.011							0.498	
		0.005							0.929	
		0.004							1.047	
		0.004							1.047	
		0.004							1.047	
		0.004							1.047	
		0.004							1.047	
		0.502								0.978
		0.108								0.876
		0.051								0.888
		0.010								0.990
		0.005								0.929
		0.004								1.019
		0.004								1.019
		0.004								1.019
		0.004								1.019

Test #	actual Miner's number	Fraction Hi	NRSD exponent all data	LRSD exponent all data	NRSD exponent -static	LRSD exponent -static	NRSD power all data	LRSD power all data	NRSD power -static	LRSD power -static
		0.004								1.019
		0.509	0.836							
		0.101	0.458							
		0.051	0.362							
		0.010	0.485							
		0.005	0.456							
		0.002	1.024							
		0.002	1.024							
		0.002	1.024							
		0.002	1.024							
		0.002	1.024							
		0.509		0.974						
		0.101		0.863						
		0.051		0.796						
		0.010		0.726						
		0.005		0.909						
		0.002		1.010						
		0.002		1.010						
		0.002		1.010						
		0.002		1.010						
		0.002		1.010						
		0.512			0.824					
		0.112			0.411					
		0.052			0.323					
		0.011			0.426					
		0.005			0.750					
		0.003			1.083					
		0.003			1.083					
		0.003			1.083					
		0.003			1.083					
		0.003			1.083					
		0.526				0.979				
		0.101				0.879				
		0.051				0.793				
		0.010				0.842				
		0.005				0.750				
		0.003				1.040				
		0.003				1.040				
		0.003				1.040				
		0.003				1.040				

Test #	actual Miner's number	Fraction Hi	NRSD exponent all data	LRSD exponent all data	NRSD exponent -static	LRSD exponent -static	NRSD power all data	LRSD power all data	NRSD power -static	LRSD power -static
		0.003				1.040				
256	0.122	0.512								
257	0.148	0.016								
258	0.083	0.121								
259	0.168	0.115								
260	0.318	0.016								
310	0.565	0.502								
311	0.982	0.102								
312	0.141	0.019								
579	0.244	1.000								
577	0.959	1.000								
297	1.051	1.000								
621	1.664	1.000								
620	0.610	1.000								
578	0.793	1.000								
606	0.929	1.000								
129	0.969	1.000								
130	0.264	1.000								
148	0.505	1.000								
172	0.525	1.000								
623	0.549	1.000								
624	1.054	1.000								
605	0.546	1.000								
433	2.654	1.000								
580	2.566	1.000								
308	1.132	1.000								
282	0.308	1.000								
313	0.288	1.000								
622	1.454	1.000								
298	0.983	1.000								
213	1.207	0.000								
161	1.343	0.000								
171	0.699	0.000								
139	1.280	0.000								
168	0.933	0.000								
582	0.302	0.000								
434	1.702	0.000								
583	1.521	0.000								
214	1.064	0.000								
140	0.844	0.000								

Test #	actual Miner's number	Fraction Hi	NRSD exponent all data	LRSD exponent all data	NRSD exponent -static	LRSD exponent -static	NRSD power all data	LRSD power all data	NRSD power -static	LRSD power -static
617	0.777	0.000								
619	0.988	0.000								
608	0.946	0.000								
607	0.729	0.000								
616	0.686	0.000								
206	0.439	0.000								
581	0.544	0.000								
376	1.777	0.000								
554	0.693	0.000								
584	0.310	0.000								
321	0.530	0.000								
325	1.061	0.000								
618	3.515	0.000								
60/35ksi, R=0.1										
		0.509					0.990			
		0.101					0.898			
		0.055					0.827			
		0.010					0.512			
		0.005					0.388			
		0.001					0.191			
		0.001					0.301			
		0.000					1.066			
		0.000					1.066			
		0.000					1.066			
		0.513						1.005		
		0.103						0.995		
		0.050						0.987		
		0.011						0.915		
		0.005						0.864		
		0.001						0.741		
		0.001						0.646		
		0.000						1.033		
		0.000						1.033		
		0.000						1.033		
		0.503							0.990	
		0.103							0.891	
		0.054							0.798	
		0.010							0.464	
		0.005							0.357	
		0.001							0.185	

Test #	actual Miner's number	Fraction Hi	NRSD exponent all data	LRSD exponent all data	NRSD exponent -static	LRSD exponent -static	NRSD power all data	LRSD power all data	NRSD power -static	LRSD power -static
		0.001							0.299	
		0.000							1.058	
		0.000							1.058	
		0.000							1.058	
		0.507								1.003
		0.106								0.990
		0.052								0.980
		0.011								0.904
		0.005								0.834
		0.001								0.721
		0.001								0.630
		0.000								1.029
		0.000								1.029
		0.000								1.029
		0.502	0.957							
		0.103	0.707							
		0.050	0.550							
		0.010	0.232							
		0.005	0.180							
		0.001	0.172							
		0.001	0.310							
		0.000	1.029							
		0.000	1.029							
		0.000	1.029							
		0.504		0.998						
		0.102		0.966						
		0.051		0.935						
		0.010		0.784						
		0.005		0.711						
		0.001		0.680						
		0.001		0.617						
		0.000		1.015						
		0.000		1.015						
		0.000		1.015						
		0.505			0.970					
		0.102			0.787					
		0.056			0.658					
		0.010			0.326					
		0.005			0.242					
		0.001			0.211					

Test #	actual Miner's number	Fraction Hi	NRSD exponent all data	LRSD exponent all data	NRSD exponent -static	LRSD exponent -static	NRSD power all data	LRSD power all data	NRSD power -static	LRSD power -static
		0.001			0.318					
		0.000			1.092					
		0.000			1.092					
		0.000			1.092					
		0.515				1.008				
		0.103				0.988				
		0.050				0.980				
		0.010				0.882				
		0.005				0.823				
		0.001				0.614				
		0.001				0.626				
		0.000				1.056				
		0.000				1.056				
		0.000				1.056				
		1.000								
		0.500								
		0.100								
		0.050								
		0.010								
		0.005								
		0.001								
		0.001								
		0.000								
		0.000								
579	0.959	1.000								
577	1.051	1.000								
297	1.664	1.000								
621	0.610	1.000								
620	0.793	1.000								
578	0.929	1.000								
606	0.969	1.000								
129	0.264	1.000								
130	0.505	1.000								
148	0.525	1.000								
172	0.549	1.000								
623	1.054	1.000								
624	0.546	1.000								
605	2.654	1.000								
433	2.566	1.000								
580	1.132	1.000								

Test #	actual Miner's number	Fraction Hi	NRSD exponent all data	LRSD exponent all data	NRSD exponent -static	LRSD exponent -static	NRSD power all data	LRSD power all data	NRSD power -static	LRSD power -static
308	0.308	1.000								
282	0.288	1.000								
313	1.454	1.000								
622	0.983	1.000								
298	1.207	1.000								
142	0.308	0.001								
136	0.162	0.001								
134	0.396	0.004								
132	0.369	0.010								
143	0.297	0.012								
144	0.504	0.031								
133	0.169	0.038								
145	0.369	0.083								
135	0.933	0.085								
146	1.125	0.505								
137	0.511	0.520								
149	0.725	0.163								
150	0.777	0.165								
215	0.145	0.002								
275	1.183	0.083								
300	0.486	0.001								
304	1.263	0.082								
307	0.169	0.109								
302	0.626	0.000								
326	1.203	0.000								
284	1.259	0.000								
138	1.648	0.000								
131	1.624	0.000								
323	0.194	0.000								
174	0.435	0.000								
147	0.367	0.000								
205	0.180	0.000								
633	0.500	0.000								
610	0.501	0.000								
630	0.663	0.000								
609	0.676	0.000								
632	0.432	0.000								
435	2.086	0.000								
588	2.152	0.000								
634	1.881	0.000								

Test #	actual Miner's number	Fraction Hi	NRSD exponent all data	LRSD exponent all data	NRSD exponent -static	LRSD exponent -static	NRSD power all data	LRSD power all data	NRSD power -static	LRSD power -static
585	2.140	0.000								
586	1.029	0.000								
587	0.403	0.000								
47.5/35ksi, R=0.1										
		0.501					0.963			
		0.101					0.775			
		0.050					0.661			
		0.010					0.465			
		0.005					0.426			
		0.001					0.459			
		0.001					0.450			
		0.000					1.003			
		0.000					1.003			
		0.000					1.003			
		0.501						0.993		
		0.100						0.950		
		0.050						0.918		
		0.010						0.835		
		0.005						0.821		
		0.001						0.803		
		0.001						0.900		
		0.000						1.001		
		0.000						1.001		
		0.000						1.001		
		0.500							0.960	
		0.100							0.763	
		0.050							0.647	
		0.010							0.467	
		0.005							0.431	
		0.001							0.472	
		0.001							0.463	
		0.000							1.003	
		0.000							1.003	
		0.000							1.003	
		0.500								0.993
		0.100								0.947
		0.050								0.912
		0.010								0.826
		0.005								0.808
		0.001								0.825

Test #	actual Miner's number	Fraction Hi	NRSD exponent all data	LRSD exponent all data	NRSD exponent -static	LRSD exponent -static	NRSD power all data	LRSD power all data	NRSD power -static	LRSD power -static
		0.001								0.926
		0.000								1.001
		0.000								1.001
		0.000								1.001
		0.500	0.897							
		0.100	0.591							
		0.050	0.493							
		0.010	0.394							
		0.005	0.384							
		0.001	0.420							
		0.001	0.555							
		0.000	1.001							
		0.000	1.001							
		0.000	1.001							
		0.500		0.981						
		0.100		0.894						
		0.050		0.849						
		0.010		0.788						
		0.005		0.770						
		0.001		0.839						
		0.001		0.833						
		0.000		1.001						
		0.000		1.001						
		0.000		1.001						
		0.501			0.918					
		0.100			0.610					
		0.050			0.482					
		0.010			0.318					
		0.005			0.294					
		0.001			0.330					
		0.001			0.434					
		0.000			1.002					
		0.000			1.002					
		0.000			1.002					
		0.500				0.987				
		0.100				0.913				
		0.050				0.860				
		0.010				0.760				
		0.005				0.735				
		0.001				0.769				

Test #	actual Miner's number	Fraction Hi	NRSD exponent all data	LRSD exponent all data	NRSD exponent -static	LRSD exponent -static	NRSD power all data	LRSD power all data	NRSD power -static	LRSD power -static
		0.001				0.867				
		0.000				1.001				
		0.000				1.001				
		0.000				1.001				
		0.500								
		0.100								
		0.050								
		0.010								
		0.005								
		0.001								
		0.001								
		0.000								
		0.000								
		0.000								
		1.000								
		0.500								
		0.100								
		0.050								
		0.010								
		0.005								
		0.001								
		0.001								
		0.000								
177	1.009	0.010								
178	0.296	0.010								
194	0.204	0.011								
195	0.641	0.003								
196	0.247	0.002								
198	0.209	0.020								
199	0.112	0.092								
200	0.251	0.501								
201	0.083	0.021								
202	0.146	0.011								
203	0.222	0.003								
204	0.441	0.004								
209	0.105	0.501								
210	0.332	0.501								
217	0.246	0.004								
279	1.024	0.002								
280	0.126	0.010								

Test #	actual Miner's number	Fraction Hi	NRSD exponent all data	LRSD exponent all data	NRSD exponent -static	LRSD exponent -static	NRSD power all data	LRSD power all data	NRSD power -static	LRSD power -static
350	1.380	0.500								
351	0.649	0.100								
213	1.343	1.000								
161	0.699	1.000								
171	1.280	1.000								
139	0.933	1.000								
168	0.302	1.000								
582	1.702	1.000								
434	1.521	1.000								
583	1.064	1.000								
214	0.844	1.000								
140	0.777	1.000								
617	0.988	1.000								
619	0.946	1.000								
608	0.729	1.000								
607	0.686	1.000								
616	0.439	1.000								
206	0.544	1.000								
581	1.777	1.000								
376	0.693	1.000								
554	0.310	1.000								
584	0.530	1.000								
321	1.061	1.000								
325	3.515	1.000								
618	0.312	1.000								
302	0.626	0.000								
326	1.203	0.000								
284	1.259	0.000								
138	1.648	0.000								
131	1.624	0.000								
323	0.194	0.000								
174	0.435	0.000								
147	0.367	0.000								
205	0.180	0.000								
633	0.500	0.000								
610	0.501	0.000								
630	0.663	0.000								
609	0.676	0.000								
632	0.432	0.000								
435	2.086	0.000								

Test #	actual Miner's number	Fraction Hi	NRSD exponent all data	LRSD exponent all data	NRSD exponent -static	LRSD exponent -static	NRSD power all data	LRSD power all data	NRSD power -static	LRSD power -static
588	2.152	0.000								
634	1.881	0.000								
585	2.140	0.000								
586	1.029	0.000								
587	0.403	0.000								

APPENDIX D

WISPERX FATIGUE TEST SUMMARY

		Mod2 WisperX Spectrum, R=0.1							
Test	Max Load, pounds	Max Stress, MPa	Cycles	Exponent Regression	LRSD Exponent Predict	NRSD Exponent Predict	Miner's Prediction	NRSD Power Predict	LRSD Power Predict
615	5544	622.0	1	641.4					
635	5901	670.1	1	641.4					
646	4953	569.3	1	641.4					
652	4285	619.3	1	641.4					
653	5624	676.4	1	641.4					
655	5879	688.8	1	641.4					
666	5726	670.9	1	641.4					
739	5734	696.9	1	641.4					
726	5765	647.8	1	641.4					
671	5633	687.3	1	641.4					
971	2875	340.9	1276	430.2					
972	2960	343.6	2325	412.4					
973	2889	344.7	2448	410.9					
976	3115	402.9	2806	406.9					
974	3352	406.9	3130	403.6					
979	3669	402.3	3203	403.0					
978	3387	406.2	3233	402.7					
970	2914	402.9	3844	397.6					
975	3081	403.2	4044	396.1					
977	2716	405.6	5722	385.8					
1004	3026	339.5	6048	384.2					
1005	2613	341.2	13058	361.4					
1000	2945	335.4	14371	358.6					
1002	2593	340.9	18334	351.4					
1006	2698	343.2	24196	343.2					
1003	2934	340.2	24906	342.4					
1001	2810	335.5	26045	341.0					
986	2524	296.9	68426	312.5					
989	2458	297.5	80980	307.5					
983	2669	301.6	86293	305.7					
988	2543	297.0	144430	290.4					
981	2475	298.0	155850	288.2					
980	2233	297.9	167885	286.0					
985	2299	298.0	169839	285.7					
982	2462	297.2	195616	281.5					
990	2338	254.1	195751	281.5					
987	2319	297.4	231019	276.6					
999	2227	256.1	248429	274.4					

Test	Max Load, pounds	Max Stress, MPa	Cycles	Exponent Regression	LRSD Exponent Predict	NRSD Exponent Predict	Miner's Prediction	NRSD Power Predict	LRSD Power Predict
984	2270	296.8	298800	269.0					
995	2222	254.6	312744	267.6					
996	2164	259.1	432307	258.1					
991	2202	255.0	598438	248.5					
998	2175	255.6	680774	244.6					
992	1878	255.9	876955	237.2					
997	1979	256.7	912240	236.0					
993	1878	253.1	1231928	227.1					
1016	1550	189.7	12289518	159.2					
1007	1550	185.6	14130978	155.0					
			12983		414				
			92466		327.75				
			836664		241.5				
			1952961		207				
			2649			414			
			41142			327.75			
			503058			241.5			
			1298580			207			
			13409				414		
			117716				327.75		
			984459				241.5		
			2284731				207		
			2649					414	
			41142					327.75	
			1863144					241.5	
			1E+07					207	
			1497						414
	644		28311						327.75
	31		1118946						241.5
	1		6777417						207

DISTRIBUTION

T. Almeida
TPI Composites Inc.
373 Market Street
Warren, RI 02885

H. Ashley
Dept. of Aeronautics and
 Astronautics Mechanical Engr.
Stanford University
Stanford, CA 94305

K. Bergey
University of Oklahoma
Aero Engineering Department
Norman, OK 73069

R. Blakemore
Enron Wind Corp.
13681 Chantico Road
Tehachapi, CA 93561
C. P. Butterfield
NREL
1617 Cole Boulevard
Golden, CO 80401

G. Bywaters
Northern Power Systems
Box 999
Waitsfield,VT 05673

J. Cadogan
Office of Geothermal & Wind
 Technology
EE-12
U.S. Department of Energy
1000 Independence Avenue SW
Washington, DC 20585

D. Cairns
Montana State University
Mechanical & Industrial Engineering Dept.
220 Roberts Hall
Bozeman, MT 59717

S. Calvert
Office of Geothermal & Wind
 Technology
EE-12
U.S. Department of Energy
1000 Independence Avenue SW
Washington, DC 20585

J. Chapman
OEM Development Corp.
840 Summer St.
Boston, MA 02127-1533

Kip Cheney
PS Enterprises
222 N. El Segundo, #576
Palm Springs, CA 92262

C. Christensen
Enron Wind Corp.
13681 Chantico Road
Tehachapi, CA 93561

R. N. Clark
USDA
Agricultural Research Service
P.O. Drawer 10
Bushland, TX 79012

J. Cohen
Princeton Economic Research, Inc.
1700 Rockville Pike
Suite 550
Rockville, MD 20852

C. Coleman
Northern Power Systems
Box 999
Waitsfield, VT 05673

C. A. Cornell
Civil Engineering Department
Stanford University
Stanford, CA 94305

K. J. Deering
The Wind Turbine Company
515 116th Avenue NE
No. 263
Bellevue, WA 98004

A. J. Eggers, Jr.
RANN, Inc.
744 San Antonio Road, Ste. 26
Palo Alto, CA 94303

D. M. Eggleston
DME Engineering
1605 W. Tennessee Ave.
Midland, TX 79701-6083

P. R. Goldman
Director
Office of Geothermal & Wind
  Technology
EE-12
U.S. Department of Energy
1000 Independence Avenue SW
Washington, DC 20585

G. Gregorek
Aeronautical & Astronautical Dept.
Ohio State University
2300 West Case Road
Columbus, OH 43220

D. Griffin
Global Energy Concepts
5729 Lakeview Drive NE, Ste. 100
Kirkland, WA 98033

C. Hansen
Windward Engineering
4661 Holly Lane
Salt Lake City, UT 84117

C. Hedley
Headwaters Composites
105 E. Adams St.
Three Forks, MT 59752

S. Hock
Wind Energy Program
NREL
1617 Cole Boulevard
Golden, CO 80401

Bill Holley
3731 Oakbrook Court
Pleasanton, CA 94588

K. Jackson
Dynamic Design
123 C Street
Davis, CA 95616

E. Jacobsen
Enron Wind
13000 Jameson Rd.
Tehachapi, CA 93561

D. Malcolm
Global Energy Concepts
5729 Lakeview Drive NE, Ste. 100
Kirkland, WA 98033

J. F. Mandell   (20)
Montana State University
302 Cableigh Hall
Bozeman, MT 59717

T. McCoy
Global Energy Concepts
5729 Lakeview Drive NE, Ste. 100
Kirkland, WA 98033

L. McKittrick
Montana State University
Mechanical & Industrial Engineering Dept.
220 Roberts Hall
Bozeman, MT 59717

P. Migliore
NREL
1617 Cole Boulevard
Golden, CO 80401

W. Musial
NREL
1617 Cole Boulevard
Golden, CO 80401

NWTC Library (5)
NREL
1617 Cole Boulevard
Golden, CO 80401

B. Neal
USDA
Agricultural Research Service
P.O. Drawer 10
Bushland, TX 79012

V. Nelson
Department of Physics
West Texas State University
P.O. Box 248
Canyon, TX 79016

J. W. Oler
Mechanical Engineering Dept.
Texas Tech University
P.O. Box 4289
Lubbock, TX 79409

T. Olsen
Tim Olsen Consulting
1428 S. Humboldt St.
Denver, CO 80210

R. G. Rajagopalan
Aerospace Engineering Department
Iowa State University
404 Town Engineering Building
Ames, IA 50011

J. Richmond
MDEC
3368 Mountain Trail Ave.
Newbury Park, CA 91320

Michael Robinson
NREL
1617 Cole Boulevard
Golden, CO 80401

D. D. Samborsky
Dept. of Chemical Engineering
Montana State University
Cableigh Hall
Bozeman, MT 59717

D. Sanchez
U.S. Dept. of Energy
Albuquerque Operations Office
P.O. Box 5400
Albuquerque, NM 87185

L. Schienbein
Sustainable Energy Technologies
350 Hills Street, #108
Richland, WA 99352

R. Sherwin
Atlantic Orient
PO Box 1097
Norwich, VT 05055

Brian Smith
NREL
1617 Cole Boulevard
Golden, CO 80401

K. Starcher
AEI
West Texas State University
P.O. Box 248
Canyon, TX 79016

F. S. Stoddard
79 S. Pleasant St. #2A
Amherst, MA 01002

A. Swift
University of Texas at El Paso
320 Kent Ave.
El Paso, TX 79922

R. W. Thresher
NREL
1617 Cole Boulevard
Golden, CO 80401

S. Tsai
Stanford University
Aeronautics & Astronautics
Durand Bldg. Room 381
Stanford, CA 94305-4035

W. A. Vachon
W. A. Vachon & Associates
P.O. Box 149
Manchester, MA 01944

C. P. van Dam
Dept. of Mech. and Aero. Eng.
Univ. of California, Davis
One Shields Avenue
Davis, CA 95616-5294

B. Vick
USDA, Agricultural Research Service
P.O. Drawer 10
Bushland, TX 79012

N. K. Wahl   (10)
Engineering Department
Montana Tech of The Univ. of Montana
1300 West Park Street
Butte, MT 59701

R. E. Wilson
Mechanical Engineering Dept.
Oregon State University
Corvallis, OR 97331

M. Zuteck
MDZ Consulting
931 Grove Street
Kemah, TX 77565